

City Research Online

City St George's, University of London

Citation: Chatterjee, J. (1993). The mechanisms of some reactions of nitrogen dioxide with alkenes and aromatic compounds. (Unpublished Doctoral thesis, City, University of London)

This is the accepted version of the paper.

This version of the publication may differ from the final published version. To cite this item please consult the publisher's version.

Permanent repository link: https://openaccess.city.ac.uk/id/eprint/29332/

Copyright and Reuse: Copyright and Moral Rights remain with the author(s) and/or copyright holders. Copies of full items can be used for personal research or study, educational, or not-for-profit purposes without prior permission or charge, unless otherwise indicated, provided that the authors, title and full bibliographic details are credited, a hyperlink and/or URL is given for the original metadata page and the content is not changed in any way. For full details of reuse please refer to City Research Online policy.

City Research Online: http://openaccess.city.ac.uk/ publications@citystgeorges.ac.uk

THE MECHANISMS OF SOME REACTIONS OF NITROGEN DIOXIDE WITH ALKENES AND AROMATIC COMPOUNDS

by

Julie Chatterjee

A thesis submitted in part fulfilment of the requirements for the degree of Doctor of Philosophy

Department of Chemistry,
The City University,
London.

April 1993

To my Mother and Father

LIST OF CONTENTS

	Page
ACKNOWLEDGEMENTS	viii
DECLARATION	ix
ABSTRACT	x
CHAPTER 1: GENERAL LITERATURE SURVEY	2
1.1 Nitration by nitrogen dioxide	2
1.1.1 Structure of nitrogen dioxide-dinitrogen tetraoxide	2
1.1.2 The nitrogen dioxide-dinitrogen tetraoxide equilibrium	3
1.1.3 Nitration of unsaturated compounds	6
1.1.4 Nitration of aromatic and polycyclic aromatic compounds	18
1.1.5 Nitration of paraffins	29
1.1.6 Nitration of phenol compounds	30
1.2 Reactions of nitrogen dioxide with fuel/lubricant components	33
1.2.1 Chemical reactants and reactions in an engine	33
1.2.2 Nitrogen oxides	34
1.2.3 Fuel hydrocarbons	35
1.2.4 Oxidation of fuel and lubricant hydrocarbons	35
1.2.5 Reactions of alkenes with nitrogen oxides	35
1.2.6 Fuel as a source of deposits	36
1.2.7 Lubricant as a material source and reaction medium in deposit formation	36
1.3 The present study	37
CHAPTER 2: KINETIC STUDIES OF THE REACTIONS OF STYRENE, ALLYLBENZENE, 4-PHENYLBUT-1-ENE AND 1-DODECENE WITH NITROGEN DIOXIDE	41
2.1 Introduction	41

2.2 Experimental 45
2.2.1 Variation of nitrogen dioxide concentration 45
2.2.2 Reaction of allylbenzene with nitrogen dioxide 46
2.2.2.1 Variation of temperature 46
2.2.2.2 Variation of $[H_2O]$ 46
2.2.2.3 Measurement of the rate of reaction under a N_2 atmosphere 47
2.2.2.4 Influence of light 47
2.3 Results 48
2.3.1 The reaction of styrene with nitrogen dioxide 48
2.3.2 The reaction of allylbenzene with nitrogen dioxide 49
2.3.2.1 Variation of $[N_2O_4]_t$ 49
2.3.2.2 Variation of temperature 49
2.3.2.3 Variation of $[H_2O]$ 50
2.3.2.4 Influence of oxygen on the reaction of allylbenzene with nitrogen dioxide 50
2.3.2.5 Influence of light on the reaction of allylbenzene with nitrogen dioxide 50
2.3.3 The reaction of 4-phenylbut-1-ene with nitrogen dioxide 51
2.3.4 The reaction of 1-dodecene with nitrogen dioxide 51
2.4 Discussion 73
2.4.1 Discussion of related work 103

CHAPTER 3: PRODUCT STUDIES OF THE REACTIONS OF STYRENE, ALLYLBENZENE,4-PHENYLBUT-1-ENE AND 1-DODECENE WITH NITROGEN DIOXIDE 117
3.1 Introduction 117
3.2 Experimental 118
3.2.1 Preparation of product mixtures from the reactions of styrene, allylbenzene, 4-phenylbut-1-ene and 1-dodecene with nitrogen dioxide 118

3.2.2 I.R. studies of the reaction of allylbenzene with nitrogen dioxide 118
3.2.3 Reaction of allylbenzene with ^{15}N-labelled nitrogen dioxide 118
3.2.4 Reaction of allylbenzene with 10000 ppm and 50 ppm gaseous nitrogen dioxide 119
3.3 Results 120
3.3.1 The reaction of allylbenzene with nitrogen dioxide 120
3.3.1.1 Reaction of allylbenzene with 10000 ppm and 50 ppm gaseous nitrogen dioxide 154
3.3.2 The reactions of styrene, 4-phenylbut-1-ene and 1-dodecene with nitrogen dioxide 159
3.4 Discussion 170

CHAPTER 4: C.I.D.N.P.STUDIES OF THE REACTIONS OF STYRENE, ALLYLBENZENE AND 1-DODECENE WITH NITROGEN DIOXIDE 173
4.1 Introduction 173
4.2 C.K.O. Theory 174
4.3 Experimental 178
4.4 Results 178
4.4.1 The reaction of styrene with ^{15}N-labelled nitrogen dioxide 178
4.4.2 The reaction of allylbenzene with ^{15}N-labelled nitrogen dioxide 179
4.4.3 The reaction of 4-phenylbut-1-ene with ^{15}N-labelled nitrogen dioxide 179
4.4.4 The reaction of 1-dodecene with ^{15}N-labelled nitrogen dioxide 180
4.5 Discussion 191

CHAPTER 5: CONCLUDING DISCUSSION FOR THE REACTIONS OF STYRENE, ALLYLBENZENE, 4-PHENYLBUT-1-ENE AND 1-DODECENE WITH NITROGEN DIOXIDE 204
5.1 Mechanistic implications 204

CHAPTER 6: THE REACTIONS OF NAPHTHALENE AND 2-METHYLNAPHTHALENE WITH NITROGEN DIOXIDE 209
6.1 Introduction 209
6.2 Experimental 210
6.2.1 Kinetic measurements 210
6.2.2 Product measurements 210
6.2.3 Measurement of reactivities by the competition technique 211
6.3 Results 212
6.3.1 The reaction of naphthalene with nitrogen dioxide 212
6.3.1.1 Kinetic and product measurements 212
6.3.2 The reaction of 2-methylnaphthalene with nitrogen dioxide 213
6.3.2.1 Kinetic measurements 213
6.3.2.2 Product measurements 214
6.3.3 Relative reactivities 231
6.3.3.1 Naphthalene 231
6.3.3.2 2-Methylnaphthalene 237
6.4 Discussion 241

CHAPTER 7: THE REACTION OF 1-METHYLBUTYLBENZENE WITH NITROGEN DIOXIDE 247
7.1 Introduction 247
7.2 Experimental 247
7.2.1 The reaction of 1-methylbutylbenzene with gaseous nitrogen dioxide 247
7.2.2 Measurement of the reactivity of 1-methylbutylbenzene by the competition technique 247
7.3 Results 248
7.3.1 The reaction of 1-methylbutylbenzene with gaseous nitrogen dioxide 248
7.3.2 Measurement of the reactivity of 1-methylbutylbenzene by the competition technique 255
7.4 Discussion 258

CHAPTER 8: THE REACTIONS OF POLYSUBSTITUTED BISPHENOLS WITH NITROGEN DIOXIDE 260
8.1 Introduction 260
8.2 Experimental 261
8.2.1 Kinetic measurements 261
8.2.2 Product measurements 261
8.3 Results 262
8.3.1 The reaction of bis(4-hydroxy-3,5-di-t-butylphenyl)methane (AN2) with nitrogen dioxide 262
8.3.1.1 Product measurements 262
8.3.1.2 Kinetic measurements 263
8.3.2 The reaction of 2,2-bis(4-hydroxy-3,5-di-t-butylphenyl)propane (IONOX 400) with nitrogen dioxide 272
8.3.2.1 Product measurements 272
8.3.2.2 Kinetic measurements 273
8.4 Discussion 282

CHAPTER 9: CONCLUDING DISCUSSION 290

CHAPTER 10: EXPERIMENTAL 296
10.1 Materials 296
10.1.1 Nitrogen dioxide and solvents 296
10.1.2 Aromatic compounds 296
10.2 Gas-liquid chromatography 297
10.2.1 GLC conditions for allylbenzene/nitrogen dioxide product mixtures 297
10.3 GLC/MS Analysis 298
10.3.1 GC/EIMS 298
10.3.2 GC/CIMS 298
10.4 Instrumentation 298
10.5 Temperature measurements 299

APPENDIX 300

REFERENCES 301

ACKNOWLEDGEMENTS

I would like to thank Drs. R.G. Coombes, J.R. Barnes, R.C. Coy and M.J. Fildes for the continual advice and encouragement shown throughout the course of this research.

My special thanks are also due to Drs. S.R. Nattrass and A.G. Osborne for useful discussions on n.m.r. work, Mr. Jeff Abrahams, Mr. D.M. James, and Ms Jane Belden for being helpful and patient whilst typing my thesis.

I also wish to thank Shell Research Ltd. for the award of a research studentship.

DECLARATION

I hereby grant powers of discretion to the City University Library to allow this thesis to be copied in whole or in part without further reference to myself.

Julie Chatterjee,
April 1993

ABSTRACT

The reactions in solution with nitrogen dioxide/ dinitrogen tetraoxide of a range of organic compounds, chosen as model compounds for those present in car engine fuel and oil, have been studied.

A main emphasis has been on the reactivity of a number of alkenes. Allylbenzene, which has the possibility of allylic reaction, has been studied in detail. The products of these reactions were dinitro, α,β-nitro-nitrite, α,β-nitro-hydroxy and α,β-nitro-nitrate adducts. Allylic products were absent. Kinetic studies established both $NO_2^{\cdot}$ and N_2O_4 as reactive species with the alkenes, but studies of chemically induced dynamic nuclear polarisation were dominated by the $NO_2^{\cdot}$ reaction. The intermediacy of radical pair species on the pathways to the dinitro and nitro-nitrite adducts was confirmed.

Naphthalene and 2-methylnaphthalene were much less reactive towards nitrogen dioxide/dinitrogen tetraoxide, although rates relative to benzene were established. No compelling evidence for a greater reactivity of 1-methylbutylbenzene than the hexadecane solvent towards nitrogen dioxide/dinitrogen tetraoxide was obtained even at 150°C.

Studies of the commercial antioxidants AN2 (bis(4-hydroxy-3,5-di-t-butylphenyl)methane) and IONOX 400 (2,2-bis(4-hydroxy-3,5-di-t-butylphenyl)propane) revealed a noteworthy difference. The former gave a reaction second-order in $NO_2^{\cdot}$ and yielded the corresponding 2,5-dienone, whereas the latter gave two equivalents of 2,6-di-t-butyl-4-nitrophenol in a reaction first-order in $NO_2^{\cdot}$.

CHAPTER 1

GENERAL LITERATURE SURVEY

1. GENERAL LITERATURE SURVEY

1.1 Nitration by nitrogen dioxide

1.1.1 Structure of nitrogen dioxide - dinitrogen tetraoxide

The monomer $NO_2^{\cdot}$ is a free-radical species with a volume susceptibility, $\chi = 3 \times 10^{-15}$ c.g.s.[1] which is in good agreement with the quantum theory prediction.[2] The ionisation potential of $NO_2^{\cdot}$ is 956 kJ mol^{-1} based on the appearance potential of NO_2^+ in studies using nitromethane.[3] The electron affinity of $NO_2^{\cdot}$ has been calculated, from values of the lattice energies of the nitrites, as 156 kJ mol^{-1}.[4] $NO_2^{\cdot}$ is an angular molecule with N-O bond lengths 1.19 Å[5] and the ONO angle 134°.[6]

$NO_2^{\cdot}$ exists as a mixture with N_2O_4 under most conditions. The structure of the dimer is still in dispute. All the bands in the infra-red spectra of the solid,[7] liquid[7,8] and gaseous [7,8] N_2O_4 have been assigned as fundamental frequencies, and combinations and overtones thereof, for the coplanar structure (I).

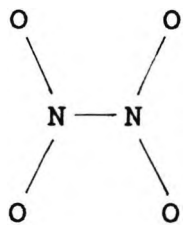

(I)

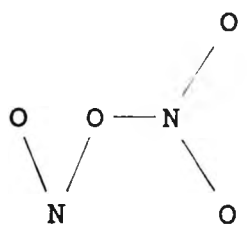

(II)

An isomeric structure for N_2O_4 (II) has been postulated,[9] based on chemical evidence which continually demonstrates the ease and readiness of the following reaction

$$N_2O_4 \longrightarrow NO^+ + NO_3^- \qquad (1.1)$$

and the complete absence of the alternative heterolysis to NO_2^+ and NO_2^-, even as an intermediate stage, e.g. there is ready exchange of $N^{15}O_3^-$ between tetramethylammonium nitrate and solvent liquid dinitrogen tetraoxide, and with metals, nitrate ions and nitric oxide are formed. The bands observed in the infra-red spectrum during this study, however, have not been observed by other workers.[7,8,10]

Electron diffraction measurements[11] on gaseous N_2O_4 and X-ray crystallographic studies[12] on the solid also suggest structure (I).

1.1.2 <u>The nitrogen dioxide-dinitrogen tetraoxide equilibrium</u>

N_2O_4 exists in a strongly temperature- and concentration -dependent equilibrium with the monomer, $NO_2^{\cdot}$

$$2\ NO_2^{\cdot} \underset{k_{-1}}{\overset{k_1}{\rightleftharpoons}} N_2O_4 \qquad (1.2)$$

$$K = \frac{k_{-1}}{k_1} = \frac{[NO_2^{\cdot}]^2}{[N_2O_4]} \qquad (1.3)$$

both in the gas-phase and in solution. The dimer is predominant at lower temperatures, but vapour-density measurements indicate complete conversion into the monomer above 140°C. At 26.7°C about 20 per cent of the tetraoxide exists in the simpler form. It is believed that above 140°C N_2O_4 decomposes to form nitric oxide and oxygen, a change which is complete at 619.5°C.[13]

The equilibrium has been found to be rapid in the gas phase[14] with $k_1 = 4.2 \times 10^5\ dm^3mol^{-1}s^{-1}$ and $k_{-1} = 6.4 \times 10^4\ s^{-1}$

at 25°C. The equilibrium constant, K, varies from the gas phase[15] (0.151 mol dm^{-3}) to solution in carbon tetrachloride or cyclohexane[16] (1.77 x 10^{-4} mol dm^{-3}).

From these data the equilibrium constant can be calculated at any temperature using the known value of the enthalpy of dissociation of N_2O_4 and equation 1.4.

$$\ln\left[\frac{K(T_2)}{K(T_1)}\right] = -\frac{\Delta H^\circ_{diss}}{R}\left[\frac{1}{T_2} - \frac{1}{T_1}\right] \qquad (1.4)$$

Table 1.1 lists the values of K for the equilibrium in cyclohexane solution for some temperatures employed in the present work. The value of K at 30°C shown in Table 1.1 was taken from a piece of work carried out by Pryor et al.[42] so that a comparison with this work could be made. The value of K at 30°C calculated using equation 1.4 is, however, found to be 2.66 x 10^{-4} mol dm^{-3}. At convenient temperatures and concentrations, comparable amounts of $NO_2^\bullet$ and N_2O_4 exist in solutions of nitrogen dioxide. The UV spectra of $NO_2^\bullet$ and N_2O_4 have been separated in the gas-phase[17] and at 430 nm, $NO_2^\bullet$ is the only absorbing species with an extinction coefficient of 150 $dm^3 mol^{-1} cm^{-1}$.

Table 1.1: Variation of K (equation 1.4) with temperature for the dissociation of N_2O_4 in carbon tetrachloride or cyclohexane[16]

T/K	10^4 K/mol dm^{-3}
298	1.77
298.4	1.83
303	2.644

Because of the equilibrium, written reports concerning $NO_2^\bullet$ and N_2O_4 are often confusing because it is not always clear whether the author is referring to one or both species. In this work, the convention is adopted that the names 'nitrogen dioxide' or 'dinitrogen tetraoxide' refer to the equilibrium mixture

containing both species, while the formulae $NO_2^{\bullet}$ and N_2O_4 refer to those particular individual species.

1.1.3 Nitration of unsaturated compounds

The reaction of unsaturated aliphatic compounds with nitrogen oxides usually leads to the formation of unstable solids or oils, from which it is often difficult to isolate the pure substance. Wieland [18,19] was one of the first research workers who studied the interaction of alkenes with dinitrogen tetraoxide and nitrogen oxide gases. He found that the products of this reaction were dinitro compounds which were formed according to equation 1.5.

$$R\text{-}CH{=}CH\text{-}R' + N_2O_4 \longrightarrow R\text{-}CHNO_2\text{-}CHNO_2\text{-}R' \quad (1.5)$$

where R and R′ are saturated alkyl groups. Similar dinitro compounds were also obtained on nitration of mixed aliphatic aromatic compounds with the general formula of $C_6H_5CH{=}CH\text{-}R$ and Ar-CH=CH-Ar using dinitrogen tetraoxide.

Wieland[59] also studied the nitration of unsaturated hydrocarbons containing conjugated double bonds:

$$R\text{-}CH{=}CH\text{-}CH{=}CH\text{-}R' \quad (III)$$

Treating a suspension of 1,4-diphenylbutadiene in absolute ether with a solution of dinitrogen tetraoxide in a mixture of ether and petroleum ether, with cooling, gave 1,4-diphenyl-1,4-dinitrobut-2-ene. Thus the nitro groups add on not to two adjacent carbon atoms (in positions 1,2) but to the terminal carbon atoms in a system of conjugated double bonds (1,4). The 1,4-addition in conjugated systems of this type has recently been shown to be quite general.[20]

A number of investigations have been made of the reactions of dinitrogen tetraoxide with 2,3-dimethylbut-2-ene. In ether solution Michael and Carlson[21a] obtained up to 22% of 2,3-dinitro-2,3-dimethylbutane (IV), whereas in the absence of solvent or in petroleum ether solution only low yields of the dinitro compound were formed:

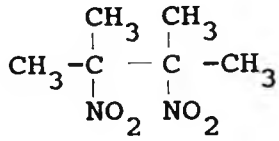

(IV)

Under these conditions, the results showed the formation of a nitro-nitrate compound (V), originally proposed by Demianov and Sidorenko.[22,23]

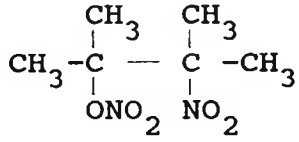

(V)

This nitric ester readily formed a double compound with the dinitro product (IV) to yield a fairly soluble crystalline solid; since it appeared in a relatively high yield only under the oxidising action of the tetraoxide, the disappearance of dinitro compound in these experiments was attributed to a conversion into double compound. Both sets of workers concluded no dinitrite[24] was formed.

Michael and Carlson[21b] also studied the action of dinitrogen tetraoxide on 2-methylpropene under a variety of conditions. In ethereal solution the reaction led to the formation of the following compounds:

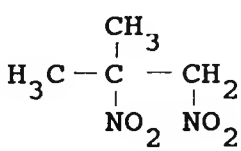

12% yield

(VI)

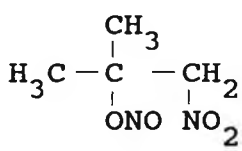

16-23% yield

(VII)

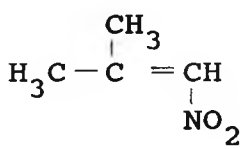

5-12% yield

(VIII)

These results were based on the yields of the reduction products, and also assumed that the isolated 1,2-diamino-2-methylpropane was formed from 1,2-dinitro-2-methylpropane.

In the absence of solvent or in petroleum ether solution a nitroso-nitrate in an approximately 13% yield was obtained:

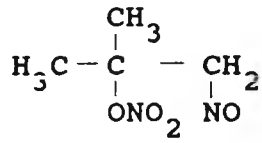

(IX)

The other products formed were not examined since they had either undergone pronounced oxidation or had decomposed and could not be separated into component parts.

If 2-methylpropene was replaced by 2-methylbut-2-ene[25] the following compound was obtained with a yield of 35% when petroleum ether was used as solvent:

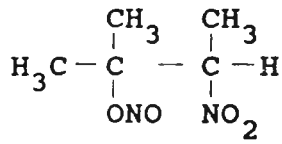

(X)

Again, the chemical nature of the remaining products from this reaction could not be established due to their instability.

When Smith[26] passed pure ethene through purified liquid nitrogen dioxide at 0°C he obtained a good yield of 1,2-dinitroethane. 1,2-dinitropropane and 1,2-dinitrobutane were obtained analogously.[27]

Levy[28a] obtained dinitroethane in a 33% yield by simultaneously passing ethene (at the rate of 30 dm^3/h) and oxygen (at the rate of 8 dm^3/h) into liquid dinitrogen tetraoxide (3 dm^3) at 0°C for 10½ h.

The same workers[28b,29] also investigated the products formed from the reaction of propene, butene, cyclohexene,

2,4,4-trimethylpent-1-ene and 2,4,4-trimethylpent-2-ene with dinitrogen tetraoxide. In the case of gaseous alkenes a stream of the hydrocarbon was passed through a solution of dinitrogen tetraoxide in ether. Liquid alkenes were added dropwise to dinitrogen tetraoxide or, alternatively, an ethereal solution of dinitrogen tetraoxide was added to the hydrocarbon. The reactions were carried out at low temperatures, from -5°C to 0°C. In some experiments a gentle stream of oxygen was passed through the reaction mixture in order to avoid the formation of nitrogen trioxide.

The studies showed that the reaction of dinitrogen tetraoxide with an alkene yields a mixture of a dinitroalkane, a nitro alcohol and a nitroalkyl nitrate. The initial products were the dinitroalkane and the nitro-nitrite. The latter was unstable and was not isolated in the pure state, but was hydrolysed on work up to form a nitro alcohol. The nitro-nitrate was believed to be formed by oxidation of the nitro-nitrite. The total yield of products ranged from 65-85%.

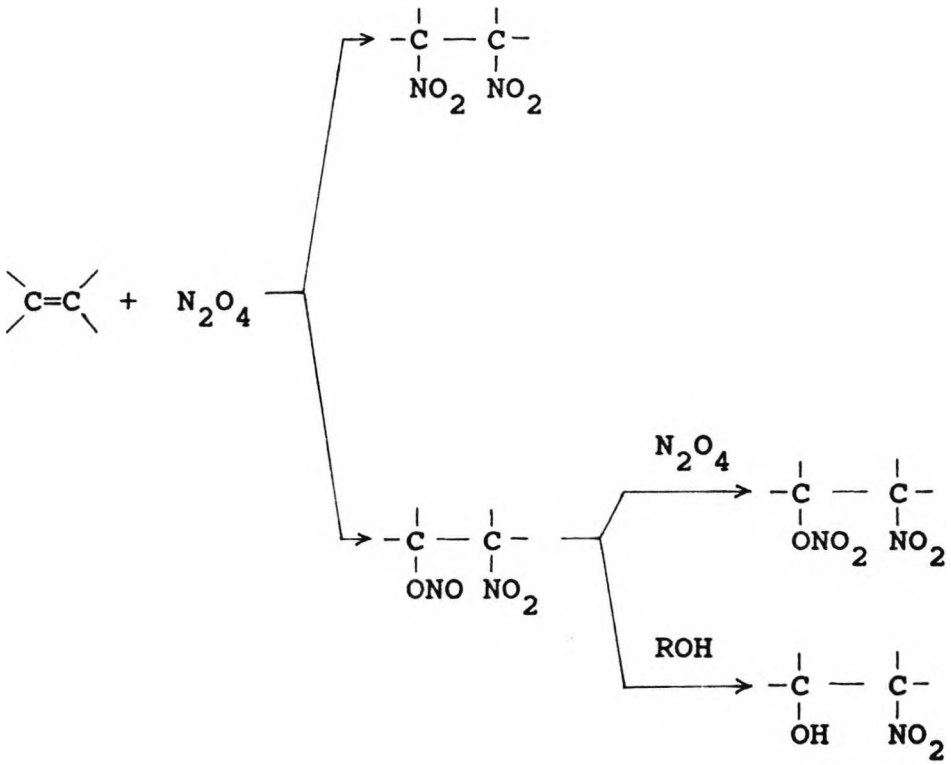

Scheme 1.1

The nitrite group always attached itself to the carbon atom linked with the fewest number of hydrogen atoms.

On the basis of these results and the solvent effect of certain ethers and esters, it was initially proposed that the reaction of dinitrogen tetraoxide with alkenes involved heterolytic addition of the tetraoxide as 'NO_2^+ NO_2^-'.[28-31] The products (vic-dinitro compounds and nitro-nitrite esters) contained not less than one C-NO_2 group, as required by an explanation involving attack by NO_2^+.

Later evidence eroded this argument considerably. Addition to diphenylacetylene[32] and to hex-3-yne[33] is non-stereospecific; this result is not expected from a heterolytic process. The orientation of addition to methyl acrylate[34] is contrary to the Markovnikov rule. These results however, are readily understood in terms of a free-radical mechanism:[34]

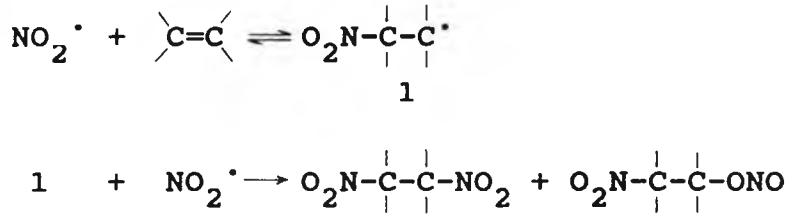

Scheme 1.2

For example, when cyclohexene is allowed to react with nitrogen dioxide in bromoform[35] or in the presence of bromotrichloromethane,[36] 2-nitro-1-bromocyclohexane is formed, suggesting the formation of a β-nitroalkyl radical intermediate. Also, product studies of the reaction of nitrogen dioxide with norbornene[37] demonstrated that the products are a mixture of cis- and trans- 1,2-dinitronorbornenes with no evidence for norbornyl cation rearrangements, which would be expected for a carbocation intermediate.

The reactions above have been utilised so that alkenes can be nitrated by a stepwise procedure involving, firstly, addition of dinitrogen tetraoxide in the presence of oxygen to the double bond to give a mixture of vic-dinitro compounds,

β-nitro-nitrites and -nitrates, and, secondly, a base-catalysed elimination reaction to generate the nitroalkene. Using this method, direct conversion of 1-octadecene into 1-nitro-1-octadecene and cyclooctene into 1-nitrocyclooctene, in 80% and 95% yield, respectively, has been achieved.[38]

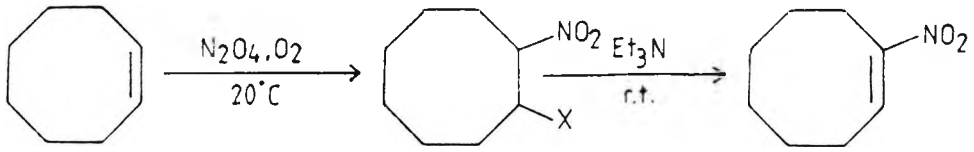

X = NO_2, ONO or ONO_2

Scheme 1.3

More recent studies performed by Pryor and his co-workers[39] show that the mechanism of nitrogen dioxide - alkene reactions changes from predominantly addition to predominantly hydrogen abstraction as the nitrogen dioxide concentration (in a carrier gas) decreases from high percent (50%) to below 10,000 ppm (1%) levels. Two mechanistic schemes were therefore proposed and these took into account the presence or absence of oxygen (Schemes 1.4 and 1.5).

Scheme 1.4

Addition Mechanism

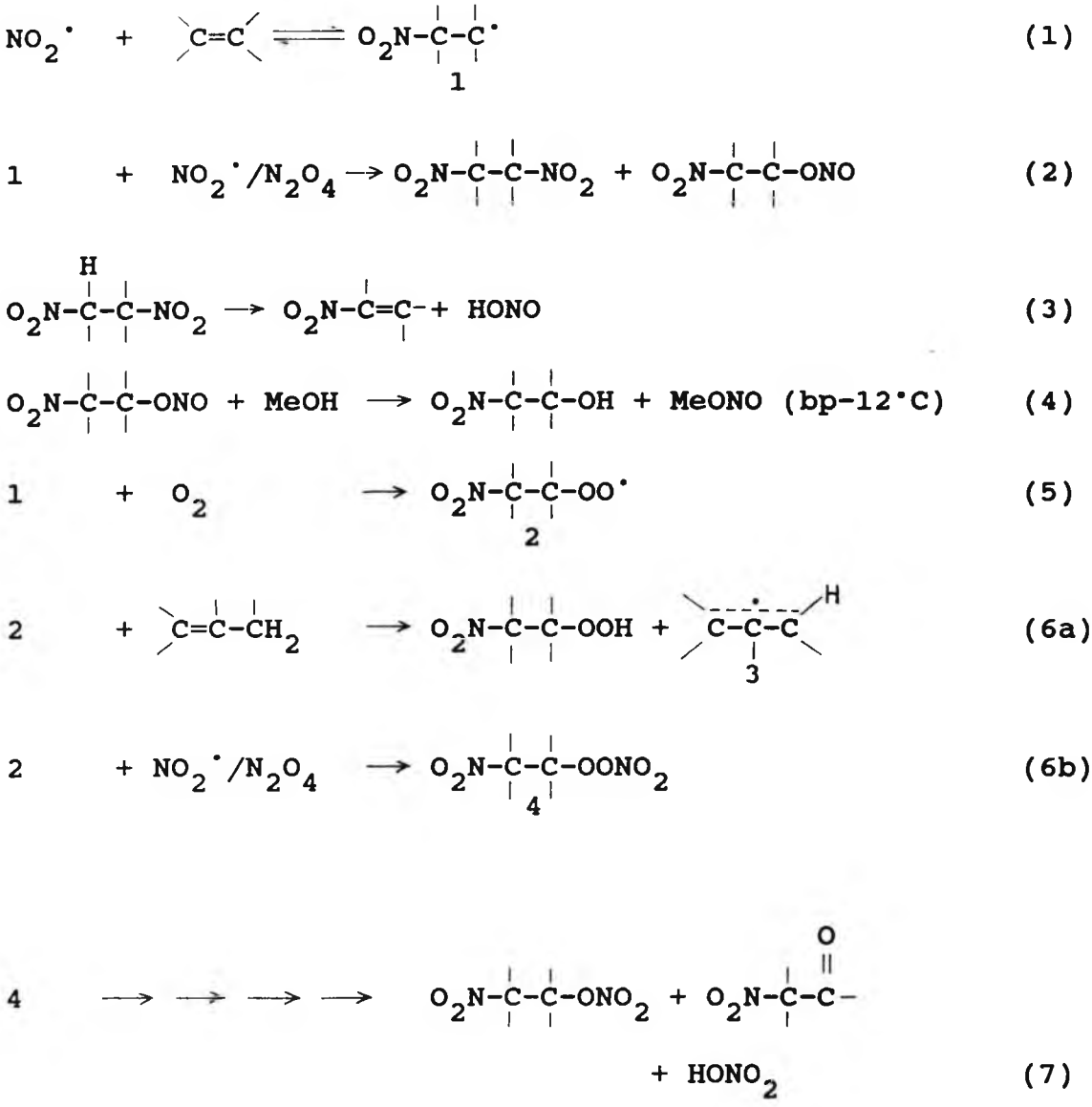

(1)

(2)

(3)

(4)

(5)

(6a)

(6b)

(7)

Scheme 1.5

Hydrogen-abstraction Mechanism

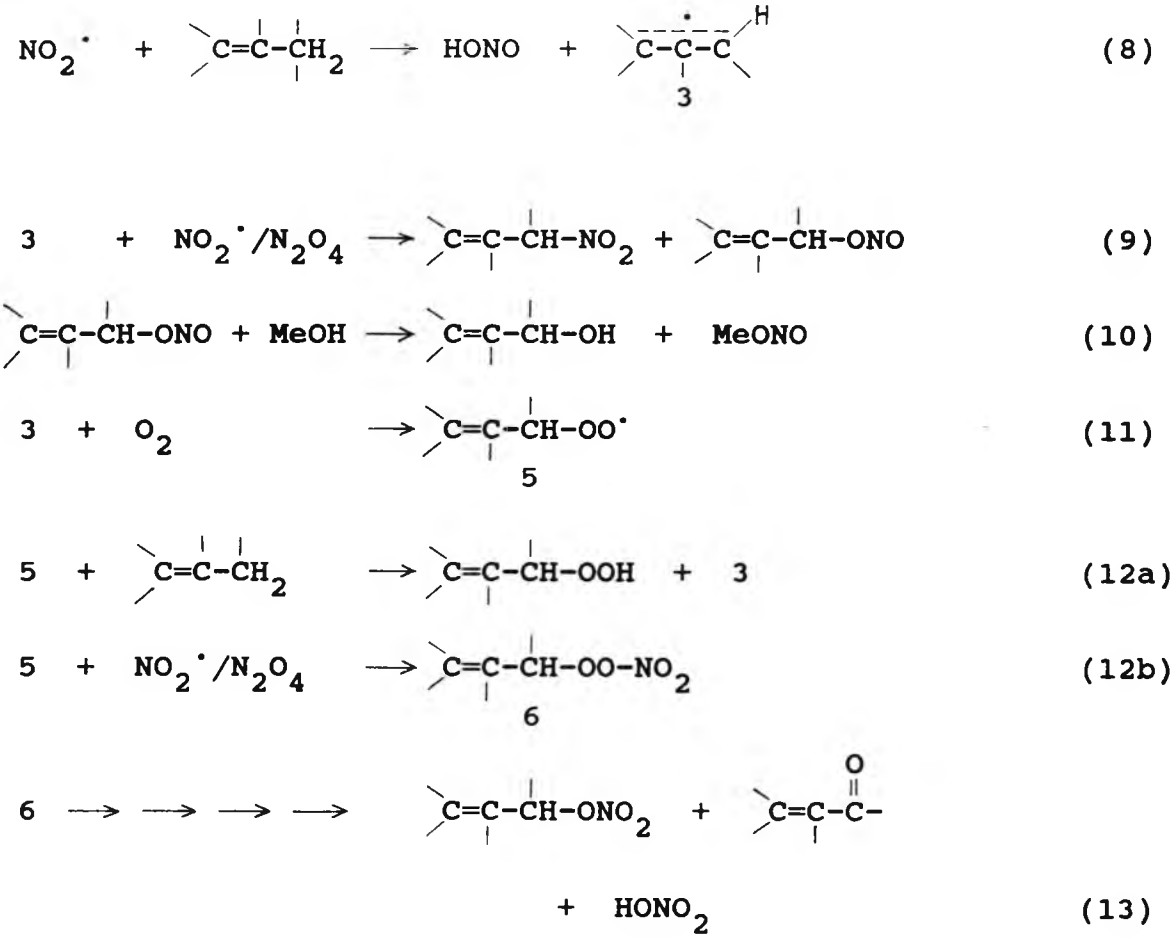

(8)

(9)

(10)

(11)

(12a)

(12b)

(13)

The reaction of cyclohexene, for example, with low concentrations of nitrogen dioxide in N_2 gave the following substitution products: 2-cyclohexenol, 2-cyclohexenyl nitrate, 3-nitrocyclohexene and 2-cyclohexenone oxime. When the reaction was carried out in the presence of oxygen or air, 2-cyclohexenol, 2-cyclohexenyl hydroperoxide, 2-cyclohexenyl nitrate and 3-nitrocyclohexene were formed. At high concentrations of nitrogen dioxide in N_2, 1-nitrocyclohexene and 2-nitrocyclohexanol were formed as the major addition products together with small amounts of 2-nitrocyclohexyl nitrate and 1,2-dinitrocyclohexane. The nature of addition products did not change upon reaction in the presence of oxygen.

E.S.R. spin trapping results with nitrogen dioxide/air/alkene gas-phase mixtures[40] (ethene, propene, 2-methylpropene, 1,3-butadiene) were consistent with the following mechanism, involving formation of a peroxyl radical:

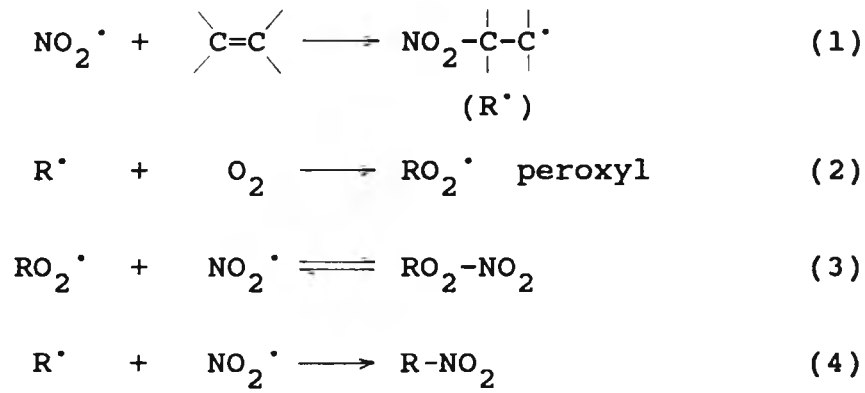

Scheme 1.6

Under the conditions used, with the concentration of O_2 about tenfold higher than that of $NO_2^{\cdot}$, the rate of reaction (2) should be faster than that of reaction (4). The data, however, indicated that a longer-lived radical precursor was produced in the gas phase when $NO_2^{\cdot}$ was allowed to react with 2-methylpropene relative to the other alkenes studied. This was interpreted as evidence that peroxyl radicals were produced, since 2-methylpropene was the only alkene studied that would give a tertiary peroxyl radical (Scheme 1.7).

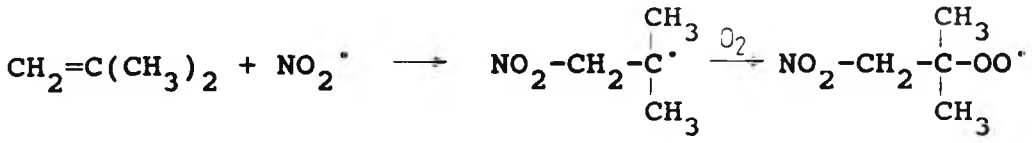

Scheme 1.7

E.S.R. spectra of nitroxide radicals ($R_2NO^{\bullet}$) formed in nitrogen oxide alkene systems (2-methylpropene, styrene and α-methylstyrene) have also been obtained.[41] The primary reaction step is again believed to be the formation of alkyl radicals, by the addition of $NO_2^{\bullet}$ to the methylene carbon of alkenes. The nitric oxide then scavenges an alkyl radical and the nitroso compound formed traps a second $R^{\bullet}$:

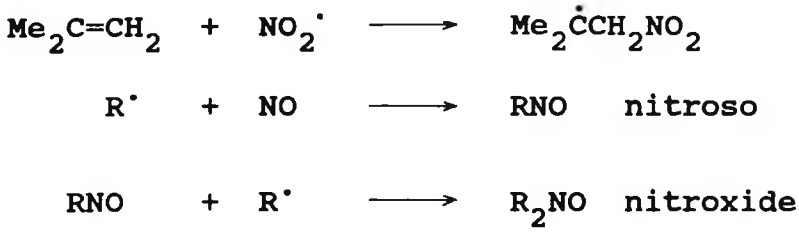

Scheme 1.8

As a comparison to earlier work,[39] Pryor et. al. have studied the rates of reaction of alkenes with nitrogen dioxide in solution.[42] At high concentrations of $NO_2^{\bullet}/N_2O_4$, a kinetic dependence that is first-order in N_2O_4 or second-order in $NO_2^{\bullet}$ was observed. As the concentration of $NO_2^{\bullet}/N_2O_4$ approached zero, the kinetic order in $NO_2^{\bullet}$ approached unity. The authors believe that these data indicate the presence of at least two reaction paths : one involving N_2O_4 in an addition mechanism and the other involving $NO_2^{\bullet}$. The reaction of the monomer was thought to proceed, at least in part, through an allylic hydrogen abstraction mechanism. The results of this study are discussed in greater detail in Section 2.4.2.

The nitration of 2-ethylbut-1-ene with ^{15}N-labelled nitrogen dioxide has been studied at high concentrations by ^{15}N n.m.r. spectroscopy,[43] to detect the presence or absence of a ^{15}N C.I.D.N.P. effect in the nitration products. The ^{15}N nuclear polarisation in the dinitro and nitro-nitrito product was consistent with the separate addition of two $NO_2^{\cdot}$ radicals to the alkene, in contrast to Pryor's kinetic results[42] above (see also Section 4.5).

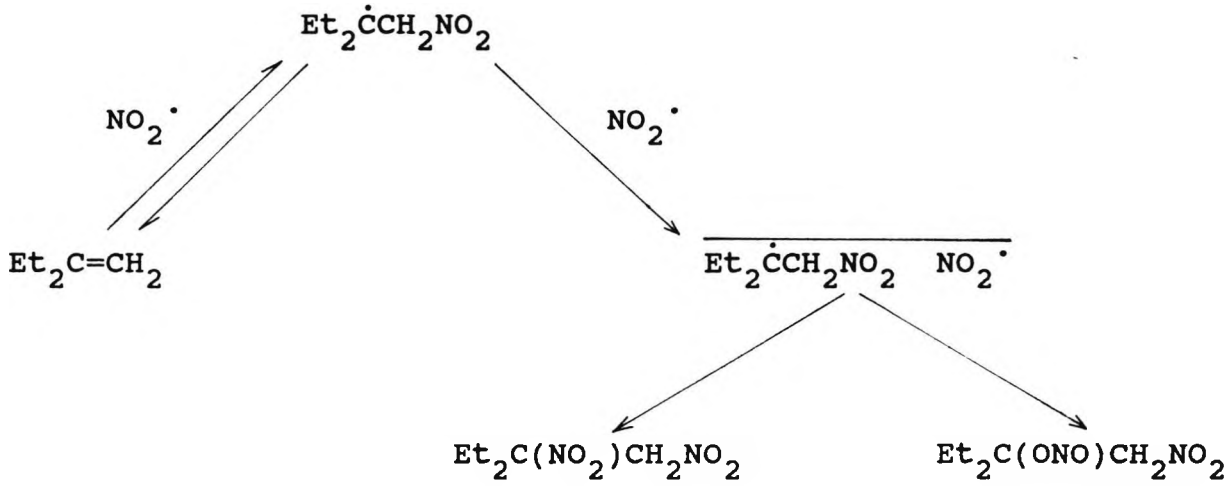

Scheme 1.9

Nitrogen dioxide reacts with phenylethenes to yield several products[44] (PhCHO, PhCOCN, $PhCO_2H$, $PhCH{=}CHNO_2$, $PhCOCH_2NO_2$, $PhCH(OH)CH_2NO_2$) that were also explained by radical addition of two NO_2 molecules to give the 2-nitro-1-phenylethylnitrite intermediate (2) (Scheme 1.10).

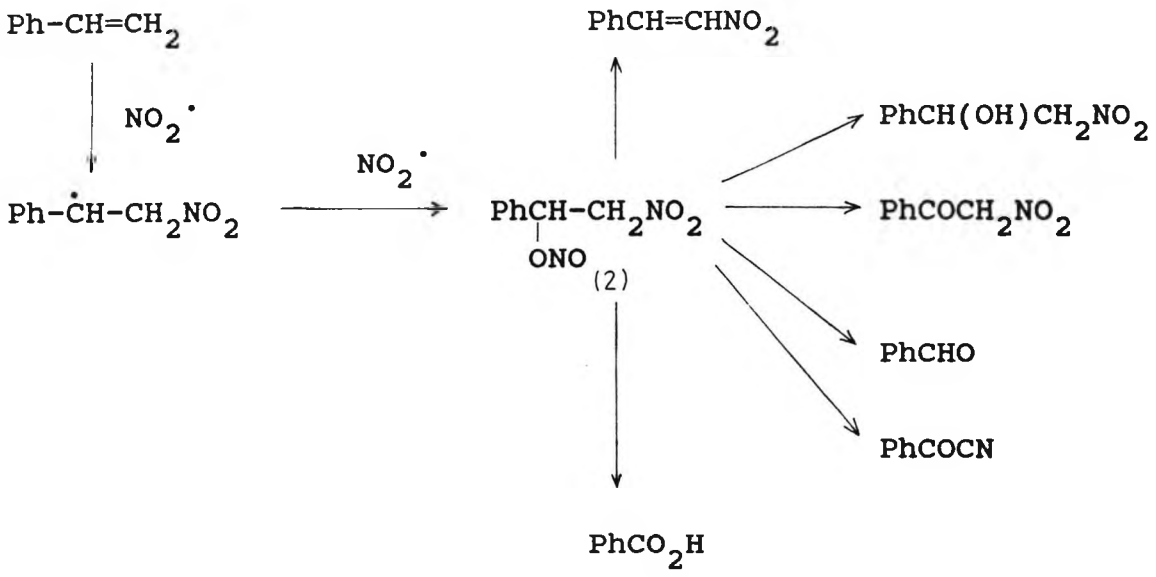

Scheme 1.10

Further evidence for the radical pathway came from the reactivities of a number of p-substituted styrenes towards $NO_2^{\cdot}$, relative to styrene itself. The resulting Hammett plot gave a low value of ρ (-0.91), which indicated that a carbocation intermediate was unlikely to be involved.

1.1.4 Nitration of aromatic and polycyclic aromatic compounds

The study of the nitration of aromatic compounds with nitrogen oxides dates relatively far back. Wieland[45] obtained poor yields of nitrobenzene , 1,3,5-trinitrobenzene and picric acid when he reacted nitrogen dioxide with benzene at 80°C in a sealed tube. Friedburg[46] investigated the reaction in carbon disulphide and recorded low yields of mono- and dinitrobenzenes and these results were later confirmed.[47] More recently, the nitration of benzene in liquid dinitrogen tetraoxide has been reported[48] to occur only when nitric oxide and oxygen are simultaneously bubbled through the solution at 0°C. Dinitrobenzenes were formed though nitrobenzene was not nitrated under similar conditions. The ratio of dinitrobenzenes was significantly different from that obtained by mixed acid nitration, thus prompting the postulation of a radical mechanism involving $NO_3^{\bullet}$ as a one-electron oxidant.

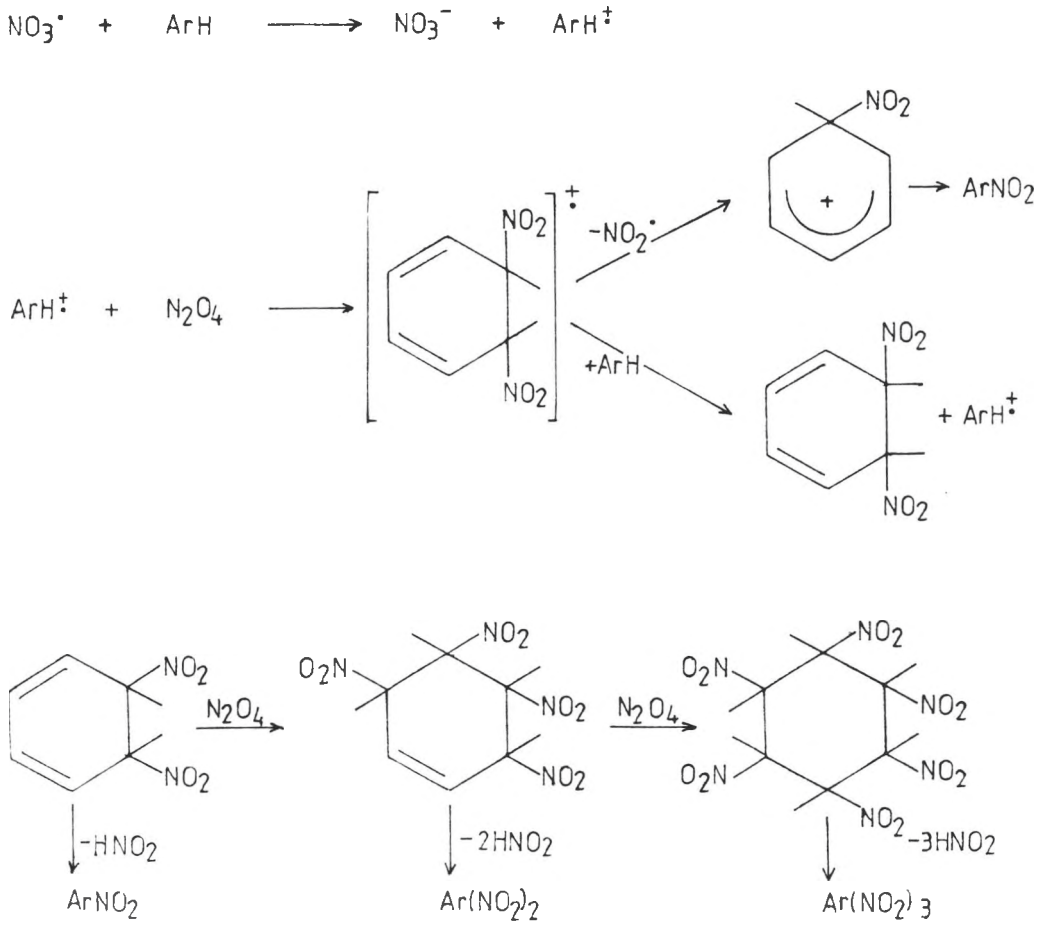

Scheme 1.11

In his extensive surveys of nitrations, Titov[35] postulates the formation of nitro products from aromatic compounds as follows:

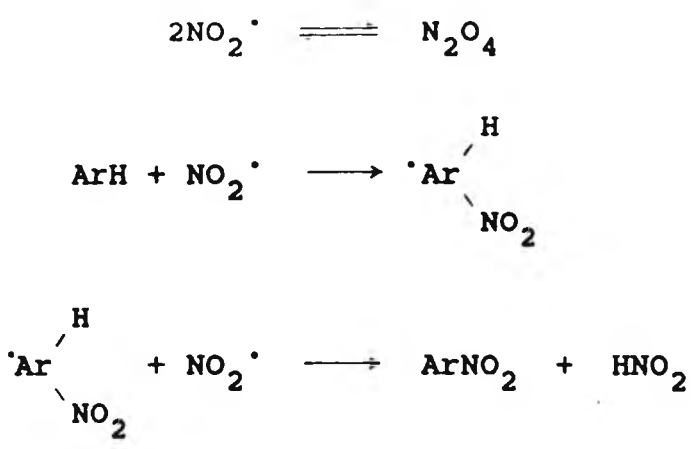

Scheme 1.12

A similar explanation for the formation of oxidation products was proposed,

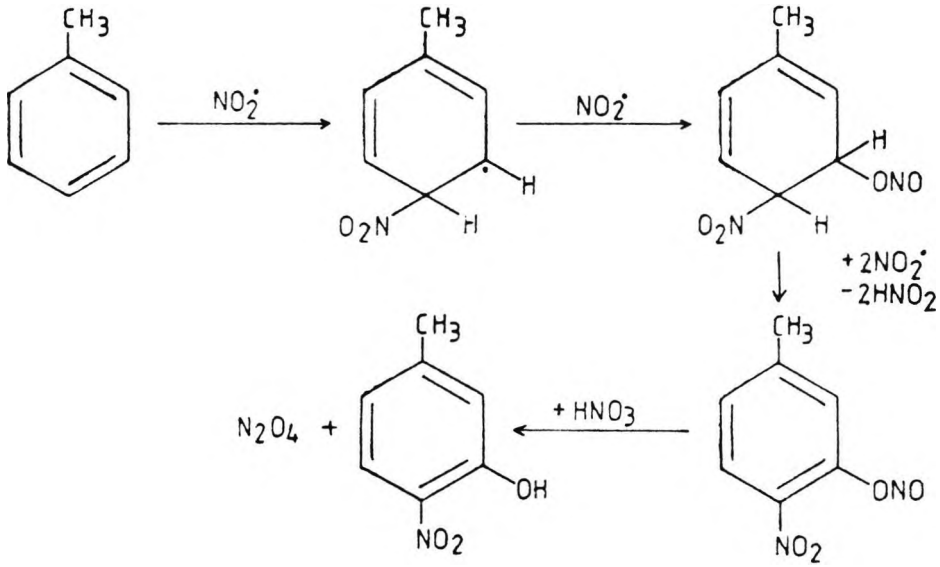

Scheme 1.13

Schaarschmidt and Smolla[49] reported the slow reaction of nitrogen dioxide with toluene at room temperature. 41-44% of nitrotoluenes were formed together with oxalic acid, benzoic acid, phenol and benzaldehyde. When this reaction was carried

out in carbon tetrachloride, a 45% conversion into nitrotoluenes was observed. Higher yields of nitroaromatics required the use of Friedel-Crafts catalysts.[50,51]

A study of the reaction of dinitrogen tetraoxide with a range of methyl substituted benzenes and anisole in nitromethane has been carried out.[52] From the data on competitive nitration experiments no clear cut decision was made on the electrophile in the reaction. For methyl, o/m/p-dimethyl, and 1,2,4-trimethylbenzene the electrophile appeared to be of comparable selectivity to the nitronium ion, whilst for the more reactive substrates such as 1,2,4,5-tetramethylbenzene, nitration via nitrosation was believed to assume increasing importance. Thus, no conclusion was reached concerning the reaction mechanism and clearly important product studies were not performed.

Nitration by nitrogen tetraoxide in carbon tetrachloride of a range of aromatic compounds demonstrated an anomalous juxtaposition of inter- and intramolecular selectivity in a low conversion reaction.[53] Toluene, for example, gave two distinct types of reaction. At low concentrations of dinitrogen tetraoxide (less than 0.2 mol dm^{-3}), the isomer distributions were characterised by a high percentage of m-nitrotoluene. When higher concentrations of dinitrogen tetraoxide were used, the isomer data showed initially a high percentage of m-nitrotoluene but as the reaction proceeded, the ratio began to resemble an isomer distribution expected for electrophilic attack. At even higher dinitrogen tetraoxide concentrations (ca. 1 mol dm^{-3}) the isomer distributions showed a low percentage of the m-nitro isomer and appeared to indicate the operation of an electrophilic mechanism. The rates of nitration from low to high concentrations of dinitrogen tetraoxide were found to be extremely low and reactions were characterised by low yields of nitrotoluenes. It was shown that these data were a result of nitration by some species in the reaction solution and not of the diversion of mononitrotoluenes to oxidation products. The other alkylbenzene substrates studied also appeared to give unusual isomeric proportions with low concentrations of dinitrogen tetraoxide. Ethylbenzene in particular yielded almost

exclusively the m-nitro isomer.

The intermolecular selectivities between aromatic substrates of dinitrogen tetraoxide in carbon tetrachloride were also of interest.[53] The toluene:benzene ratio for dinitrogen tetraoxide remained fairly constant over the range of concentrations where the change of selectivity between positions in toluene had already been observed. At low dinitrogen tetraoxide concentrations, the effective species associates a selectivity between benzene and toluene approaching that of the nitronium ion (1:17-30) with almost an absence of intramolecular selectivity. The values of relative reactivity of the alkylbenzenes studied compared to benzene are collected in Table 1.2.

Table 1.2: Relative reactivity to dinitrogen tetraoxide in carbon tetrachloride by competition.

substrate	rate
mesitylene	280
o-xylene	100
toluene	40
benzene	1
hexadeuteriobenzene	1
chlorobenzene	0.2
p-dichlorobenzene	0.02

The relative rates for mesitylene, o-xylene and toluene are those expected for an eletrophile of comparable selectivity to the nitronium ion, but for the halogenobenzenes the values obtained are those for an electrophile less selective than the nitronium ion.

Dinitrogen pentaoxide in carbon tetrachloride solution has been found to react with aromatic compounds (eg toluene) by two different mechanisms to yield the nitro substituted aromatic compounds.[54,55] At high nitrogen pentaoxide concentrations an autocatalytic reaction involves nitration by the nitronium ion. The other mechanism, favoured by low concentrations of dinitrogen pentaoxide in dry solvent, was originally believed to involve the N_2O_5 molecule as an electrophilic species but more recent work[55] has established that this process has the characteristics of a radical reaction (high proportion of m-nitro product from toluene) and appears to involve a similar nitrating species to that in operation in nitration by dinitrogen tetraoxide in carbon tetrachloride.[53]

Nitration of p-dimethoxybenzene by nitrogen tetraoxide in carbon tetrachloride[56] was held to proceed by slow nitrosation followed by rapid oxidation of the nitroso-intermediate by N_2O_4. In view of current ideas concerning nitrous acid catalysis, the evidence for this mechanism is not convincing.

Shorygin and Topchiev[57] achieved a quantitative yield of 1-nitronaphthalene from the reaction of nitrogen dioxide and naphthalene at 150°C. Early work on the nitration of anthracene by dinitrogen tetraoxide in glacial acetic acid,[48] benzene[47] and nitrobenzene[58] reported 9,10-anthraquinone as the sole product. This was followed by a study reporting an 80% yield of 9,10-dinitroanthracene when anthracene was allowed to react with a large excess of dinitrogen tetraoxide in chloroform at 0°C.[59] More recently it was shown that for nitration in dichloromethane, 9-nitroanthracene and 9,10-anthraquinone were formed with a high overall yield.[60] The important observation was that the ratio of 9-nitroanthracene to 9,10-anthraquinone changed from 1.64 to 0.35 when the reaction was carried out in a solution saturated with water; no indication was given of the water content of the original solution. Quinones were not detected on nitration of benzene, naphthalene or phenanthrene.[60] Tokiwa et al.[61] also reported no quinone from phenanthrene. The nitration of naphthalene by nitrogen dioxide in dichloromethane led to a 92% yield with a 1-nitro:2-nitro ratio of 11.6 at 25°C,[60] a ratio similar to that obtained by nitronium ion nitration. There are,

however, discrepancies between these data and the findings of Radner.[62] He concluded that while most of the polycyclic aromatic hydrocarbons (PAHs) studied were nitrated in high yields, three, namely naphthalene, triphenylene and fluoranthene gave lower yields and product ratios different from those expected for nitronium ion nitration. These three compounds required longer reaction times and/or acid catalysis in order to facilitate product formation. The results from this study are summarised in Table 1.3.

Table 1.3: Nitration of polycyclic aromatic hydrocarbons with dinitrogen tetraoxide

PAH	Catalytic amount of CH_3SO_3H added	Reaction time/h	Yield [a]/%	Isomer distribution [c]/%	
Perylene	NO	0.2	95[b]	3-nitro	99.2
				1-	0.8
Pyrene	NO	0.5	97[b]	1-	100
Anthracene	NO	1	>90[c,d]	9-	100
				6-	97
Chrysene	NO	24	>90[c]	other mononitro	3
Naphthalene	NO	48	59[c]	1-	96
				2-	4
Fluorene	NO	24	>90[c]	3-	1
	YES	2	92[b]	4-	9
Fluoranthene	NO	24	75[c]	3-	63
	YES	0.4	90[c]	8-	27
				other mononitro	10
Binaphthyl	NO	24	>90[c]	4-	100
	YES	1	89[b]		
Triphenylene	NO	120	50[c]	1-	22
	YES	2	92[b]	2-	78

[a] yield based on PAH. [b] Isolated yield. [c] Determined by GLC

[d] 5-7% of 9,10-anthraquinone was formed.

The mechanism of nitration of PAHs by dinitrogen tetraoxide in dichloromethane was investigated further by the same workers.[63] From studies on relative reactivities, isomer distributions, and the effect of acid, base and nitrosonium ion on the reaction, a mechanism involving initial attack of a novel electrophile, nitrosated dinitrogen tetraoxide, was proposed. The initially formed σ-complex was suggested to be transformed into the nitro σ-complex via a pathway involving radical pairs, thus explaining the observation by others of C.I.D.N.P. effects on the reaction path of nitrous acid catalysed nitration, a reaction proposed to follow the same reaction scheme.

Pryor and his co-workers[60] have also considered the nature of the initial step of the nitration of PAHs by nitrogen dioxide. They proposed two possible schemes for the reaction; one involving rate-determining σ-complex formation, the other rate-determining initial electron transfer. The existence of linear-free energy relationships was tested between rate data and molecular orbital parameters based on the two models. Since better correlation was obtained within the latter model (especially when the data for benzene was omitted) it was suggested that the more easily ionised polycyclic aromatic hydrocarbons underwent nitration by an electron-transfer mechanism:

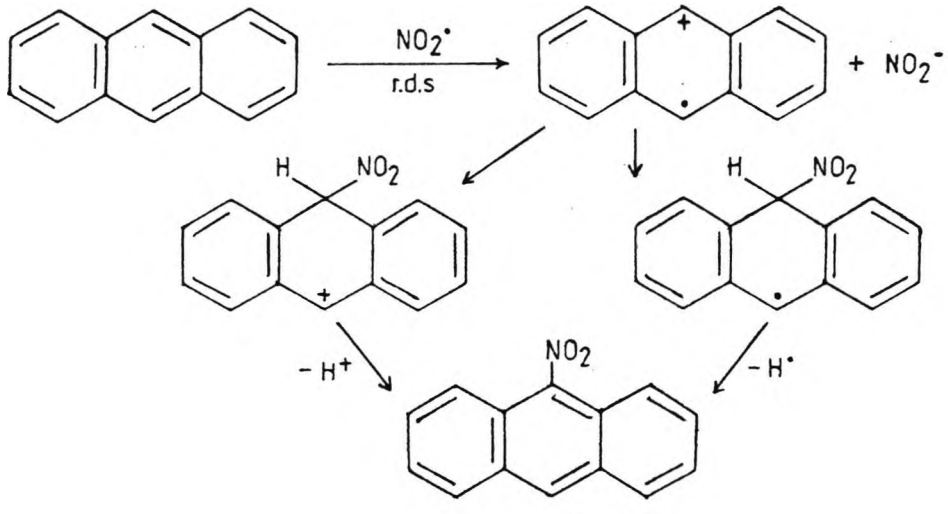

Scheme 1.14

It was also shown that this mechanism could account for the formation of anthraquinone from the reaction of the radical cation with water.

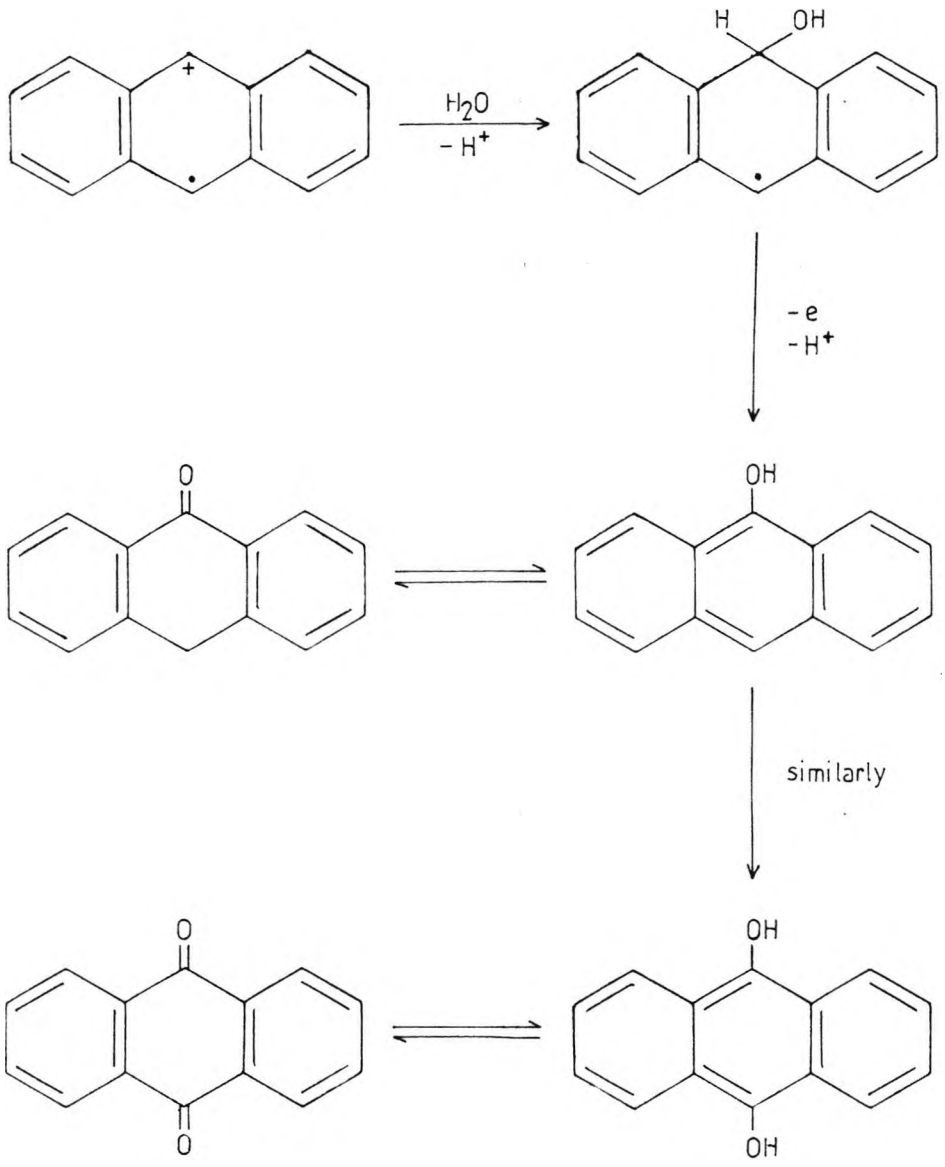

Scheme 1.15

Some water would always be present due to the formation of nitrous acid as a reaction product.

$$2HNO_2 \longrightarrow NO + NO_2 + H_2O \qquad (1.6)$$

but, as observed, added water would increase the yield of anthraquinone.

If this mechanism is to be accepted it must be assumed that since the polycyclic aromatic hydrocarbons studied react at different rates, the rate of electron transfer to nitrogen dioxide is not diffusion controlled. The authors state that it is not surprising that product distribution is similar to nitronium ion nitration since both processes (in their view) involve rate determining electron-transfer followed by collapse to give a σ-complex.

Schmitt et al.[64] also observed in gas-phase work that aromatic radical cations ($ArH^{+\bullet}$) readily react with nitrogen dioxide to give the σ-bonded $Ar\text{-}HNO_2^+$. The radical cations giving the σ-intermediate were those from benzene, methylbenzenes up to mesitylene and 1,2,4-trimethylbenzene, phenol and several fluorobenzenes up to 1,2,4-trifluorobenzene. The reaction of naphthalene to give the σ-bonded $C_{10}H_8\text{-}NO_2^+$ was found, however, to be surprisingly slow compared with other electron-rich systems.

The coupling reactions of a series of methylnaphthalene radical cation hexafluorophosphates with nitrogen dioxide have been studied in CH_2Cl_2 at low temperatures.[65] Yields of nitro derivatives were generally higher with the β-methyl than with the α-methyl substituted naphthalenes and the isomer distributions were different from those obtained in electrophilic aromatic nitration and nitrous acid catalysed nitration. $Pyrene^+$ hexafluorophosphate, however, did not yield nitropyrenes upon treatment with nitrogen dioxide. This confirmed the view that only radical cations of aromatics with E° values > 1.7 V could take part in successful coupling reactions with nitrogen dioxide.

A more recent investigation of the nitration of naphthalene with nitrogen dioxide in carbon tetrachloride[66] appears to conflict considerably with earlier work.[60] In this study, the reaction was postulated to occur via a free-radical mechanism, and was characterised by low 1-nitronaphthalene/ 2-nitronaphthalene ratios and the formation of unexpected dinitronaphthalene isomers, 1,3-dinitronaphthalene and 2,3-dinitronaphthalene, at low conversions (Scheme 1.14). The reaction of naphthalene (2M; 1.5ml) with nitrogen dioxide (2M; 2.4ml) for 24 h in CCl_4, for example, led to a 12% conversion with a 1-nitro:2-nitro ratio of 9.7 at 25°C (c.f. 92% yield in previous report).

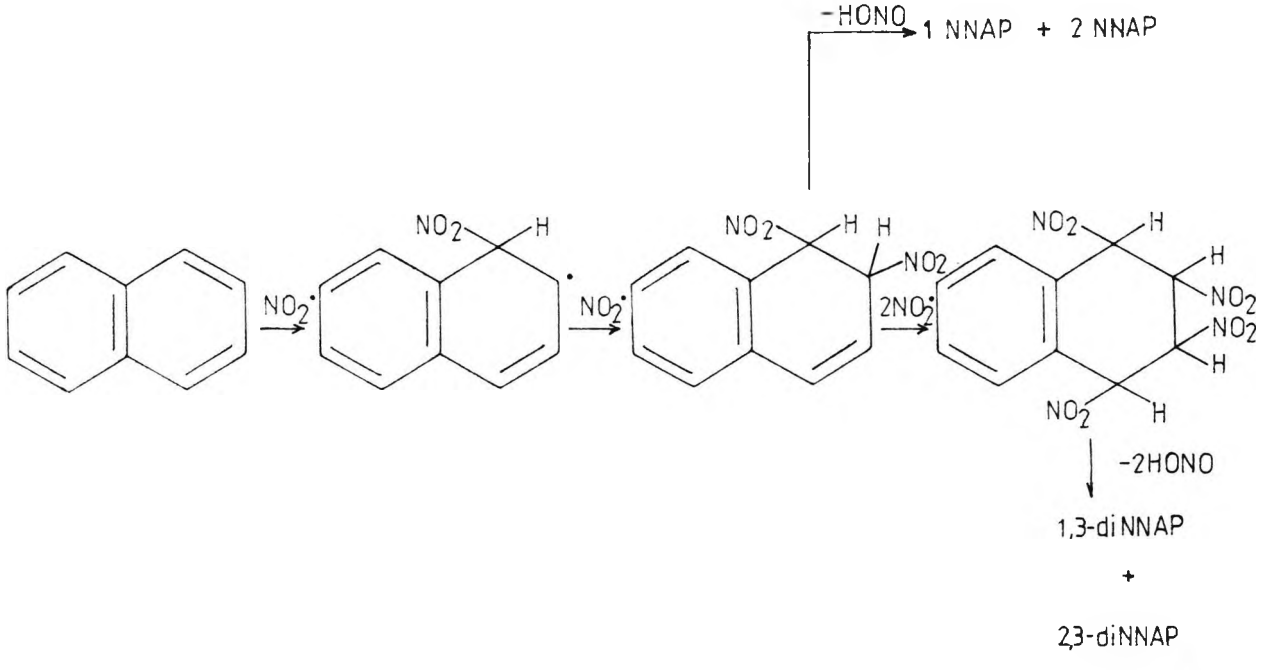

Scheme 1.16

The nitro substituent was found to have a small activating effect toward free-radical nitration in 2-nitronaphthalene while it had no noticeable effect in 1-nitronaphthalene, contrasting sharply with conventional electrophilic nitration where the nitro substituent has a very strong deactivating effect.

1.1.5 Nitration of paraffins

The many chemical conversions that take place with paraffin chain nitration have been summarised in a review by Titov.[35] According to general theory, the rate-determining step is believed to be the formation of a free alkyl radical:

$$R\text{-}H + NO_2^{\bullet} \longrightarrow R^{\bullet} + HNO_2 \qquad (1.7)$$

In 1940, based on this radical mechanism, a route for the formation of lower nitro-compounds by nitration at high temperature was proposed. Depending on the distribution of the unpaired electron $NO_2^{\bullet}$ throughout all nitrogen and oxygen atoms, Titov concluded that the reaction of $NO_2^{\bullet}$ with a free alkyl radical $R^{\bullet}$ not only gives rise to nitro compound (XI) but also to alkyl nitrite (XII).

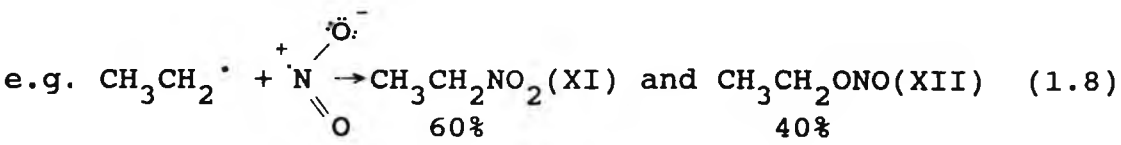

Between 300 - 500°C the R-ONO decomposes to produce a free ethoxy- and then methyl radical, which in turn reacts with $NO_2^{\bullet}$ to form nitromethane and methyl nitrite.

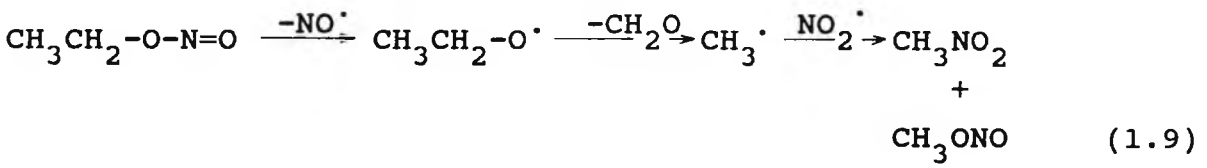

In the presence of oxygen $NO_2^{\bullet}$ initiates oxidation.

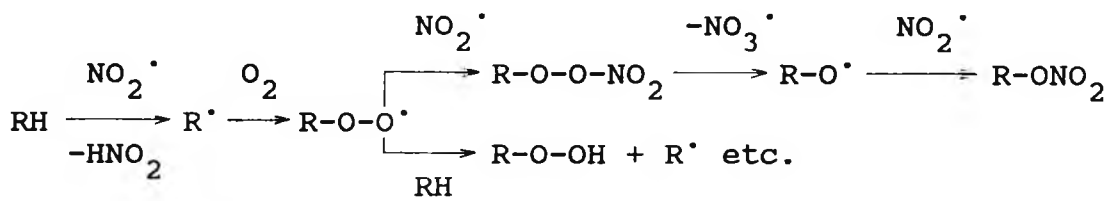

Scheme 1.17

But on saturation with O_2, the increased reaction rate of NO_2 with the paraffin chain is largely due to the formation of $NO_3^{\cdot}$ and $NO_2^{\cdot}$ during the conjugate oxidation of NO and $NO_2^{\cdot}$.

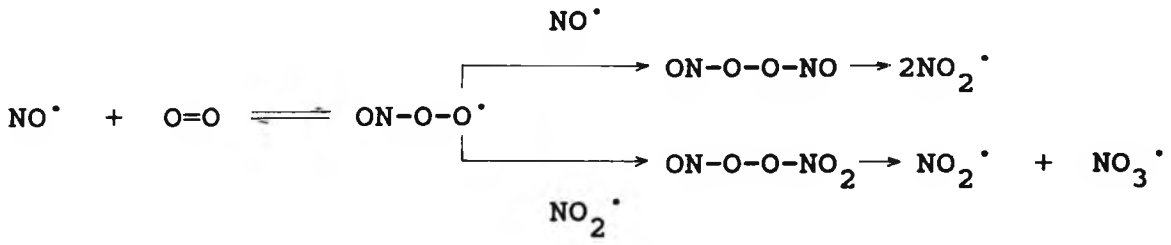

Scheme 1.18

The formation of alkenes during nitration of paraffins proceeds by β-hydrogen abstraction from free radicals by $NO_2^{\cdot}$.

$$\cdot CH_2\text{-}CH_2\text{-}H + NO_2^{\cdot} \xrightarrow{400\,^{\circ}C} CH_2{=}CH_2 + HNO_2 \qquad (1.10)$$

1.1.6 Nitration of phenol compounds

Frankland and Farmer[67] and Wieland[45] noted that nitrogen dioxide reacts much more readily with phenol than with aromatic hydrocarbons. The reaction gave o- and p-nitrophenols in good yields, but anisole did not react under similar conditions. The cresols have been reported to be polynitrated,[45,57,68] but the complete product distribution was not mentioned.

The mechanism of the reaction of nitrogen dioxide with mono- and polysubstituted phenols has been studied in great depth.[69] Nitration occurs at the ortho and para positions relative to the hydroxyl group.

Reactions were found to show excellent first-order behaviour in the phenols. The observed orders of the reactions in $[NO_2^{\bullet}]$ vary but can be explained by the following scheme:

$$ArOH + NO_2^{\bullet} \rightleftharpoons ArO^{\bullet} + HNO_2$$

$$ArO^{\bullet} + NO_2^{\bullet} \longrightarrow \text{products (via a dienone intermediate)}$$

Scheme 1.19

Major results of the study were explained by the mechanism shown in Fig. 1. For clarity, all substituents are not included. For the reactions of the phenols unsubstituted at the 2,6-positions, if the reaction was second-order in $NO_2^{\bullet}$, the proton-loss in step (3) was rate-limiting and the equilibria (1) and (2) were to the L.H.S. Where the 2,6-positions were blocked, and the reaction was second-order in $NO_2^{\bullet}$, a step subsequent to step (1) was rate-limiting (see discussion in Section 8.4).

Some of the reactions became first-order in $NO_2^{\bullet}$ at higher nitrogen dioxide concentrations. This was explained by step (1) becoming rate-limiting under these conditions. Where zeroth-order behaviour in $NO_2^{\bullet}$ was observed, the equilibrium (2) was to the R.H.S. and the 2,4-dienone was formed in bulk. The rate of the reaction was then limited by either step (3) where the 2,6-positions were vacant, or by step (4) in the case of the sterically hindered phenols (Section 8.4). For some less activated phenols, e.g. iodophenol, p-hydroxybenzonitrile, the order in $NO_2^{\bullet}$ was three. This phenomenon was explained on the basis of a third molecule of $NO_2^{\bullet}$ being involved in the rate-limiting rearrangement of the dienone (Step 4).

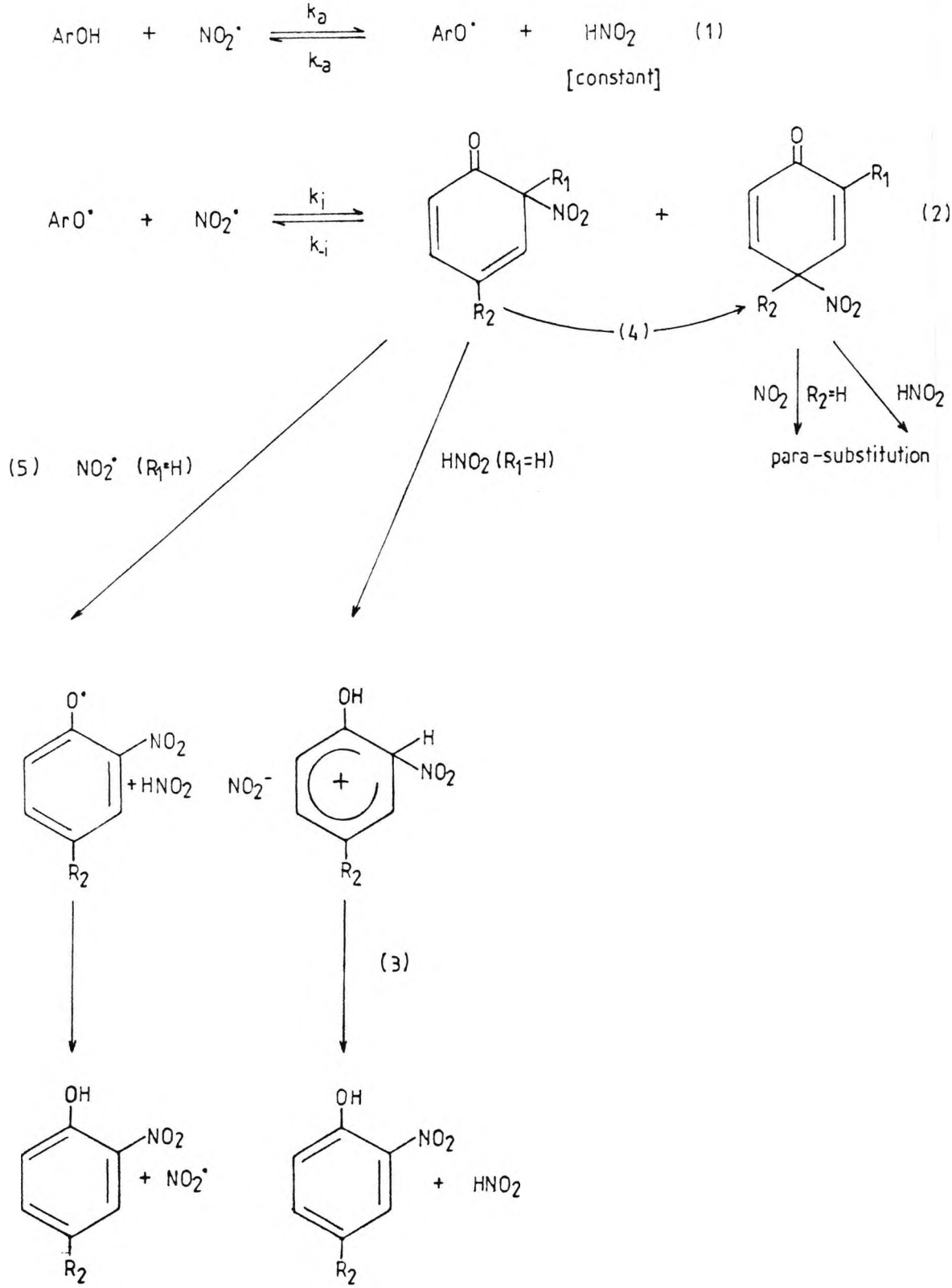
ArOH + NO2· ⇌ ArO· + HNO2 (1)
ka
k-a
[constant]
ArO· + NO2· ⇌ (2)
ki
k-i
R1
NO2
R2
(4)
NO2 R2=H
HNO2
para-substitution
(5) NO2· (R1=H)
HNO2 (R1=H)
O·
+HNO2
NO2-
OH
H
(3)
+ NO2·
+ HNO2

FIG. 1

1.2 Reactions of Nitrogen Dioxide with Fuel/Lubricant components

Nitrogen oxides, NO_x, play an important role in the degradation of lubricating oil in internal combustion engines. It is well established that unburned and incompletely burned fuel and lubricant oxidise, condense and polymerise in the crankcase producing varnish and sludge. Nitrogen dioxide can also react chemically with mineral oil components of a lubricant and hydrocarbon diluents, which originated from the fuel, and this contributes to the formation of engine deposits and to oil oxidation and thickening.[70,71,72] In particular, reaction with the additives present in the lubricant, e.g. antioxidants, dispersants and anti-wear compounds, causes a loss of functional performance and reduces the useful life of the lubricant. The trends towards leaner-burning engines, higher engine temperatures (resulting in higher nitrogen oxide levels) and longer life lubricants will exacerbate these problems. Thus, there is a continuing need to understand the details of reactions of nitrogen dioxide with fuel and lubricant constituents, to assist in alleviating these harmful effects.

1.2.1 Chemical Reactants and Reactions in an Engine

Nitrogen oxides, formed during combustion, come into contact and react with fuel and oil components in the piston/cylinder areas, and enter the crankcase environment as part of gases which leak past the piston rings. These blow-by gases travel through the engine and come into contact with the oil in different locations depending on the type of ventilation system. The composition of blow-by gases typically falls in the ranges shown in Table 1.4,[72-74] and gives an indication of the amount of NO_x that comes into contact with the lubricating oil.

COMBUSTION PRODUCTS	15-20%	
AIR AND FUEL	80-85%	
(O_2	16-17%)	
NO_X	8-500	ppm
$NO_2^{\cdot}$	0.3-155	ppm

Table 1.4 : BLOW-BY COMPOSITION

1.2.2 **Nitrogen Oxides**

An important component of blow-by is nitrogen oxide which is formed from the nitrogen and oxygen in the air. With excess of oxygen, nitrogen oxide is converted to the dioxide and the two gases coexist in a temperature dependent equilibrium, equation 1.11.

$$2NO + O_2 \rightleftharpoons 2NO_2^{\cdot} \qquad (1.11)$$

NO predominates at high temperatures while a shift towards $NO_2^{\cdot}$ occurs at lower temperatures. Thus the principal component in exhaust is NO due to the high temperatures and low oxygen levels. At the lower temperatures and higher oxygen contents found in the crankcase, the fraction of NO_x from blow-by which is $NO_2^{\cdot}$ increases.

Since nitrogen dioxide is a very reactive odd-electron molecule, capable of a wide variety of reactions, it can greatly affect oxidation reactions in the blow-by and the crankcase vapour space.

1.2.3 Fuel Hydrocarbons

In the precombustion reactions, the fuel hydrocarbon molecules lose hydrogen atoms. The hydrocarbon radicals formed undergo thermal decomposition by carbon-carbon cleavage and hydrogen stripping in the presence of oxygen to yield relatively stable alkenes.

Further reactions with oxygen form peroxides which decompose to yield aldehydes, ketones and smaller alkenes.[75-77] Thus, the alkenes entering the crankcase as a part of the blow-by have been formed in incomplete combustion of fuel or may be present as components of the fuel. Generally, emissions and blow-by contain low molecular weight alkenes and acetylene, which form by carbon-carbon cleavages in alkenes and alkyl groups of alkylaromatics.[75,78]

1.2.4 Oxidation of Fuel and Lubricant Hydrocarbons

In the oxidation of hydrocarbons, the initial product is a hydroperoxide. Saturated hydrocarbons are generally much more resistant to autoxidation than alkenes, but the alkyl side chains on aromatics are readily attacked.[79]

In the presence of oxygen, $NO_2^{\cdot}$ initiates oxidation of hydrocarbons.[80] The vapour phase nitration gives both nitrated and oxidised products.[81] Secondary reactions convert hydroperoxides to alcohols and carbonyl compounds[80] which are assumed to condense, yielding polymeric engine deposits of high oxygen content.

1.2.5 Reactions of Alkenes with Nitrogen Oxides

Nitration and oxidation of alkenes take place in the gas phase in the combustion chamber, around the piston rings and in the vapour space of the crankcase.[81] The initial nitration products are unstable and undergo further reactions. Thus, vapour phase reactions of ethene and 2-methylpropene with nitrogen dioxide at 150°C, reportedly produce heavy viscous

oils.[28]

When alkenes and nitrogen oxides are picked up by the lubricant mist and the film on the cylinder walls, they may undergo liquid phase reactions which have been reported to yield compounds of the type R-CHX-CH_2-NO_2 (where X= -OH/NO_2 or -ONO_2).[82] These components are known to be the precursors primarily responsible for crankcase deposition.[83] The nitrated alkenes readily undergo elimination reactions to give nitro-alkenes which polymerise. Nitro groups leave with the formation of carbonyl groups by the Nef type reactions. Ring forming reactions can then occur.

1.2.6 Fuel as a source of deposits

The fuel is, generally, the major source of deposits in the moderate temperature range of engine operation.[83] Several fuels of widely different hydrocarbon compositions have been compared with respect to their effect and contribution to deposit formation.[84] The alkene content of the fuel was found to have the greatest effect on varnish-forming tendencies in the lubricant (see above). Fuels with higher alkylaromatics, which are known to yield alkenes by fragmentation of the alkyl groups in incomplete combustion, were also recognised as significant contributors to varnish formation.

1.2.7 Lubricant as a Material Source and Reaction Medium in Deposit Formation[84]

The crankcase lubricant, a mineral base oil or polyalphaolefin, alkylbenzene or ester synthetic oil, is oxidised, nitrated and burned during operation of the engine. The deposit precursors formed are of similar type to those resulting from the fuel.

When an oil is oxidised and nitrated to a low degree without molecular fragmentation, it does not contribute directly to deposits. In the process, however, it has become a much more reactive medium and may promote deposit formation by

interactions with free radical intermediates from the engine blow-by. Thus, deposit formation is a function not only of fuel and lubricant combustion and degradation, but also of the lubricant's suitability as a medium for free radical type oxidations and condensations. The effectiveness of a lubricant as a dispersant or solvent for the blow-by and other oxidised and nitrated materials will also influence deposit formation.

The effects of nitrogen dioxide on oxidation of hydrocarbons (hexadecane) in the presence and absence of a radical trapping antioxidant (2,6-di-tert-butyl-4-methylphenol) have also been investigated.[74] The results of this study suggest that nitrogen dioxide reacts preferentially with antioxidant. This reaction accelerates antioxidant consumption and therefore shortens the useful life of the engine oil.

1.3 The present study

The present work is concerned with a detailed kinetic and mechanistic study of the reactions of nitrogen dioxide with a number of organic compounds, which model the more reactive hydrocarbon components in fuel and lubricant. These include aromatic/alkene, aromatic and diaromatic compounds. The main objectives were to assess the reactivity of these compounds, determine the main products of reaction and assess their relevance to sludge/varnish formation. The following variables were included into the project in order to simulate engine conditions as closely as possible:

- temperature - rocker cover/crankcase temperatures were considered to be most relevant, i.e. ambient to 150°C;

- nitrogen dioxide concentration - this is important in determining the mechanism and products of reaction;

- oxygen - again this is important in determining the mechanism of reaction;

- medium - reaction in an alkane solvent was considered to be of most interest;

- water - this is present in the crankcase/rocker cover environment and collects in two ways.[85] Whilst most of the water produced during combustion is expelled through the exhaust system, some of it condenses on the cold engine parts. It then works its way past the piston rings and drops into the crankcase, together with moisture in the air drawn through the crankcase by the ventilating system.

From an academic point of view there is an interest in the relative reactivities of these compounds and the mechanisms of reactions with nitrogen dioxide.

Chapters 2 and 3 of this work deal with the kinetic and product studies of the reactions of nitrogen dioxide with styrene, allylbenzene, 4-phenylbut-1-ene and 1-dodecene. The last three compounds are known to be present in the fuel diluent and mineral oil of a lubricant, and are believed to be relatively reactive.

The reactions of naphthalene and 2-methylnaphthalene, the major diaromatics present in the mineral oil of a lubricant, with nitrogen dioxide are reported in Chapter 6.

1-methylbutylbenzene was chosen as a model for the alkylaromatics present in fuel and lubricant, and is of interest because of the presence of a tertiary H atom. The results of the study of the nitration of this compound are presented in Chapter 7.

Bis(4-hydroxy-3,5-di-t-butylphenyl)methane (AN2) and 2,2-bis(4-hydroxy-3,5-di-t-butylphenyl)propane (IONOX 400) were also selected as model compounds since they are present as additives in the lubricant and extend the previous work on monomolecular phenols,[69] and are particularly reactive towards nitrogen dioxide under engine conditions (i.e. low nitrogen dioxide concentrations and temperatures greater than 100°C).

The rates and products of the reactions of these compounds with nitrogen dioxide have been interpreted in terms of previously established mechanisms and are discussed in Chapter 8.

C H A P T E R 2

KINETIC STUDIES OF THE REACTIONS OF STYRENE, ALLYLBENZENE, 4-PHENYLBUT-1-ENE AND 1-DODECENE WITH NITROGEN DIOXIDE

2. Kinetic studies of the reactions of styrene, allylbenzene, 4-phenylbut-1-ene and 1-dodecene with nitrogen dioxide

2.1 Introduction

Over the years the reaction of nitrogen dioxide with alkenes has received considerable interest from both a mechanistic viewpoint and as a route to the formation of various environmental toxicants.[86-90] A comparison of Pryor's earlier work[39] to the gas-phase studies[86-90] or to studies in solution[30,35-37,92] reveals some interesting discrepancies. Most notably, while Pryor has reported the formation of two different types of products, addition products and allylic substitution products, other authors have observed only addition products. Furthermore, Pryor found that varying the concentration of nitrogen dioxide changes the addition/substitution ratio; as the nitrogen dioxide concentration is decreased, the relative amounts of substitution products increase. These observations were made first with cyclohexene[39] and were later supported using methyl oleate as the substrate.[91]

To explain the products cited above,[39] it was proposed that the reaction of nitrogen dioxide with alkenes occurs by two mechanisms, each of which might involve $NO_2^{\bullet}$, N_2O_4 or both. These pathways are summarised in Schemes 2.1 and 2.2.[39] Scheme 2.1 represents the radical addition mechanism proposed by other authors.[30,35-37,92] In the gas-phase, particularly at the low nitrogen dioxide concentrations used experimentally in the gas-phase studies,[86-90] the $NO_2^{\bullet}/N_2O_4$ equilibrium favours the monomer. With the exception of some early work,[93,94] the gas-phase reactions of nitrogen dioxide with alkenes are first order in $NO_2^{\bullet}$.[86-90] The anomalous reports are for the reaction of nitrogen dioxide with ethene and propene at elevated temperatures with little or no dioxygen present,[93,94] reactions that were reported to be 1.8 order in $NO_2^{\bullet}$ and 1.2 order in alkene. All the other gas-phase work was done in the presence of dioxygen, and under these

conditions, equation 4 is more important than equation 3 and dioxygen rather than $NO_2^{\bullet}$ traps the β-nitroalkyl intermediate 1. Therefore, the stoichiometry is near 1:1 for $NO_2^{\bullet}$ and the alkene and the kinetics can be expected to approach first-order in $NO_2^{\bullet}$.[89,90]

In solution, particularly at high nitrogen dioxide concentrations, the $NO_2^{\bullet}/N_2O_4$ equilibrium constant favours the dimer, so equation 2, involving N_2O_4, might be the major pathway for this reaction; this reaction would be second-order in $NO_2^{\bullet}$.If nitrogen dioxide is present in concentrations much higher than dioxygen is, then equation 3 will predominate over eq 4, and the intermediate 1 will be trapped by $NO_2^{\bullet}$. The products will be dinitro compounds and nitro-nitrites, and the stoichiometry would be expected to be 2:1 $NO_2^{\bullet}$ to alkene as is observed experimentally.[30,35-37,39,92]

The second pathway, represented in Scheme 2.2,[39] involves hydrogen atom abstraction, a process that ultimately leads to the formation of allylic substitution products. While in principle the first step in this sequence could involve $NO_2^{\bullet}$ or N_2O_4, allylic substitution products are observed only at low nitrogen dioxide concentrations and, therefore, probably involve $NO_2^{\bullet}$. The hydrogen abstraction pathway is expected to be first-order in $NO_2^{\bullet}$, since the first step (equation 5) should be rate-limiting. The stoichiometry should be 2:1 in the absence of oxygen or in the presence of much more nitrogen dioxide than dioxygen, since $NO_2^{\bullet}$ would be the trapping species.

As a comparison to the gas-phase work Pryor et. al. have also studied the rates of reaction of alkenes with nitrogen dioxide in solution.[42] The results of this study are discussed in Section 2.4.2.

Scheme 2.1

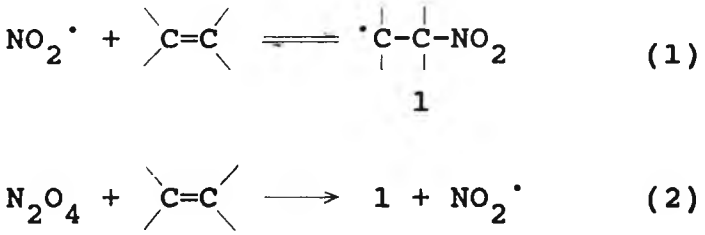

Scheme 2.2

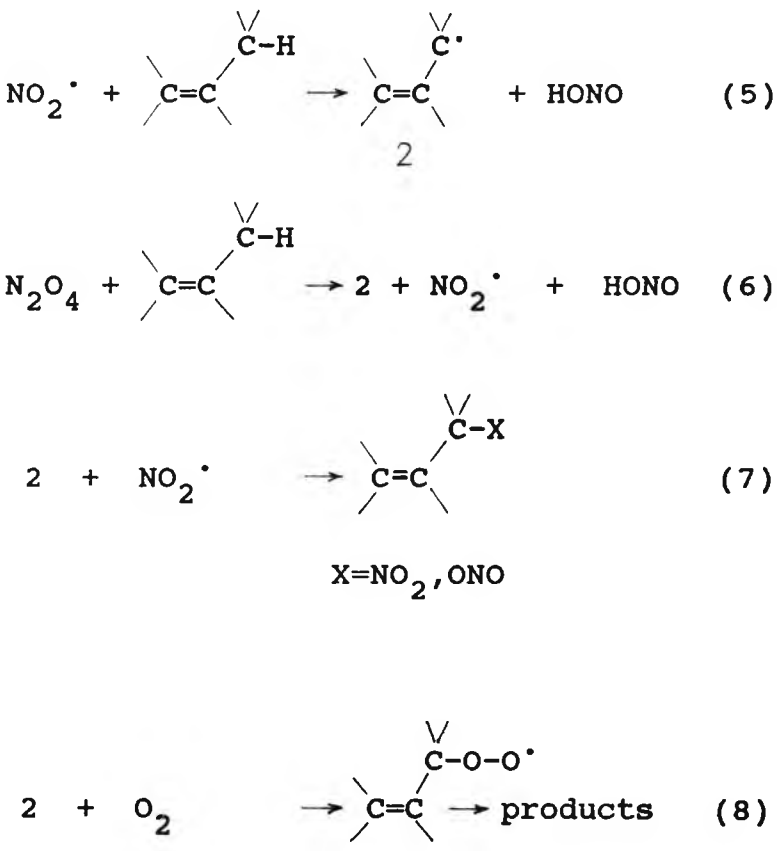

In this chapter we examine the reactivity of nitrogen dioxide towards alkenes as a function of the nitrogen dioxide concentration in order to investigate the above findings and elucidate the mechanism of formation of deposit precursors in internal combustion engines.

Kinetics of the initial reactions were performed in cyclohexane at 30°C. All the reactions were found to be first order in the alkene when the nitrogen dioxide was in a large excess. Conditions of temperature, presence of water, oxygen and light were also varied to see how these parameters affect the kinetics of the reaction of allylbenzene with nitrogen dioxide. The results from this work are discussed in the context of previous studies.

2.2 Experimental

Kinetic studies were performed in cyclohexane under conditions of a large excess of nitrogen dioxide. Absolute rates of reaction were determined by g.l.c.

2.2.1 Variation of nitrogen dioxide concentration

Solutions of nitrogen dioxide in cyclohexane (100 ml) were thermostatted in a waterbath at 30°C for 15 mins before the alkene was added. The initial concentration of $NO_2^{\bullet}$ was measured at 25.4 ± 0.1°C in a Perkin Elmer Lambda-5 spectrophotometer using the gas-phase extinction coefficient of 150 $dm^3 mol^{-1} cm^{-1}$ at 430 nm (this value was assumed to be invariant with temperature). 1 cm quartz cells fitted with silicone rubber septa, held in place with Quickfit screw-caps[95], were used for these measurements. The total stoichiometric concentration of N_2O_4 was then calculated using equation 2.1.

$$[N_2O_4]_t = \frac{[NO_2^{\bullet}]^2}{K_d} + \tfrac{1}{2}[NO_2^{\bullet}] \qquad (2.1)$$

At 25.4°C, $K_d = 1.83 \times 10^{-4}$ mol dm^{-3}

The equilibrium constant K_d at 30°C, $[NO_2^{\bullet}]^2/[N_2O_4] = 2.644 \times 10^{-4}$ mol dm^{-3} was calculated from the thermochemical data of Redmond and Wayland.[16] The values of $[NO_2^{\bullet}]$ and $[N_2O_4]$ at the temperature of the experiment were obtained by solving the quadratic equation 2.1 for $[NO_2^{\bullet}]$ and substituting this value into equation 2.2, since $[N_2O_4]_t$ is known.

$$[N_2O_4] = [N_2O_4]_t - \tfrac{1}{2}[NO_2^{\bullet}] \qquad (2.2)$$

A known quantity of alkene was added to the nitrating solution by microsyringe and the mixture was thoroughly shaken. The reaction was followed by removal of samples (1 ml) at suitable times. These samples were treated with water to prevent further reaction, and the organic layer was

analysed quantitatively by g.l.c. on a Pye 104 gas chromatograph fitted with a flame ionisation detector. Analysis was possible with a 2 metre x 31.75 mm silicone 5% SE30 column at 80°C and a nitrogen flow rate of 20 ml min^{-1}; for the 1-dodecene product solutions the temperature of the column and flow rate were increased to 100°C and 25 ml min^{-1} respectively.

The concentration of alkene in each sample was determined by a method based on relative response factors. The relative response factor of alkene was measured with respect to nitrobenzene, an internal standard, which was added just prior to analysis.

2.2.2 Reaction of allylbenzene with nitrogen dioxide

2.2.2.1 Variation of temperature

Kinetic measurements of the reaction of nitrogen dioxide with allylbenzene were made at 30, 40 and 50°C. At temperatures above 50°C the reaction was too fast to be monitored by the sampling technique used.

2.2.2.2 Variation of $[H_2O]$

The cyclohexane solvent used in all the kinetic experiments was dried over 4A molecular sieves before use. The maximum solubility of water in this solvent is quoted in the literature as being 3.45 x 10^{-2} mol dm^{-3}.[96] Attempts were made to measure accurately the moisture content of cyclohexane by near I.R. spectrophotometry,[97] but since the absorption bands due to cyclohexane mask the H_2O absorption band at 1900 nm, this approach was abandoned.

For experiments in cyclohexane saturated with water, a sample of cyclohexane (150 cm^3) was shaken with water (15 cm^3) for 2 hours and kept undisturbed in a separating funnel overnight. 100 cm^3 of organic layer was removed and a solution of nitrogen dioxide was made up. This was thermostatted in a waterbath at 30°C for 15 min before

addition of allylbenzene. The change in concentration of allylbenzene with time was then monitored by g.l.c.

In order to study the effect of an excess of water on the course of a reaction, 1 ml of water was added to the solvent (100 ml) before addition of nitrogen dioxide and allylbenzene. The reaction solution was mechanically agitated by placing the flask on a shaker, and samples were removed at periodic intervals as before.

2.2.2.3 Measurement of the rate of reaction under a N_2 atmosphere

A vacuum line was used for this experiment. The rotary pump was switched on. Cyclohexane (50 ml) was placed in a round bottomed flask and was degassed by a series of 7 freeze-thaw cycles. Nitrogen dioxide, in a boiling tube was also degassed and transferred to the reaction flask by immersing the latter in liquid nitrogen. The flask was then removed from the vacuum system and filled with nitrogen via a syringe attached directly to a N_2 gas line.

The solution of nitrogen dioxide in cyclohexane was thermostatted in a waterbath at 30°C for 15 min prior to addition of allylbenzene. All syringes were flushed with nitrogen before use. Samples were removed at periodic intervals by syringe and injected into a volume of water (2 ml) to quench the reaction.

2.2.2.4 Influence of light

The flask used in this experiment was coated with black paint and wrapped in aluminium foil, in order to exclude all light from the reaction. A solution of nitrogen dioxide was made up, and thermostatted in a waterbath at 30°C before addition of allylbenzene. Kinetic measurements were carried out using the usual sampling technique.

2.3 Results

2.3.1 The reaction of styrene with nitrogen dioxide

The rate of reaction of styrene (9.69×10^{-3} mol dm^{-3}) with nitrogen dioxide (0.11 mol dm^{-3}) was too high to be monitored by g.l.c.; product formation was essentially complete within 2 min (Table 2.1). Hence, very little kinetic information could be obtained for this reaction.

t/s	height of 2-nitro-1-phenylethanol g.l.c. peak (mm)
111	30.8
950	29.3

Table 2.1

2.3.2 The reaction of allylbenzene with nitrogen dioxide

2.3.2.1 Variation of $[N_2O_4]_t$

The initial absorbance values measured for each nitrogen dioxide solution are shown in Table 2.2, together with the calculated values of $[NO_2^{\cdot}]$, $[N_2O_4]$ and $[N_2O_4]_t$. Reactions were performed with nitrogen dioxide in an excess, with $[N_2O_4]_t$ in the range 0.05 - 0.35 mol dm^{-3}, and with allylbenzene in the range 4×10^{-3} - 1×10^{-2} mol dm^{-3}. The results from a typical run are given below:

$$[PhCH_2CHCH_2]_o = 1.1 \times 10^{-2} \text{ mol dm}^{-3}$$
$$[N_2O_4]_{t,o} = 0.23 \text{ mol dm}^{-3}$$

The change in concentration of allylbenzene was monitored over three half lives (Table 2.3). The rate of nitration was shown to be first-order in allylbenzene by a linear plot of $\log_{10}$[allylbenzene] against time (Fig. 2.1). From the slope of this graph, the observed first-order rate coefficient, $k_{obs} = 4.17 \times 10^{-3} s^{-1}$. The variation of k_{obs} with $[NO_2^{\cdot}]$ and $[N_2O_4]$ for the reaction is shown in Table 2.4, and a plot of k_{obs} against $[NO_2^{\cdot}]$ is shown in Fig. 2.2.

2.3.2.2 Variation of temperature

Values of rate coefficient, k_{obs}, at various temperatures (30°C - 50°C) are given in Table 2.5. The Arrhenius plot of ln k_{obs} against reciprocal temperature, illustrated in Fig. 2.3, affords the values of the activation parameters for the reaction.

$$E_a = 66.4 \text{ kJ mol}^{-1}$$
$$A = 65.0 \times 10^7 \text{ dm}^3 \text{ mol}^{-1} s^{-1}$$

2.3.2.3 Variation of $[H_2O]$

The reaction of allylbenzene with nitrogen dioxide in cyclohexane saturated with water, was investigated over the $[N_2O_4]_t$ range 0.09 - 0.46 mol dm^{-3}. Under these conditions, good first order kinetic plots were observed over three half lives, demonstrating that the reaction is first order in allylbenzene (see Table 2.6 and Fig. 2.4). The values of k_{obs} obtained are shown in Table 2.7 and Fig. 2.18.

The first order plot of $\log_{10}$[allylbenzene] against time for the reaction carried out in the presence of an excess of water ([allylbenzene] = 9.36 x 10^{-3} mol dm^{-3}, $[N_2O_4]_{t,o}$ = 0.08 mol dm^{-3}) is shown in Fig. 2.5. From the slope of the graph, $k_{obs} = 1.75 \times 10^{-3} s^{-1}$.

2.3.2.4 Influence of oxygen on the reaction of allylbenzene with nitrogen dioxide

Fig. 2.6 shows the first order plot of $\log_{10}$[allylbenzene] against time for the reaction carried out in the absence of oxygen ([allylbenzene] = 1.21 x 10^{-2}mol dm^{-3}, $[N_2O_4]_{t,o}$ = 0.19 mol dm^{-3}, $[O_2]_{max.} \sim 1.2 \times 10^{-3}$mol dm^{-3} i.e. [allylbenzene] >> $[O_2]_{max.}$) From the slope of the graph, $k_{obs} = 3.98 \times 10^{-3} s^{-1}$.

2.3.2.5 Influence of light on the reaction of allylbenzene with nitrogen dioxide

The first order plot of $\log_{10}$[allylbenzene] against time for the reaction carried out in the absence of light ([allylbenzene) = 9.95 x 10^{-3} mol dm^{-3}, $[N_2O_4]_{t,o}$ = 0.10 mol dm^{-3}) is shown in Fig. 2.7. From this graph, the rate coefficient $k_{obs} = 2.31 \times 10^{-3} s^{-1}$.

2.3.3 The reaction of 4-phenylbut-1-ene with nitrogen dioxide

The reaction of 4-phenylbut-1-ene ($\sim$0.01 mol dm^{-3}) with nitrogen dioxide was studied over the $[N_2O_4]_t$ concentration range (0.08 - 0.23 mol dm^{-3}). The results from a typical run are given below:

$$[PhCH_2CH_2CH{=}CH_2]_o = 1.03 \times 10^{-2} \text{ mol } dm^{-3}$$
$$[N_2O_4]_{t,o} = 0.20 \text{ mol } dm^{-3}$$

The concentration of 4-phenylbut-1-ene was monitored over three half-lives (Table 2.8) and the plot of $\log_{10}$[4-phenylbut-1-ene] against time is a straight line (Fig. 2.8), demonstrating that the reaction is first-order in the alkene. From the slope of this graph, the observed first-order rate coefficient, $k_{obs} = 5.66 \times 10^{-3} s^{-1}$. The variation of k_{obs} with $[NO_2^{\bullet}]$ and $[N_2O_4]$ for the reaction is shown in Table 2.9, and a plot of k_{obs} against $[NO_2^{\bullet}]$ is shown in Fig. 2.9.

2.3.4 The reaction of 1-dodecene with nitrogen dioxide

The concentration of alkene was $\sim$ 0.01 mol dm^{-3} and $[N_2O_4]_t$ was varied over the range 0.06 - 0.24 mol dm^{-3}. The results from a typical run are given below:

$$[CH_3(CH_2)_9CH{=}CH_2]_o = 9.81 \times 10^{-3} \text{ mol } dm^{-3}$$
$$[N_2O_4]_{t,o} = 0.11 \text{ mol } dm^{-3}$$

A good first-order kinetic plot was observed over three half-lives (Table 2.10 and Fig. 2.10), demonstrating that the reaction is first-order in 1-dodecene. From the slope of this graph, the observed first-order rate coefficient, $k_{obs} = 3.99 \times 10^{-3} s^{-1}$. The variation of k_{obs} with $[NO_2^{\bullet}]$ and $[N_2O_4]$ for the reaction is shown in Table 2.11, and a plot of k_{obs} against $[NO_2^{\bullet}]$ is shown in Fig. 2.11.

Table 2.2: Calculation of $[NO_2^{\cdot}]$, $[N_2O_4]$ and $[N_2O_4]_t$ values from absorbance readings for the reaction of allylbenzene with nitrogen dioxide in cyclohexane at 30°C

A*	$[NO_2^{\cdot}]$/mol dm^{-3}	$[N_2O_4]$/mol dm^{-3}	$[N_2O_4]_t$/mol dm^{-3}
0.489	3.66×10^{-3}	0.051	0.052
0.641	4.88×10^{-3}	0.090	0.092
0.788	6.06×10^{-3}	0.139	0.142
0.848	6.54×10^{-3}	0.162	0.165
0.991	7.68×10^{-3}	0.223	0.227
1.053	8.18×10^{-3}	0.253	0.257
1.141	8.88×10^{-3}	0.298	0.303
1.222	9.53×10^{-3}	0.344	0.348

* $A = A_{NO_2} + A_s$

where A_{NO_2} = absorbance due to $NO_2^{\cdot}$

$A_s = 0.031$ = absorbance due to solvent, cyclohexane, at 430nm

Table 2.3: Change in concentration with time during the reaction of allylbenzene with nitrogen dioxide in cyclohexane at 30°C

t/s	$10^3[PhCH_2CH=CH_2]$	$\log_{10}[PhCH_2CH=CH_2]$
81	9.90	-2.00
138	8.05	-2.09
208	5.90	-2.23
288	4.10	-2.39
370	2.74	-2.56
497	1.66	-2.78
670	0.90	-3.05

$[PhCH_2CH=CH_2]_o = 1.1 \times 10^{-2}$ mol dm^{-3}, $[N_2O_4]_t = 0.23$ mol dm^{-3}

$k_{obs} = 4.17 \times 10^{-3} s^{-1}$

Fig. 2.1: Typical first-order plot of $\log_{10}$[allylbenzene] against time for the reaction of nitrogen dioxide with allylbenzene in cyclohexane at 30°C

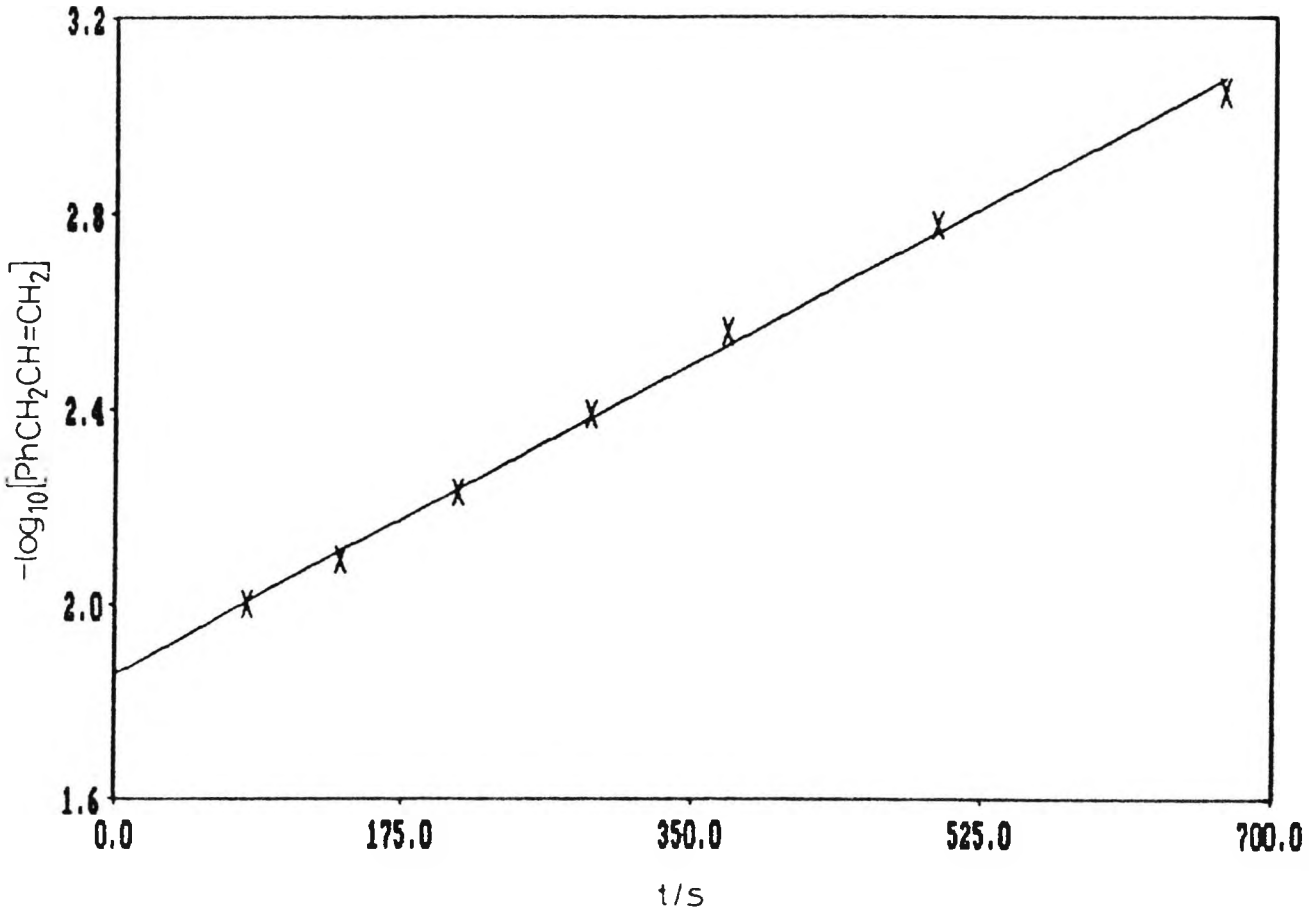

Table 2.4: Variation of k_{obs} with $[N_2O_4]_t$ for the reaction of allylbenzene with nitrogen dioxide in cyclohexane at 30°C

k_{obs}/s^{-1}	$[N_2O_4]_t$/mol dm^{-3}	$[NO_2^{\cdot}]$/mol dm^{-3}	$[N_2O_4]$/mol dm^{-3}
1.25×10^{-3}	0.052	3.66×10^{-3}	0.051
2.28×10^{-3}	0.092	4.88×10^{-3}	0.090
3.33×10^{-3}	0.142	6.06×10^{-3}	0.139
2.82×10^{-3}	0.165	6.54×10^{-3}	0.162
4.17×10^{-3}	0.227	7.68×10^{-3}	0.223
4.49×10^{-3}	0.257	8.18×10^{-3}	0.253
5.34×10^{-3}	0.303	8.88×10^{-3}	0.298
5.25×10^{-3}	0.348	9.53×10^{-3}	0.344

Fig. 2.2: Plot of k_{obs} against $[NO_2^{\bullet}]$ for the reaction of allylbenzene with nitrogen dioxide in cyclohexane at 30°C

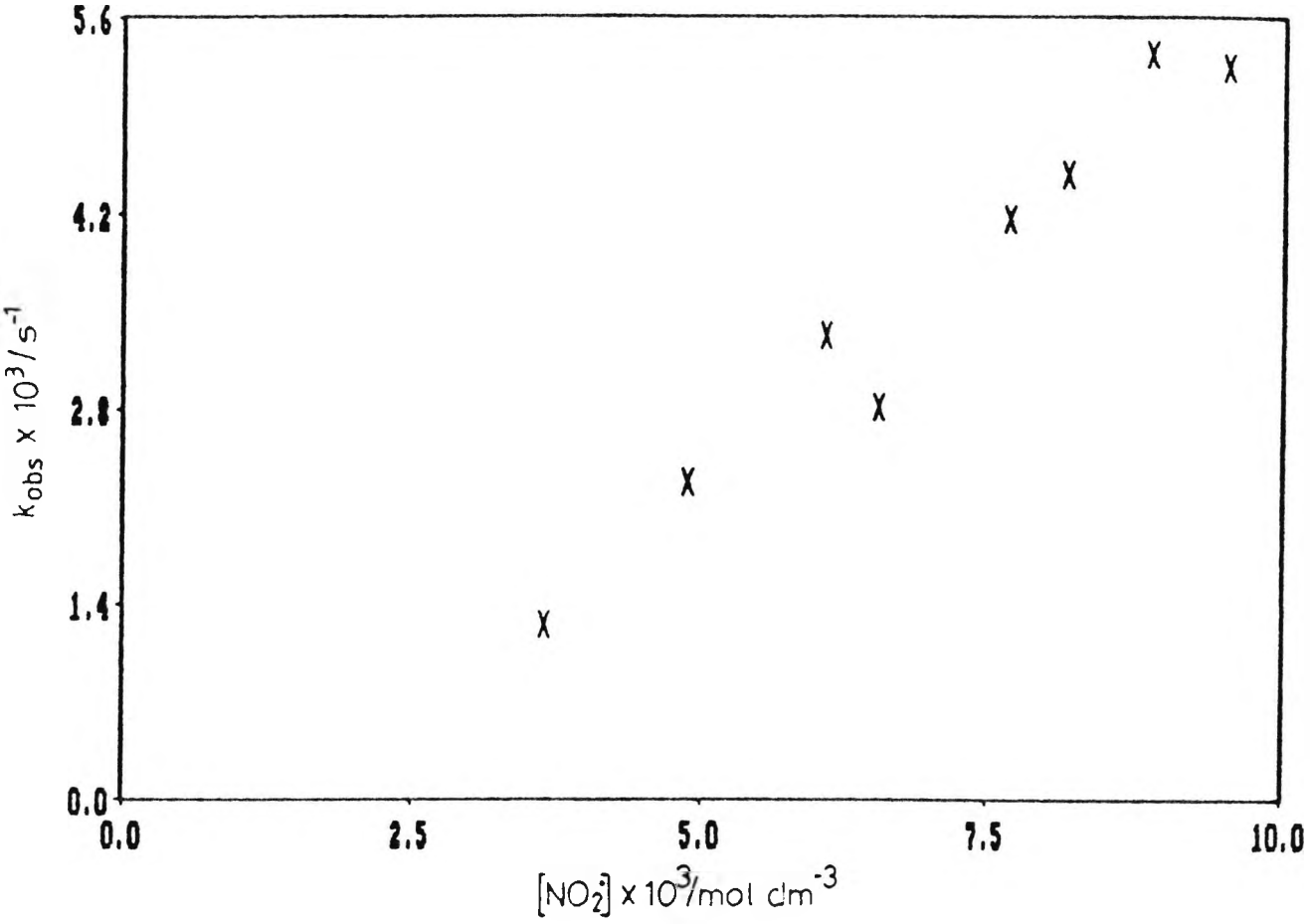

Table 2.5: Variation of rate coefficients with temperature

T/K	$[allylbenzene]_o$/mol dm^{-3}	$[N_2O_4]_t$/mol dm^{-3}	k_{obs}/s^{-1}
303	7.35×10^{-3}	0.092	2.28×10^{-3}
313	9.62×10^{-3}	0.092	5.39×10^{-3}
333	9.99×10^{-3}	0.084*	11.30×10^{-3}

*This nitrogen dioxide concentration is considered to be close enough to 0.093 mol dm^{-3} in order to construct an Arrhenius plot

Fig. 2.3: Arrhenius plot of ln k_{obs} against reciprocal temperature for the reaction of allylbenzene with nitrogen dioxide in cyclohexane

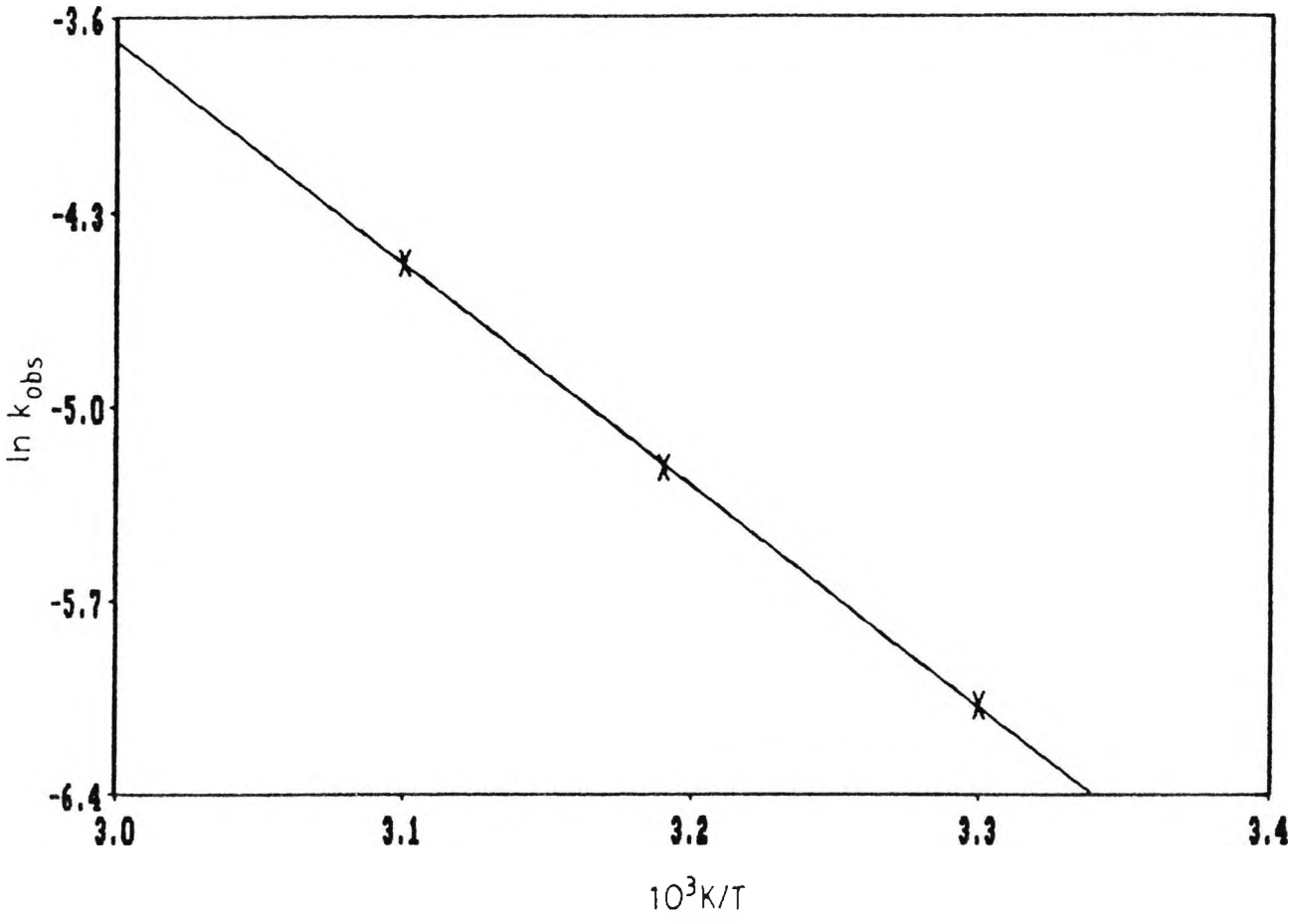

Table 2.6: Change in concentration with time during the reaction of allylbenzene with nitrogen dioxide in cyclohexane (saturated with water) at 30°C

t/s	$10^3[PhCH_2CH=CH_2]$	$\log_{10}[PhCH_2CH=CH_2]$
71	9.47	-2.02
130	7.86	-2.10
191	6.56	-2.18
252	4.95	-2.31
388	3.00	-2.52
480	2.31	-2.64
667	1.18	-2.93

$[PhCH_2CH=CH_2]_o = 1.1 \times 10^{-2}$ mol dm^{-3}, $[N_2O_4]_t = 0.25$ mol dm^{-3}

$k_{obs} = 3.52 \times 10^{-3} s^{-1}$

Fig. 2.4: Typical first-order plot of $\log_{10}$[allylbenzene] against time for the reaction of allylbenzene with nitrogen dioxide in cyclohexane (saturated with water) at 30°C

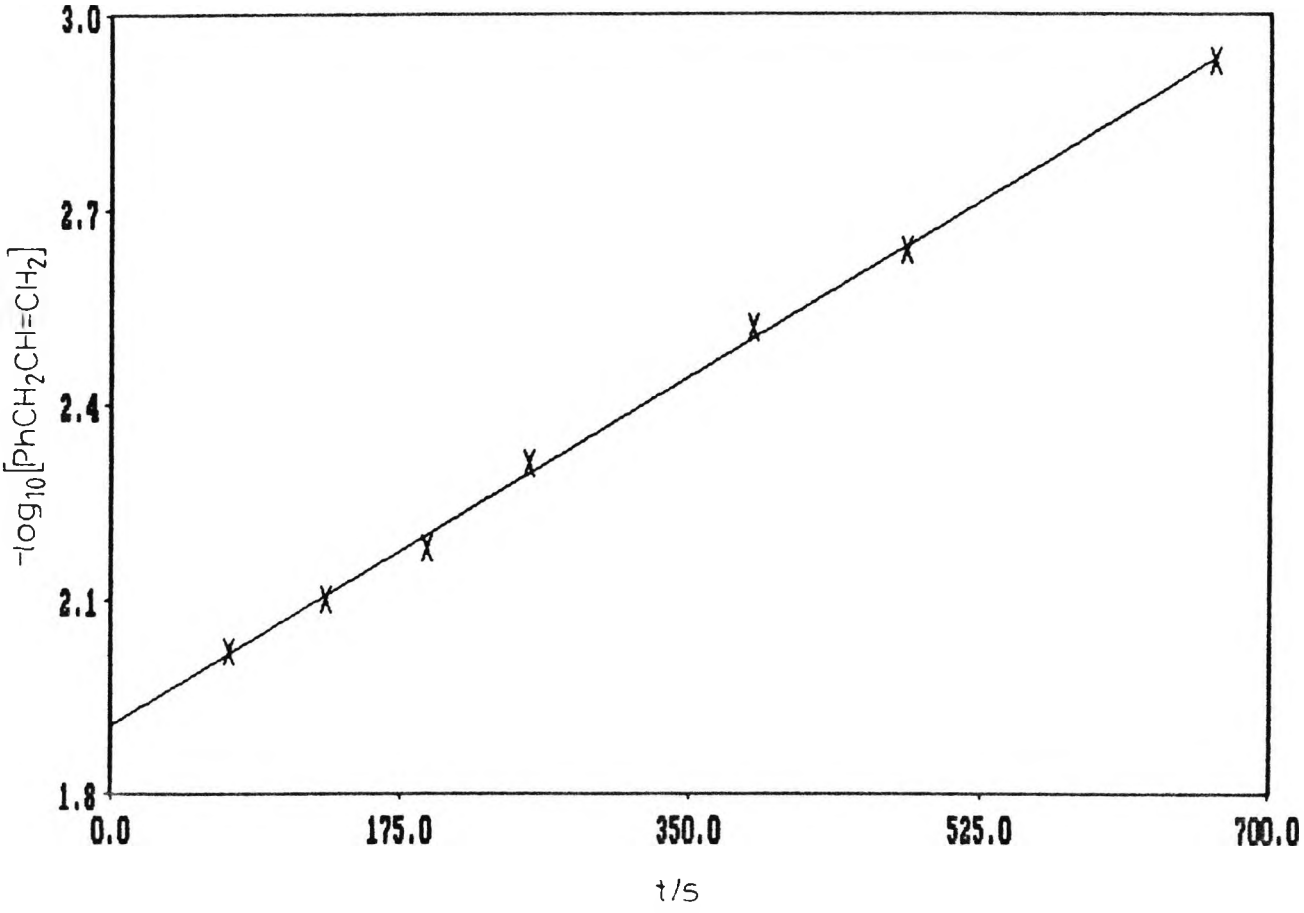

Table 2.7: Variation of k_{obs} with $[N_2O_4]_t$ for the reaction of allylbenzene with nitrogen dioxide in cyclohexane (saturated with water) at 30°C

k_{obs}/s^{-1}	$[N_2O_4]_t$/mol dm^{-3}	$[NO_2^{\cdot}]$/mol dm^{-3}	$[N_2O_4]$/mol dm^{-3}
1.75×10^{-3}	0.094	4.93×10^{-3}	0.092
3.52×10^{-3}	0.254	8.13×10^{-3}	0.250
6.15×10^{-3}	0.458	10.9×10^{-3}	0.453

Fig. 2.5: First-order plot of $\log_{10}$[allylbenzene] against time for the reaction of allylbenzene with nitrogen dioxide in cyclohexane at 30°C, in the presence of excess water

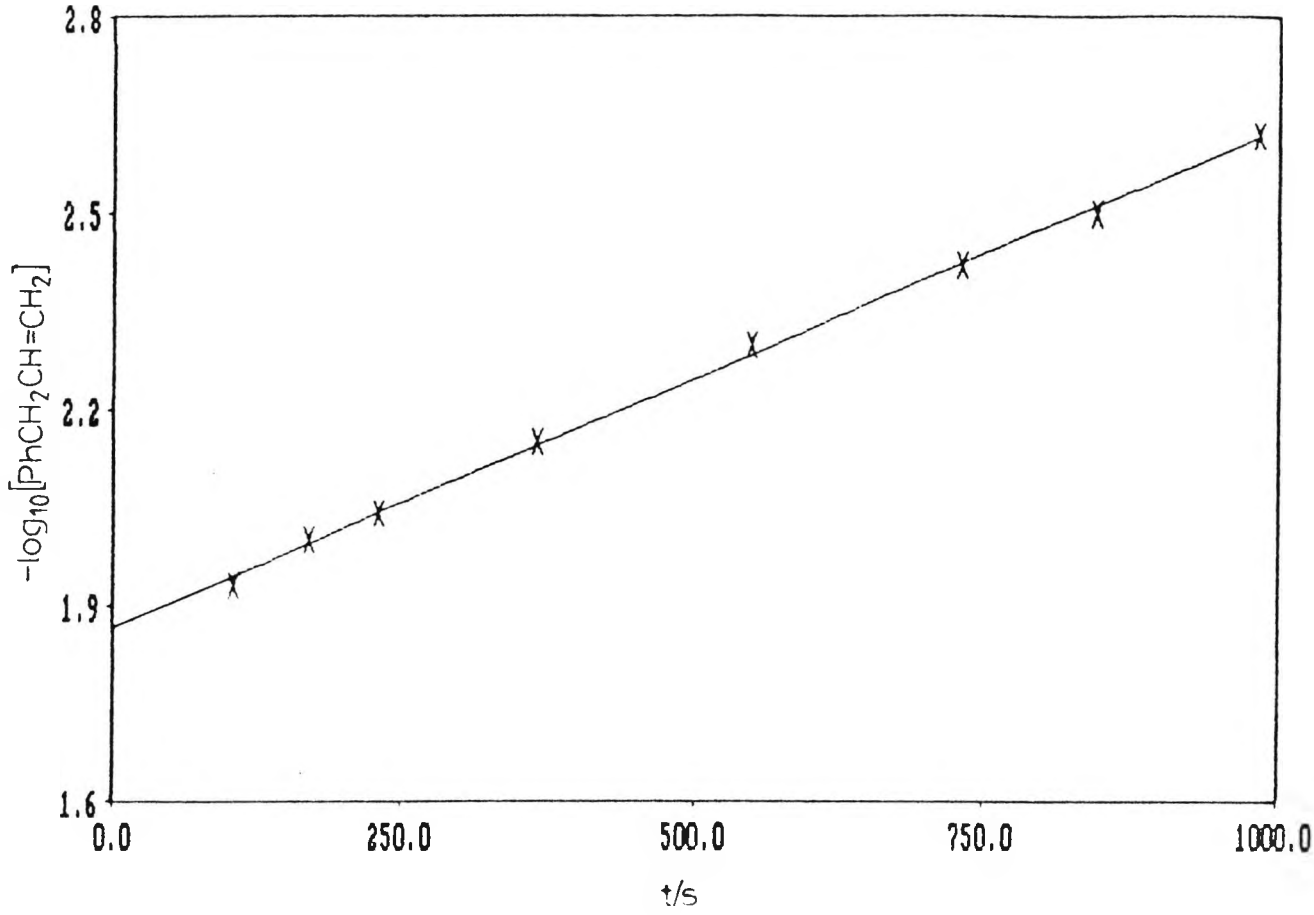

Fig. 2.6: First-order plot of $\log_{10}$[allylbenzene] against time for the reaction of allylbenzene with nitrogen dioxide in cyclohexane at 30°C, in the absence of oxygen

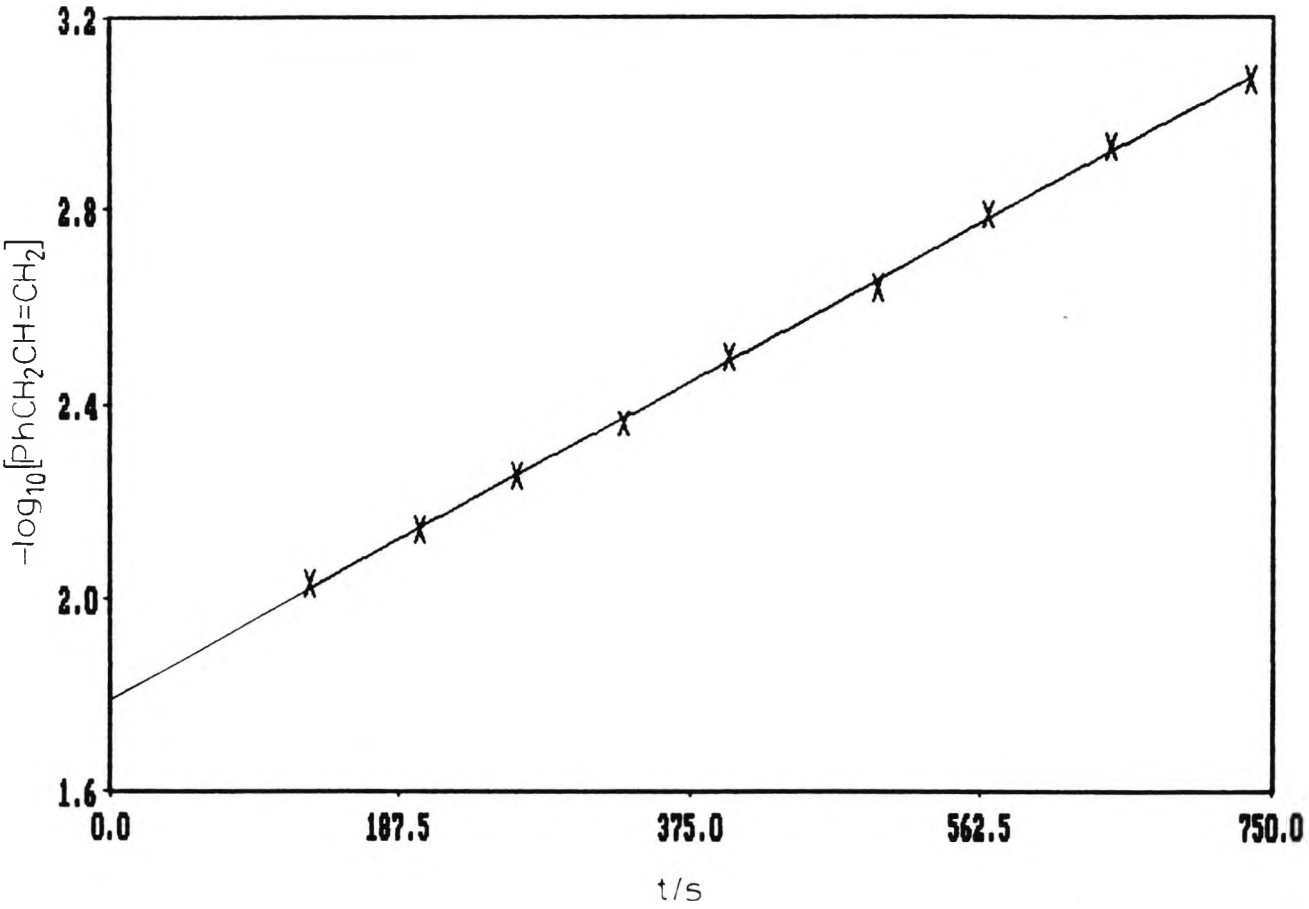

Fig. 2.7: First-order plot of $\log_{10}$[allylbenzene] against time for the reaction of allylbenzene with nitrogen dioxide in cyclohexane at 30°C, in the absence of light

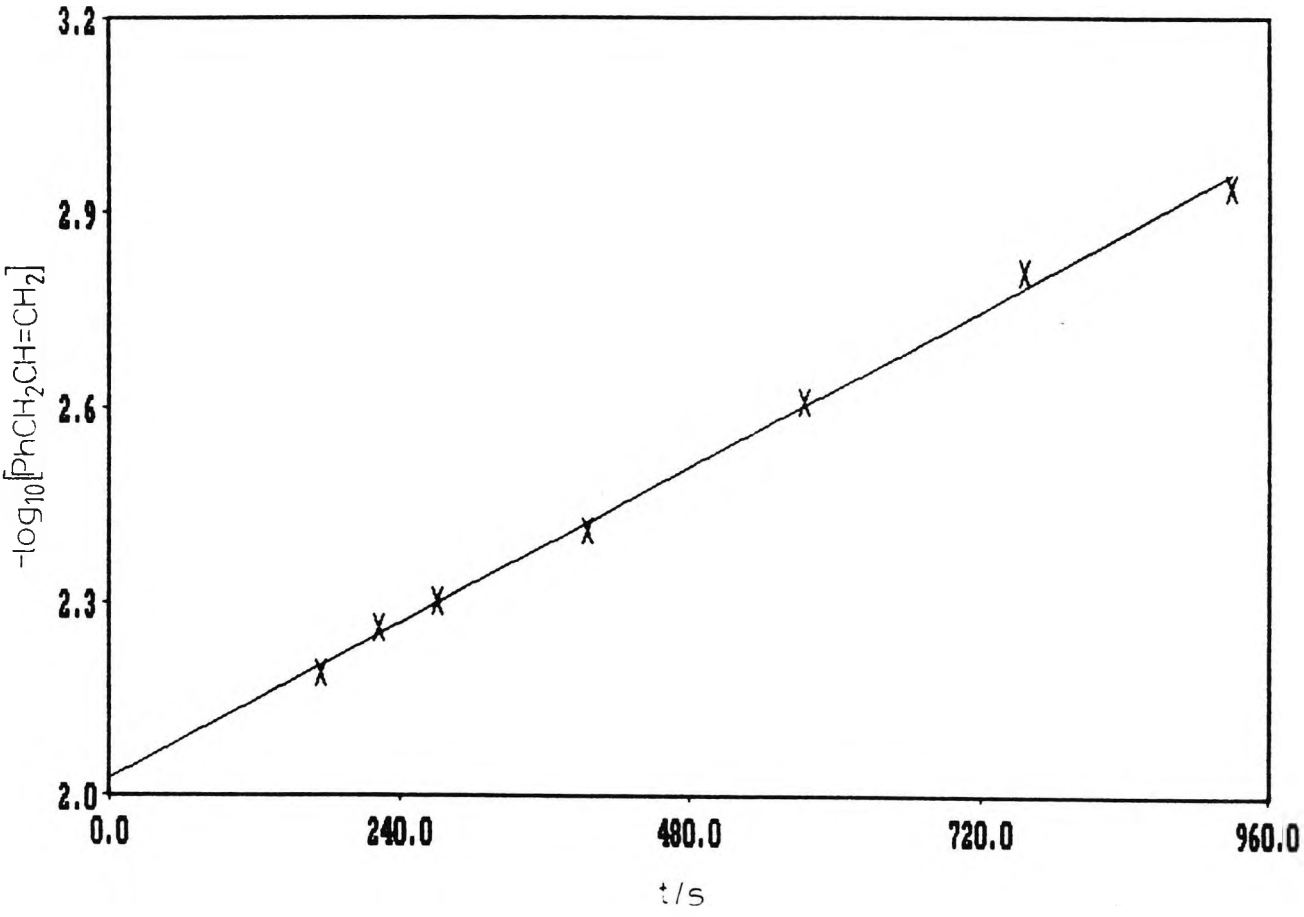

Table 2.8: Change in concentration with time during the reaction of 4-phenylbut-1-ene with nitrogen dioxide in cyclohexane at 30°C.

t/s	$10^3[PhCH_2CH_2CH=CH_2]$	$\log_{10}[PhCH_2CH_2CH=CH_2]$
86	6.98	-2.16
134	5.31	-2.27
178	4.37	-2.36
221	3.10	-2.51
265	2.49	-2.60
324	1.90	-2.72
408	1.11	-2.95
461	0.85	-3.07

$[PhCH_2CH_2CH=CH_2] = 1.03 \times 10^{-2}$ mol dm^{-3}; $[N_2O_4]_t = 0.20$ mol dm^{-3}

$k_{obs} = 5.66 \times 10^{-3} s^{-1}$

Fig. 2.8: Typical first-order plot of $\log_{10}$[phenylbut-1-ene] against time for the reaction of 4-phenylbut-1-ene with nitrogen dioxide in cyclohexane at 30°C

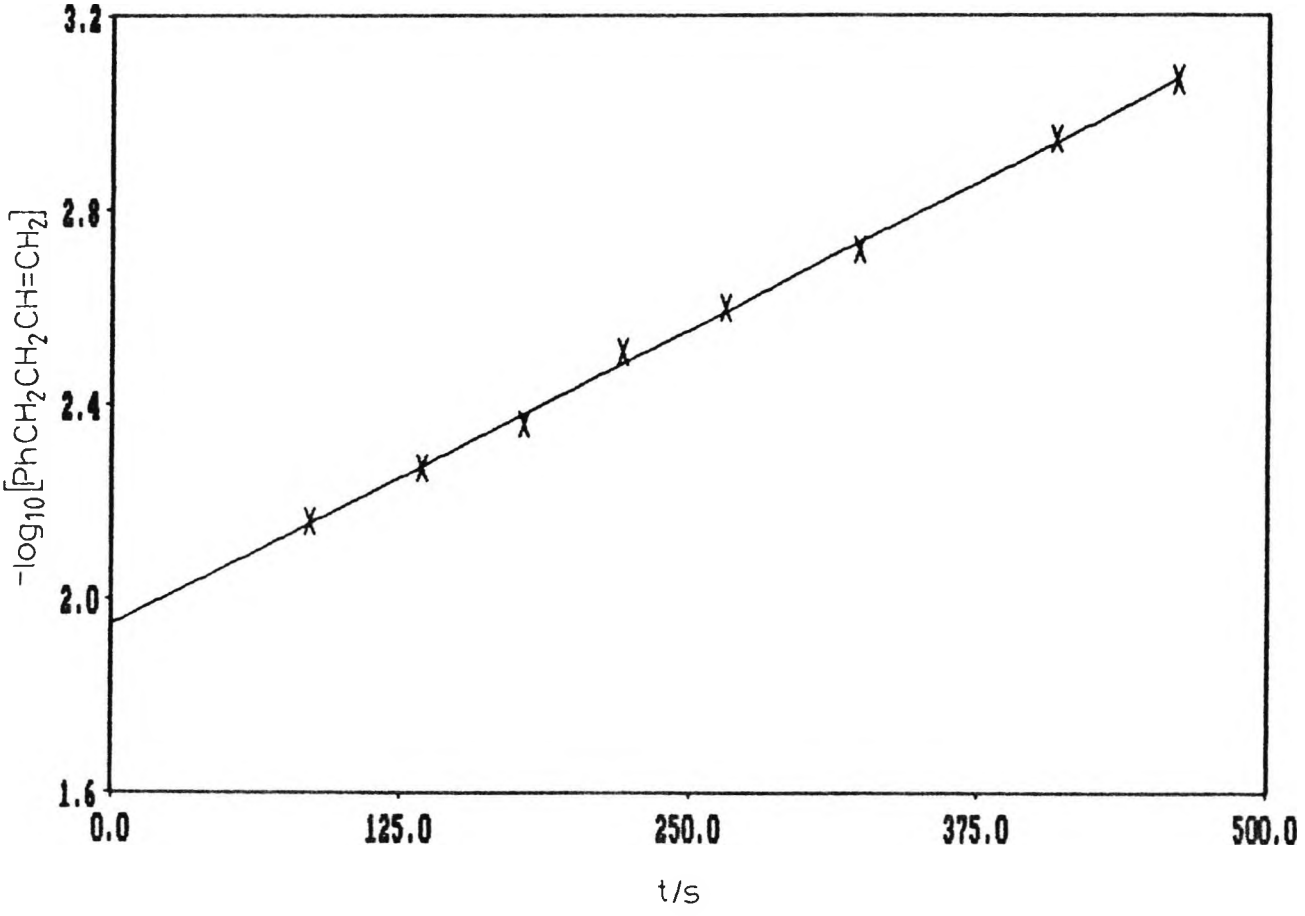

Table 2.9: Variation of k_{obs} with $[N_2O_4]_t$ for the reaction of 4-phenylbut-1-ene with nitrogen dioxide in cyclohexane at 30°C

k_{obs}/s^{-1}	$[N_2O_4]_t$/mol dm^{-3}	$[NO_2^{\cdot}]$/mol dm^{-3}	$[N_2O_4]$/mol dm^{-3}
2.67×10^{-3}	0.080	4.54×10^{-3}	0.078
3.20×10^{-3}	0.100	5.08×10^{-3}	0.098
4.16×10^{-3}	0.140	6.02×10^{-3}	0.137
4.16×10^{-3}	0.180	6.83×10^{-3}	0.177
5.66×10^{-3}	0.203	7.27×10^{-3}	0.200
5.87×10^{-3}	0.229	7.72×10^{-3}	0.226

Fig. 2.9: Plot of k_{obs} against $[NO_2^{\cdot}]$ for the reaction of 4-phenylbut-1-ene with nitrogen dioxide in cyclohexane at 30°C

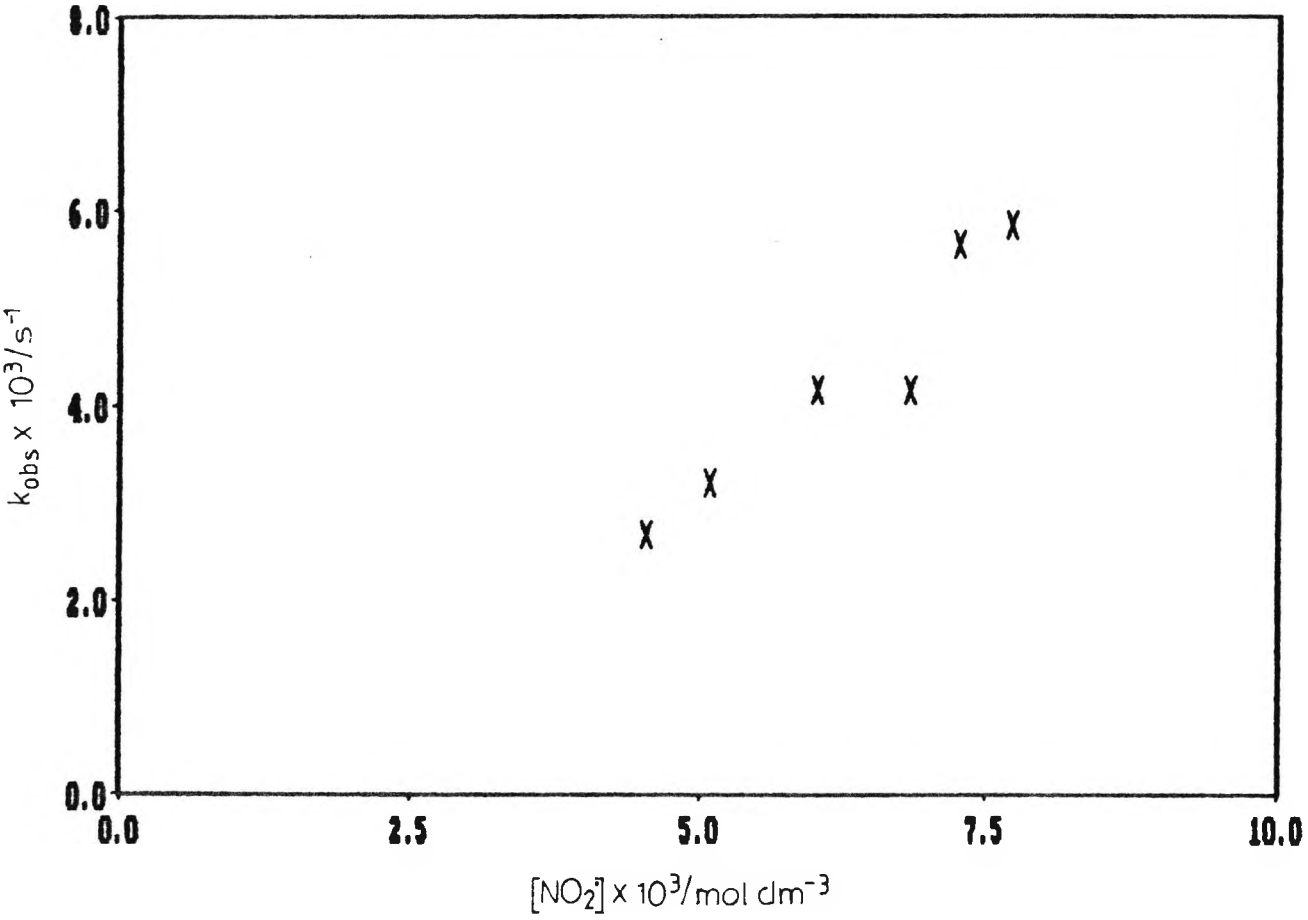

Table 2.10: Change in concentration with time during the reaction of 1-dodecene with nitrogen dioxide in cyclohexane at 30°C

t/s	$10^3[CH_3(CH_2)_9CH=CH_2]$	$\log_{10}[CH_3(CH_2)_9CH=CH_2]$
135	6.32	-2.20
199	4.67	-2.33
262	3.53	-2.45
338	2.74	-2.56
437	1.88	-2.73
520	1.03	-2.99
599	0.92	-3.04
679	0.69	-3.16
767	0.54	-3.27

$[CH_3(CH_2)_9CH=CH_2]_o = 9.81 \times 10^{-3}$ mol dm^{-3}; $[N_2O_4]_t = 0.11$ mol dm^{-3}

$k_{obs} = 3.99 \times 10^{-3} s^{-1}$

Fig. 2.10: Typical first-order plot of $\log_{10}$[1-dodecene] against time for the reaction of 1-dodecene with nitrogen dioxide in cyclohexane at 30°C

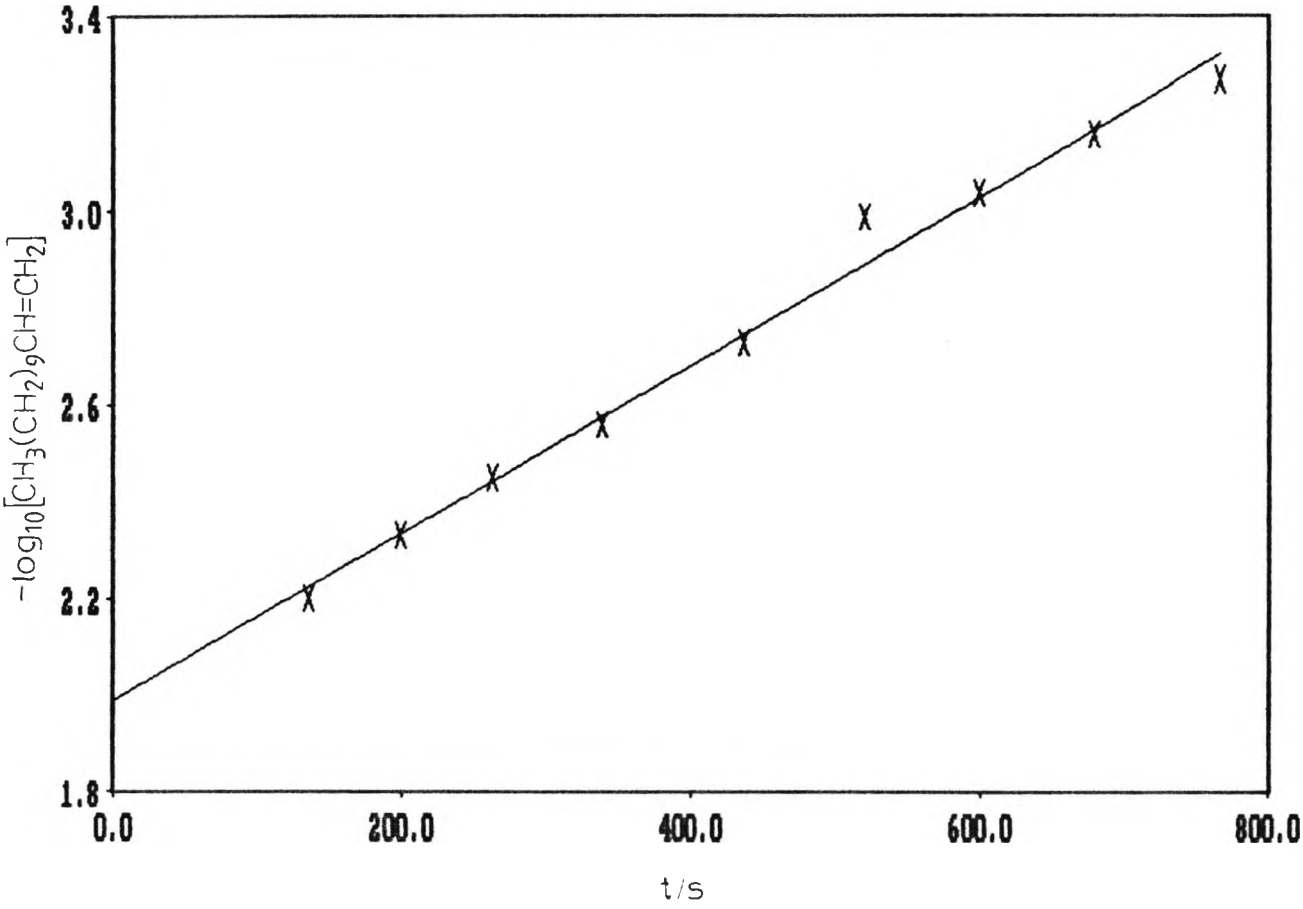

Table 2.11: Variation of k_{obs} with $[N_2O_4]_t$ for the reaction of 1-dodecene with nitrogen dioxide in cyclohexane at 30°C

k_{obs}/s^{-1}	$[N_2O_4]_t$/mol dm^{-3}	$[NO_2^{\cdot}]$/mol dm^{-3}	$[N_2O_4]$/mol dm^{-3}
2.72×10^{-3}	0.067	4.16×10^{-3}	0.065
3.99×10^{-3}	0.106	5.23×10^{-3}	0.103
4.70×10^{-3}	0.133	5.87×10^{-3}	0.130
5.90×10^{-3}	0.175	6.73×10^{-3}	0.171
7.88×10^{-3}	0.231	7.75×10^{-3}	0.227

Fig. 2.11: Plot of k_{obs} against $[NO_2^{\cdot}]$ for the reaction of 1-dodecene with nitrogen dioxide in cyclohexane at 30°C

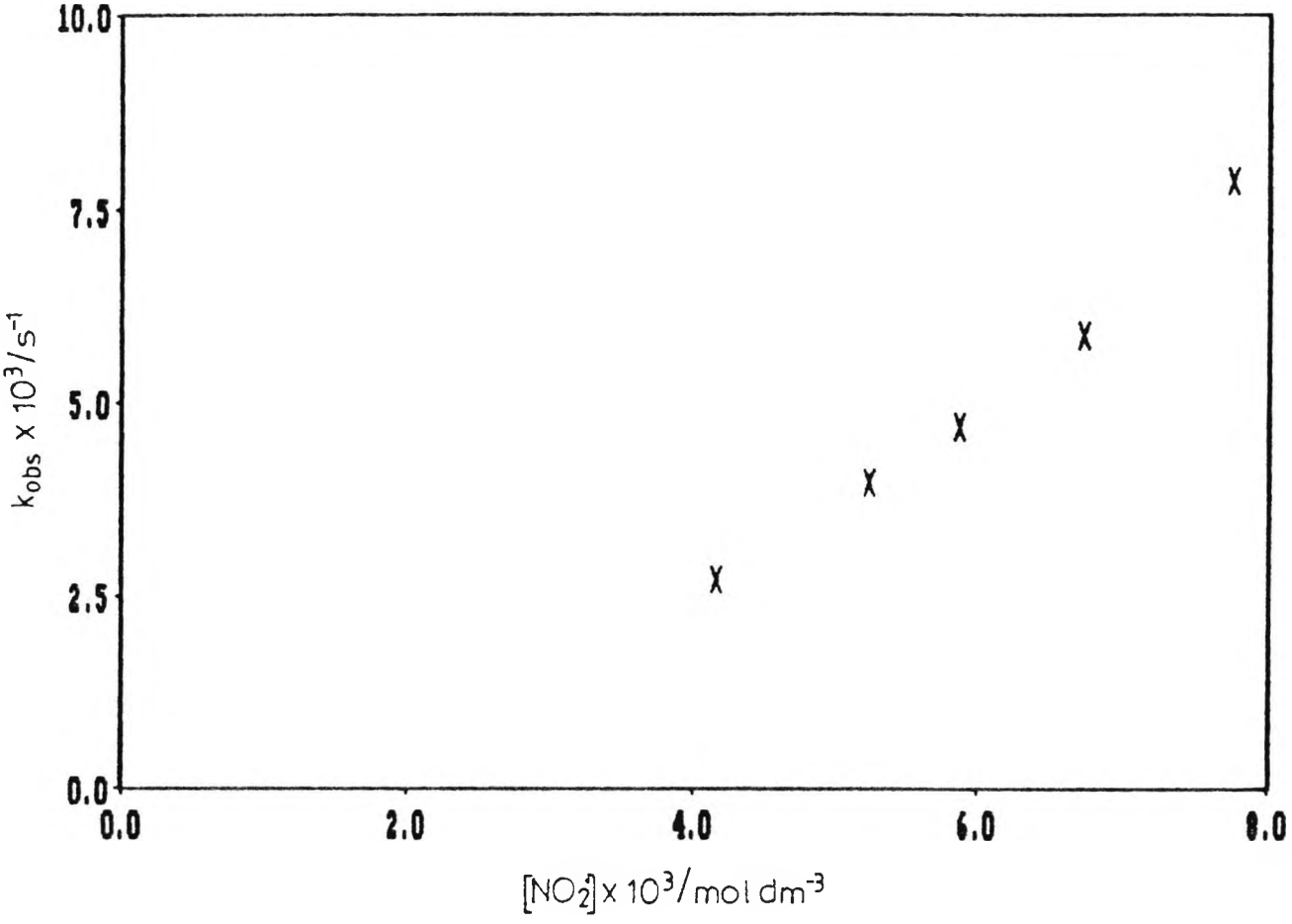

2.4 Discussion

The reactions of alkenes with nitrogen dioxide exhibit good first-order behaviour in the alkene when nitrogen dioxide is in a large excess. The rates of reaction were measured as first-order rate coefficients and the data collected were analysed in a number of ways. The consistency of the results producing smooth curves of rate coefficients vs. $NO_2^{\bullet}$ and N_2O_4 concentrations indicates the reproducibility of the results.

Values of k_{obs} at 30°C are shown in Figs. 2.12 - 2.14, plotted against $[NO_2^{\bullet}]$ and Figs. 2.15 - 2.17 plotted against $[N_2O_4]$. From these plots, it is clear that there is not a first-order dependence of rate on $[NO_2^{\bullet}]$ or $[N_2O_4]$.

For experiments in cyclohexane saturated with water, the values of k_{obs} obtained for the reaction of allylbenzene with nitrogen dioxide indicate that the presence of water has little effect on the rate of reaction (Fig. 2.18). In all experiments, reaction rates were monitored by removal of samples (1 ml) at periodic intervals. These samples were then treated with water (2 ml) to prevent further reaction and analysed directly by g.l.c. The effect of excess water on the course of reaction of allylbenzene with nitrogen dioxide was determined by the addition of 1 ml of water to the solvent (100 ml) before addition of nitrogen dioxide and substrate. The proportion of water used in this experiment was much less than that used to quench the reaction in individual samples, and was apparently not sufficient to extract and hydrolyse the nitrogen dioxide. Reaction must have continued as before addition in the organic phase. The absence of light and oxygen also have no effect on the observed rate of reaction of allylbenzene with nitrogen dioxide (Fig. 2.18).

A trend in the graphs of the observed first-order rate coefficients vs. $[NO_2^{\bullet}]$ for allylbenzene (Fig. 2.12), 4-phenylbut-1-ene (Fig. 2.13) and 1-dodecene (Fig. 2.14) was noted. The data could be accommodated only poorly by straight line plots manipulated to pass through the origin, however, if

no such manipulation was carried out, the line of best fit appeared to intercept the negative ordinate axis. By calculating the least squares fit for each line, when passage through the origin was not assumed, similar intercepts on the x-axis were identified (Figs. 2.19 - 2.21).

Two possible sources of error exist in the data used to calculate $NO_2^{\cdot}$ concentrations, and these were examined further in order to establish their contribution to the trend in the above graphs:

1) the value of K_{eq} [16] - equilibrium constant for the dissociation of N_2O_4 in cyclohexane,

2) the value of ϵ [17] - gas phase extinction coefficient of $NO_2^{\cdot}$ at 430 nm.

The literature value for K_{eq} was measured over a wide range of temperatures, under stringent experimental conditions, and is therefore considered to be accurate.

The concentration of $NO_2^{\cdot}$ was measured using the gas-phase extinction coefficient of 150 $dm^3mol^{-1}cm^{-1}$ at 430 nm. This value was assumed to be identical in solution and invariant with temperature. Altering the extinction coefficient to a value of 500 $dm^3mol^{-1}cm^{-1}$ and 25 $dm^3mol^{-1}cm^{-1}$ respectively, does not, however, manipulate the line of either graph through the origin (representative examples of this effect on the graph of k_{obs} vs $[NO_2^{\cdot}]$ for allylbenzene are shown in Figs. 2.22 and 2.23).

In view of the unsatisfactory nature of the plots of k_{obs} vs. $[NO_2^{\cdot}]$, the order of reaction in $NO_2^{\cdot}$ was investigated further The $\log_{10}k_{obs}$ vs. $\log_{10}[NO_2^{\cdot}]$ graphs for allylbenzene, 4-phenylbut-1-ene and 1-dodecene were plotted (Figs. 2.24 - 2.26) and the apparent orders in $NO_2^{\cdot}$ were found to be 1.5, 1.4 an 1.7 respectively. These results suggest that the kinetic data might be accommodated by a combination of first- and second-order reactions in $NO_2^{\cdot}$. The kinetic expression shown in equation 2.4 represents a kinetic scheme of this type:

$$\frac{-d[\text{Alkene}]}{dt} = k_{obs}[\text{Alkene}] \quad (2.3)$$

$$\frac{-d[\text{Alkene}]}{dt} = k_2[\text{Alkene}][NO_2^{\cdot}] + k_3[\text{Alkene}][NO_2^{\cdot}]^2 \quad (2.4)$$

$$= k_2[\text{Alkene}][NO_2^{\cdot}] + k_2'[\text{Alkene}][N_2O_4] \quad (2.5)$$

where $k_2' = k_3K$

$$k_{obs} = k_2[NO_2^{\cdot}] + k_3[NO_2^{\cdot}]^2 \quad (2.6)$$

$$\frac{k_{obs}}{[NO_2^{\cdot}]} = k_2 + k_3[NO_2^{\cdot}] \quad (2.7)$$

Scheme 2.3

Plots of $k_{obs}/[NO_2^{\cdot}]$ vs. $[NO_2^{\cdot}]$ (eq 2.7) were constructed for each alkene (Tables 2.12 - 2.14 and Figs. 2.27 - 2.29). By calculating the least squares fit for each line, the values of the second-and third-order rate coefficients, k_2, k_2' and k_3 were obtained (Table 2.15).

Table 2.15: Values of second-and third-order rate coefficients obtained for the reactions of allylbenzene, 4-phenylbut-1-ene and 1-dodecene with nitrogen dioxide in cyclohexane at 30°C

	k_2/mol^{-1}dm^{3}s^{-1}	k_2'/mol^{-1}dm^{3}s^{-1}	k_3/mol^{-2}dm^{6}s^{-1}
allylbenzene	0.26	9.20×10^{-3}	34.8
4-phenylbut-1-ene	0.37	1.31×10^{-3}	49.5
1-dodecene	0.24	2.58×10^{-3}	97.5

The graphs of the calculated rate constant k_{CALC} ($k_2[NO_2^{\cdot}]+k_3[NO_2^{\cdot}]^2$) vs. $[NO_2^{\cdot}]$ give good agreement with the experimental data and these derived rate coefficients clearly describe the system well within experimental error (Tables 2.12 - 2.14 and Figs. 2.30 - 2.32).

The results then indicate the existence of two reaction pathways, one first-order in $NO_2^{\cdot}$ and the other first-order in N_2O_4 (or second-order in $NO_2^{\cdot}$), and that this behaviour is quite general.

It is difficult to envisage a reaction involving $NO_2^{\cdot}$ which second-order in that species coexisting with a reaction which is first-order in the same species. It is also not possible to explain the results in terms of a change in rate-limiting step in a two stage $NO_2^{\cdot}$ reaction such as that represented by equations 2.8 and 2.9. In order for a change of order to occur here the second stage would have to be rate-limiting at low $NO_2^{\cdot}$

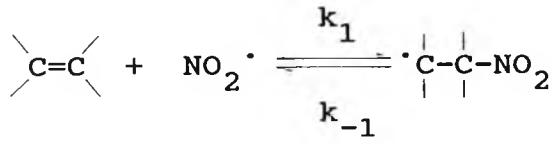

(2.8)

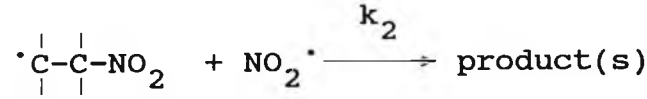

(2.9)

concentrations, giving second order behaviour in $NO_2^{\bullet}$, allowing the first stage to become rate-limiting at high concentrations of $NO_2^{\bullet}$ when $k_2 >> k_{-1}$. The latter case would give first-order dependence of rate on $NO_2^{\bullet}$. A change in rate-limiting stage analogous to this does indeed occur in the reaction of phenol with nitrogen dioxide in cyclohexane[69] (Chapter 1). This predicted behaviour is, however, at variance with the observations in the present study where the order of reaction tends to second in $NO_2^{\bullet}$ at high concentrations of $NO_2^{\bullet}$ and to unity as the concentration of $NO_2^{\bullet}$ approaches zero.

A scheme which is consistent with the observed results is shown below:

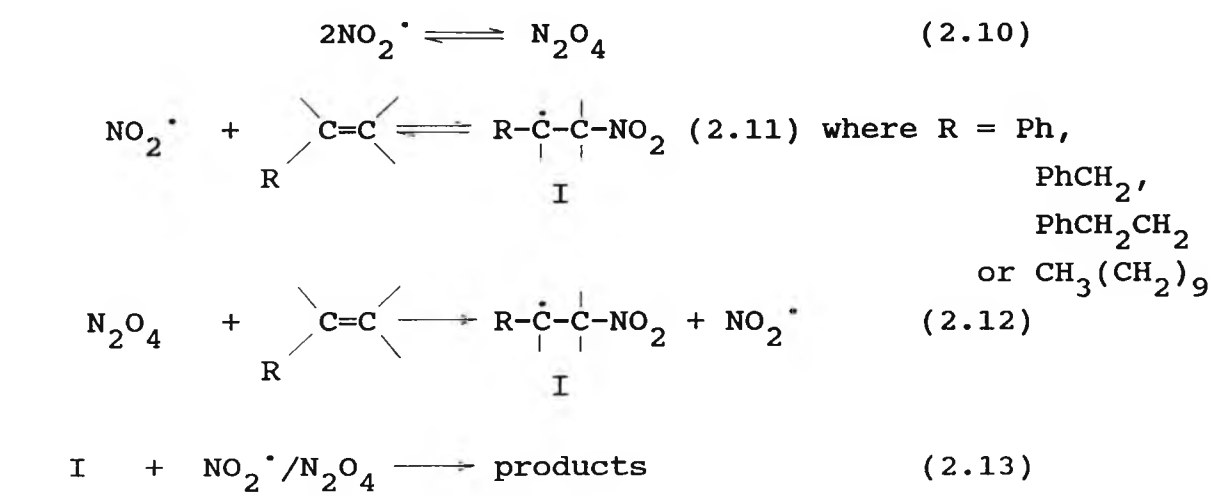

(2.10)

(2.11) where R = Ph, $PhCH_2$, $PhCH_2CH_2$ or $CH_3(CH_2)_9$

(2.12)

(2.13)

Scheme 2.5

Homolytic pathways are written consistent with earlier studies[30,35-37,92] and product and C.I.D.N.P. studies (Chapters 3 and 4). The rate coefficients k_2 and k_2' in Table 2.15 are the rate coefficients of a bimolecular reaction of each of the alkenes

with $NO_2^{\cdot}$ and N_2O_4 respectively, step 2.13 being fast in each case The data indicate that $NO_2^{\cdot}$ is a factor of 29, 28 and 9 more reactive than N_2O_4 towards allylbenzene, 4-phenylbut-1-ene and 1-dodecene respectively in these reactions.

Fig. 2.12: Plot of k_{obs} against $[NO_2^{\bullet}]$ for the reaction of allylbenzene with nitrogen dioxide in cyclohexane at 30°C

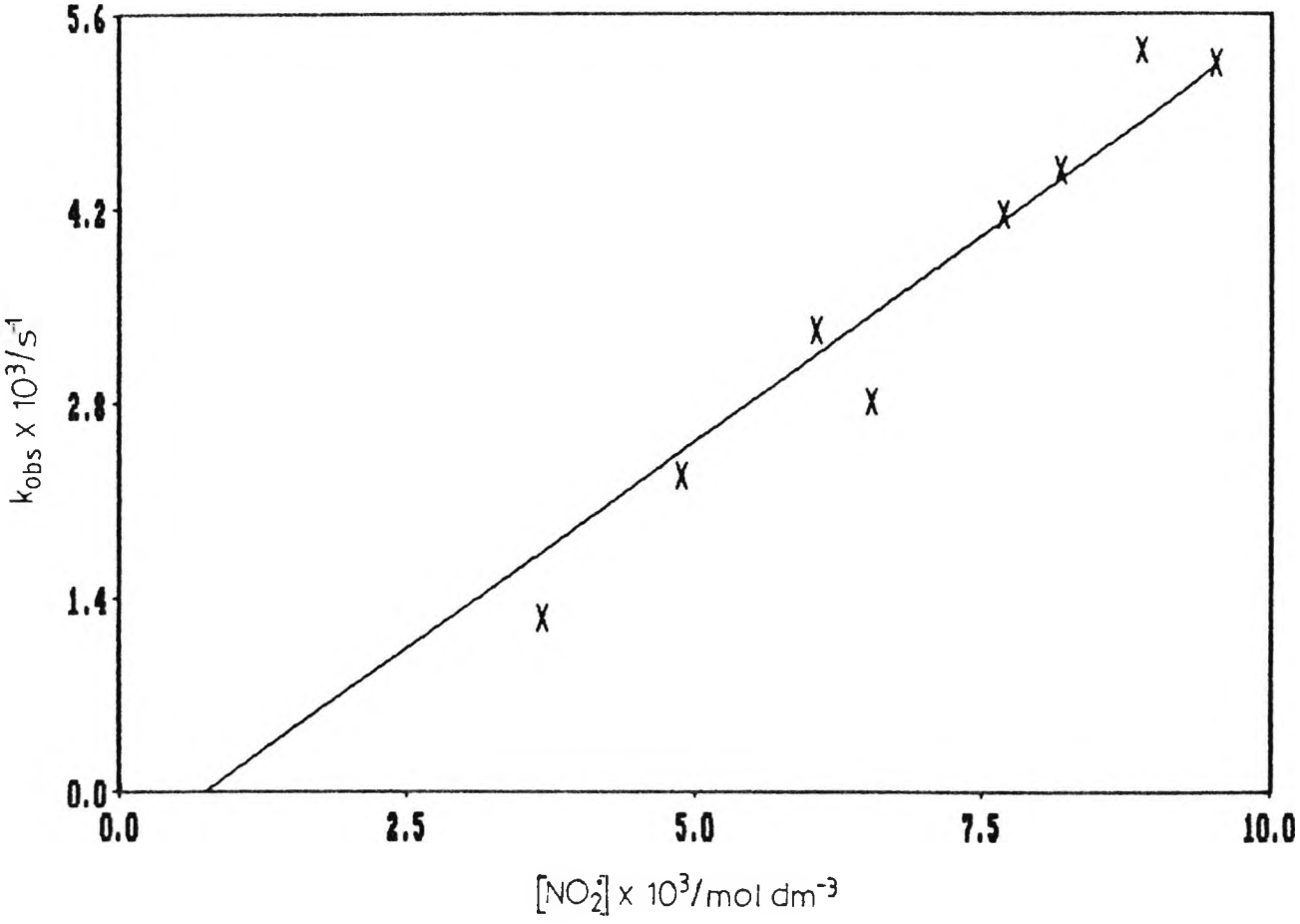

Fig. 2.13: Plot of k_{obs} against $[NO_2^{\cdot}]$ for the reaction of 4-phenylbut-1-ene with nitrogen dioxide in cyclohexane at 30°C

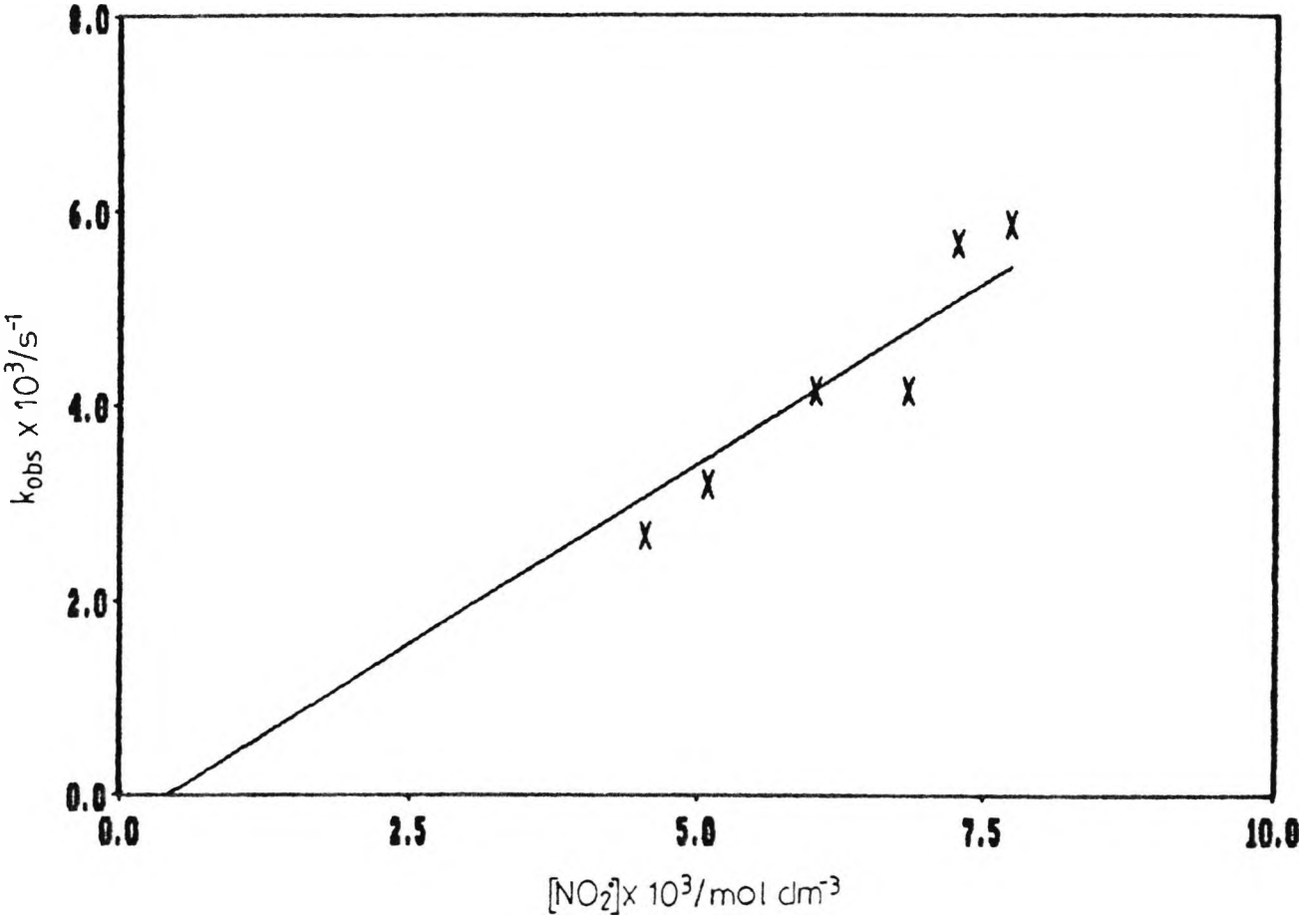

Fig. 2.14: Plot of k_{obs} against $[NO_2^{\cdot}]$ for the reaction of 1-dodecene with nitrogen dioxide in cyclohexane at 30°C

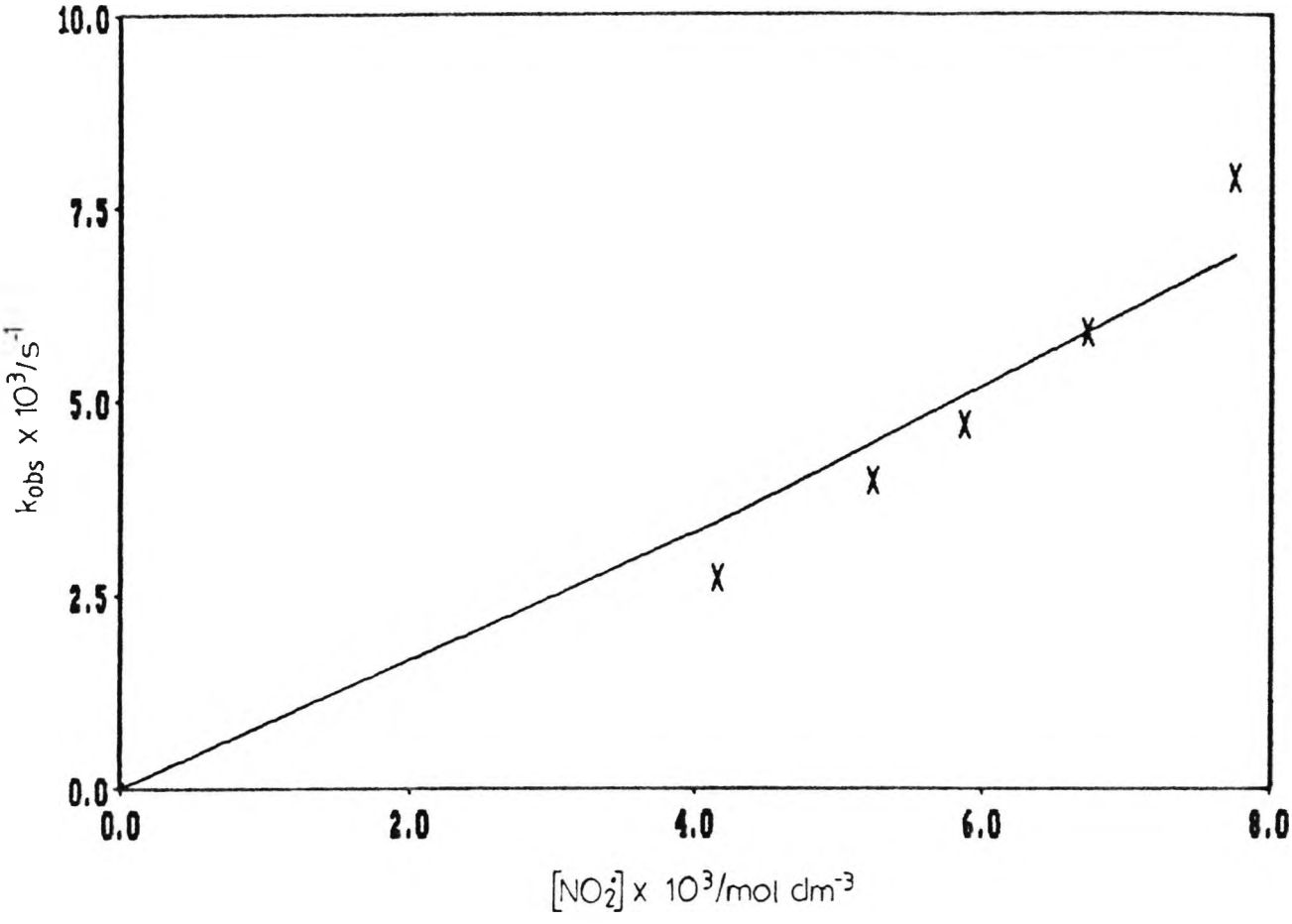

Fig. 2.15: Plot of k_{obs} against $[N_2O_4]$ for the reaction of allylbenzene with nitrogen dioxide in cyclohexane at 30°C

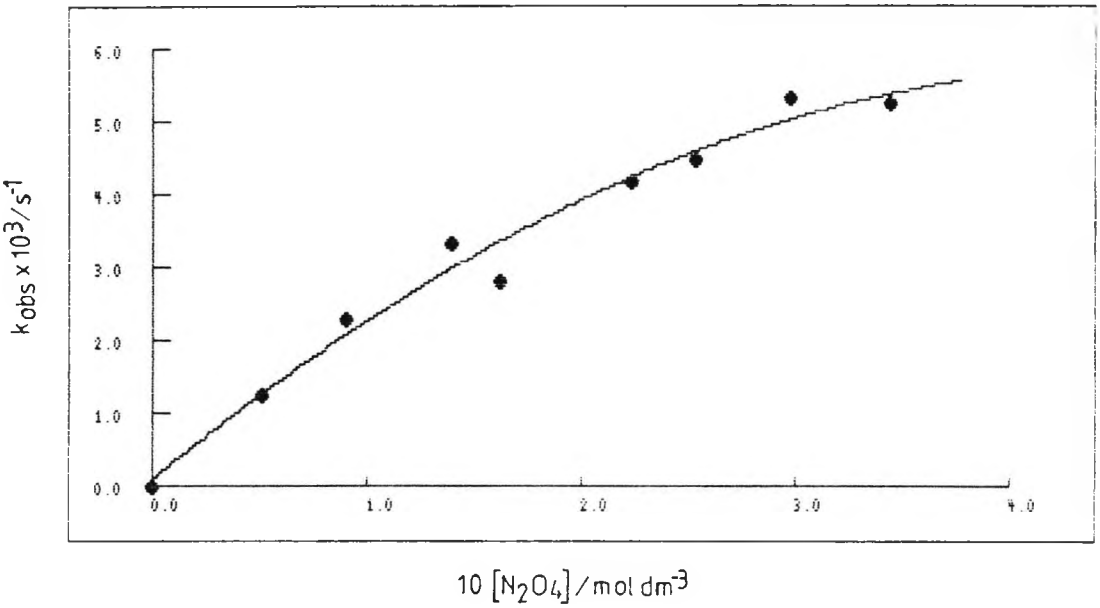

Fig. 2.16: Plot of k_{obs} against $[N_2O_4]$ for the reaction of 4-phenylbut-1-ene with nitrogen dioxide in cyclohexane at 30°C

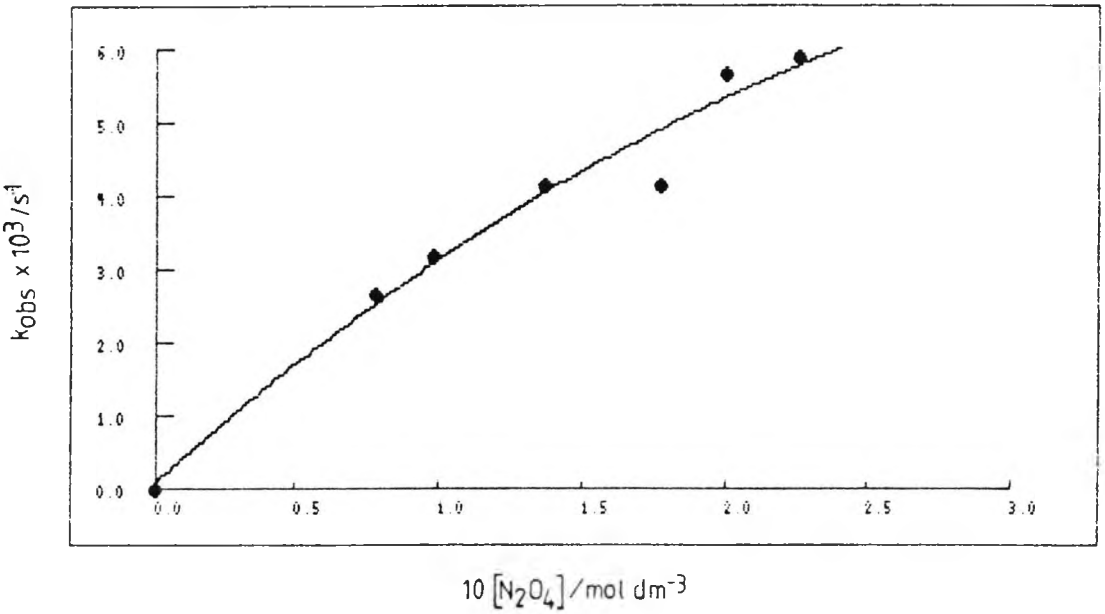

Fig. 2.17: Plot of k_{obs} against $[N_2O_4]$ for the reaction of 1-dodecene with nitrogen dioxide in cyclohexane at 30°C

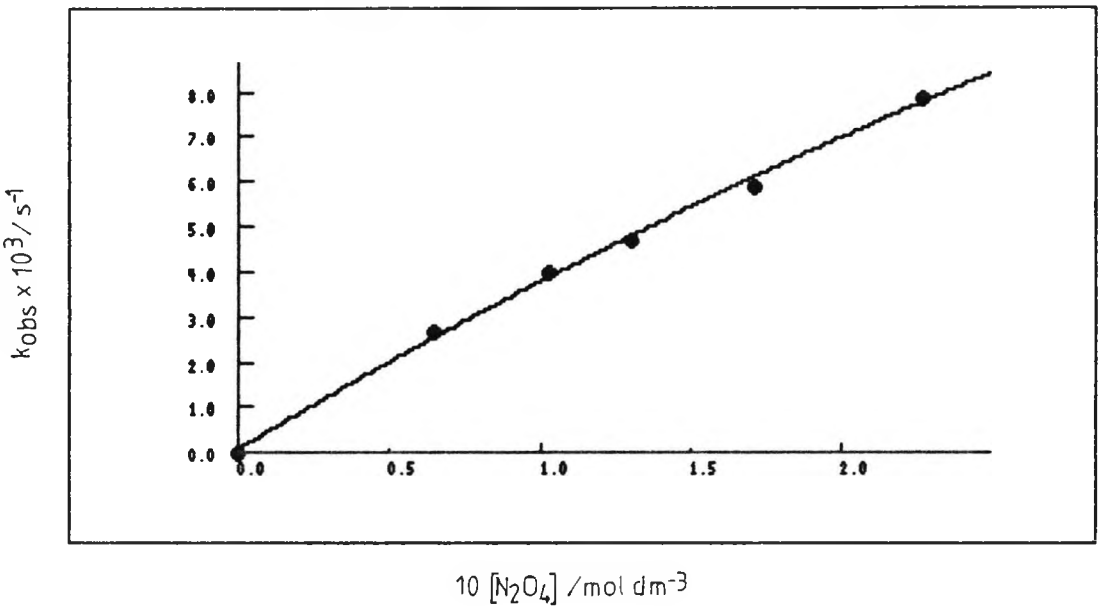

Fig. 2.18: Plot of k_{obs} against $[NO_2^{\bullet}]$ for the reaction of allylbenzene with nitrogen dioxide in cyclohexane at 30°C

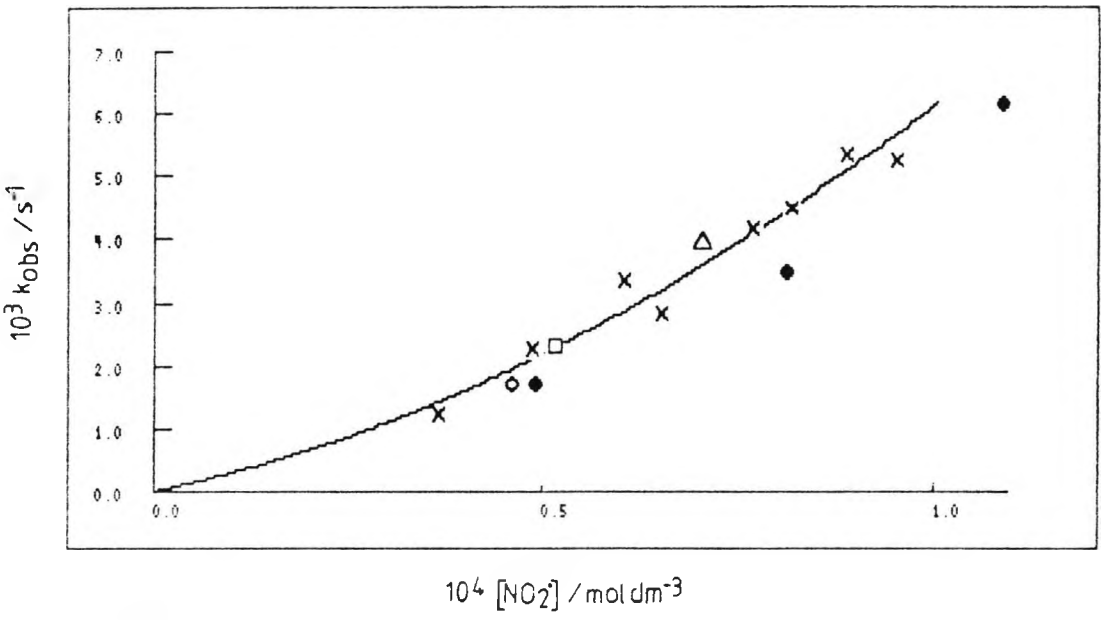

KEY

— CALCULATED DATA

x EXPERIMENTAL DATA

o EXCESS WATER

• CYCLOHEXANE SATURATED WITH WATER

△ ABSENCE OF OXYGEN

□ ABSENCE OF LIGHT

Fig. 2.19 Least squares fit for the observed rate of reaction of allylbenzene vs. [$NO_2^{\cdot}$]

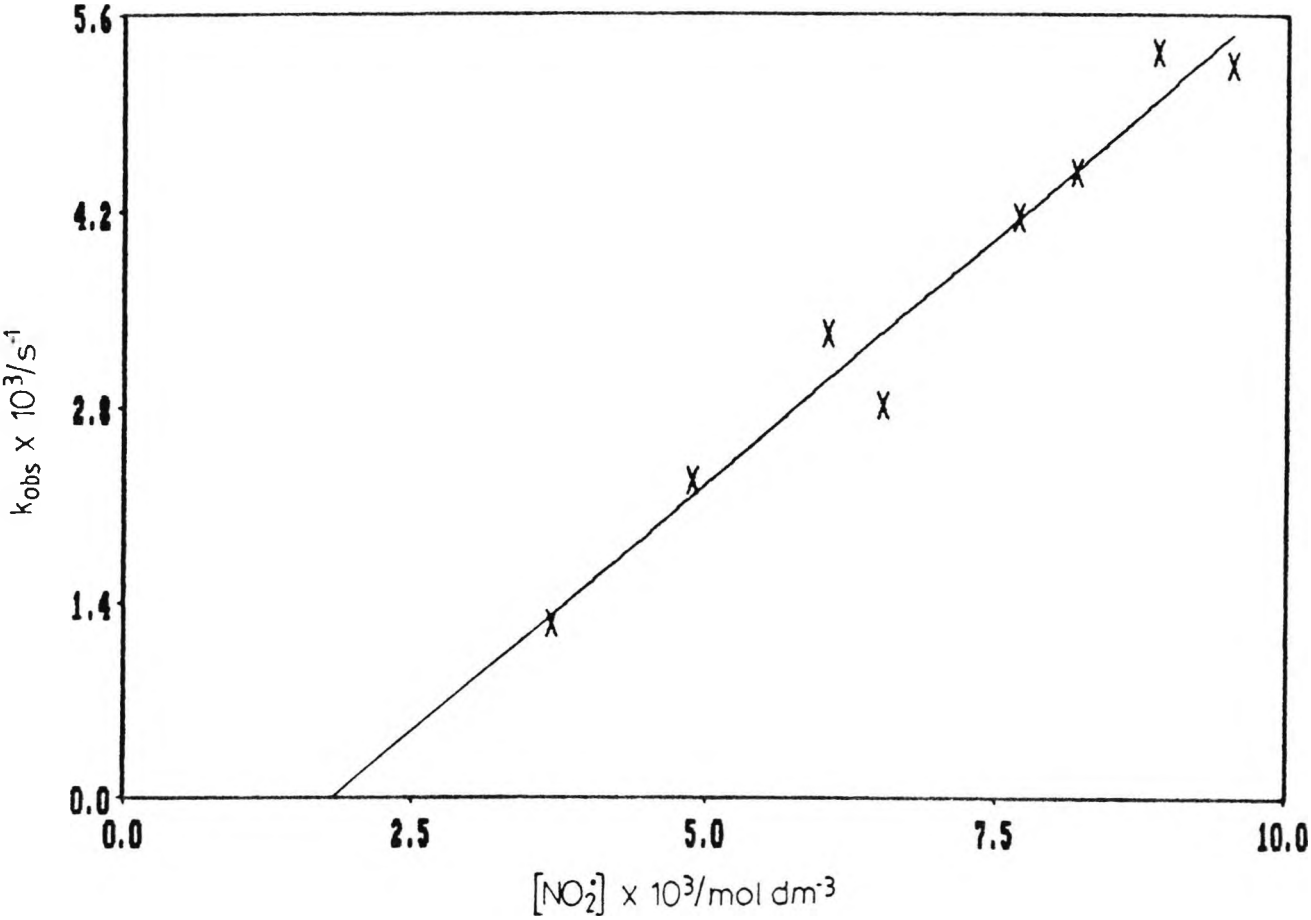

Fig. 2.20: Least squares fit for the observed rate of reaction of 4-phenylbut-1-ene vs. $[NO_2^{\bullet}]$

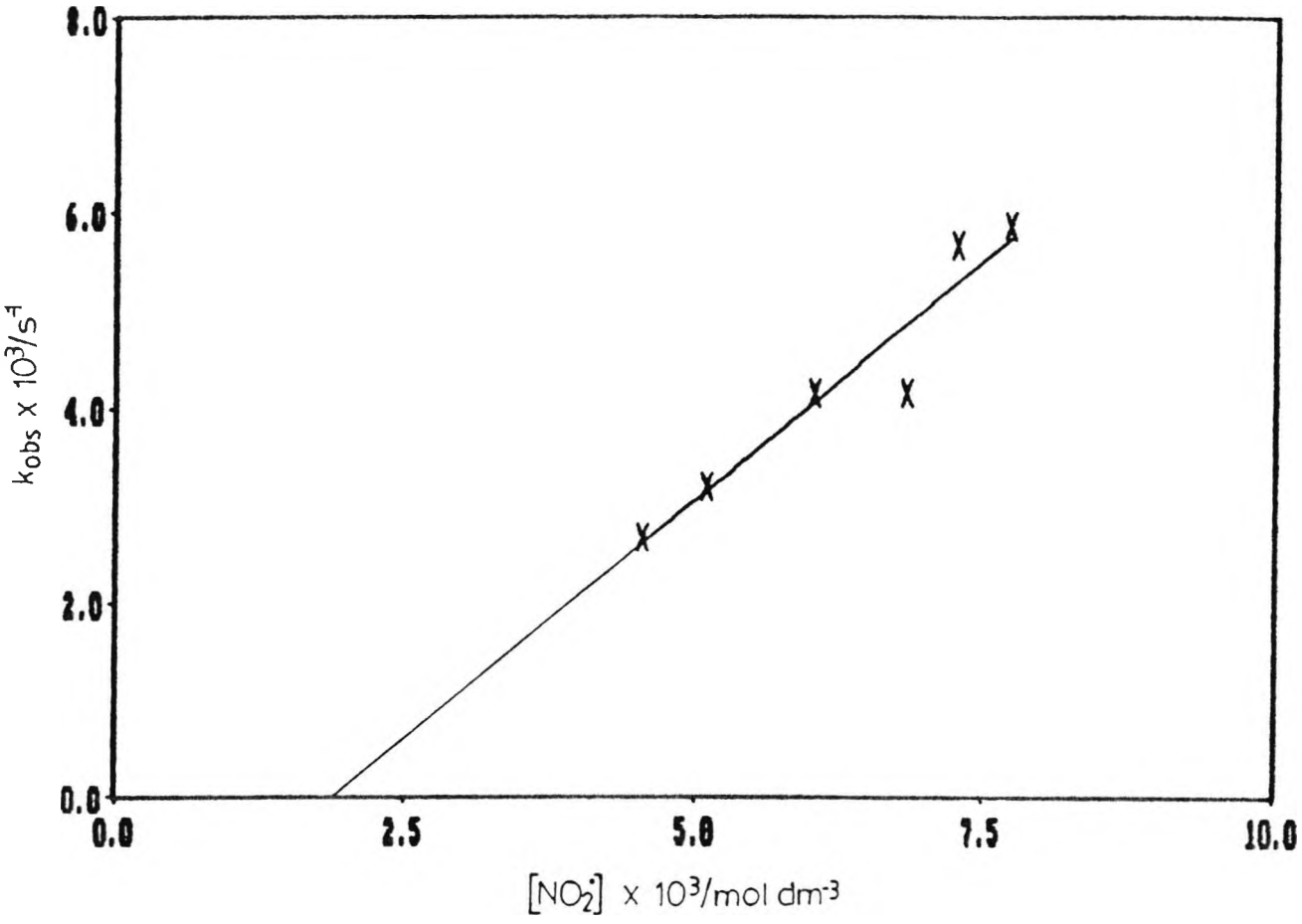

Fig. 2.21: Least squares fit for the observed rate of reaction of 1-dodecene vs. $[NO_2^{\cdot}]$

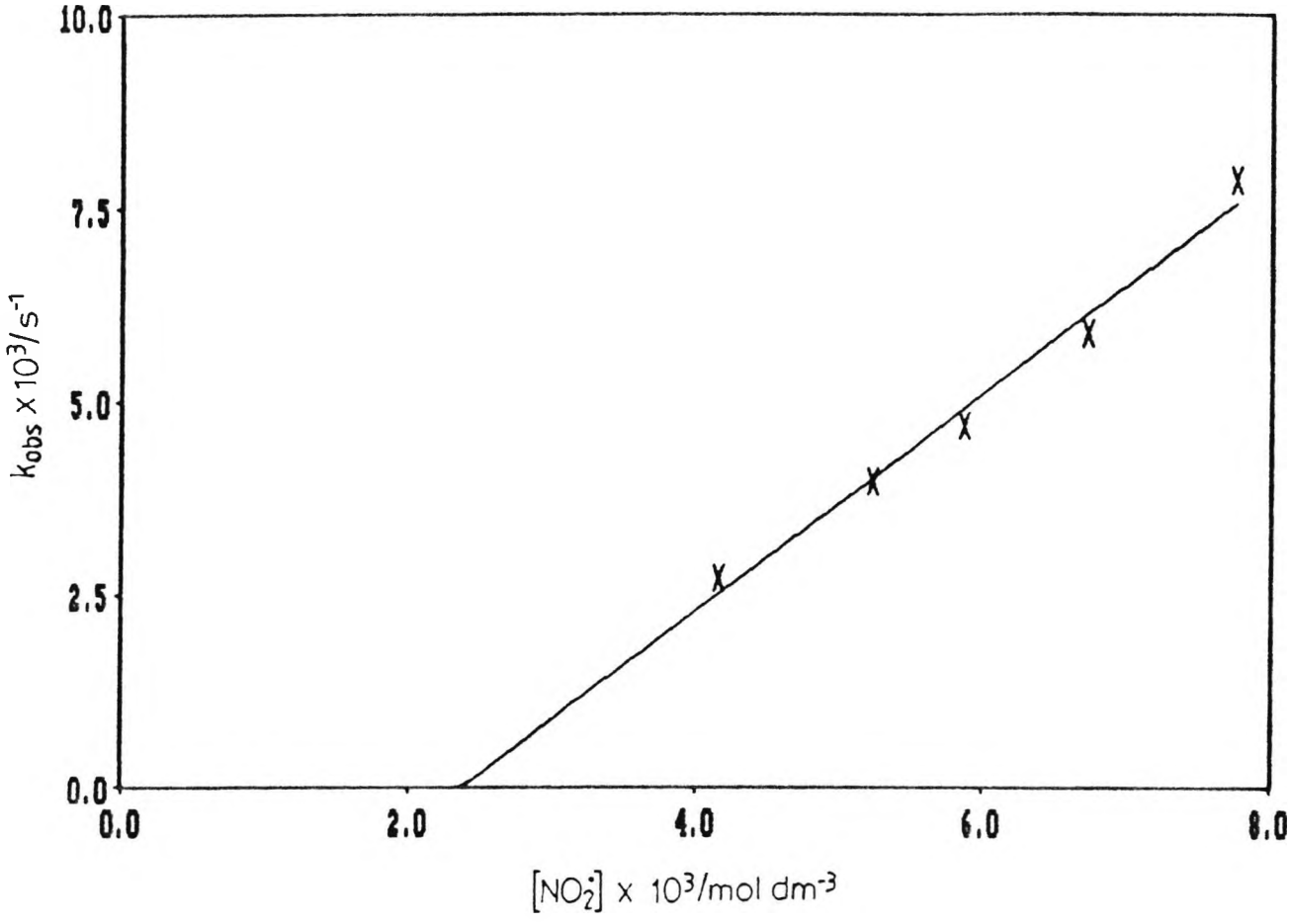

Fig. 2.22: Effect of varying the extinction coefficient ε on the graph of k_{obs} vs $[NO_2^{\cdot}]$ for allylbenzene

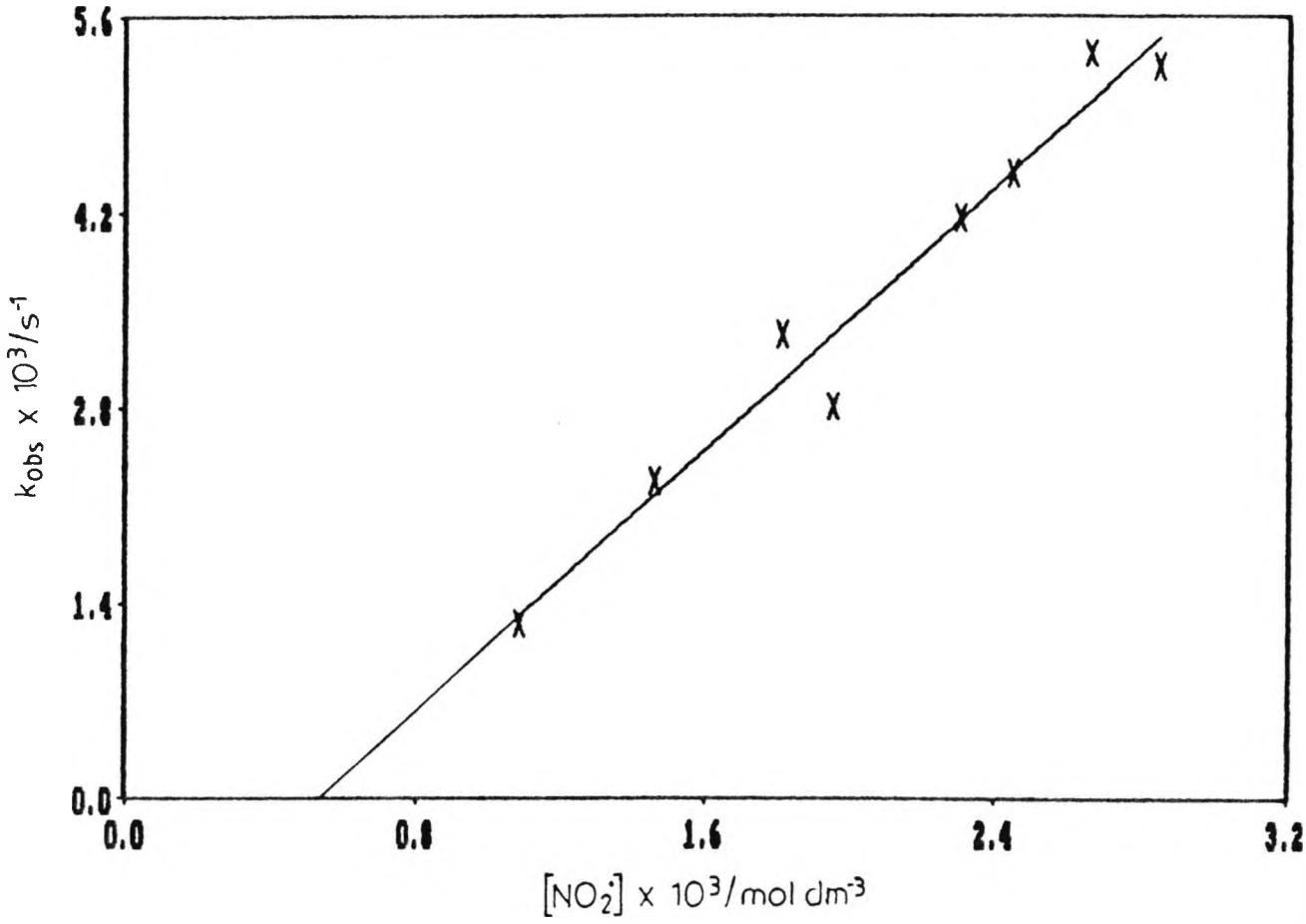

$\varepsilon = 500\ dm^3\ mol^{-1}\ cm^{-1}$

Fig. 2.23: Effect of varying the extinction coefficient ϵ on the graph of k_{obs} vs $[NO_2^{\cdot}]$ for allylbenzene

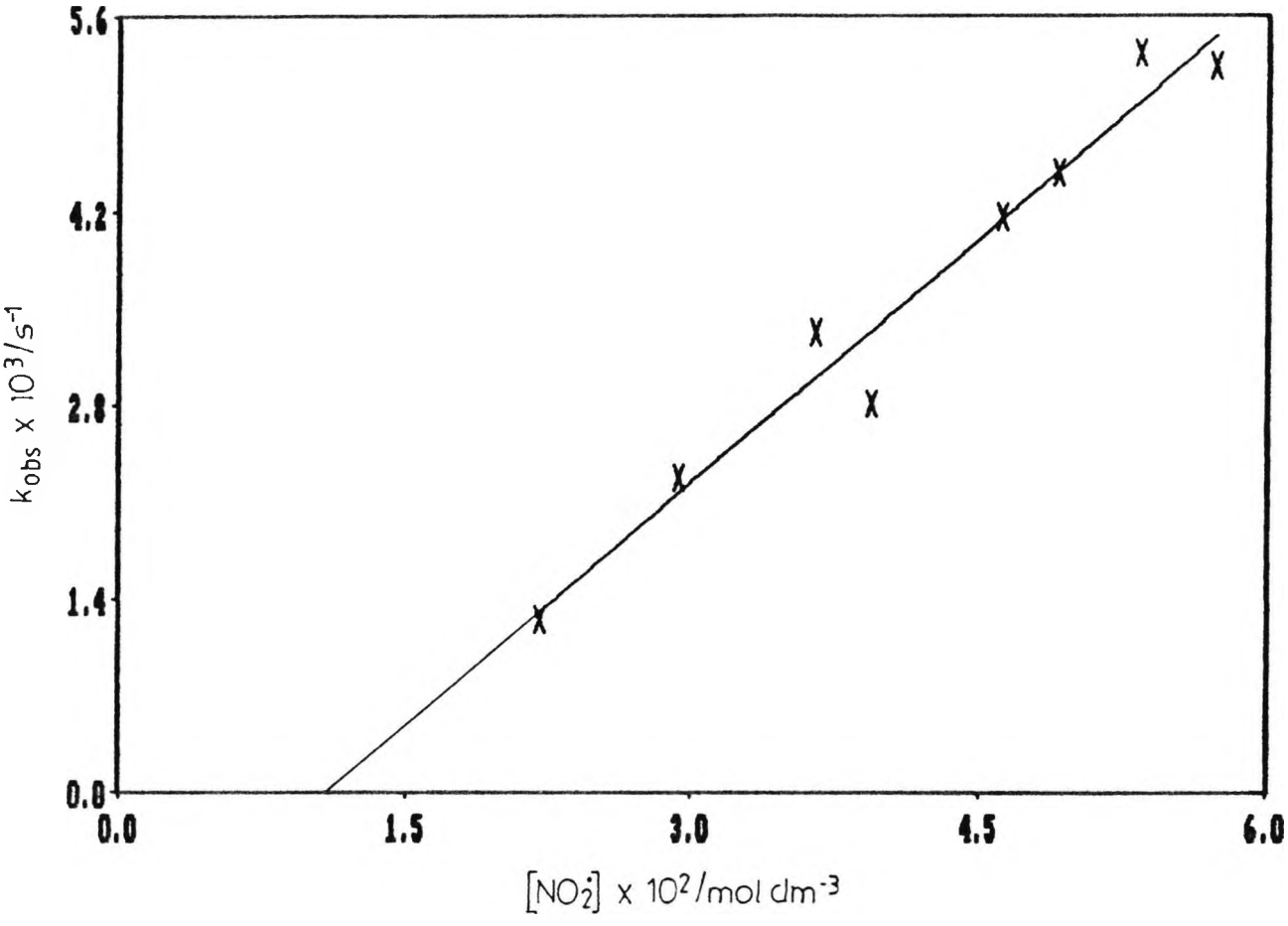

ε=25 $dm^3\ mol^{-1}\ cm^{-1}$

Fig. 2.24: Plot of $\log_{10} k_{obs}$ vs. $\log_{10}[NO_2^{\cdot}]$ for the reaction of allylbenzene with nitrogen dioxide in cyclohexane at 30°C

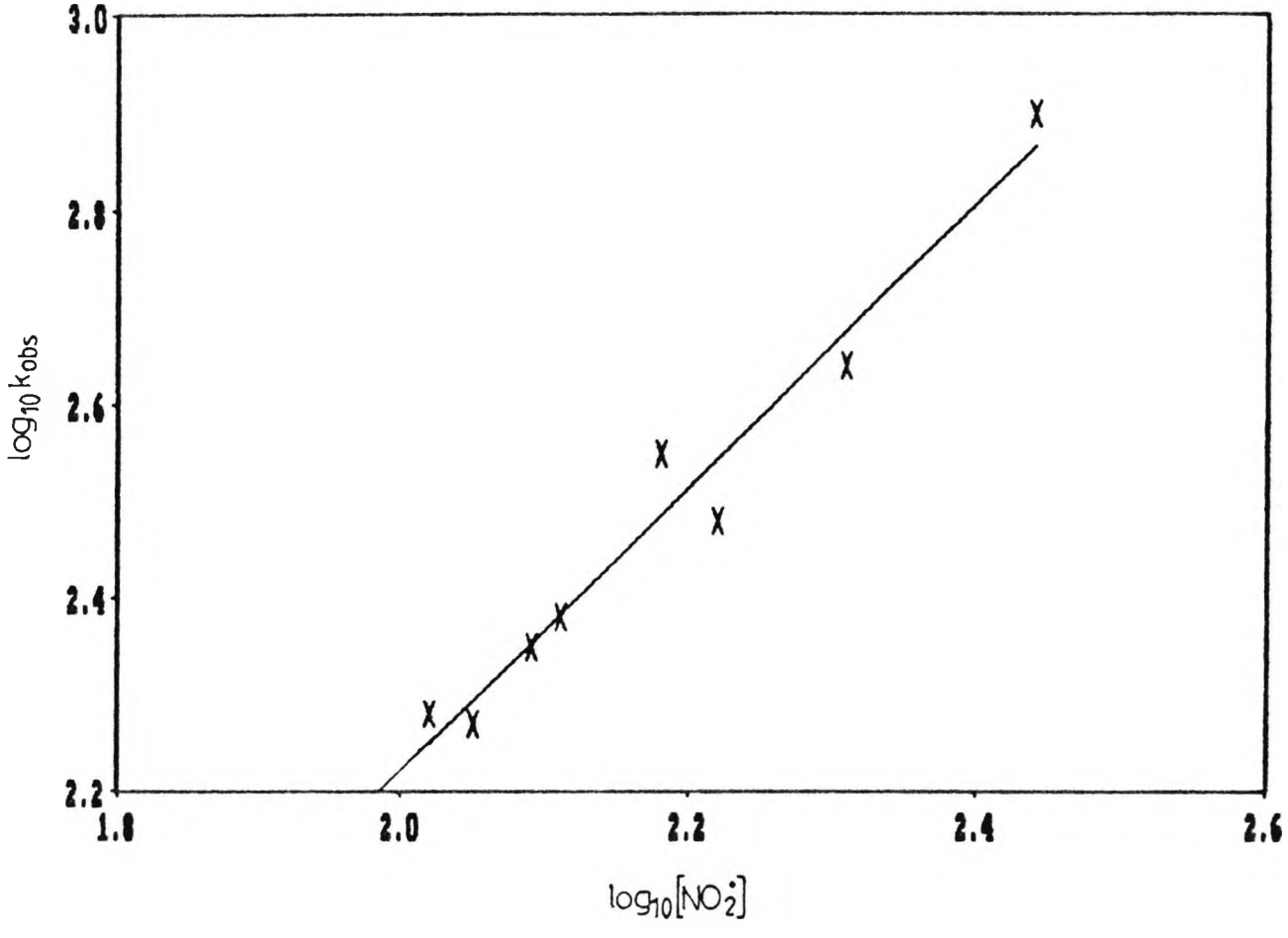

Fig. 2.25: Plot of $\log_{10}k_{obs}$ vs. $\log_{10}[NO_2^{\cdot}]$ for the reaction of 4-phenylbut-1-ene with nitrogen dioxide in cyclohexane at 30°C

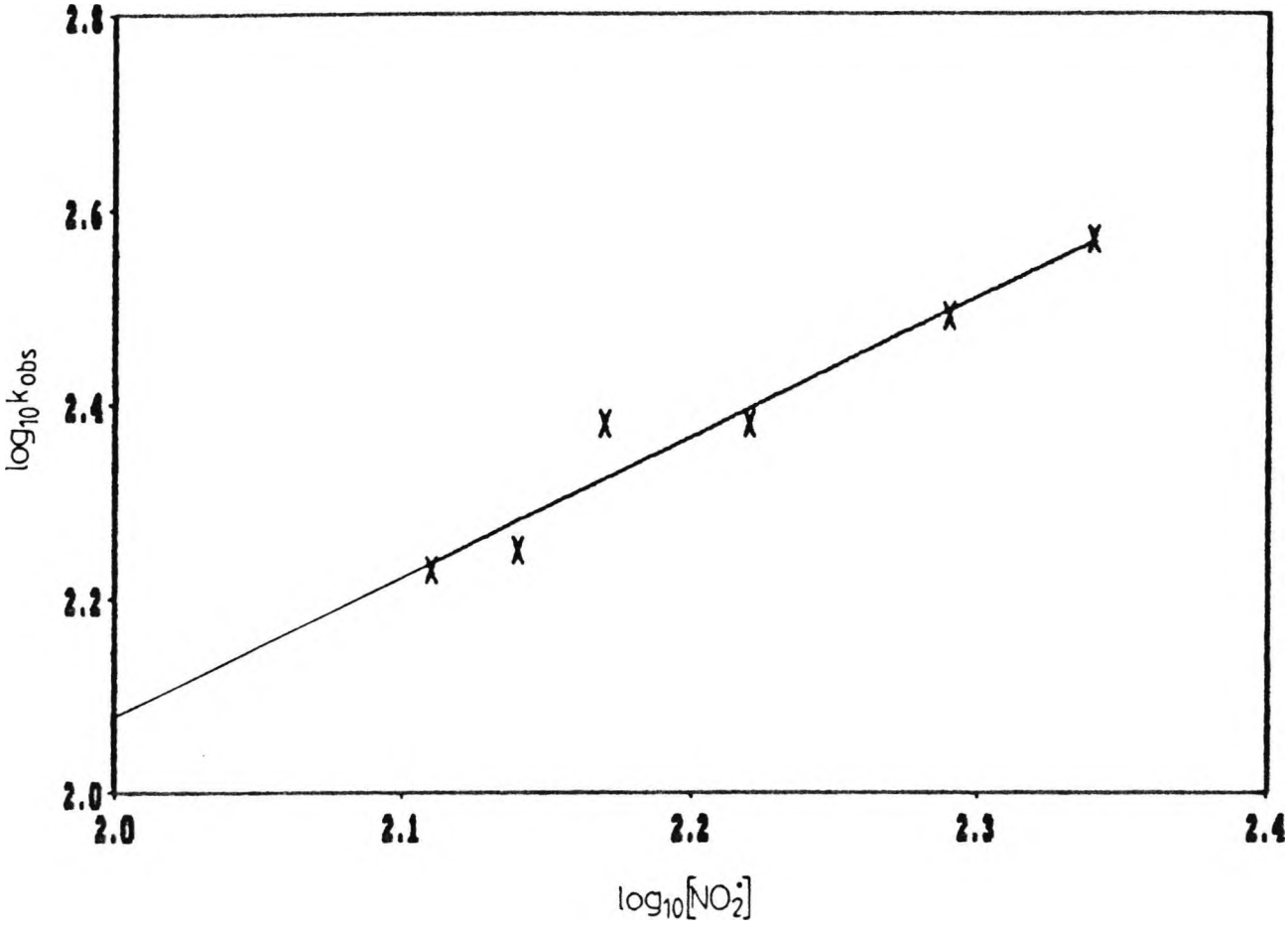

Fig. 2.26: Plot of $\log_{10} k_{obs}$ vs. $\log_{10}[NO_2^{\cdot}]$ for the reaction of 1-dodecene with nitrogen dioxide in cyclohexane at 30°C

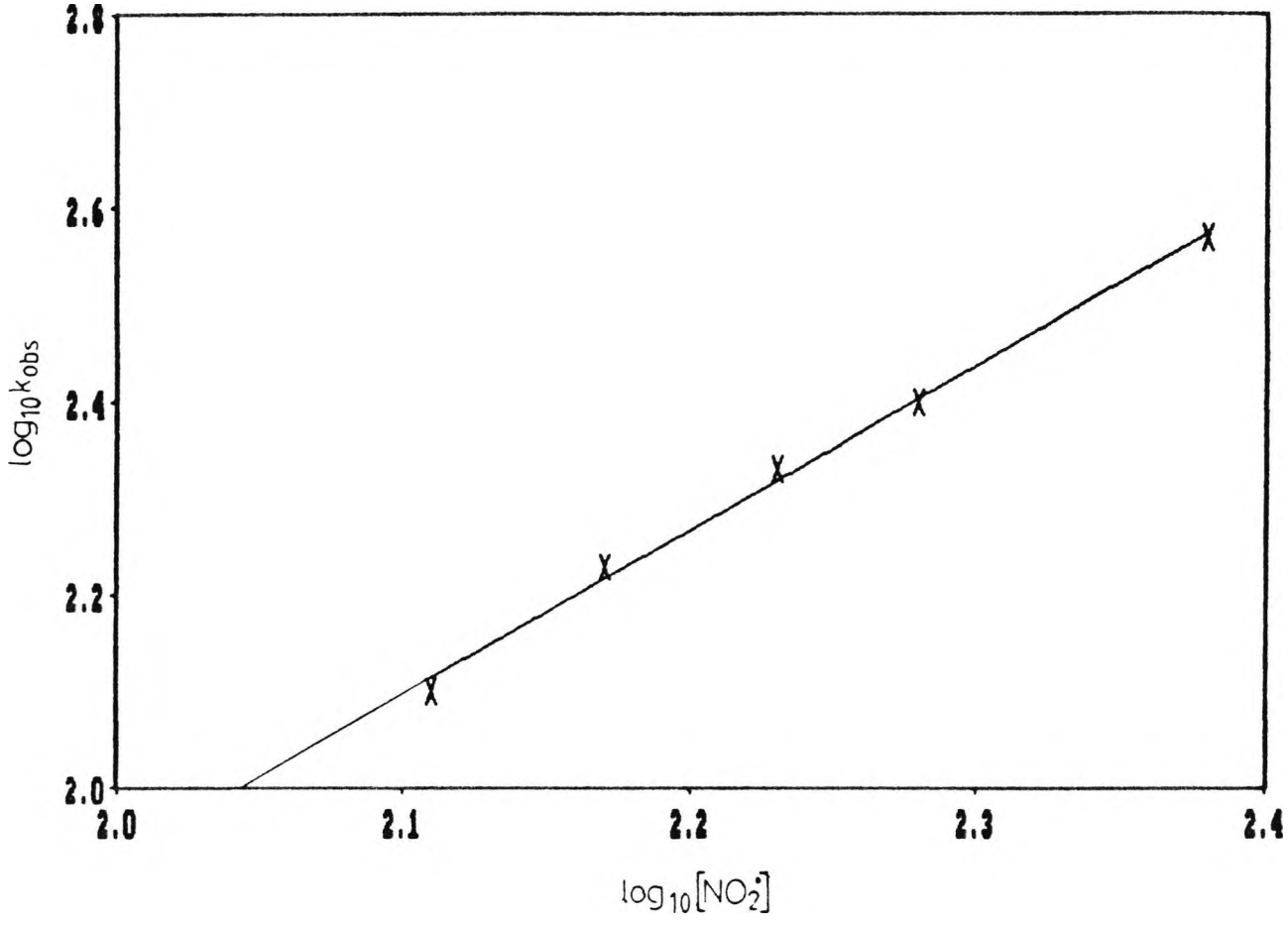

Table 2.12: Variation of $k_{obs}/[NO_2^{\cdot}]$ and k_{CALC} ($k_2[NO_2^{\cdot}] + k_3[NO_2^{\cdot}]^2$) with $[NO_2^{\cdot}]$ for the reaction of allylbenzene with nitrogen dioxide in cyclohexane at 30°C

$10^3[NO_2^{\cdot}]$/mol dm^{-3}	$10^3 k_{obs}$/s^{-1}	$k_{obs}/[NO_2^{\cdot}]$/ mol^{-1}dm^{3}s^{-1}	$10^3 k_{CALC}$/s^{-1}
3.66	1.25	0.342	1.43
4.88	2.28	0.467	2.11
6.06	3.33	0.550	2.87
6.54	2.82	0.431	3.21
7.68	4.17	0.543	4.07
8.18	4.49	0.549	4.48
8.88	5.34	0.601	5.08
9.53	5.25	0.551	5.67

$k_2 = 0.26$ mol^{-1}dm^{3}s^{-1}
$k_2' = 9.20 \times 10^{-3}$ mol^{-1}dm^{3}s^{-1}
$k_3 = 34.8$ mol^{-2}dm^{6}s^{-1}

Fig. 2.27: Plot of $k_{obs}/[NO_2^{\bullet}]$ against $[NO_2^{\bullet}]$ for the reaction of allylbenzene with nitrogen dioxide in cyclohexane at 30°C

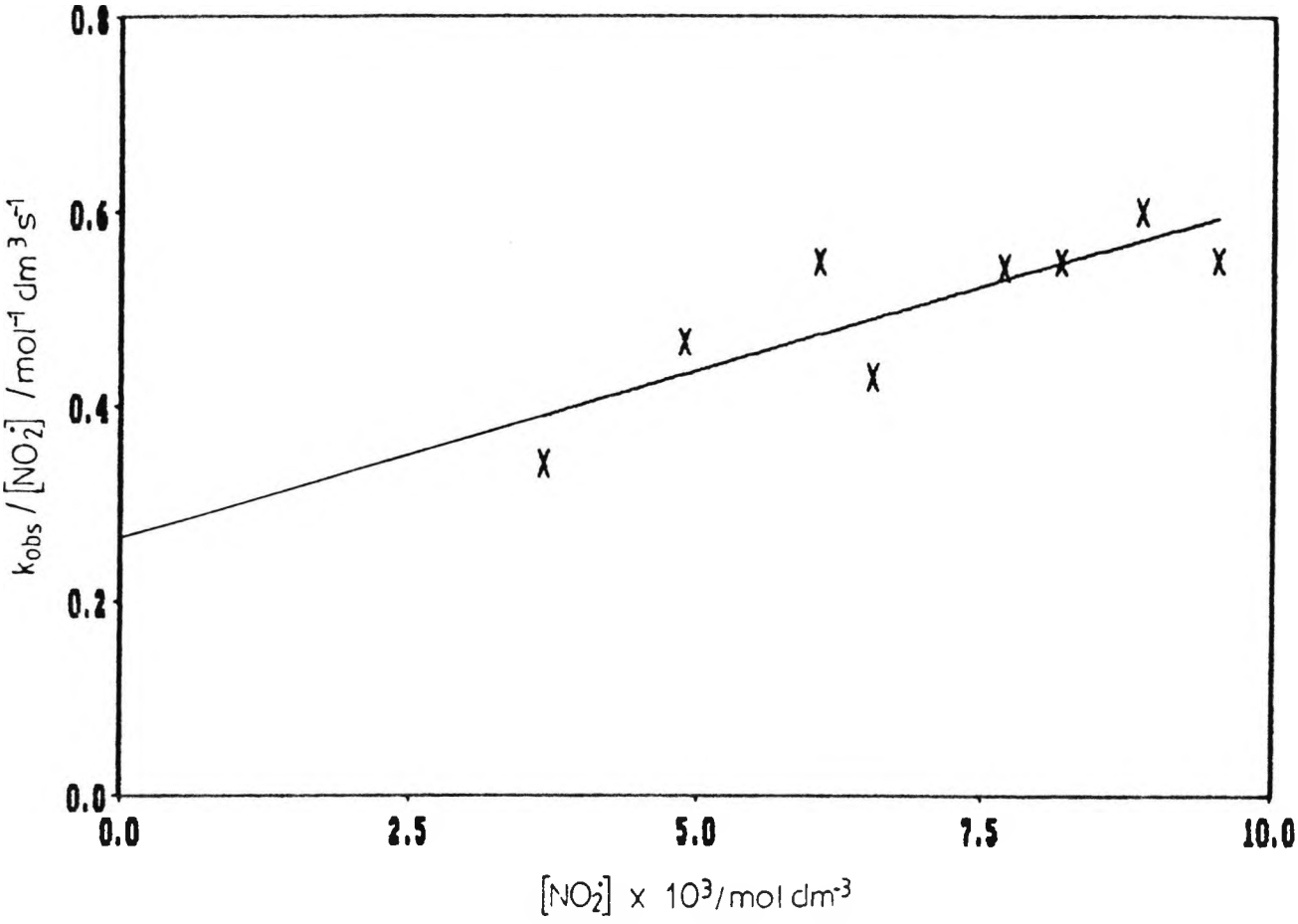

Table 2.13: Variation of $k_{obs}/[NO_2^{\cdot}]$ and k_{CALC} ($k_2[NO_2^{\cdot}] + k_3[NO_2^{\cdot}]^2$) with $[NO_2^{\cdot}]$ for the reaction of 4-phenylbut-1-ene with nitrogen dioxide in cyclohexane at 30°C

$10^3[NO_2^{\cdot}]$/mol dm^{-3}	$10^3 k_{obs}/s^{-1}$	$k_{obs}/[NO_2^{\cdot}]$/ mol^{-1}dm^{3}s^{-1}	$10^3 k_{CALC}/s^{-1}$
4.54	2.67	0.588	2.69
5.08	3.20	0.630	3.14
6.02	4.16	0.691	4.00
6.83	4.16	0.609	4.82
7.27	5.66	0.779	5.29
7.72	5.87	0.760	5.78

k_2 = 0.37 mol^{-1}dm^{3}s^{-1}
k_2' = 1.31 x 10^{-2} mol^{-1}dm^{3}s^{-1}
k_3 = 49.5 mol^{-2}dm^{6}s^{-1}

Fig. 2.28: Plot of $k_{obs}/[NO_2^{\cdot}]$ against $[NO_2^{\cdot}]$ for the reaction of 4-phenylbut-1-ene with nitrogen dioxide in cyclohexane at 30°C

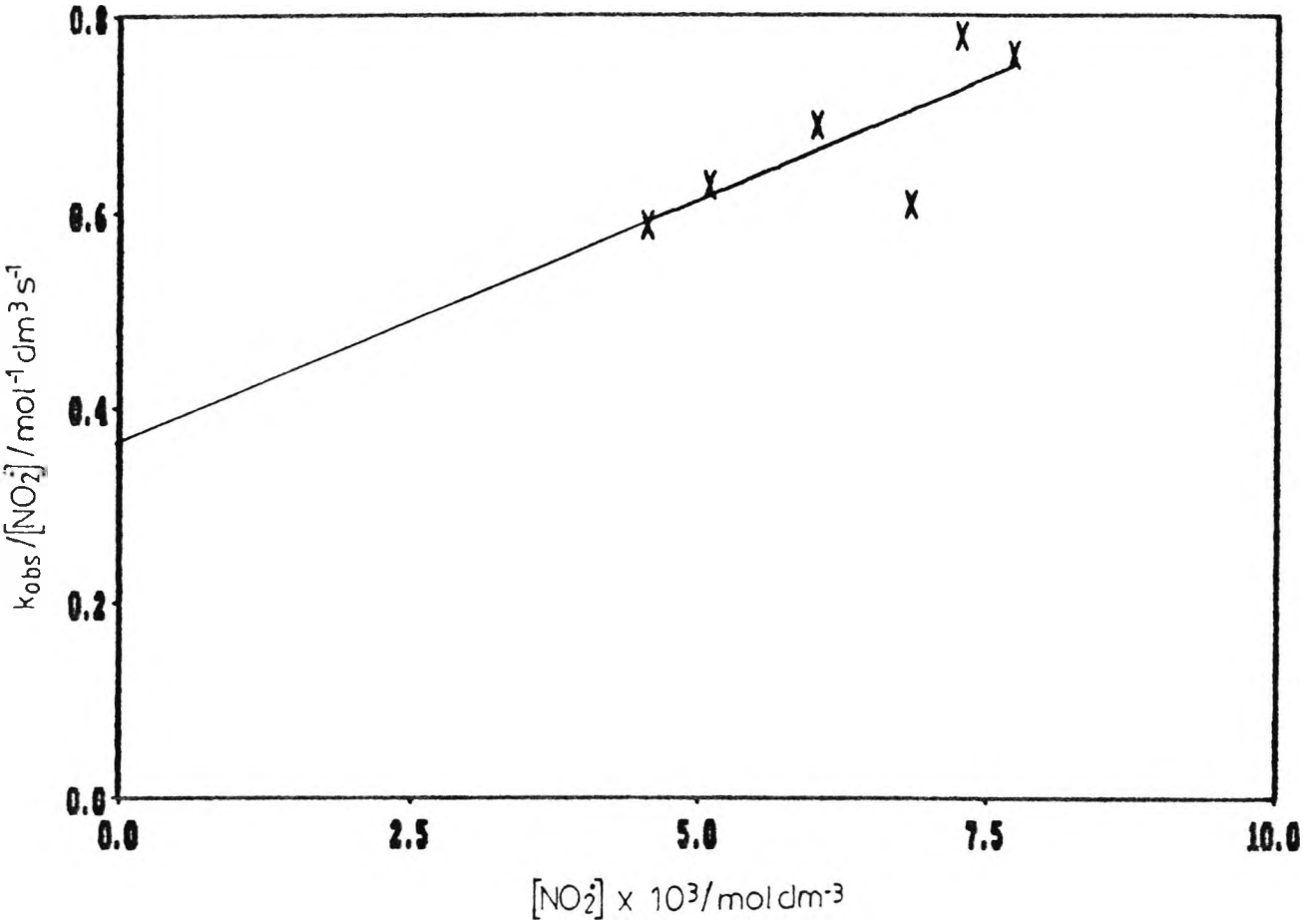

Table 2.14: Variation of $k_{obs}/[NO_2^{\cdot}]$ and k_{CALC} ($k_2[NO_2^{\cdot}] + k_3[NO_2^{\cdot}]^2$) with $[NO_2^{\cdot}]$ for the reaction of 1-dodecene with nitrogen dioxide in cyclohexane at 30°C

$10^3[NO_2^{\cdot}]$/mol dm^{-3}	$10^3 k_{obs}/s^{-1}$	$k_{obs}/[NO_2^{\cdot}]$/ mol^{-1}dm^{3}s^{-1}	$10^3 k_{CALC}/s^{-1}$
4.16	2.72	0.654	2.70
5.23	3.99	0.763	3.93
5.87	4.70	0.801	4.78
6.73	5.90	0.877	6.05
7.75	7.88	1.020	7.74

k_2 = 0.24 mol^{-1}dm^{3}s^{-1}
k_2' = 97.5 mol^{-1}dm^{3}s^{-1}
k_3 = 2.58 x 10^{-2} mol^{-2}dm^{6}s^{-1}

Fig. 2.29: Plot of $k_{obs}/[NO_2^{\cdot}]$ against $[NO_2^{\cdot}]$ for the reaction of 1-dodecene with nitrogen dioxide in cyclohexane at 30°C

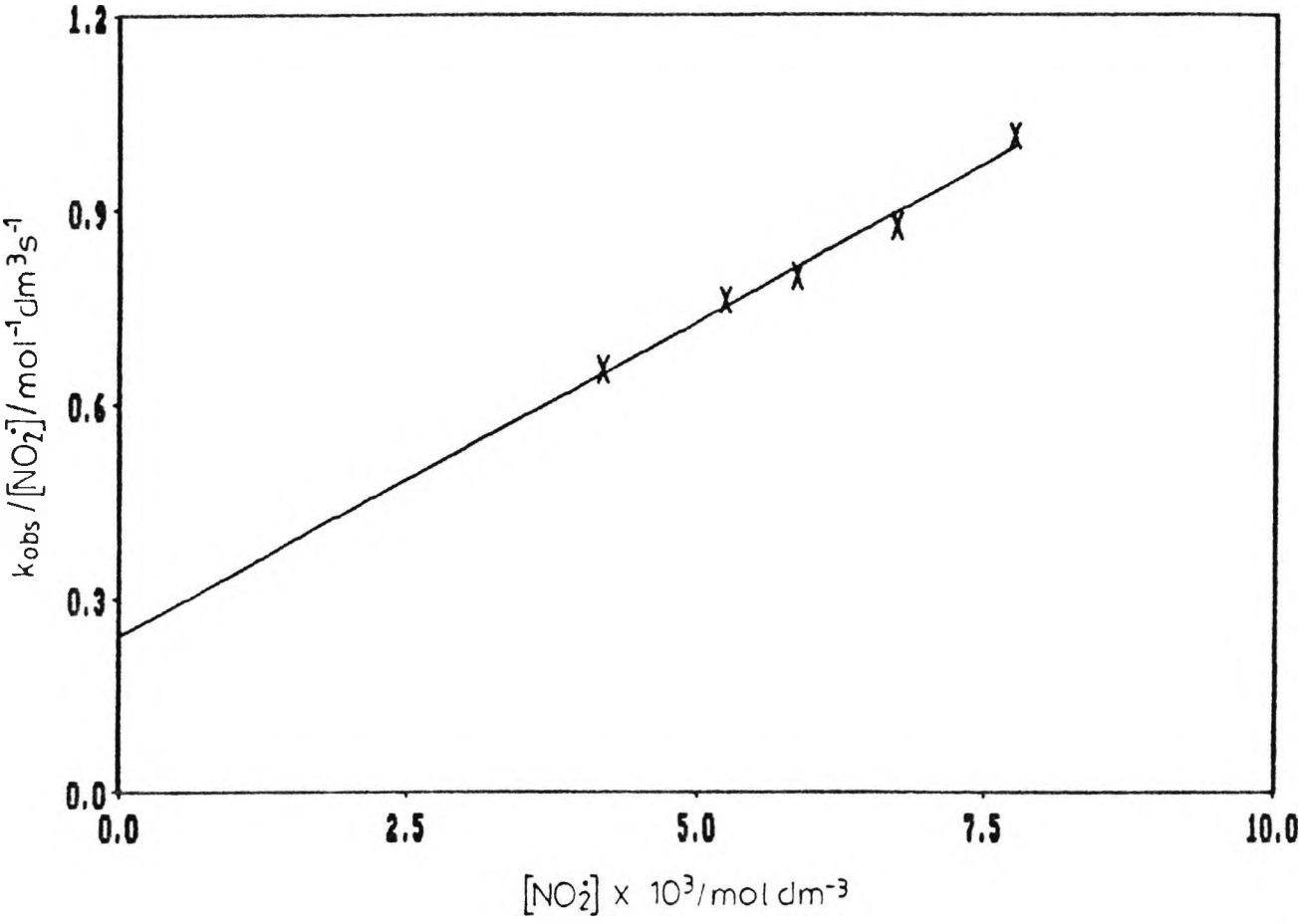

Fig. 2.30: Plot of k_{CALC} against $[NO_2^{\bullet}]$ for the reaction of allylbenzene with nitrogen dioxide in cyclohexane at 30°C

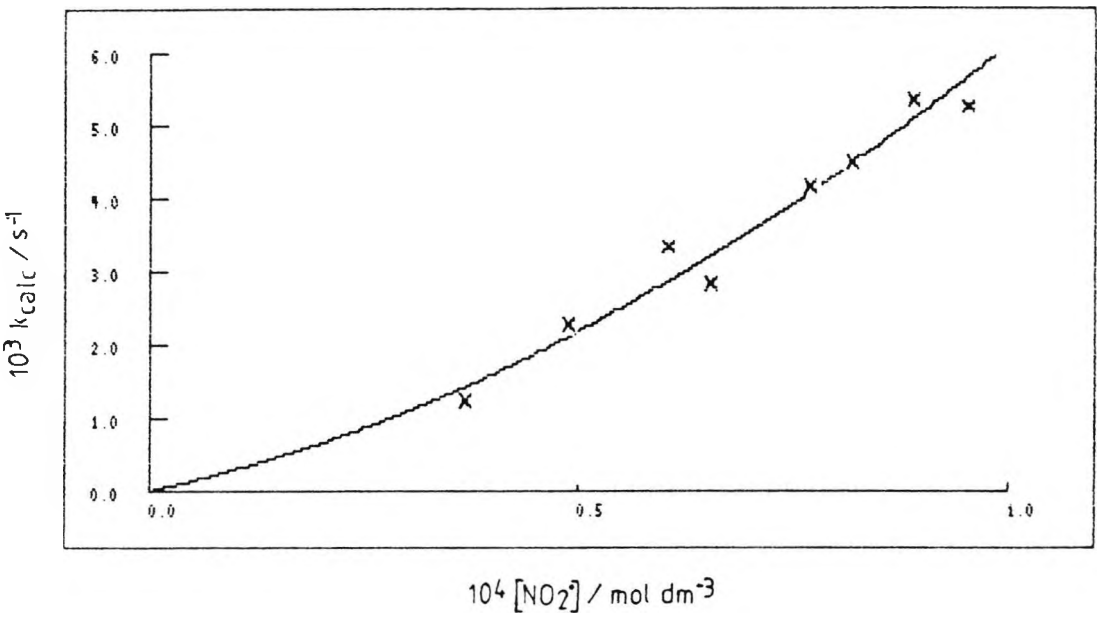

KEY

— CALCULATED DATA

x EXPERIMENTAL DATA

Fig. 2.31: Plot of k_{CALC} against $[NO_2^{\bullet}]$ for the reaction of 4-phenylbut-1-ene with nitrogen dioxide in cyclohexane at 30°C

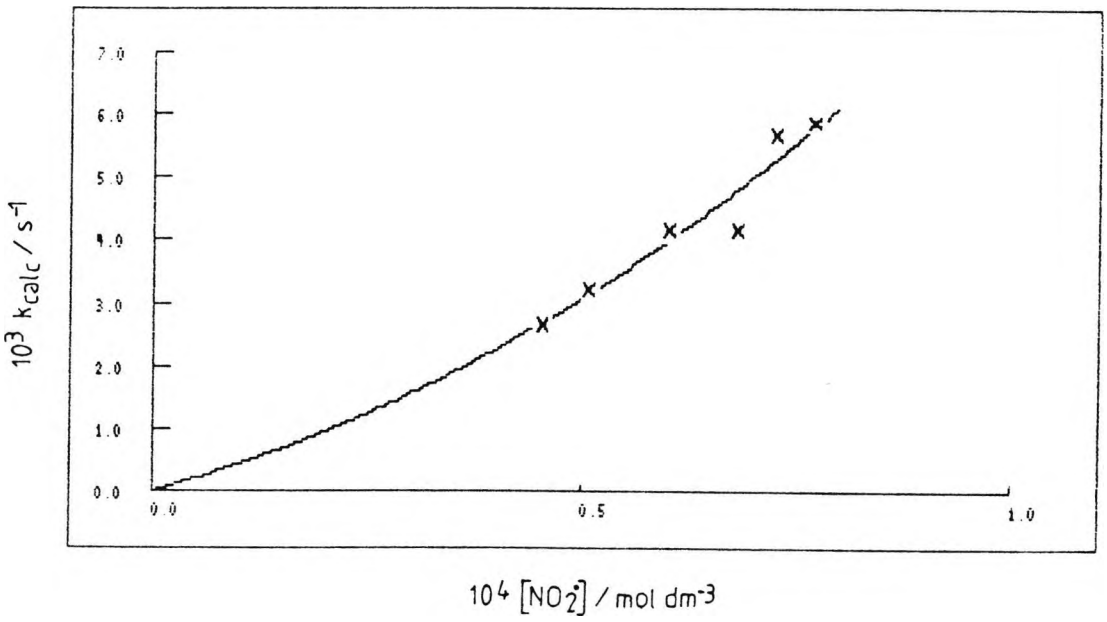

KEY

— CALCULATED DATA

x EXPERIMENTAL DATA

Fig. 2.32: Plot of k_{CALC} against $[NO_2^{\bullet}]$ for the reaction of 1-dodecene with nitrogen dioxide in cyclohexane at 30°C

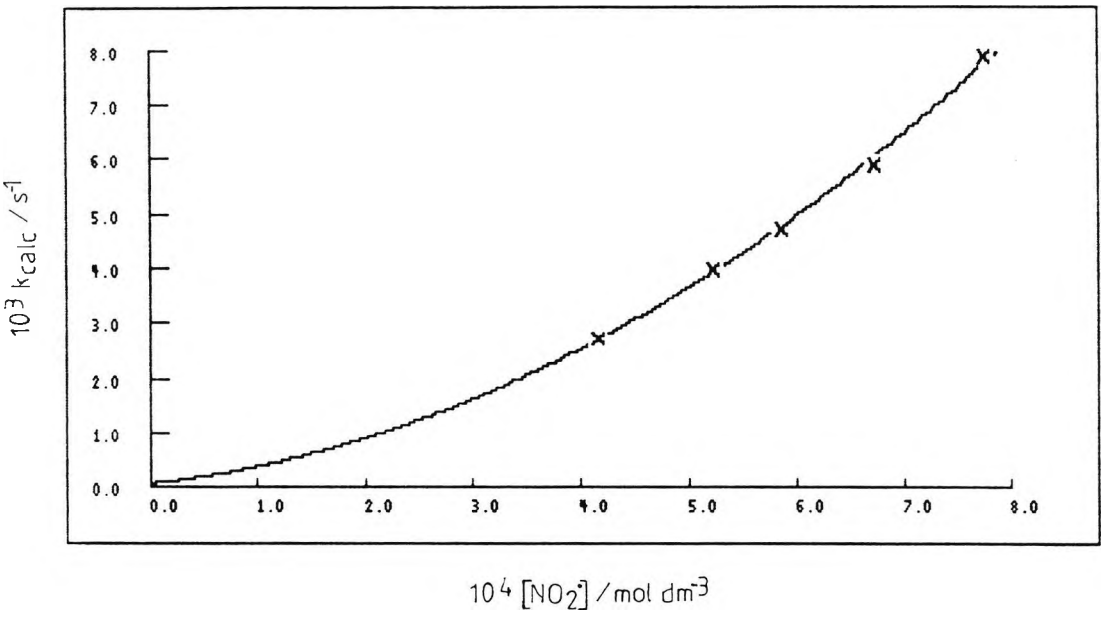

2.4.1 Discussion of related work[42]

Pryor and co-workers have also investigated the kinetics of the reactions of alkenes with nitrogen dioxide in aprotic solvents by stopped-flow spectroscopy,[42] and a discussion of this work serves as a useful comparison to the present study. The course of the reactions was followed by monitoring the loss of $NO_2^{\cdot}$ at 410 nm over a time course in which less than 10% of the $NO_2^{\cdot}$ was consumed. For some runs the reactions were followed to completion with excess alkene. The rates were calculated as $^1/_2 d[N(IV)]^*/dt$,[98] since the stoichiometry of the reactions is 2:1 $NO_2^{\cdot}$ to alkene.

Reaction orders were determined with initial rate based on the expression shown in equation 2.14, where m and n represent the order in alkene and $NO_2^{\cdot}$ respectively.

$$^1/_2 d[N(IV)]/dt = k[Alkene]^m[NO_2^{\cdot}]^n \qquad (2.14)$$

When the nitrogen dioxide concentration was held constant, the calculated reaction orders in alkene for 2,3-dimethylbut-2-ene, cyclohexene and hex-1-ene were found to be 1. At 30°C in CCl_4, and at high N(IV) (i.e.> 0.05M), the order in $NO_2^{\cdot}$ was 2 for 2,3-dimethylbut-2-ene, hex-1-ene, 3,3-dimethylbut-1-ene and cyclohexene. The rates of reactions of the last three substrates listed were measured over a wider range of nitrogen dioxide concentrations, from less than 10^{-4}-0.76 M N(IV). Representative data, collected for "single runs in which $NO_2^{\cdot}$ concentrations and rates were determined for successive small portions of the curves",[42] are illustrated in Fig. 2.33. For these substrates, the order in $NO_2^{\cdot}$ was near 2 at high $NO_2^{\cdot}$ (>10^{-3}M) and decreased to 1 as the concentration of $NO_2^{\cdot}$ was decreased (<10^{-4}M).

*N.B. N(IV) represents the quantity $[NO_2^{\cdot}] + 2[N_2O_4]$

Fig. 2.33: A plot of $\log_{10}[NO_2^{\cdot}]$ versus the $\log_{10}$ of the initial rate for 0.50M cyclohexene (circles) and 0.77M 3,3-dimethylbutene (squares), in CCl_4 at 30°C. The solid lines represent hypothetical lines that would indicate that the reactions were first order (slope=1) and second order (slope=2) in $NO_2^{\cdot}$

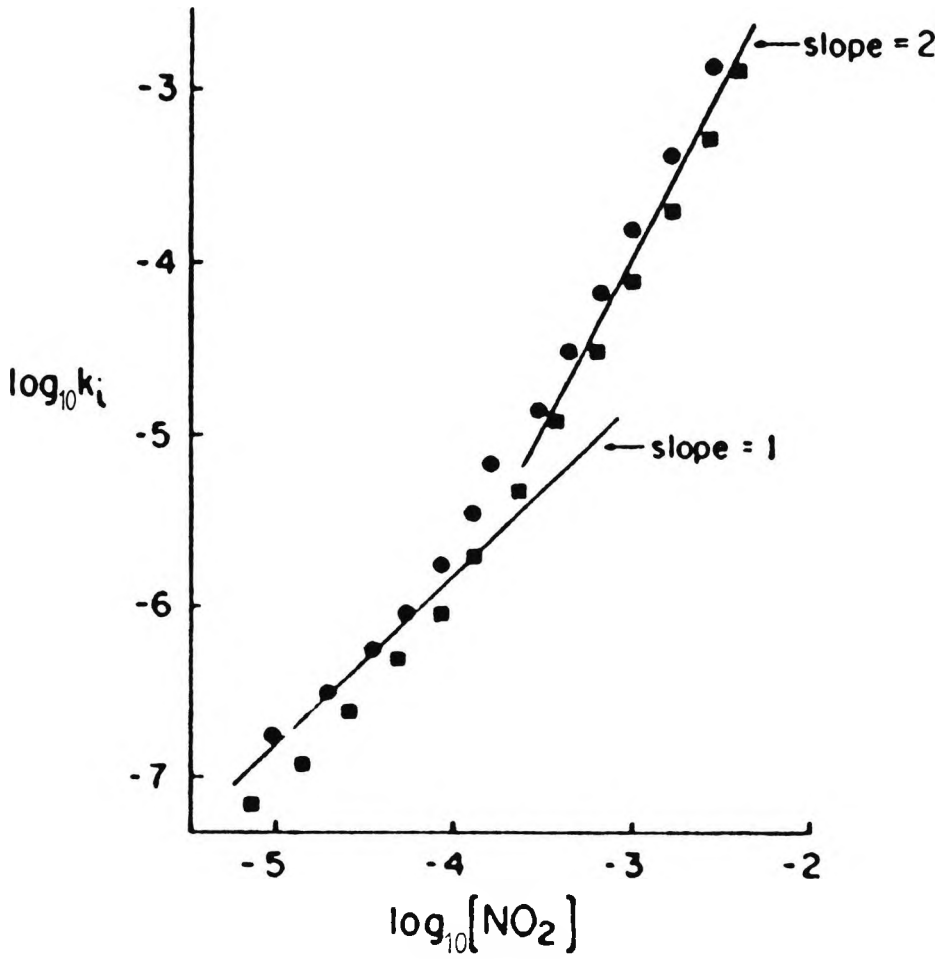

The simplest expression that fitted the data is shown in equation 2.15.

$$-{}^{1}/_{2}d[N(IV)]/dt = k_1[Alkene][NO_2^{\cdot}] + k_2[Alkene][NO_2^{\cdot}]^2 \quad (2.15)$$

and later discussion considered only reactions that exhibited first-order or second-order dependence on the $NO_2^{\cdot}$ concentration. The results of multiple-regression analyses of the data as a function of $[NO_2^{\cdot}]$ and $[NO_2^{\cdot}]^2$ are collected in Table 2.16.

The order in $NO_2^{\cdot}$ was also determined for a conjugated diene, 2,5-dimethyl-2,4-hexadiene, at high N(IV). Data collected at three N(IV) concentrations (0.02, 0.035 and 0.23 M) indicated that the order of the reaction in $NO_2^{\cdot}$ was 1.

Data were also collected at 30°C at high N(IV) concentrations in CCl_4 for some other alkenes. Generally, only a single set of concentrations was used, and the rate constant was calculated assuming that the reactions were first-order in alkene and second-order in $NO_2^{\cdot}$. These rate constants are given in Table 2.17.

Relative rates of reaction were determined by g.l.c. at high N(IV) concentrations for a number of substrates in CCl_4, hexane and CH_2Cl_2, and these are presented relative to allylbenzene in Table 2.18. Each value represents the average of at least three determinations; "if three runs did not agree to within 10%, one to three additional replicates were performed, and the average of all runs was reported."[42]

Table 2.16:Absolute rates of reaction of alkenes toward N(IV)[a]

substrate	$k_2, M^{-2}s^{-1}$	$k_1, M^{-1}s^{-1}$
hex-1-ene	$230 \pm 30 (190 \pm 7)$	(0.17 ± 0.07)
cyclohexene	$380 \pm 50 (318 \pm 13)$	(0.63 ± 0.12)
3,3-dimethylbut-1-ene	$77 \pm 10 (76 \pm 1)$	(0.02 ± 0.002)

Table 2.17: Absolute rates of reaction of alkenes toward N(IV)[a]

substrate	$k_2, M^{-2}s^{-1}$	$k_1, M^{-1}s^{-1}$
allyl cyanide	40 ± 10	
allyl chloride	60 ± 10	
allylbenzene	125 ± 10	
cyclopentene	530 ± 30	
1,4-hexadiene	1230 ± 150[b]	
norbornene	2100 ± 300	
2-methylpent-2-ene	2550 ± 150	
2,3-dimethylbut-2-ene	4350 ± 500	
2,5-dimethyl-2,4-hexadiene		18500 ± 800[c]

[a] These values were measured at 30°C in CCl_4, in the presence of at least 50 mM N(IV). The given error limits are ± 1 standard deviation; values in parentheses are calculated by a multiple-regression analysis from rates determined at several concentrations. See the text for details.

[b] This value was measured in the presence of 3mM total N(IV).

[c] This reaction is first-order in $NO_2^{\bullet}$.

Table 2.18: Relative rates of reaction of alkenes with high concentrations of N(IV)[a]

	solvent		
	CCl_4	CH_2Cl_2	hexane
allyl cyanide	0.1 ± 0.03	0.06 ± 0.01	0.4 ± 0.05
3,3-dimethyl-3-phenyl -propene	0.3 ± 0.02		
allyl chloride	0.3 ± 0.1		
3,3-dimethylbut-1-ene	0.6 ± 0.2		
allyl bromide	0.8 ± 0.1	0.6 ± 0.1	0.8 ± 0.1
allylbenzene	1.0	1.0	1.0
oct-1-ene	1.8 ± 0.1	2.4 ± 0.1	1.7 ± 0.1
hex-1-ene	2.3 ± 0.3		
methyl oleate	2.6 ± 0.1	3.6 ± 0.3	2.4 ± 0.1
cyclooctene	4.5 ± 0.3	6.4 ± 0.4	5.3 ± 0.1
α-pinene	13.0 ± 3.0	39.0 ± 1.5	16.0 ± 2.0
β-pinene	15.0 ± 3.5	40.0 ± 4.0	21.0 ± 3.0
norbornene	21.0 ± 3.5	74.0 ± 9.0	33.0 ± 4.0
2-methylpent-2-ene	16.0 ± 4.0		

[a] All results were measured at ambient temperatures in the solvent indicated, in the presence of greater than 0.1M total N(IV). Error limits are ±1 standard deviation. See the text for a discussion of experimental error.

[b] All values are reported relative to allylbenzene.

A more limited number of relative rates were determined at low concentrations of N(IV) with CCl_4 as the solvent. The substrates used, as well as the relative rates measured at high and at low N(IV), are compiled in Table 2.19.

Table 2.19: Relative rates of reactions in CCl_4 at high and low N(IV) concentrations[a]

substrates	high N(IV)	low N(IV)
diphenylmethane/oct-1-ene	<0.01	0.05
triphenylmethane/oct-1-ene	<0.02	0.25
allylbenzene/oct-1-ene	0.55(0.4)[b]	0.70 (0.5)[b]
allylbenzene/cycloctene	0.22	0.37
allylbenzene/3,3-dimethyl-3-phenyl-propene	3.0	4.3

[a] All values are $\pm$ 15%.

[b] The values in parentheses were obtained with dichloromethane as the solvent.

The rates of reaction of alkenes with high concentrations of N(IV) were measured both as absolute rates (Tables 2.16 and 2.17) and as relative rates versus allylbenzene (Table 2.18). Although experimental errors were often large and the relative rate determinations were not thermostatted, there is fairly good agreement between Tables 2.16-2.17 and 2.18.

Pryor[42] suggests that the data collected at high N(IV) concentrations for simple alkenes are consistent with a radical addition mechanism involving N_2O_4:

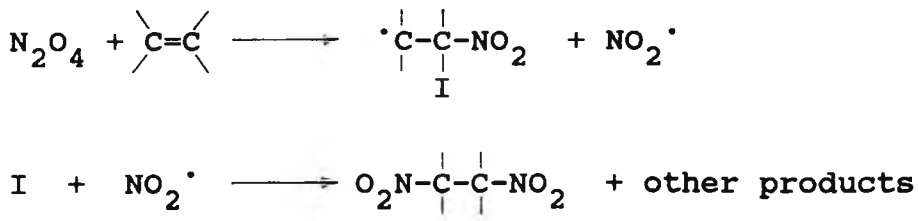

Scheme 2.6

The radical addition of N_2O_4 would be expected to be first-order in alkene and first-order in N_2O_4 (≡ second-order in $NO_2^{\bullet}$). Radical addition of $NO_2^{\bullet}$, which has been observed in the gas phase, was excluded from consideration since it should be first-order in $NO_2^{\bullet}$.

Evidence against other reactions of alkenes with N_2O_4, such as an electrophilic addition mechanism with a cationic intermediate, has been presented earlier.[30,35-37,92] This work also provided evidence against an ionic mechanism. The rate of reaction of norbornene relative to the rates of other alkenes did not support the presence of a cationic intermediate : no large rate acceleration was observed for the reaction of norbornene, although it would give a highly stabilized norbornyl cation. In addition, the differences in relative rates in the solvents studied were said to be too small to support an ionic mechanism. However, in the absence of knowledge of absolute rates this evidence is not convincing.

At lower concentrations of N(IV), an apparent increase in reactivity of the alkenes, over that expected, was observed. As shown in Fig. 2.33, the $\log_{10}$ of the initial rate does not change linearly with the $\log_{10}$ of the $NO_2^{\cdot}$ concentration. Rather, the slope is near 2 at high $NO_2^{\cdot}$ concentrations and approaches 1 as the concentration is lowered. Two possibilities were proposed to account for the kinetic order in $NO_2^{\cdot}$ in dilute solutions moving from second-order to first-order. The first was a radical addition mechanism involving $NO_2^{\cdot}$ rather than N_2O_4 in the rate-determining step. This appears to be the course of the reaction in the gas phase, and might be observed in solution at very dilute N(IV) where the concentration of $NO_2^{\cdot}$ exceeds that of N_2O_4.

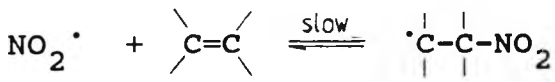

(2.16)

The second mechanism proposed was a hydrogen atom abstraction pathway which could compete with radical addition. This pathway was considered to be more favourable in solution than radical addition, and was used to account for part of the reduction of the order in $NO_2^{\cdot}$ at low N(IV) concentrations, based on the alleged increased reactivity of substrates with no olefin double bonds but readily abstractable H atoms.

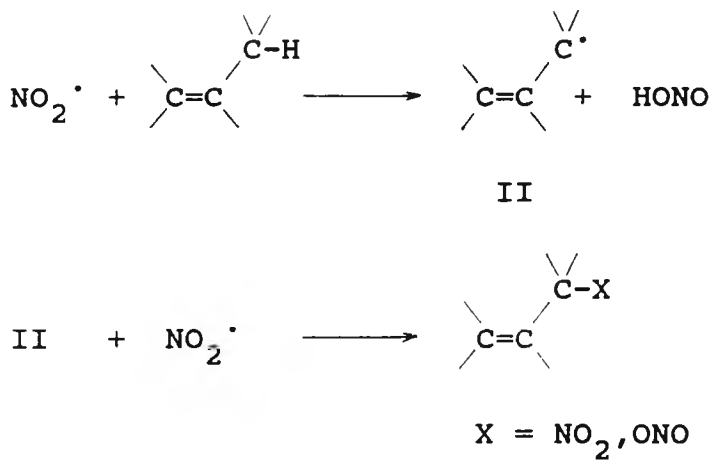

Scheme 2.7

There are, however, several disturbing points about this study. The authors[42] recognised the presence of the $NO_2^{\cdot}/N_2O_4$ equilibrium, but the reactions were made artifically fast by

the use of high concentrations of alkene and therefore had to be followed by stopped-flow spectroscopy. The rates were calculated usually over only 10% of reaction and although some runs were followed to completion, the details of only two of these experiments were reported; there is little kinetic information on the later stages of reaction.

More importantly, the data in Fig. 2.33 for the reactions in which a change from first-to second-order in $[NO_2^{\cdot}]$ was observed, were based not on a series of experiments but on "single runs in which $NO_2^{\cdot}$ concentrations and rates were determined for successive small portions of the curve".[42] N.B. Fig. 2.33 is actually a plot of $\log_{10}[NO_2^{\cdot}]$ versus the $\log_{10}$ of the rate of the reaction. The title and legend for this diagram, however, describe it as a plot of $\log_{10}[NO_2^{\cdot}]$ versus the $\log_{10}$ of the <u>initial</u> rate. The second-order rate coefficients, k_1 for the reactions of cyclohexene (0.50M) and 3,3-dimethylbut-1-ene (0.77 M) with nitrogen dioxide were calculated as 0.63 $mol^{-1}dm^3s^{-1}$ and 0.02 $mol^{-1}dm^3s^{-1}$ respectively (Table 2.16). This is a very large difference and must be very sensitive to the accuracy of the results, since the graphical data represented in Fig. 2.33 for these two substrates appear to be very similar. Likewise, the difference in the third-order rate coefficients, k_2, for cyclohexene and 3,3-dimethylbut-1-ene is also significant (380 $mol^{-2}dm^6s^{-1}$ compared to 77 $mol^{-2}dm^6s^{-1}$). 2,3-dimethylbut-2-ene is a factor of 56 more reactive than 3,3-dimethylbut-1-ene towards N_2O_4. This result seems difficult to accept when the relative rates for electrophilic bromination of these two compounds, which involves cationic stabilisation, are only 7:1.[99] The kinetics of reaction of $[NO_2^{\cdot}]$ with 2,5-dimethyl-2,4-hexadiene could not be accounted for by any of the mechanisms discussed above, since this reaction appeared to be first-order in $NO_2^{\cdot}$ even at high nitrogen dioxide concentrations. The first-order rate coefficent obtained is also abnormally high and it is difficult to ascribe this to H abstraction. A possible explanation for the effect seen in Fig. 2.33 could be the increased proportion of $NO_2^{\cdot}$ in solution at low N(IV) concentrations, which would lead to radical addition of $NO_2^{\cdot}$ becoming more important than addition of N_2O_4.

At high N(IV) concentrations, the possibility of a two stage $NO_2^{\bullet}$ reaction, with the second step being rate-limiting, should have been considered since this would lead to a second-order dependence of rate on $NO_2^{\bullet}$.

To further test the likelihood of allylic hydrogen atom abstraction competing with radical addition, a relative reactivity study was carried out using low levels of N(IV) with substrates of differing ease of allylic hydrogen atom abstraction (Table 2.19). It should be noted that these reactions were not thermostatted, and although the authors[42] state that a clear trend emerges, this is difficult to see as compounds such as allylbenzene were not considerably more reactive at low N(IV) - relative rate of reaction for allylbenzene/1-octene was 0.55 at high N(IV) cf. value of 0.70 at low N(IV).

The most significant anomaly arises for the reaction of 3,3-dimethylbut-1-ene with nitrogen dioxide. This substrate appears to react in an analogous way to cyclohexene and yet does not have allylic hydrogen atoms. According to Table 2.16, the k_1 value for this substrate is substantially smaller than that of cyclohexene. The similarity of the experimental curves in Fig. 2.33, however, must make one question this result, which if correct, indicates that there is an extreme sensitivity to experimental error.

We conclude that evidence is presented for a second-order dependence on $[NO_2^{\bullet}]$ at high N(IV). The evidence presented for a change to a first-order dependence at low N(IV) is less convincing, based apparently on single runs followed over concentration changes in $[NO_2^{\bullet}]$ of 3 orders of magnitude, with large concentrations of products building in the solutions. There seems to be no compelling evidence for allylic H abstraction being responsible for any change in order and the relative rates reported for the dimethylbutenes, cf. polar bromination, are difficult to ascribe to a free radical addition mechanism.

A plot of $\log_{10}[NO_2]$ versus the $\log_{10}$ of the rate for the reaction of allylbenzene (0.5 mol dm^{-3}) with nitrogen dioxide in cyclohexane at 30°C was constructed using the rate coefficients determined in the present study (Fig. 2.34). A comparison of this plot with Pryor's results shown in Fig. 2.33 for cyclohexene is given below. Rates were calculated according to equation 2.4 over the NO_2 concentration range 10^{-2} - 10^{-5} mol dm^{-3} (Table 2.20).

$$\frac{-d[Alkene]}{dt} = k_2[Alkene][NO_2^{\cdot}] + k_3[Alkene][NO_2^{\cdot}]^2 \qquad (2.4)$$

where $k_2 = 0.26$ mol^{-1}dm^{3}s^{-1}
$k_3 = 34.8$ mol^{-2}dm^{6}s^{-1}
and [Allylbenzene] = 0.5 mol dm^{-3}

As shown in Fig. 2.34, the rates of the reaction of allylbenzene with nitrogen dioxide are approximately ten-fold higher than those of the reaction of cyclohexene with nitrogen dioxide. The $\log_{10}$ of the rate does not change linearly with the $\log_{10}$ of the $NO_2^{\cdot}$ concentration. The slope is 1.3 at high $NO_2^{\cdot}$ concentrations and approaches 1.0 as the concentration of $NO_2^{\cdot}$ is lowered. The change in slope occurs at a similar $NO_2^{\cdot}$ concentration to Fig. 2.33 (5.6×10^{-4} cf. 3×10^{-4}) and at a higher $\log_{10}$ rate (-4.2 cf. -5.2). The two sets of data show some similarities but significant differences, and it is reasonable to attribute these to the experimental method used by Pryor, as described above.

Table 2.20: Change in rate with $[NO_2^{\bullet}]$ for the reaction of allylbenzene (0.50M) with nitrogen dioxide in cyclohexane at 30°C

$[NO_2^{\bullet}]$	$\log_{10}[NO_2]$	$\log_{10}(-d[Alkene]/dt)$
1×10^{-5}	-5.0	-5.89
2×10^{-5}	-4.7	-5.58
4×10^{-5}	-4.4	-5.28
6×10^{-5}	-4.2	-5.10
8×10^{-5}	-4.1	-4.98
1×10^{-4}	-4.0	-4.88
2×10^{-4}	-3.7	-4.57
4×10^{-4}	-3.4	-4.26
6×10^{-4}	-3.2	-4.07
8×10^{-4}	-3.1	-3.94
1×10^{-3}	-3.0	-3.83
2×10^{-3}	-2.7	-3.48
4×10^{-3}	-2.4	-3.10
6×10^{-3}	-2.2	-2.86
8×10^{-3}	-2.1	-2.67
1×10^{-2}	-2.0	-2.52

[Alkene] = 0.50M

Fig. 2.34 Plot of $\log_{10}[NO_2]$ versus the $\log_{10}$ of the rate for the reaction of allylbenzene (0.50M) with nitrogen dioxide in cyclohexane at 30°C (LEAST SQUARES FIT)

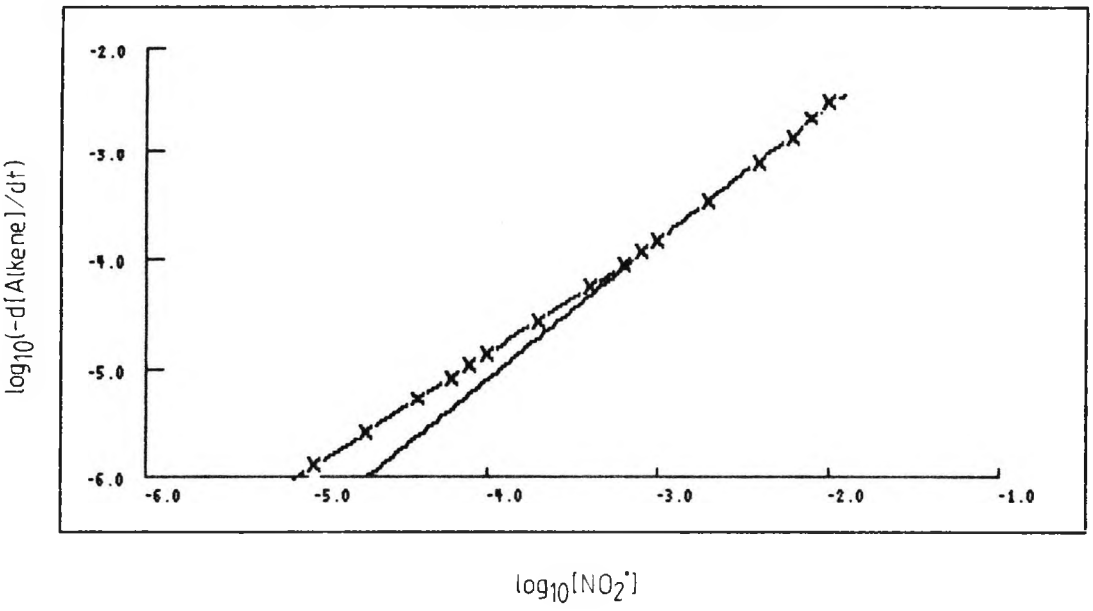

C H A P T E R 3

PRODUCT STUDIES OF THE REACTIONS OF STYRENE, ALLYLBENZENE, 4-PHENYLBUT-1-ENE AND 1-DODECENE WITH NITROGEN DIOXIDE

3 Product studies of the reactions of styrene, allylbenzene, 4-phenylbut-1-ene and 1-dodecene with nitrogen dioxide

3.1 Introduction

A wide variety of separation (TLC, GLC, GC/EIMS, GC/CIMS) and spectroscopic techniques (I.R., ^{1}H n.m.r., ^{13}C n.m.r., ^{15}N n.m.r.) have been used to aid product analysis for the reactions of styrene, allylbenzene, 4-phenylbut-1-ene and 1-dodecene with nitrogen dioxide. The results from these experiments and interpretations of the various spectra obtained are given in the following chapter.

In addition, the reaction of allylbenzene with 10,000 ppm and 50 ppm gaseous nitrogen dioxide has been studied in order to establish the nature of products under these conditions, and to detect the presence or absence of allylic substitution products at low concentrations of nitrogen dioxide.

3.2 Experimental

3.2.1 Preparation of product mixtures from the reactions of styrene, allylbenzene, 4-phenylbut-1-ene and 1-dodecene with nitrogen dioxide

A solution of nitrogen dioxide in cyclohexane (100 ml) was made up and thermostatted in a waterbath at 30°C for 15 min. A known quantity of alkene was added to the nitrating solution by microsyringe and the mixture was thoroughly shaken. After a 1 h reaction period, the cyclohexane was removed on a rotary evaporator and replaced with a suitable solvent for analysis.

The following additional experiments were carried out on the reaction of allylbenzene with nitrogen dioxide.

3.2.2 I.R. studies of the reaction of allylbenzene with nitrogen dioxide

A solution of nitrogen dioxide in carbon tetrachloride was made up and allylbenzene added. An aliquot of this reaction mixture was removed immediately and injected into a sealed, fixed path length NaCl cell. The reaction was followed in a Perkin Elmer 983G infrared spectrophotometer, with spectra being recorded at periodic intervals.

3.2.3 Reaction of allylbenzene with ^{15}N-labelled nitrogen dioxide

$$PbO + 2H^{15}NO_3 \longrightarrow Pb(^{15}NO_3)_2 + H_2O$$

$$Pb(^{15}NO_3)_2 \longrightarrow {}^{15}N_2O_4 + PbO_2$$

Powdered litharge was added gradually to a boiling solution of nitric acid (1.2 ml, 40%, 98 atom % ^{15}N) with constant stirring, until an excess remained. The solution was filtered whilst hot in order to remove residual lead oxide, and the filtrate was placed on a rotary evaporator to remove water.

The white crystalline product obtained was further dried in an oven overnight.

The lead nitrate was heated using a bunsen burner. After about one minute brown fumes of gaseous nitrogen dioxide were given off and were passed directly into cyclohexane where they dissolved. Heating was continued until no more nitrogen dioxide bubbles could be seen to be entering the solvent.

The initial concentration of nitrogen dioxide was measured at 25.4 ± 0.1°C in a Perkin Elmer Lambda-5 spectrophotometer. Allylbenzene was added to the nitrating solution via a microlitre syringe, and the mixture was then heated in a waterbath at 30°C for 1.5 h. Subsequent evaporation of the solvent led to the formation of a viscous liquid. This was separated into its various components by preparative t.l.c. (70% ethylacetate:ether). Acetone was used as the work-up solvent. Thus, ^{15}N-labelled samples of the crude product mixture and the major component of this mixture were generated.

3.2.4 Reaction of allybenzene with 10000 ppm and 50 ppm gaseous nitrogen dioxide

A solution of allylbenzene in cyclohexane was placed in a two-necked flask fitted with a condenser, purged with N_2, exposed to 10000 ppm gaseous nitrogen dioxide/N_2 for 2 h at 30°C, and purged again with N_2 (to remove any unreacted nitrogen dioxide). After the final purging, the reaction solution was transferred to a 100 ml flask. The solvent was removed on a rotary evaporator and replaced with a small volume of methanol. This product solution, together with an internal standard (4-nitroveratrole), was then analysed by g.l.c.

The time of reaction was increased to 5 h in an additional experiment. An identical set of runs was also carried out with 50 ppm nitrogen dioxide/N_2.

N.B. Any unreacted nitrogen dioxide was trapped in a 3 dm^3 beaker containing water.

3.3 Results

3.3.1 The reaction of allylbenzene with nitrogen dioxide

^{1}H n.m.r. confirmed the loss of the olefinic bond in allylbenzene (5.4δ - 6.4δ, m, 1H) upon its reaction with nitrogen dioxide (Figs. 3.1 and 3.2). In the proton decoupled ^{13}C n.m.r. spectrum of the crude product mixture, 6 CH_2 signals, 3 CH signals and 8 aromatic carbon signals are seen (Table 3.1 and Fig. 3.3). If a C_9H_{10} carbon skeleton is assumed, the number of aliphatic carbon signals indicates the presence of two major components and one minor component, with the skeletal structure of (I):

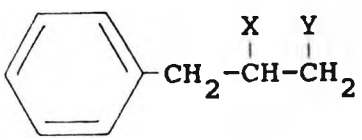

(I)

Since coupling information is totally lost in the proton decoupled ^{13}C n.m.r. spectrum, a DEPT (Fig. 3.4) experiment was carried out in order to determine CH_n multiplicity. This technique is particularly useful for differentiating between CH_2, CH and quaternary carbons - CH_2 C's appear as inverted signals, CH C's appear as upright signals and quaternary carbons disappear.

G.L.C. confirmed the presence of 3 components with retention times of 6.9 min (PEAK A) , 13 min (PEAK B) and 16.2 min (PEAK C) - Fig. 3.5.

In a separate experiment, the crude mixture was analysed by GC/CIMS using NH_3 as the reagent gas (Table 3.2 and Fig. 3.6). This technique also separated 3 components which correspond to peaks A, B and C in the g.l.c. In the mass spectra of A and B, a molecular ion peak (MNH_4^+) at m/z = 181 suggests the presence of an addition compound which decomposes in the mass spectrometer to probably form a nitroalkene:

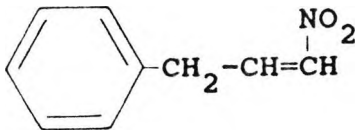

(II)

The most retained component in the chromatogram (Peak C) has a molecular ion at m/z = 199 which led to the following structural assignment:

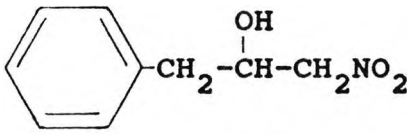

(III)

The mass spectra of the three peaks separated by GC/EIMS each contained a molecular ion peak (M^+) at m/z = 163, which confirmed the presence of 3 addition compounds which decompose to form the nitroalkene with the structure of (II) (Table 3.3 and Fig. 3.7). In one case the nitroalkene was formed by thermal degradation of (III). Oxidation products, in very low concentrations, were also detected in the g.l.c.

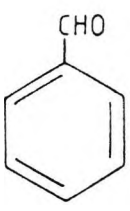

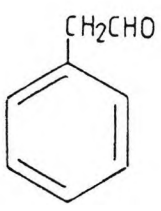

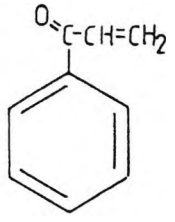

In the I.R. spectrum of the crude mixture, bands assignable to OH, =C-H, C=C, NO_2 and $-ONO_2$ functional groups are seen (Table 3.4). 1-nitro-3-phenylpropan-2-ol (III) is believed to be formed by the hydrolysis of the corresponding nitro-nitrite compound. This mechanism was substantiated by following the reaction of allylbenzene (0.01 mol dm^{-3}) with nitrogen dioxide (0.09 mol dm^{-3}) by I.R. In the initial spectrum the two peaks appearing at 1686 cm^{-1} and 1602 cm^{-1} are characteristic of -O-N=O frequencies. These bands slowly disappear as the reaction proceeds and were not present in the final spectrum taken after 150 min (Fig. 3.8).

Proton coupled and decoupled ^{15}N n.m.r. spectra of the crude mixture were recorded using $CDCl_3$ (Fig. 3.9), CD_3COCD_3 (Fig. 3.11) and C_6H_{12}/C_6D_{12} (Fig. 3.12) as solvents. These show 4 $-NO_2$ peaks and 1 $-ONO_2$ peak (Table 3.5) which were assigned according to the region in which they lie in the spectrum,[100] and by determining the ^1H environment of each ^{15}N signal from ^{15}N - ^1H coupling experiments (Fig. 3.10) - see below. The nitro-nitrate compound was only partially soluble in C_6H_{12}/C_6D_{12} and so the $-ONO_2$ signal was not discernible in this spectrum.

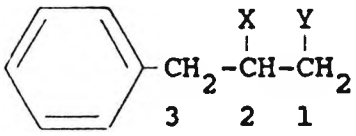

The 1-nitro groups are split into quartets apparently because the coupling constants between the NO_2 group and the protons on carbons 1 and 2 are very similar. Likewise, the signal due to the 2-nitro group is split into a multiplet by the proton on carbon 2 and the methylene protons.

Further product analysis required separation of the mixture into its various components. This was achieved by thin layer chromatography. Preparative t.l.c. using silica plates eluted with ethylacetate : diethyl ether (70:30) consistently gave separation into three distinct bands.:

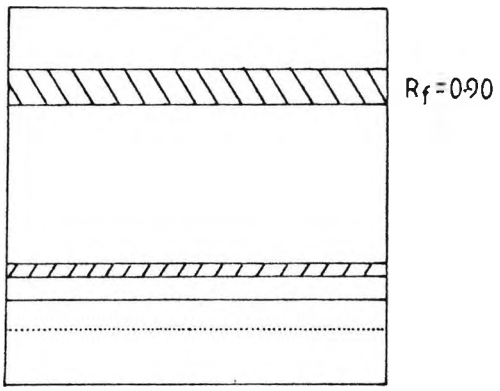

The major band (R_f = 0.90) was scraped off the plate and was extracted with acetone. Removal of the solvent gave an orange oil.

The ^{13}C n.m.r. spectra of this component (Table 3.6 and Fig. 3.13) correspond to that of one of the products in the crude mixture and therefore indicate that this compound is an addition product with the skeletal structure of (I):

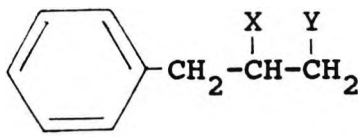

(I)

^{1}H n.m.r. (Fig. 3.14) supported this result, since there are no signals in the region 5.4δ - 6.4δ due to an olefinic double bond. G.L.C. confirmed the presence of one major component which corresponds to peak C in the g.l.c. of the crude mixture. The ^{15}N n.m.r. spectrum recorded using $CDCl_3$ (Fig. 3.15) shows one nitro peak at 11.64 p.p.m., which is split into a quartet in the proton coupled spectrum (Fig. 3.15), indicating the presence of a 1-nitro group (cf. NO_2 peak in mixture at 11.91 p.p.m. $CDCl_3$). In addition, the I.R. spectrum has bands assignable to OH,=C-H, C=C and $-NO_2$ functional groups (Table 3.7). The above findings led to the following structural assignment for the major component in the crude mixture:

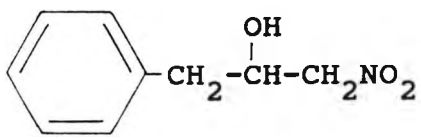

(III)

The n.m.r. data obtained by subtracting the ^{15}N spectrum of III from that of the crude mixture, identifies the second major product as 1,2-dinitro-3-phenylpropane.

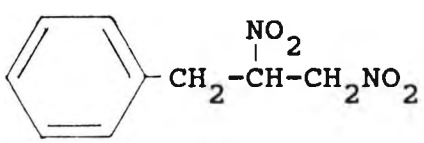

(IV)

The ^{15}N n.m.r. signals at 4.29 p.p.m. (q) and 12.49 p.p.m. (m) in Fig. 3.9 correspond to the 1-nitro and 2-nitro groups respectively in (IV). This assignment was supported by the fact that the difference in shift values between these two signals is very similar to that found between the nitro groups assigned to 1,2-dinitro-3-phenylpropane in the C.I.D.N.P. experiments (Section 4.5).

The ^{13}C n.m.r. spectra agree well with the simulated spectra of these compounds (Table 3.8).

The remaining nitro and nitrate peaks in the I.R. and ^{15}N n.m.r. of the crude mixture suggest that the minor component in the crude mixture is a nitro-nitrate compound.

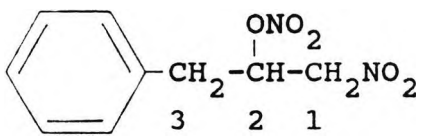

(V)

This compound is only partially soluble in C_6H_{12}/C_6D_{12}, with the result that the nitro signal is only just discernible in Fig. 3.12 and the nitrate signal disappears completely. This evidence lends further support to the assignment of the ^{15}N n.m.r. signal at 28.533 p.p.m. (m) in Fig. 3.9 (Table 3.5) to the nitro group of (V). Also, in the proton coupled ^{15}N n.m.r. spectrum (Fig. 3.10), the nitro group of (V) is split into a multiplet (see above) and the nitrate group is split into a doublet by the proton on carbon 2 (the coupling between the $-ONO_2$ group and protons of carbons 1 and 3 is very weak).

The proportions of these compounds were determined by integrating the ^{15}N nitro signals in the proton coupled ^{15}N n.m.r. (CD_3COCD_3) spectrum (Fig. 3.16), on the assumption that the relaxation properties of these nitro groups are similar:

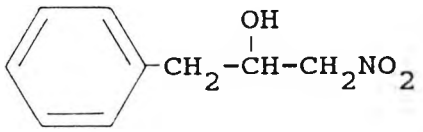

36%

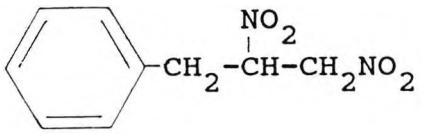

51%

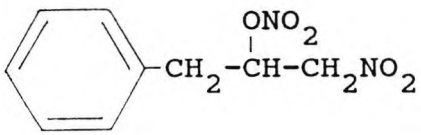

7%

There is no significant change in products or proportions over the nitrogen dioxide concentrations used in the kinetic studies (Table 3.9).

In conclusion, peak C in the g.l.c. chromatogram of the crude mixture is ascribed to the nitro-hydroxy compound. The dinitro and nitro-nitrate compounds give peaks A and B, but it is not possible to determine which peak is formed from which compound (see Section 3.4).

Fig. 3.1: ^{1}H n.m.r. ($CDCl_3$) spectrum of allylbenzene

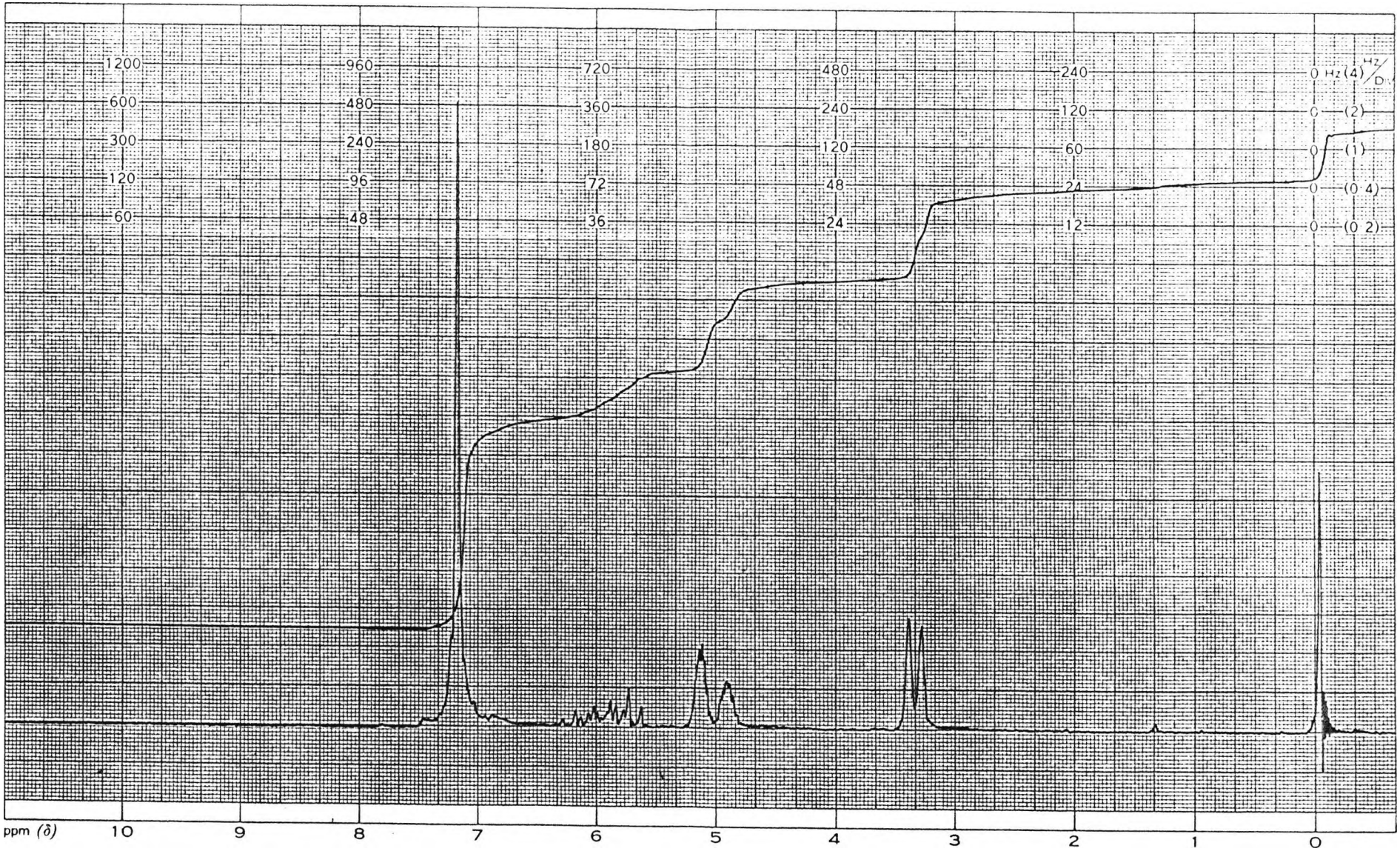

Fig. 3.2: ^{1}H n.m.r. ($CDCl_3$) spectrum of crude product mixture from the reaction of allylbenzene (0.01 mol dm^{-3}) with nitrogen dioxide (0.1 mol dm^{-3}) in cyclohexane at 30°C for 1 h

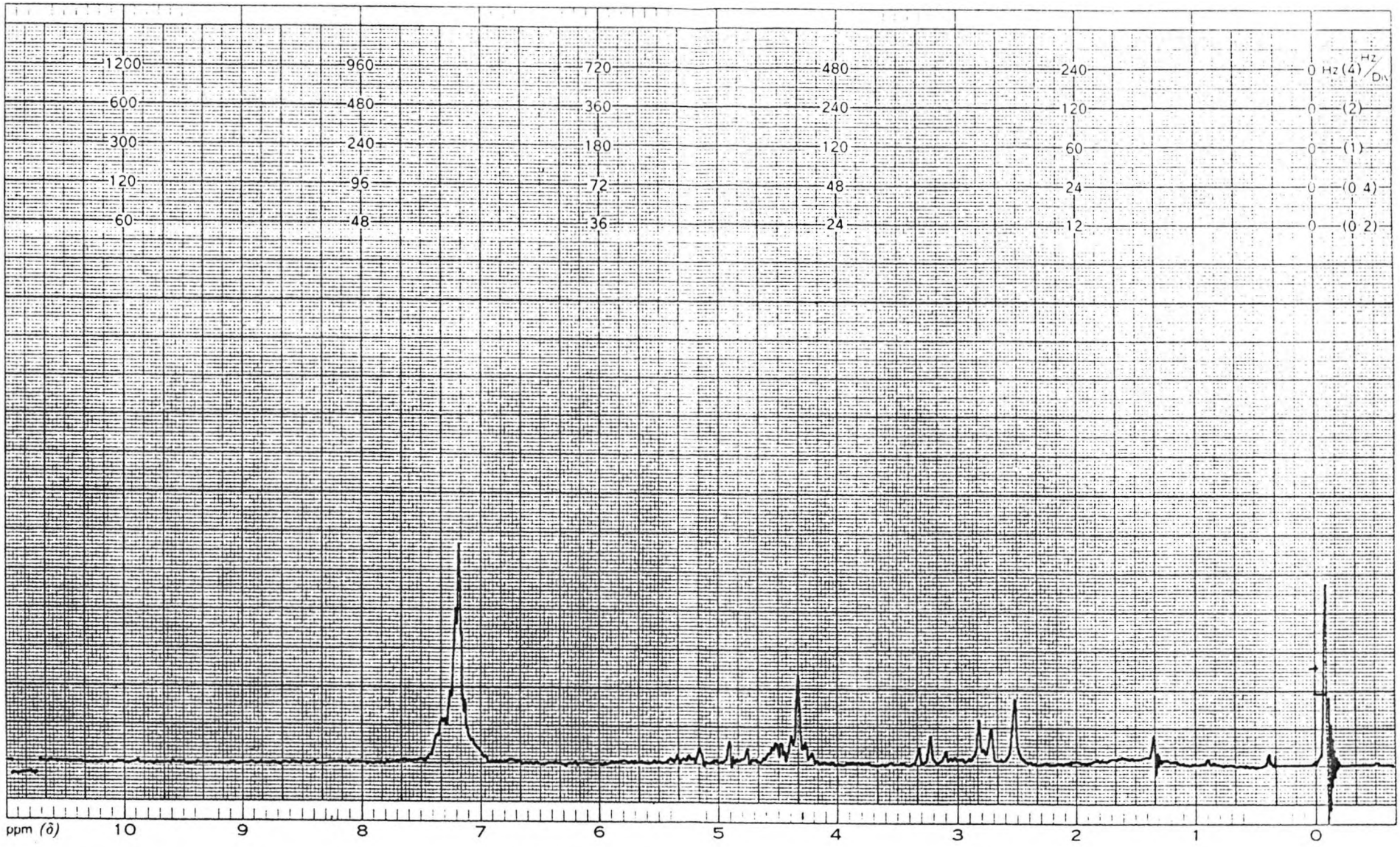

Table 3.1: Proton decoupled ^{13}C n.m.r. spectrum of crude product mixture from the reaction of allylbenzene (0.01 mol dm^{-3}) with nitrogen dioxide (0.1 mol dm^{-3}) in cyclohexane at 30°C for 1 hr

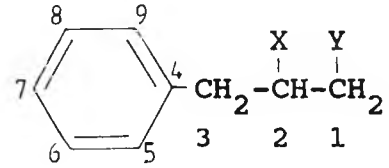

δ value	Assignment	δ value	Assignment
135.92	C4	83.11	CH-upright signal in DEPT
133.48	C4	79.75	CH_2-inverted signal in DEPT
132.81	C4	78.72	CH-upright signal in DEPT
129.36	C5,C9	77.56	
128.89	C6,C8	77.09	$CDCl_3$
		76.62	
128.44	C7		
127.96	C7	74.11	CH_2-inverted signal in DEPT
127.24	C7	73.06	CH_2-inverted signal in DEPT
		69.58	CH-upright signal in DEPT
		40.32	CH_2-inverted signal in DEPT
		37.16	CH_2-inverted signal in DEPT
		36.55	CH_2-inverted signal in DEPT

Fig. 3.3: Proton decoupled ^{13}C n.m.r. ($CDCl_3$) spectrum of crude product mixture from the reaction of allylbenzene (0.01 mol dm^{-3}) with nitrogen dioxide (0.1 mol dm^{-3}) in cyclohexane at 30°C for 1 h

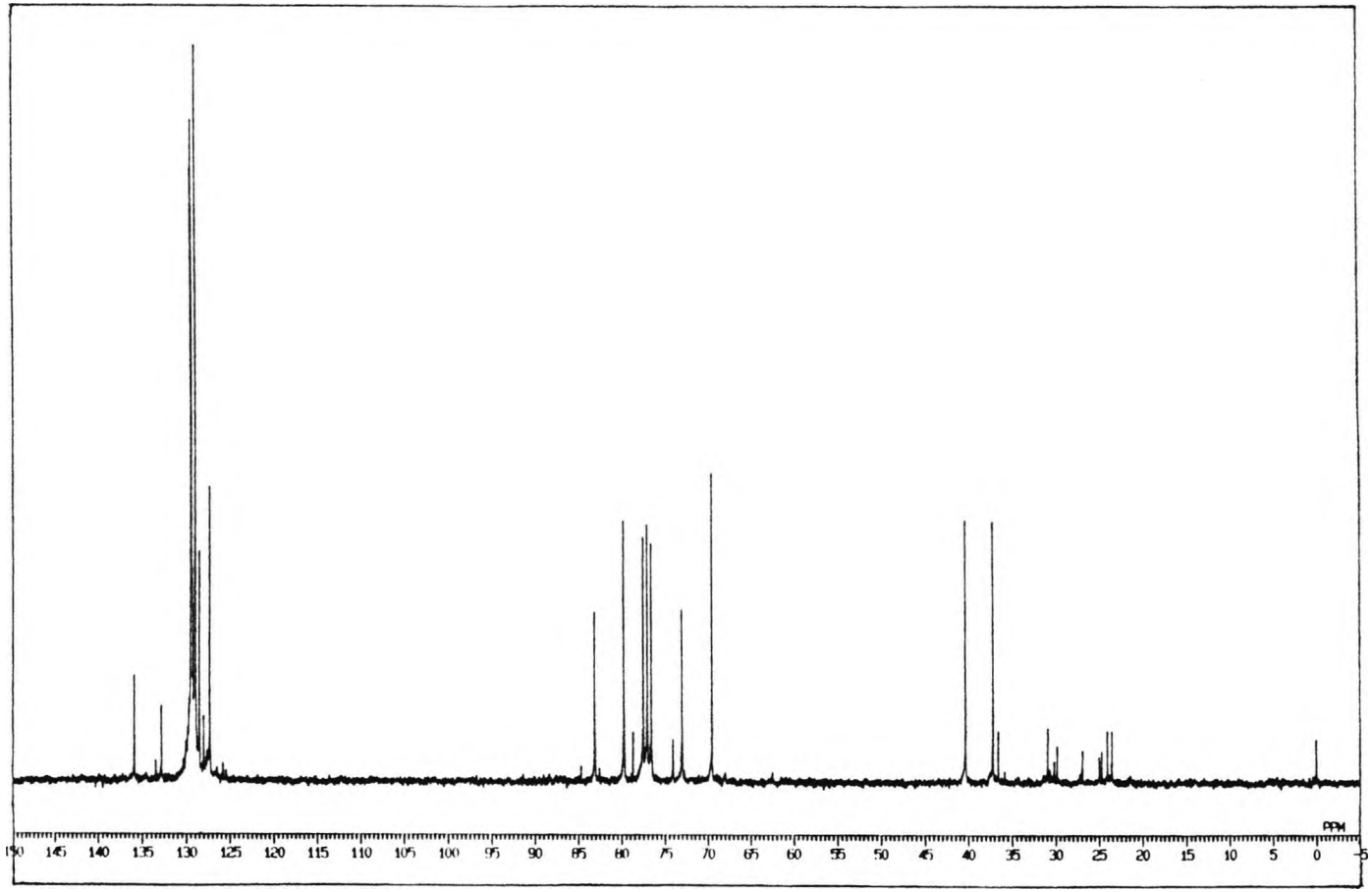

Fig. 3.4: DEPT ($CDCl_3$) spectrum of crude product mixture from the reaction of allylbenzene (0.01 mol dm^{-3}) with nitrogen dioxide (0.1 mol dm^{-3}) in cyclohexane at 30°C for 1 h

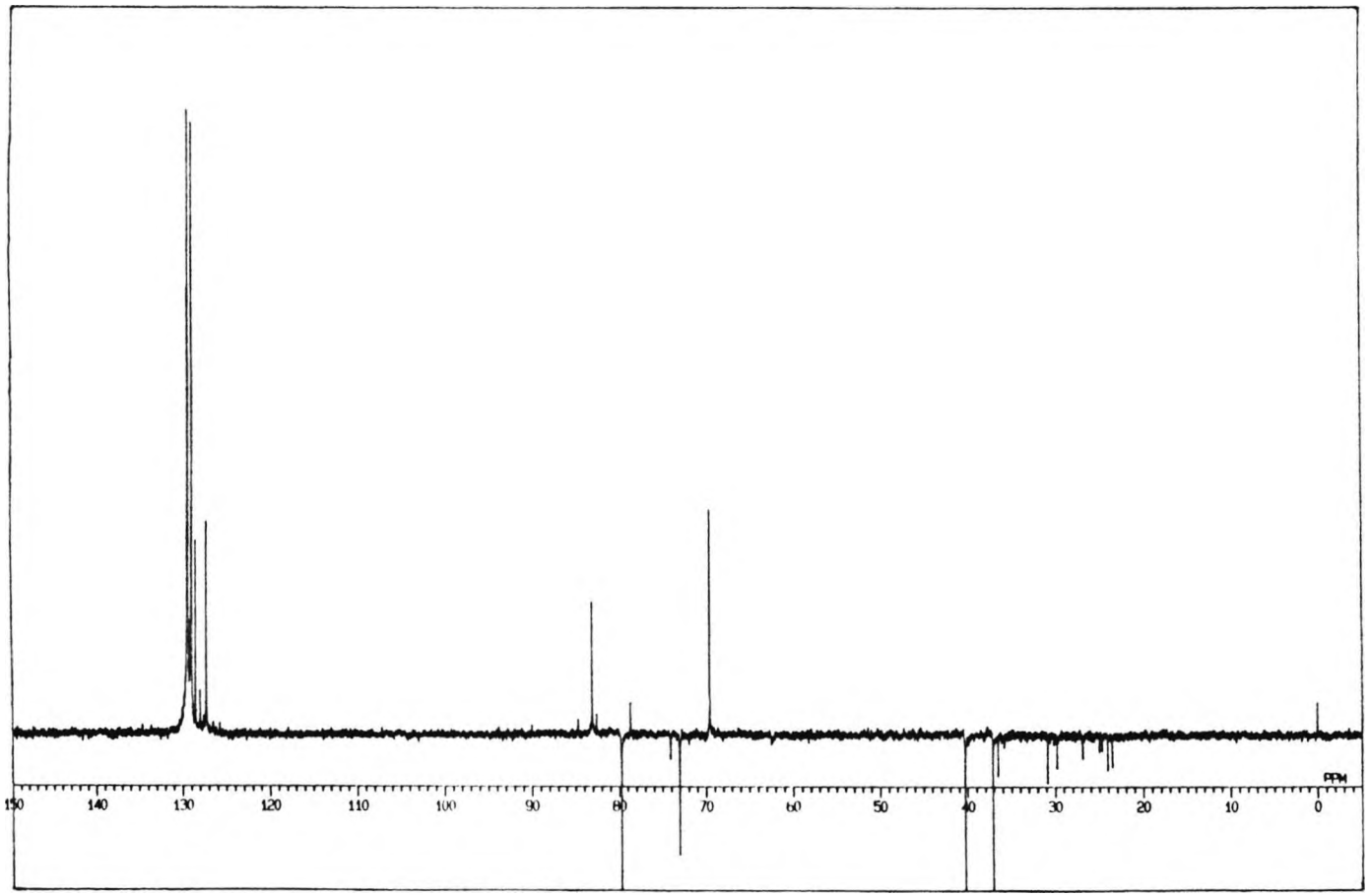

Fig. 3.5: GLC chromatogram of crude product mixture from the reaction of allylbenzene (0.01 mol dm^{-3}) with nitrogen dioxide (0.1 mol dm^{-3}) in cyclohexane at 30°C for 1 h
(see Section 10·2·1)

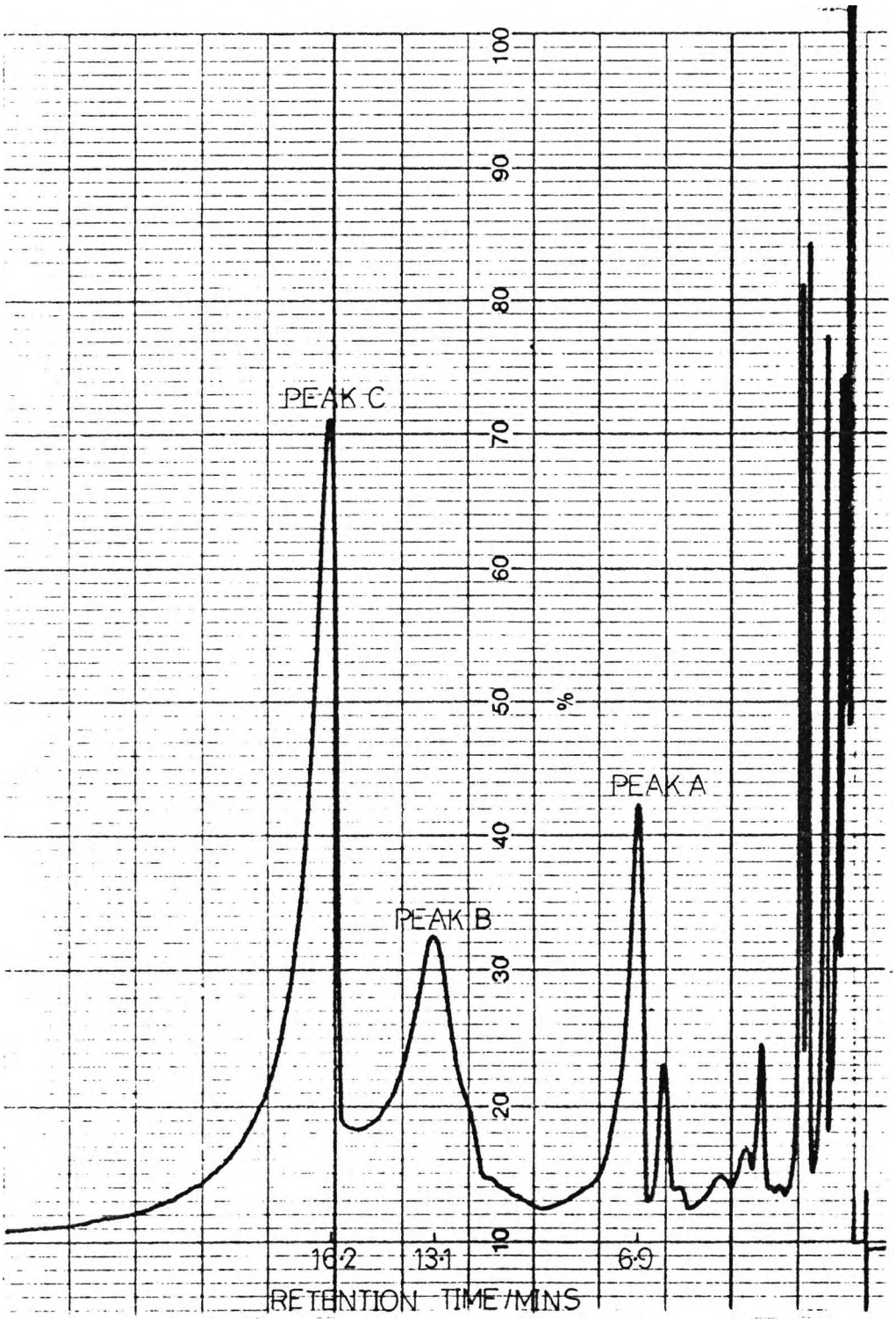

Table 3.2: GC/CIMS (NH_3) chromatogram of crude product mixture from the reaction of allylbenzene (0.01 mol dm^{-3}) with nitrogen dioxide (0.1 mol dm^{-3}) in cyclohexane at 30°C for 1 h
(see Section 10·3·2)

	m/z	relative abundance	Assignment
Peak A	181	100.00	$C_6H_5CH_2CH{=}CHNO_2 \cdot NH_4^+$
	116	6.07	$C_9H_8^+$
	106	3.71	$C_7H_6O^+$
	77	3.07	$C_6H_5^+$
	52	12.10	$C_4H_4^+$
Peak B	181	32.99	$C_6H_5CH_2CH{=}CHNO_2 \cdot NH_4^+$
	132	100.00	$C_9H_8O^+$
	117	13.10	$C_9H_9^+$
	106	3.11	$C_7H_6O^+$
	77	1.55	$C_6H_5^+$
Peak C	199	43.69	$C_6H_5CH_2CHOHCH_2NO_2 \cdot NH_4^+$
	182	1.35	$C_6H_5CH_2CHOHCH_2NO_2 \cdot H^+$
	106	6.24	$C_7H_6O^+$
	91	2.58	$C_7H_7^+$
	77	1.80	$C_6H_5^+$
	52	11.07	$C_4H_4^+$

Fig. 3.6: GC/CIMS (NH_3) chromatogram of crude product mixture from the reaction of allylbenzene (0.01 mol dm^{-3}) with nitrogen dioxide (0.1 mol dm^{-3}) in cyclohexane at 30°C for 1 h
(see Section 10·3·2)

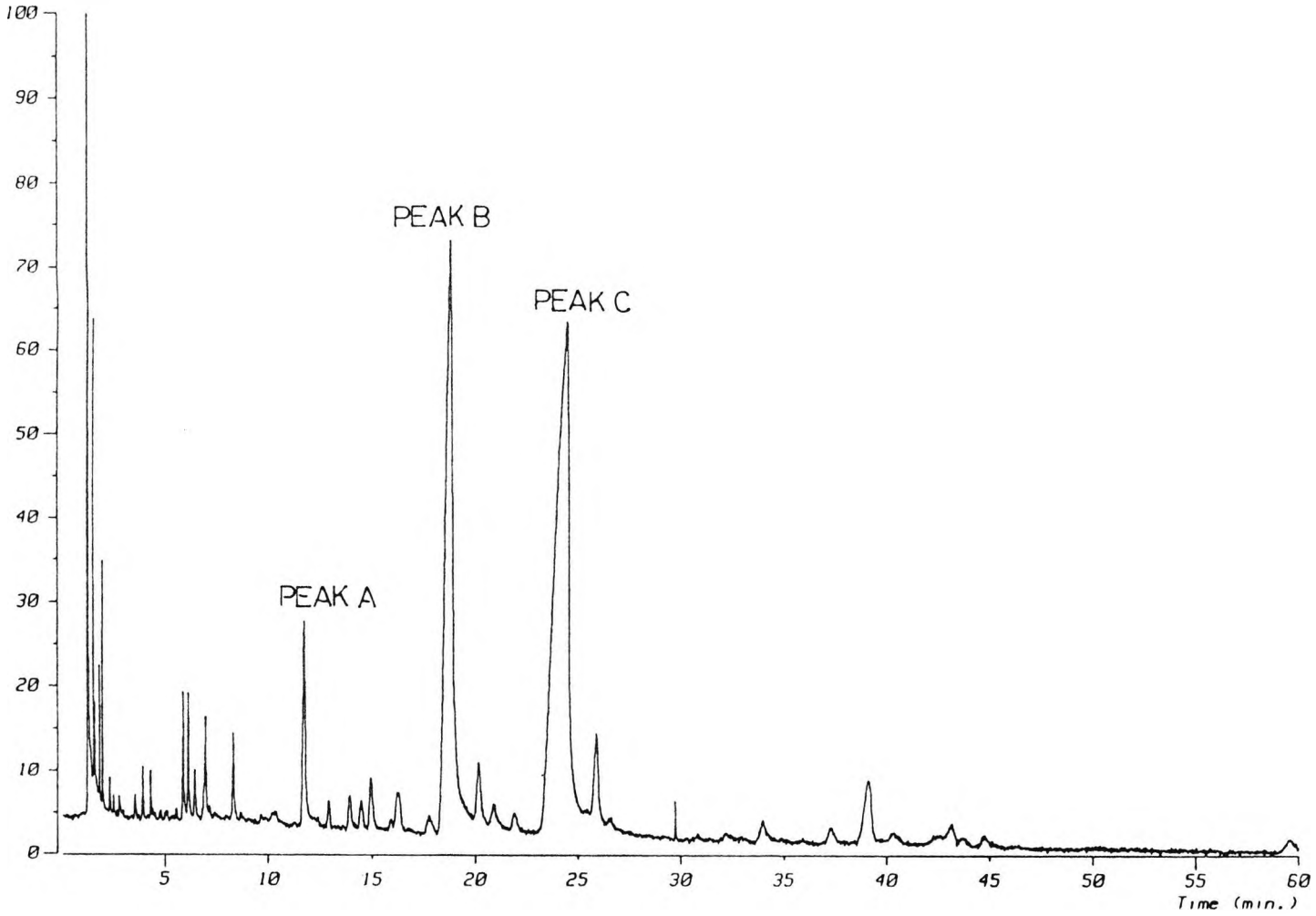

Fig. 3.6: ..... cont'd.

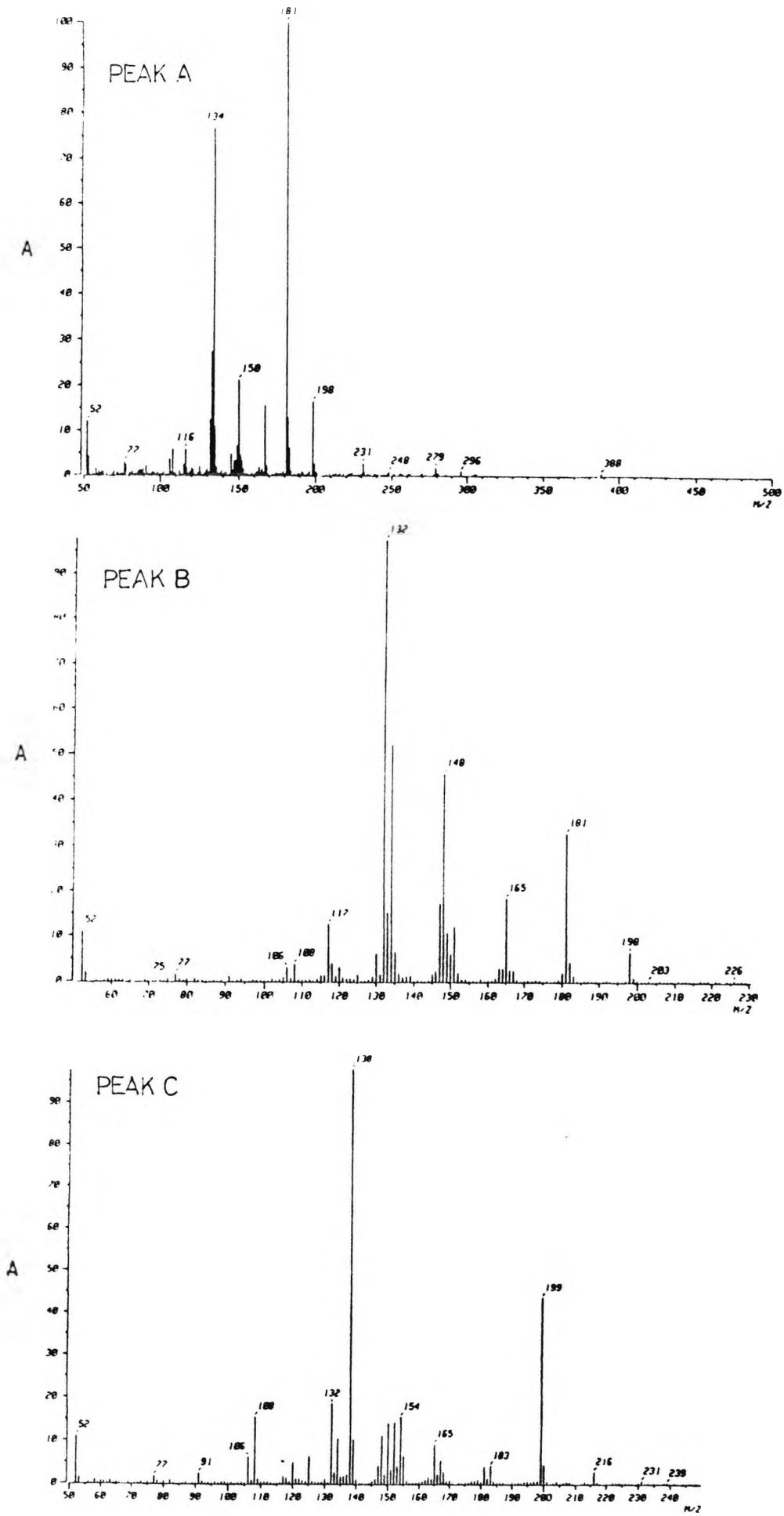

Table 3.3: GC/EIMS chromatogram of crude product mixture from the reaction of allylbenzene with nitrogen dioxide in cyclohexane at 30°C for 1 h (see Section 10·3·1)

Peak		m/z
	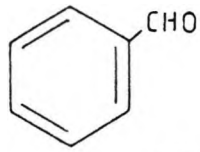	106(64%;M^+),105(71%), 77(100%),51(52%)
	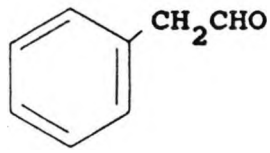	120(23%;M^+), 91(100%), 51(7%)
	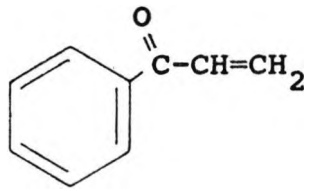	132(61%;M^+), 131(100%), 104(86%),77(73%),51(27%)
PEAK A	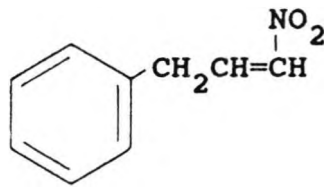	163(6%;M^+), 116(100%), 115(71%),91(23%)
PEAK B	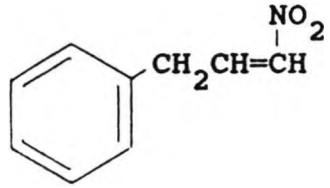	163(40%;M^+), 117(100%), 116(50%),115(91%),77(23%) 51(31%)
PEAK C	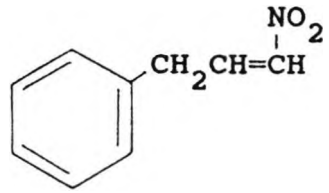	163(1%;M^+), 120(22%),117 (14%),91(100%),77(5%), 51(8%)

Fig. 3.7: GC/EIMS chromatorgram of crude product mixture from the reaction of allylbenzene with nitrogen dioxide in cyclohexane (see Section 10-3-1)

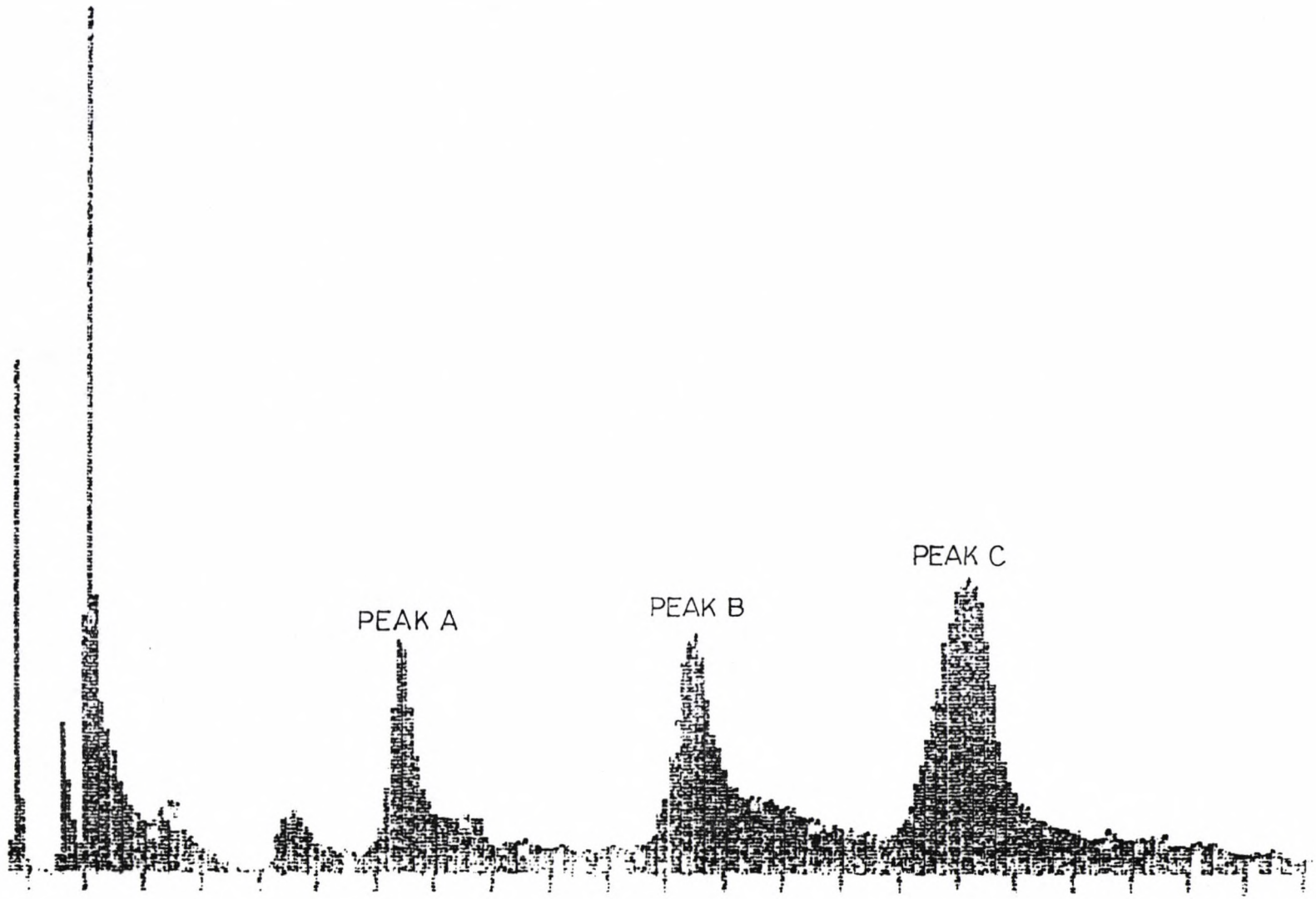

Table 3.4: I.R. spectrum of crude product mixture from the reaction of allylbenzene (0.01 mol dm^{-3}) with nitrogen dioxide (0.1 mol dm^{-3}) in cyclohexane at 30°C for 1 h (thin film)

Peak, cm^{-1}	Assignment
3558 (m)	free and hydrogen bonded O-H
3065 (w)	aromatic = C-H stretch
3030 (m)	
2929 (m)	aliphatic C-H stretch
COMBINATION & OVERTONE BANDS (w) 2000 - 1700 cm^{-3} 4 peaks (monosubstitution - typically 4 peaks in the range 2000 - 1650 cm^{-1})	
1642 (m)	asymmetric $-O-NO_2$ stretch
1603 (m)	aromatic C=C stretch
1494 (m)	
1553 (s)	asymmetric N=O stretch $-NO_2$
1382 (m → s)	symmetric N=O stretch
1278 (m → s)	symmetric ONO_2 stretch

Fig. 3.8: IR spectra recorded during the reaction of allylbenzene (0.01 mol dm^{-3}) with nitrogen dioxide (0.09 mol dm^{-3}) in carbon tetrachloride at r.t.

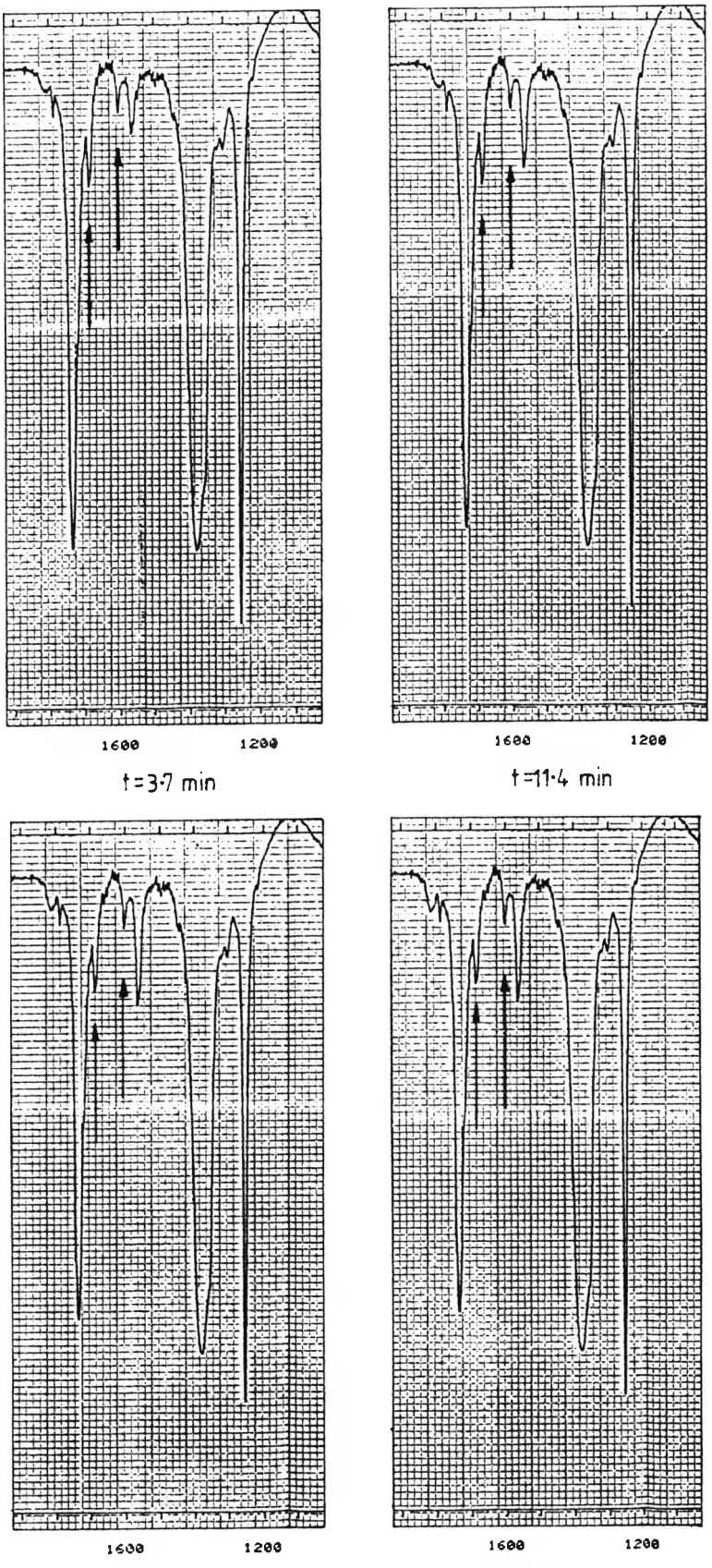

Fig. 3.8: ..... cont'd

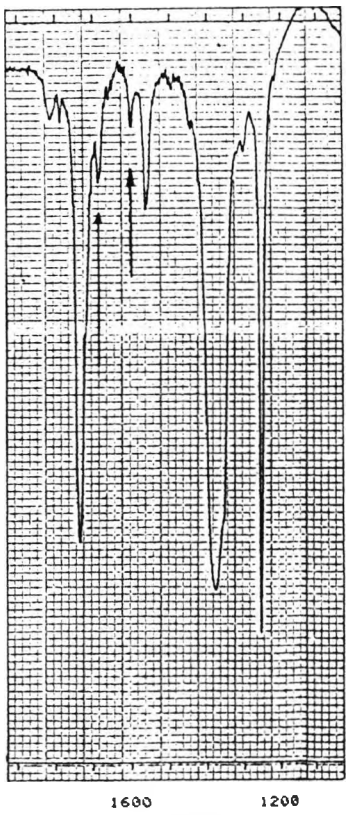

t=41·4 min

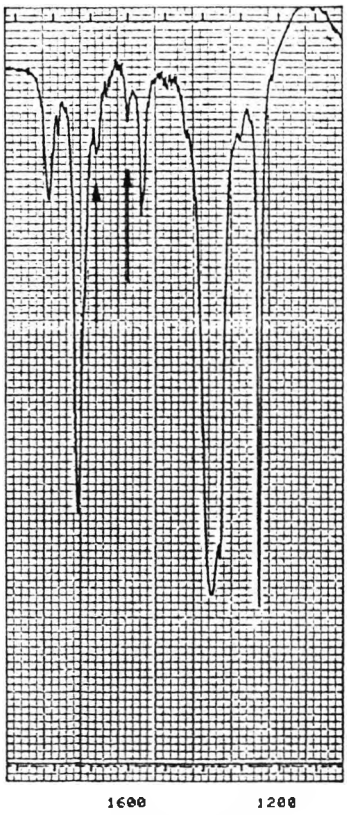

t=82·75 min

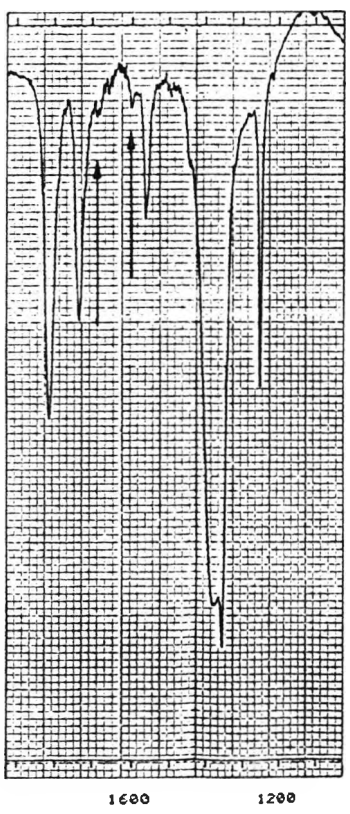

t=125·2 min

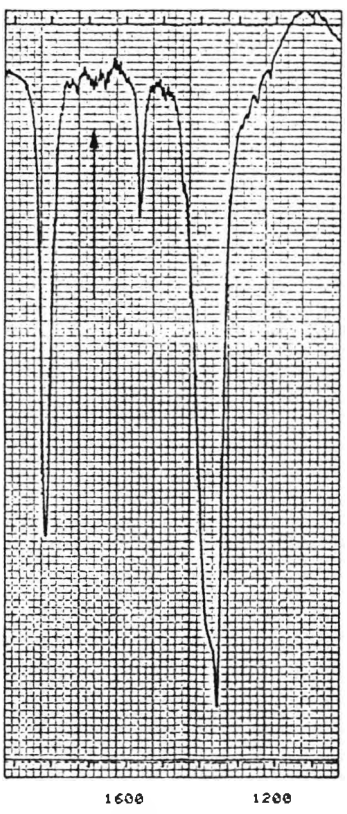

t=152·4 min

Fig. 3.9: Proton decoupled ^{15}N n.m.r. ($CDCl_3$) spectrum of crude product mixture from the reaction of allylbenzene (6.93×10^{-3} mol dm^{-3}) with ^{15}N-labelled nitrogen dioxide (0.05 mol dm^{-3}) in cyclohexane at 30°C for 1.5 h ($Ph^{15}NO_2$ in $CDCl_3$ set at 0 ppm)

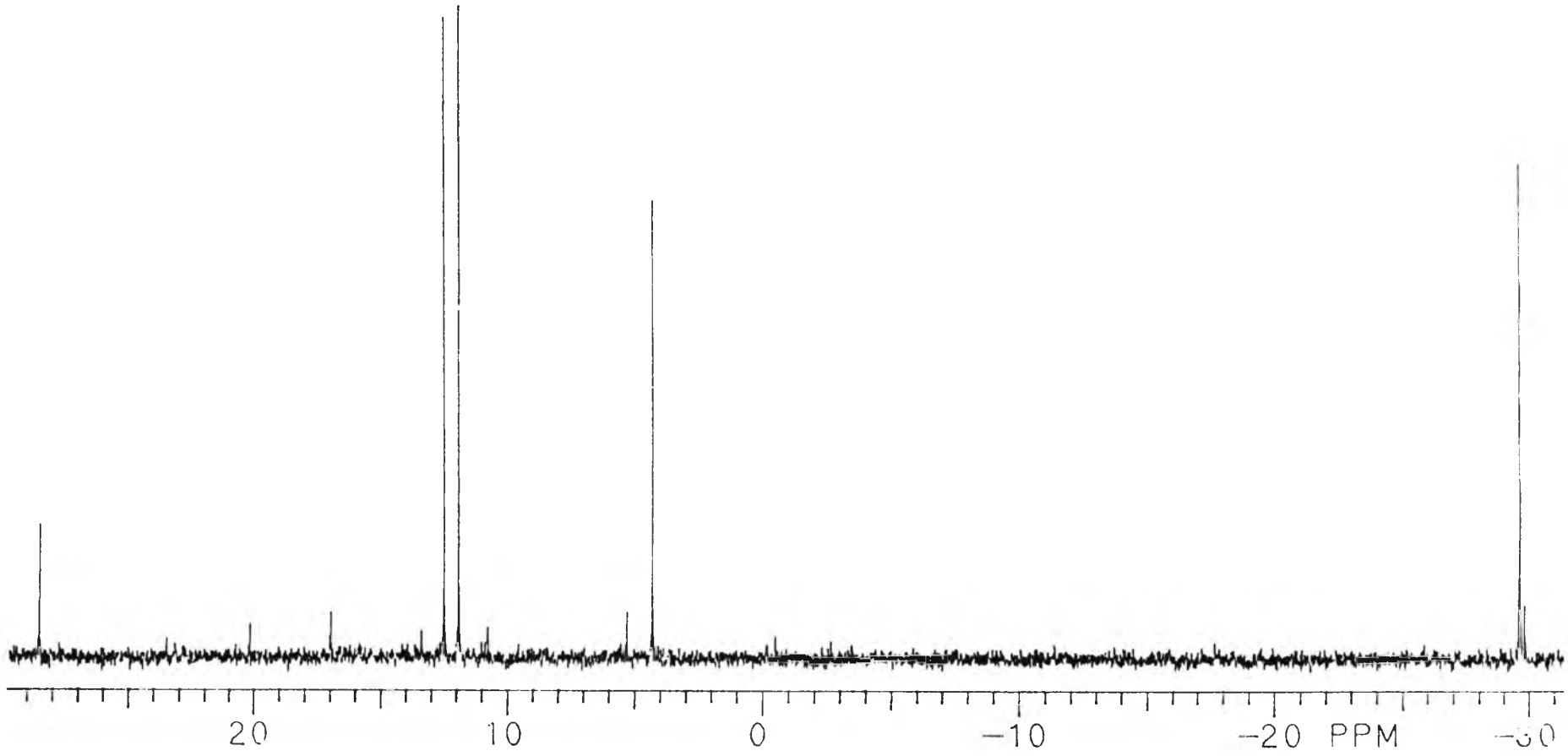

Fig. 3.10: Proton coupled ^{15}N n.m.r. spectrum ($CDCl_3$) of crude product mixture from the reaction of allylbenzene (6.93×10^{-3} mol dm^{-3}) with ^{15}N-labelled nitrogen dioxide (0.05 mol dm^{-3}) in cyclohexane at 30°C for 1.5 h

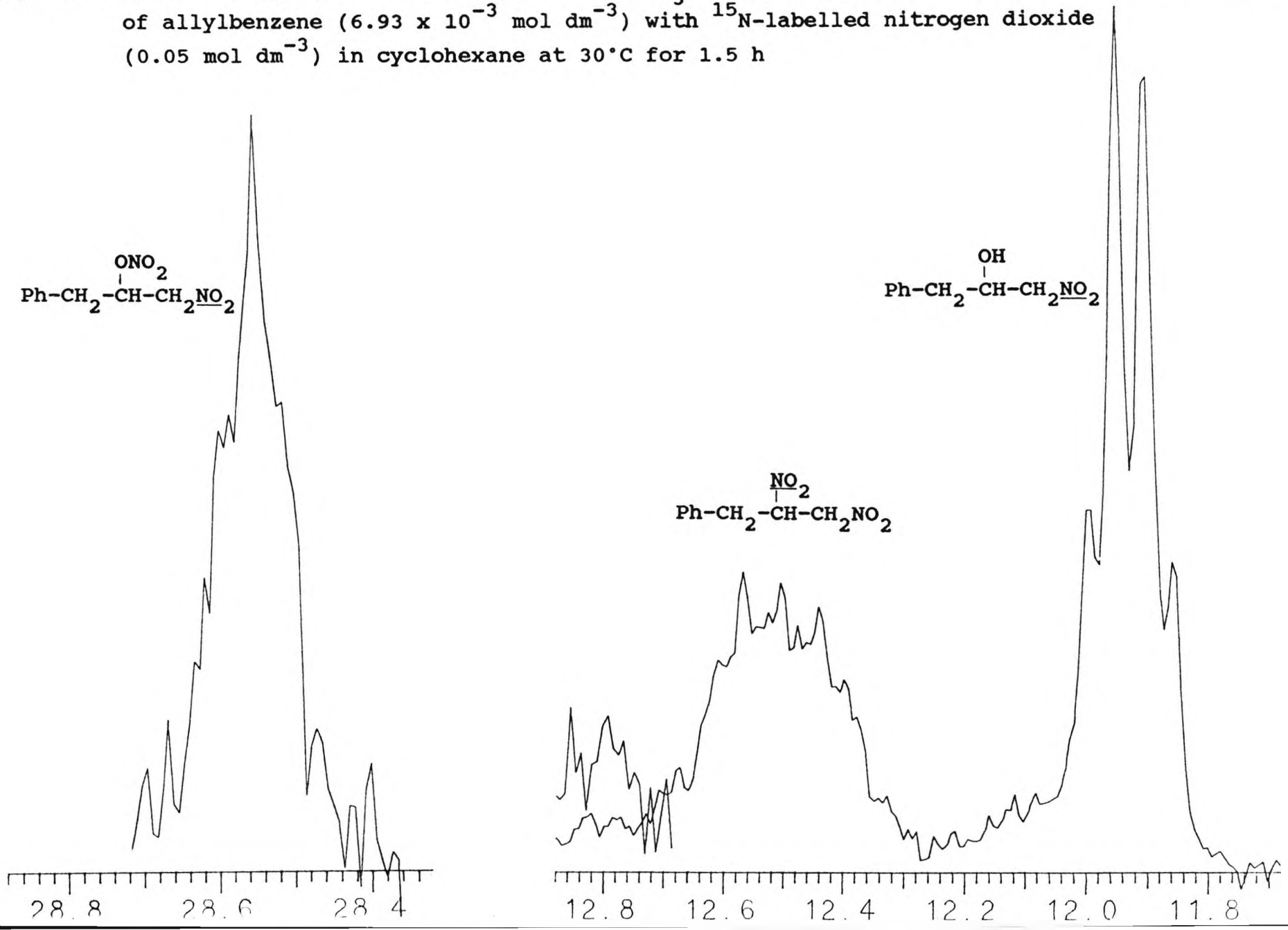

Fig. 3.10 ..... contd.

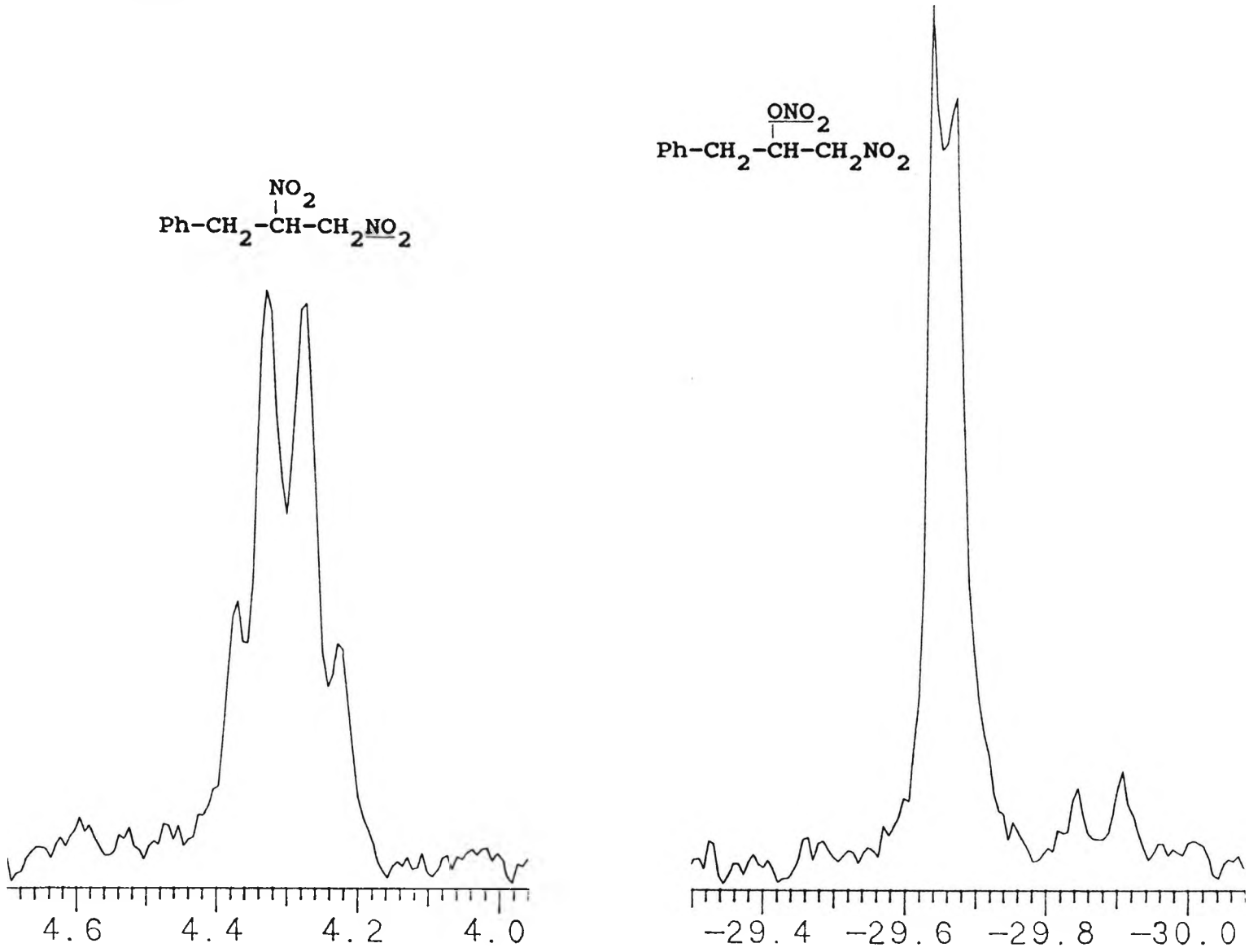

Fig. 3.11: Proton coupled ^{15}N n.m.r. spectrum (CD_3COCD_3) of crude product mixture from the reaction of allylbenzene (6.93×10^{-3} mol dm^{-3}) with ^{15}N-labelled nitrogen dioxide (0.05 mol dm^{-3}) in cyclohexane at 30°C for 1.5 h ($Ph^{15}NO_2$ in CD_3COCD_3 set at 0 ppm)

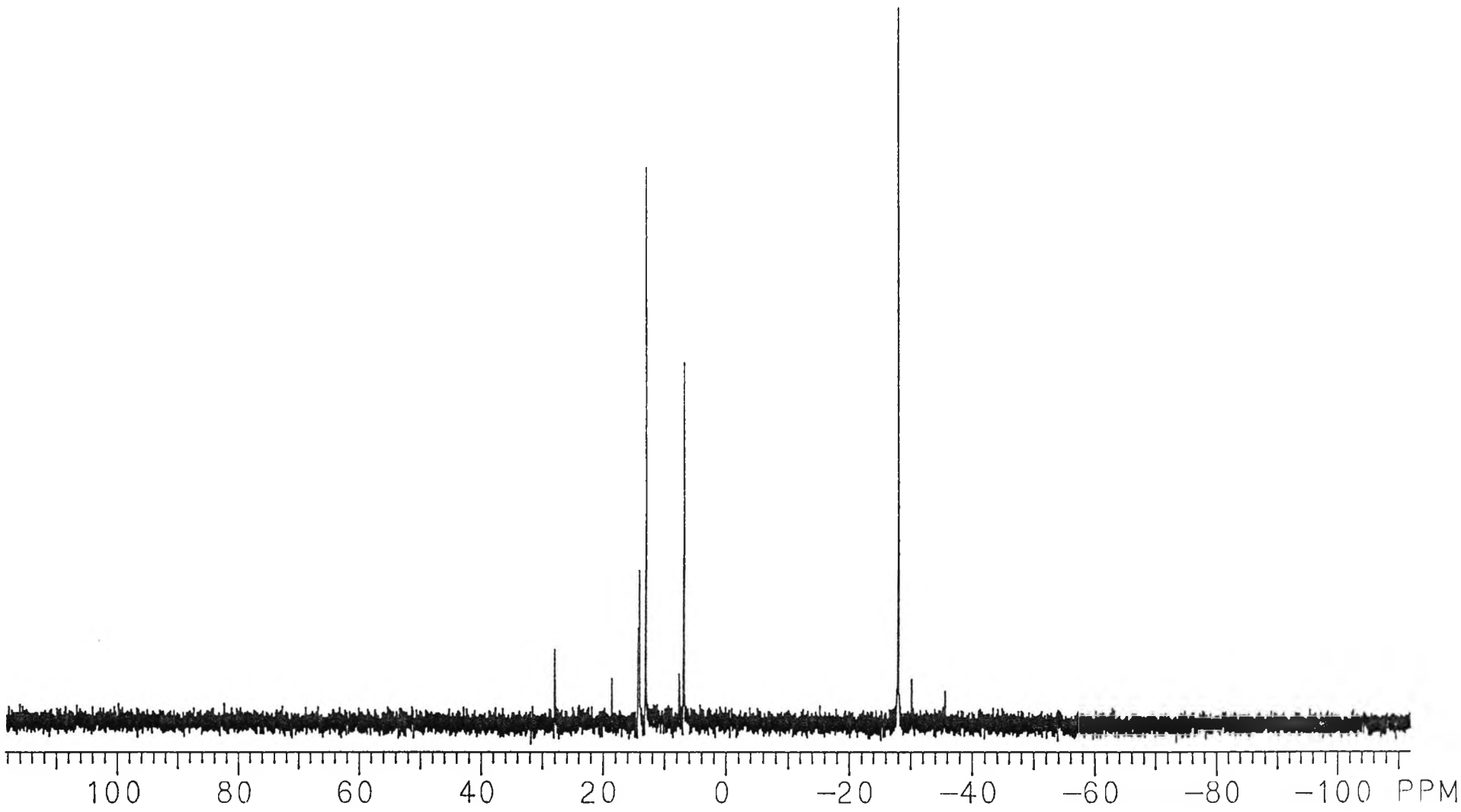

Fig. 3.12: Proton decoupled ^{15}N n.m.r. spectrum (C_6H_{12}/C_6D_{12}) of crude product mixture from the reaction of allylbenzene (6.93×10^{-3} mol dm^{-3}) with ^{15}N-labelled nitrogen dioxide (0.05 mol dm^{-3}) in cyclohexane at 30°C for 1½ h ($Ph^{15}NO_2$ in $CDCl_3$ set at 0ppm)

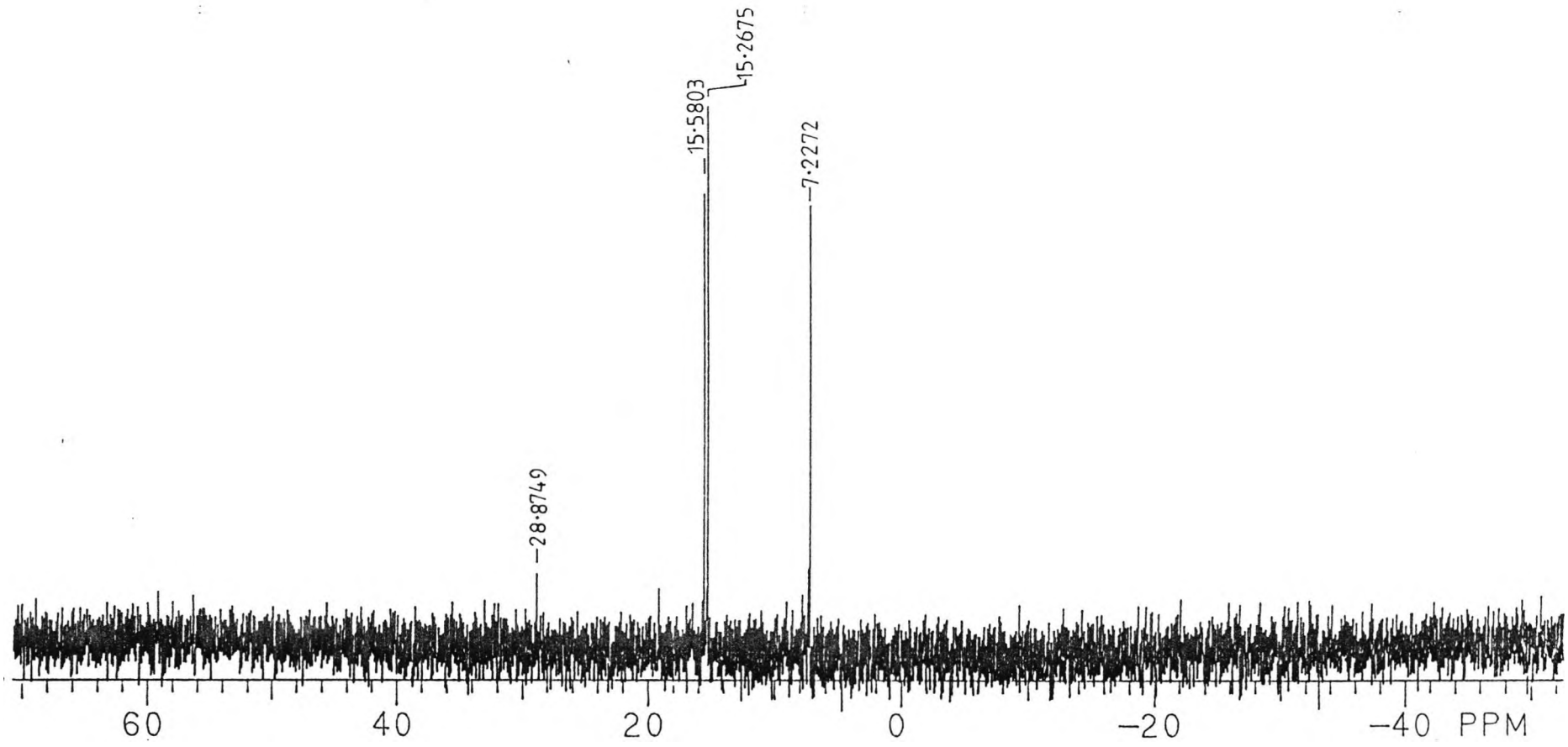

Table 3.5: ^{15}N n.m.r. spectra of crude product mixture from the reaction of allylbenzene (6.93×10^{-3} mol dm^{-3}) with ^{15}N-labelled nitrogen dioxide (0.05 mol dm^{-3}) in cyclohexane at 30°C for 1½ h

δ value in $CDCl_3$ (Fig. 3.9)	(Fig. 3.10)	Assignment[100]	J_2, J_3* ($CDCL_3$) (Fig. 3.10)
28.533	m	$Ph-CH_2-\underset{\displaystyle ONO_2}{\underset{\vert}{CH}}-CH_2\underline{\underline{NO_2}}$	1.4Hz
12.493	m	$Ph-CH_2-\underset{\displaystyle \underline{\underline{NO_2}}}{\underset{\vert}{CH}}-CH_2NO_2$	
11.916	q	$Ph-CH_2-\underset{\displaystyle OH}{\underset{\vert}{CH}}-CH_2\underline{\underline{NO_2}}$	1.9Hz
4.293	q	$Ph-CH_2-\underset{\displaystyle NO_2}{\underset{\vert}{CH}}-CH_2\underline{\underline{NO_2}}$	1.9Hz
-29.291	d	$Ph-CH_2-\underset{\displaystyle \underline{\underline{ONO_2}}}{\underset{\vert}{CH}}-CH_2NO_2$	J_2=1.3Hz

*J_2,J_3 represent 2/3 bond coupling constants (Section 3.3.1)

Table 3.6: Proton decoupled ^{13}C n.m.r. spectrum of 1-nitro-3-phenylpropan-2-ol isolated from the reaction of allylbenzene (0.01 mol dm^{-3}) with nitrogen dioxide (0.1 mol dm^{-3}) in cyclohexane at 30°C for 1 h

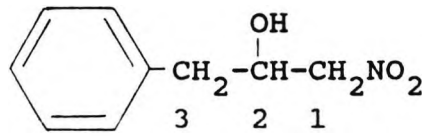

δ value	Assignment
136.06 (135.92*)	C4
129.36 (129.36)	C5,C9
128.88 (128.89)	C6,C8
127.22 (127.24)	C7
79.86 (79.75)	CH_2-inverted signal in DEPT
77.56 77.07 76.60	$CDCl_3$
69.58 (69.58)	CH-upright signal in DEPT
40.52 (40.32)	CH_2-inverted signal in DEPT

* The numbers in parentheses refer to the corresponding δ values in the proton decoupled ^{13}C n.m.r. spectrum of the crude product mixture

Fig. 3.13: Proton decoupled ^{13}C n.m.r. and DEPT spectra of 1-nitro-3-phenylpropan-2-ol isolated from the reaction of alylbenzene (0.01 mol dm^{-3}) with nitrogen dioxide (0.1 mol dm^{-3}) in cyclohexane at 30°C for 1 h

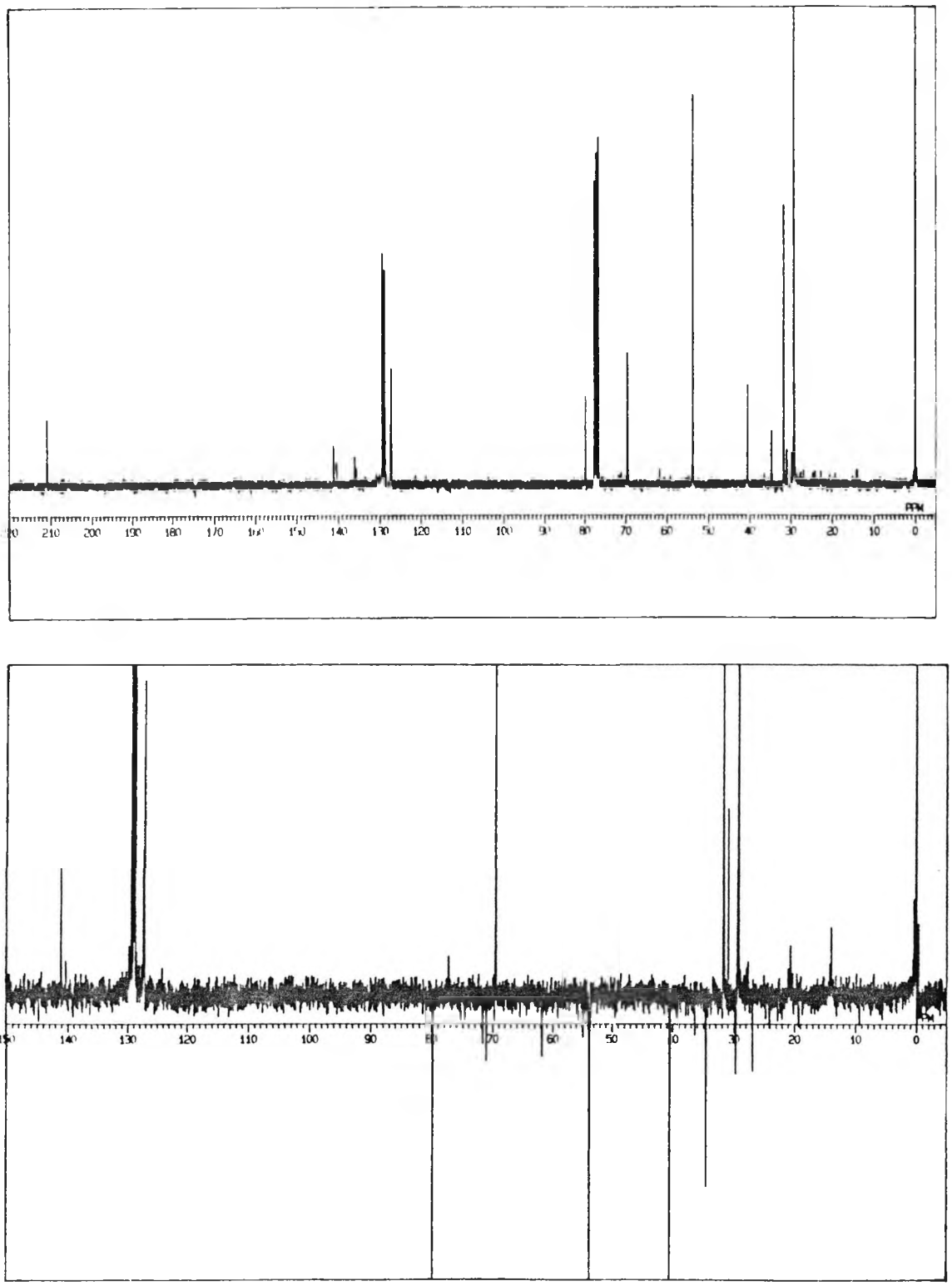

Fig. 3.14: ^{1}H n.m.r. ($CDCl_3$) spectrum of 1-nitro-3-phenylpropan-2-ol isolated from the reaction of allylbenzene (0.01 mol dm^{-3}) with nitrogen dioxide (0.1 mol dm^{-3}) in cyclohexane at 30°C for 1 h

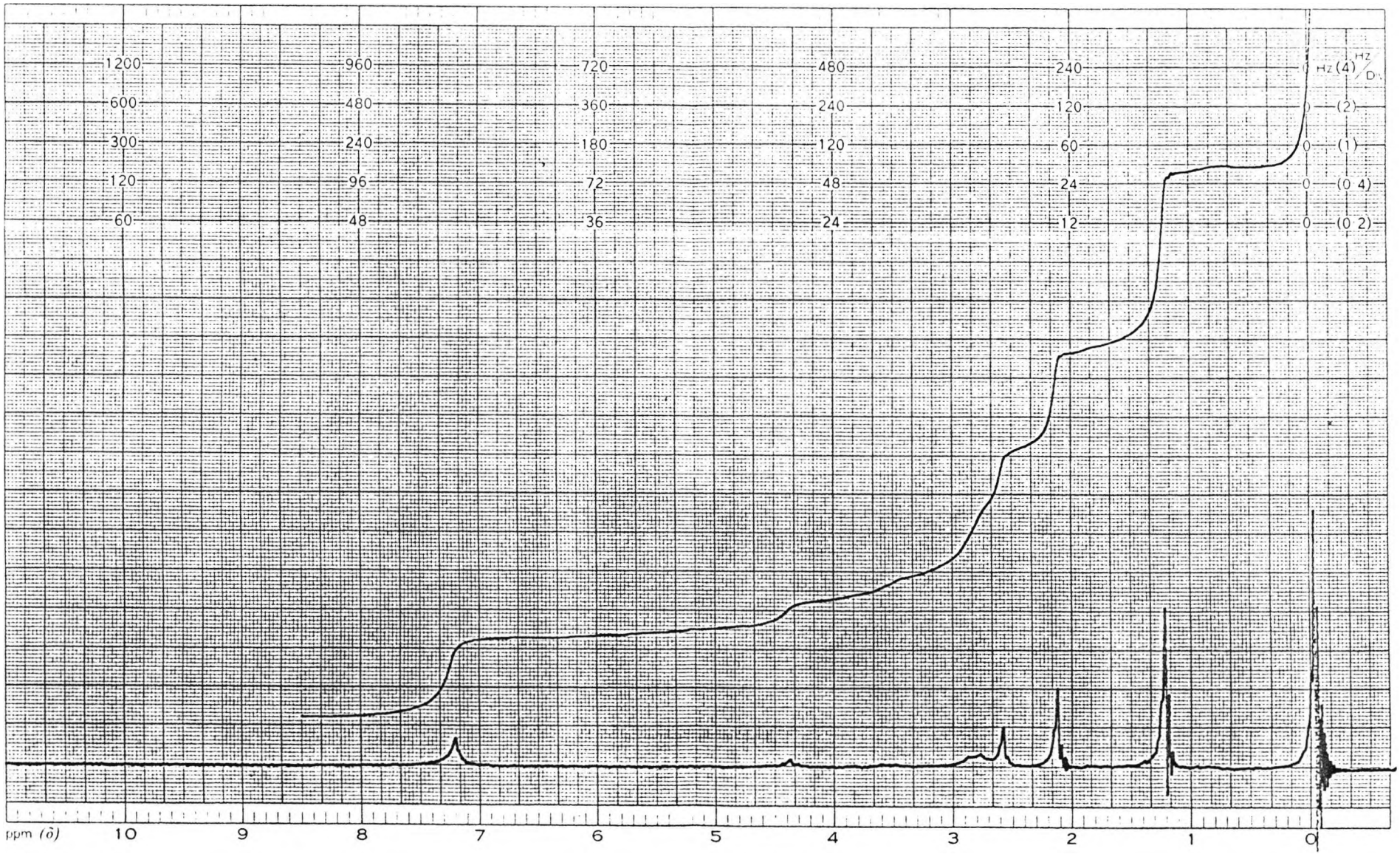

Fig. 3.15: Proton coupled ^{15}N n.m.r. spectra of 1-nitro-3-phenylpropan-2-ol isolated from the reaction of allylbenzene (6.93×10^{-3} mol dm^{-3}) with nitrogen dioxide (0.05 mol dm^{-3}) in cyclohexane at 30°C for 1 h ($Ph^{15}NO_2$ in $CDCl_3$ set at 0 ppm)

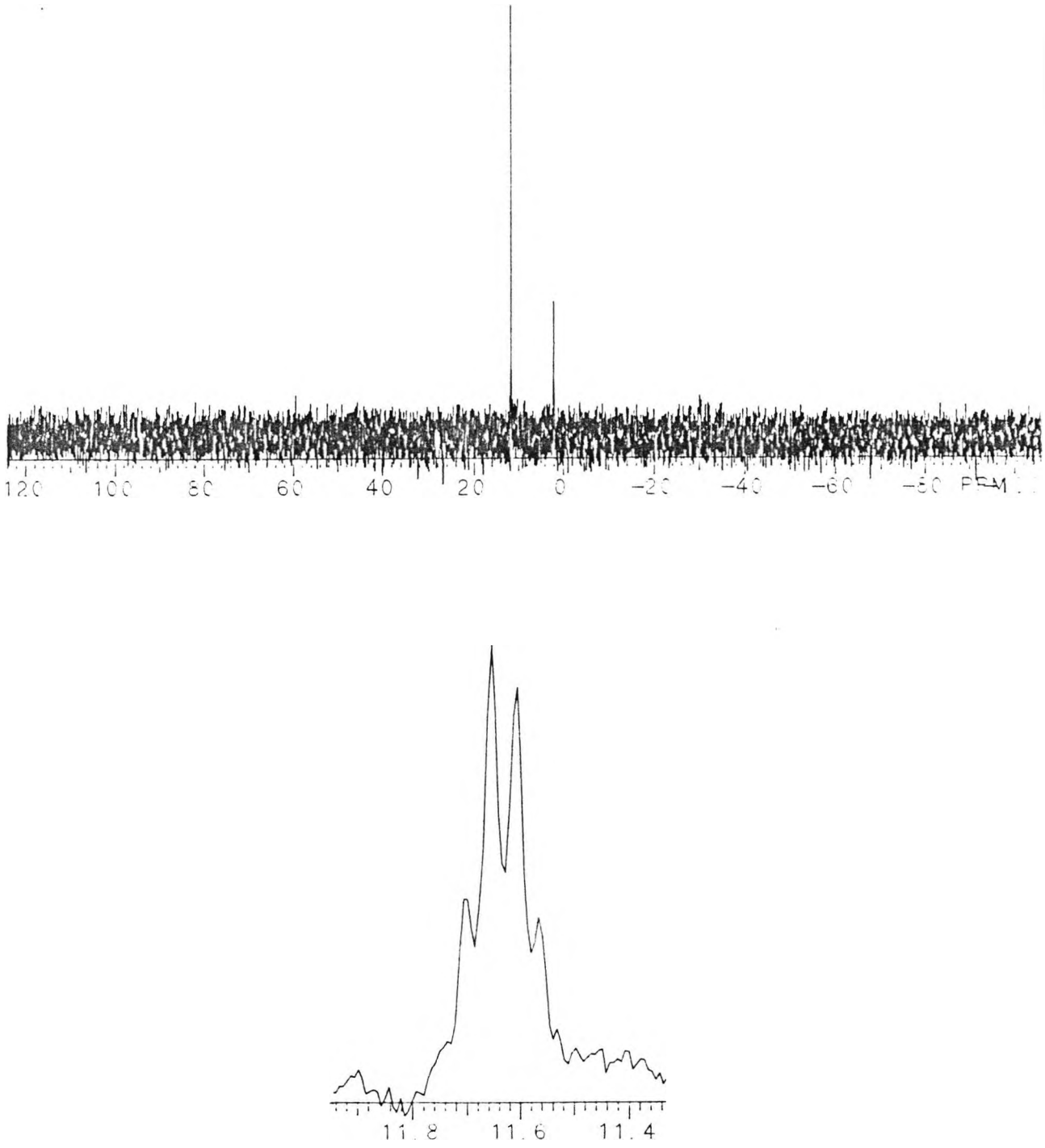

Table 3.7: I.R. spectrum of 1-nitro-3-phenylpropan-2-ol (thin film)

Peak, cm^{-1}	Assignment
3417 (m)	free and hydrogen bonded O-H
3062 (w → m) 3028 (m)	aromatic =C-H stretch
2923 (m)	aliphatic C-H stretch

COMBINATION & OVERTONE BANDS (w) 2000 - 1800 cm^{-1}
3 peaks (monosubstitution - typically 4 peaks in the range 2000 - 1650 cm^{-1})

1603 (m) 1494 (m)	aromatic C=C stretch in correct range for monosubstituted benzene ring
1550 (s)	asymmetric N=O stretch $-NO_2$
1382 (m → s)	symmetric N=O stretch

Table 3.8: Comparison of actual and simulated spectra of 1-nitro-3-phenylpropan-2-ol and 1,2-dinitro-3-phenylpropane

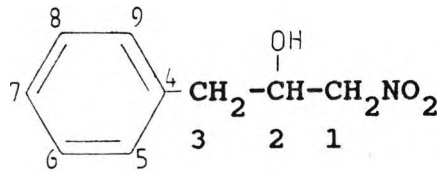

	ACTUAL SPECTRUM	SIMULATED SPECTRUM*
C1	79.75	80.5
C2	69.58	69.1
C3	40.32	42.0
C4	135.92	137.8
C5	129.36	129.0
C6	128.89	128.6
C7	127.24	127.3
C8	128.89	128.6
C9	129.36	129.0

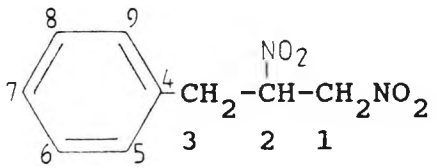

C1	83.11	89.6
C2	73.06	79.5
C3	37.16	38.5
C4	132.81	136.6
C5	129.36	129.0
C6	128.89	128.6
C7	128.44	127.2
C8	128.89	128.6
C9	129.36	129.0

*Data for simulated spectra obtained from STN database bureau

Fig. 3.16: Determination of yields of products from the reaction of allylbenzene (6.93×10^{-3} mol dm^{-3}) with nitrogen dioxide (0.05 mol dm^{-3}) in cyclohexane at 30°C for 1 h by integration of ^{15}N n.m.r. signals in proton coupled ^{15}N n.m.r. (CD_3COCD_3) spectrum of crude product mixture

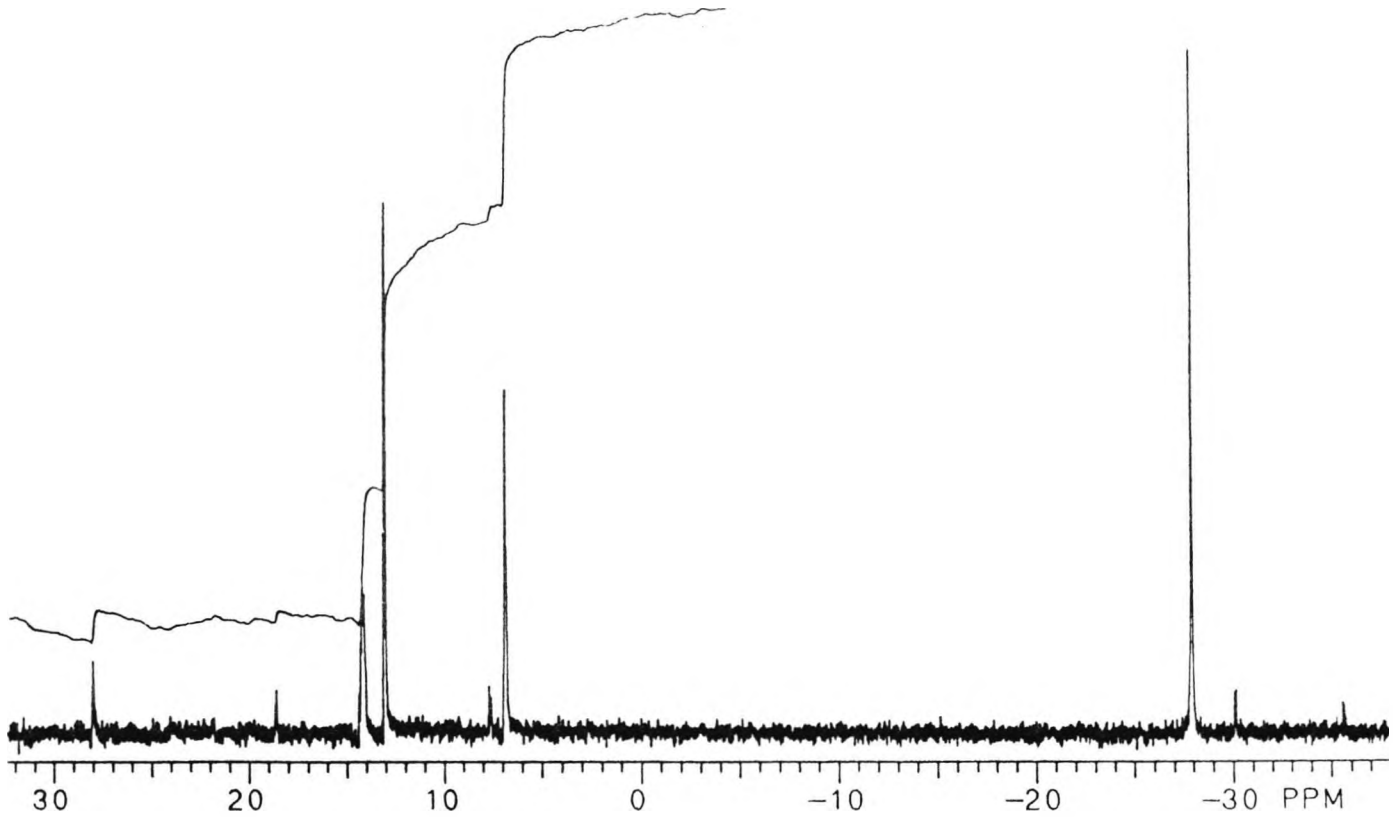

Table 3.9: Variation of product yields* with $[N_2O_4]_t$ for the reaction of allylbenzene with nitrogen dioxide in cyclohexane at 30°C

$[N_2O_4]_t$/mol dm^{-3}	1-nitro-3-phenylpropan-2-ol	Peak B	Peak A
0.1	1	0.51	0.35
0.2	1	0.48	0.23
0.3	1	0.47	0.25

*determined from the relative peak areas in the g.l.c. chromatograms of the crude product mixtures

3.3.1.1 Reaction of allylbenzene with 10000 ppm and 50 ppm gaseous nitrogen dioxide

The reaction of allylbenzene (0.01 mol dm^{-3}) with 10000 ppm sparged gaseous nitrogen dioxide in cyclohexane at 30°C gave 1-nitro-3-phenylpropan-2-ol, 1,2-dinitro-3-phenylpropane and 1-nitro-3-phenyl-2-propylnitrate as the products of reaction after both a 2 h and 5 h reaction period (Figs. 3.17 and 3.18).

The chromatogram of the products from the reaction of allylbenzene (0.01 mol dm^{-3}) with 50 ppm sparged gaseous nitrogen dioxide (5 h) is shown in Fig. 3.19. The main difference from the reaction with 10000 ppm nitrogen dioxide is the absence of the peak due to 1-nitro-3-phenylpropan-2-ol. The main product of the reaction (peak A) was either 1,2-dinitro-3-phenylpropane or 1-nitro-3-phenyl-2-propylnitrate (Section 3.4). In the ^{1}H n.m.r. spectrum (Fig. 3.20) signals due to unreacted allylbenzene and an addition product are seen. The most significant observation is that no allylic substitution products (5.1δ - 5.6δ) were detected in the mixture from the reaction of allylbenzene with low concentrations of nitrogen dioxide.

Fig. 3.17: G.L.C. chromatogram of the products from the reaction of allylbenzene (0.01 mol dm^{-3}) with 10000 ppm sparged gaseous nitrogen dioxide in cyclohexane at 30°C for 2 h (see Section 10·2·1)

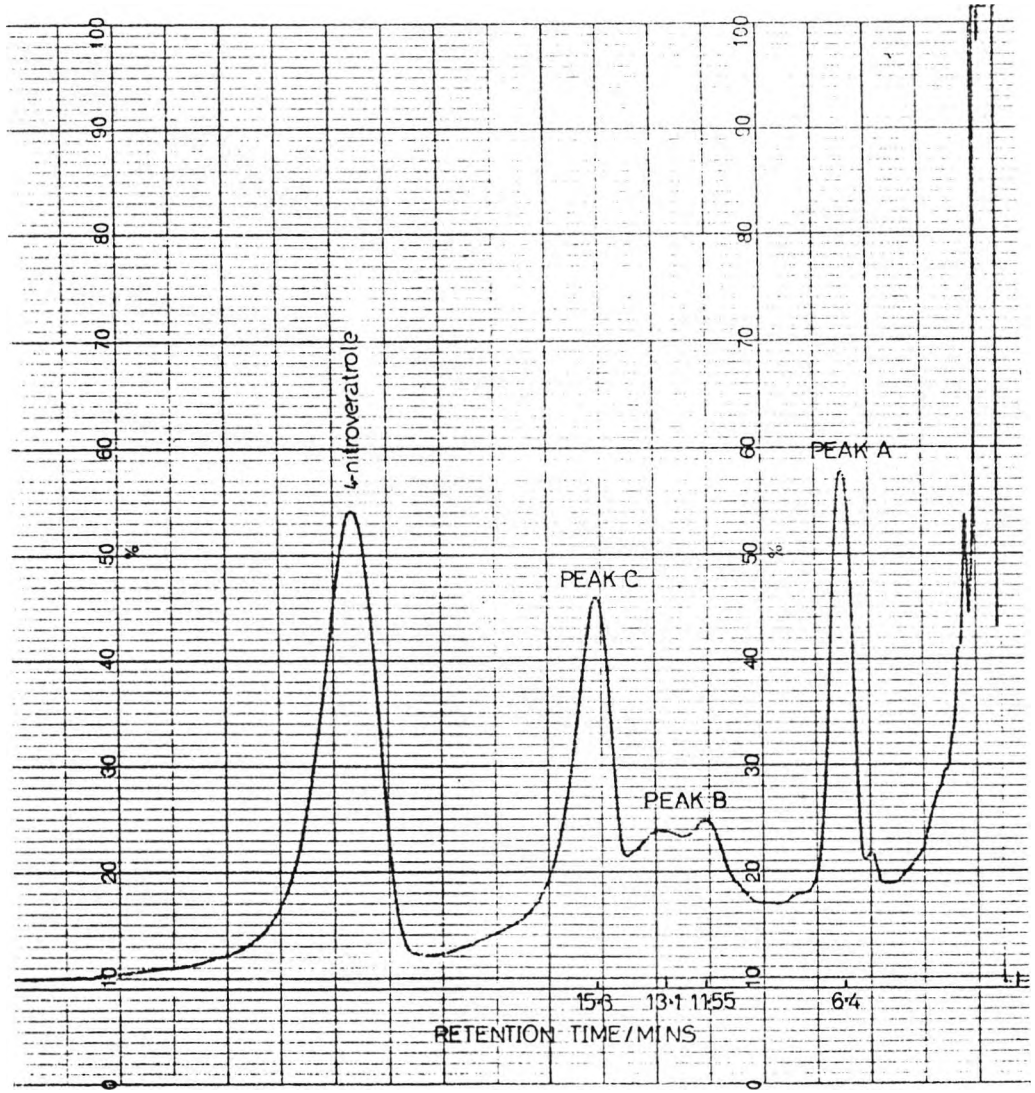

Fig. 3.18: G.L.C. chromatogram of the products from the reaction of allylbenzene (0.01 mol dm^{-3}) with 10000 ppm sparged gaseous nitrogen dioxide in cyclohexane at 30°C for 5 h (see Section 10·2·1)

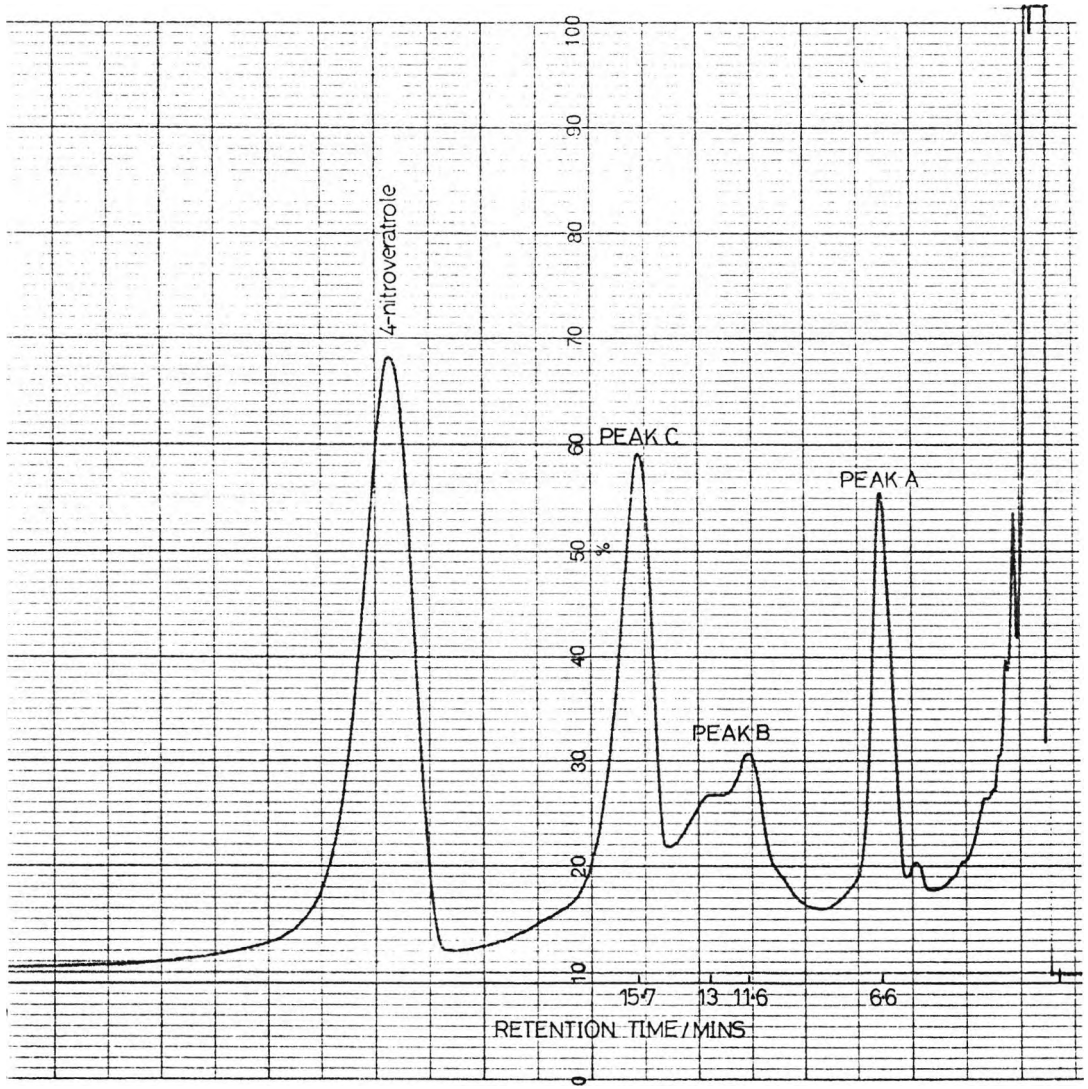

Fig. 3.19: G.L.C. chromatogram of the products from the reaction of allylbenzene (0.01 mol dm^{-3}) with 50 ppm sparged gaseous nitrogen dioxide in cyclohexane at 30°C for 5 h (see Section 10·2·1)

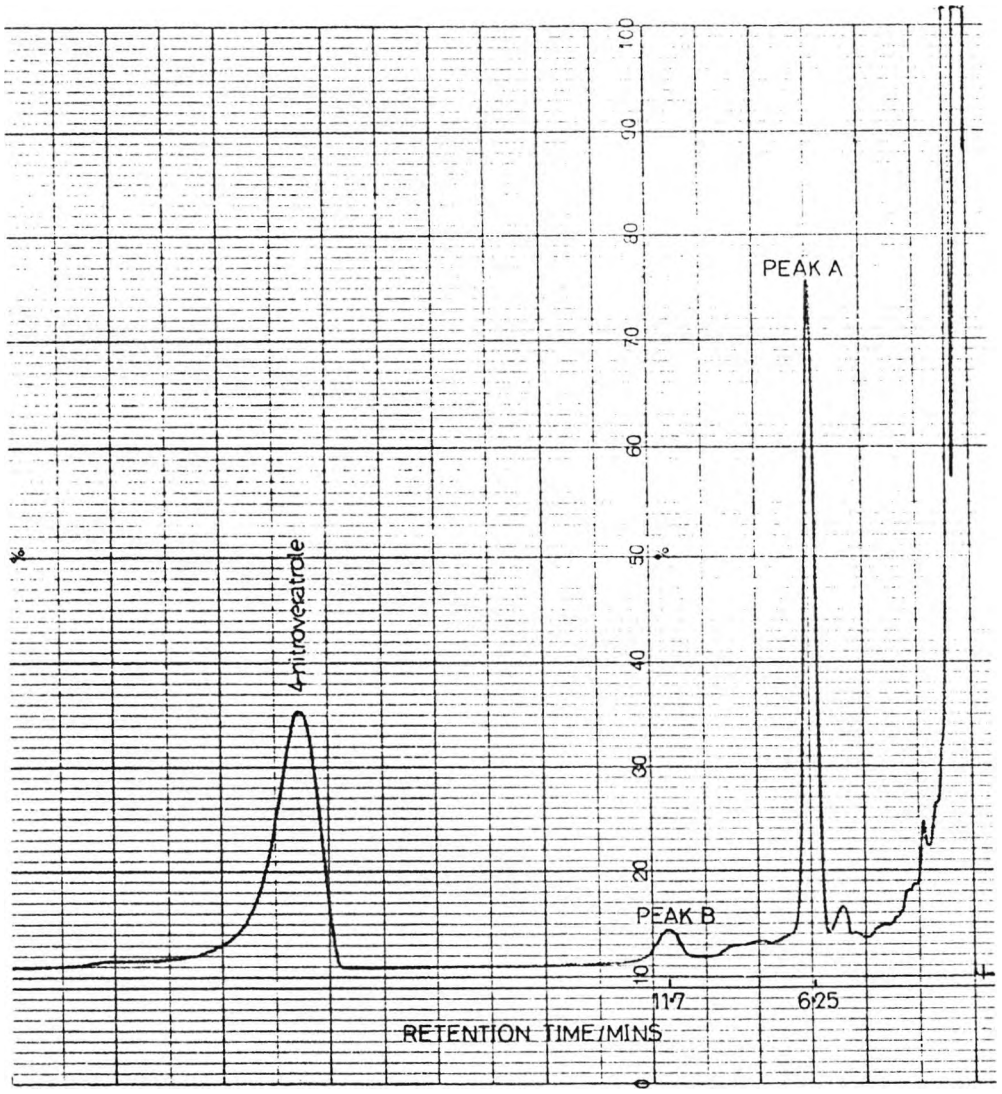

Fig. 3.20: ^{1}H n.m.r. ($CDCl_3$) spectrum of the products from the reaction of allylbenzene (0.01 mol dm^{-3}) with 50 ppm sparged gaseous nitrogen dioxide in cyclohexane at 30°C for 5 h

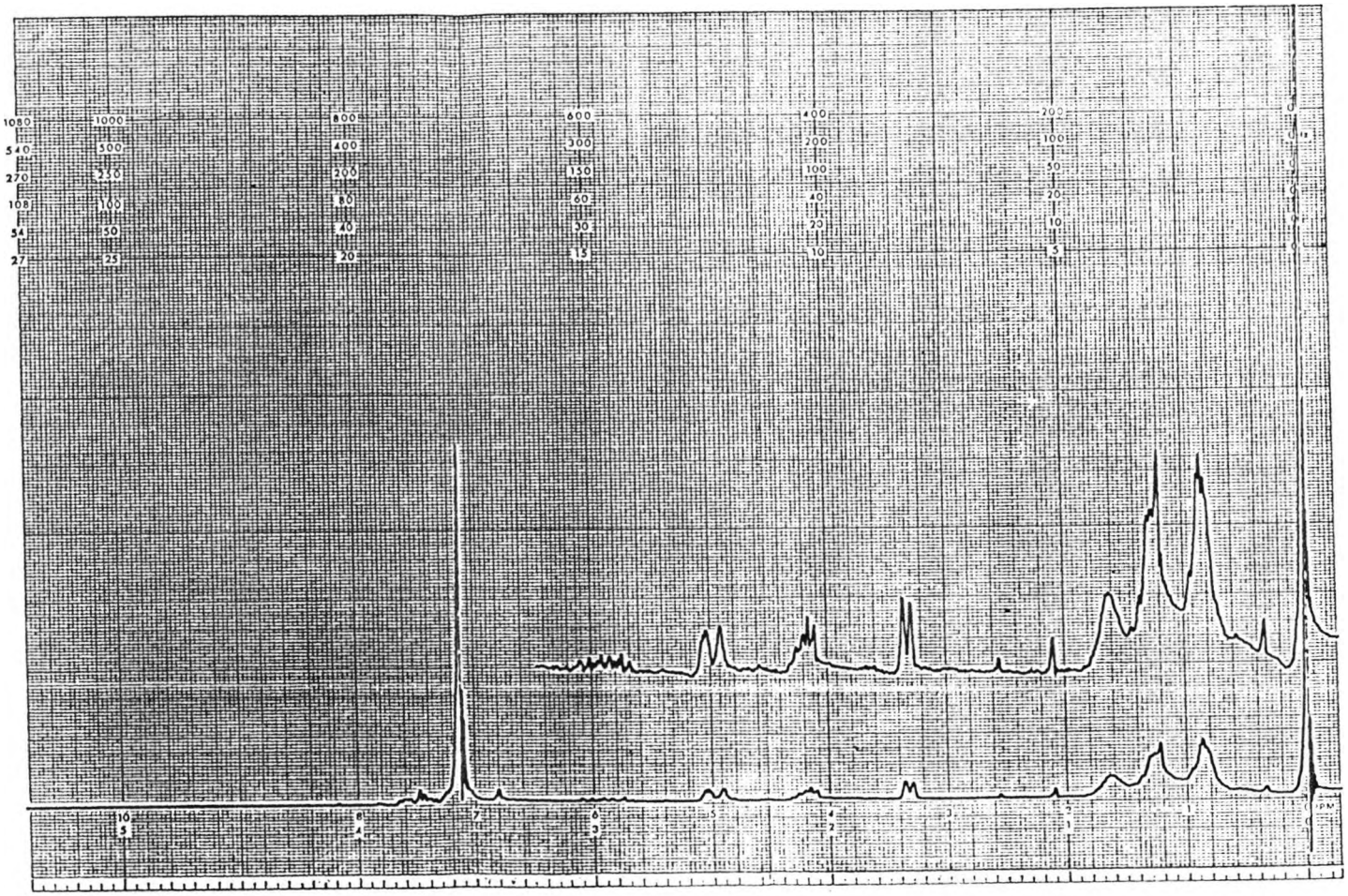

3.3.2 The reactions of styrene, 4-phenylbut-1-ene and 1-dodecene with nitrogen dioxide

^1H n.m.r. confirmed the loss of the C=C bond in styrene (6.5δ - 7δ), 4-phenylbut-1-ene (5.5δ - 6.3δ) and 1-dodecene (5.5δ - 6.3δ) upon their reactions with nitrogen dioxide (Figs. 3.21 - 3.26 respectively). The I.R. spectra of the crude mixtures show peaks due to -OH, -C-H, C=C, NO_2, -ONO and ONO_2 functional groups (Tables 3.10 - 3.12). GC/CIMS, although successful in detecting molecular ions in the chromatogram of the allylbenzene product mixture, was not helpful for characterising products from the above reaction. For styrene, 3 peaks were separated, one of which contained a molecular ion at m/z = 149, indicating the presence of 1-nitro-2-phenylethene (Table 3.13). The mass spectra of the products from the reactions of 4-phenylbut-1-ene and 1-dodecene with nitrogen dioxide only contained molecular fragments. More conclusive product information for the reactions of the above alkenes with nitrogen dioxide was obtained from C.I.D.N.P. experiments (Chapter 4).

Fig.3.21: ^{1}H n.m.r. ($CDCl_3$) spectrum of styrene

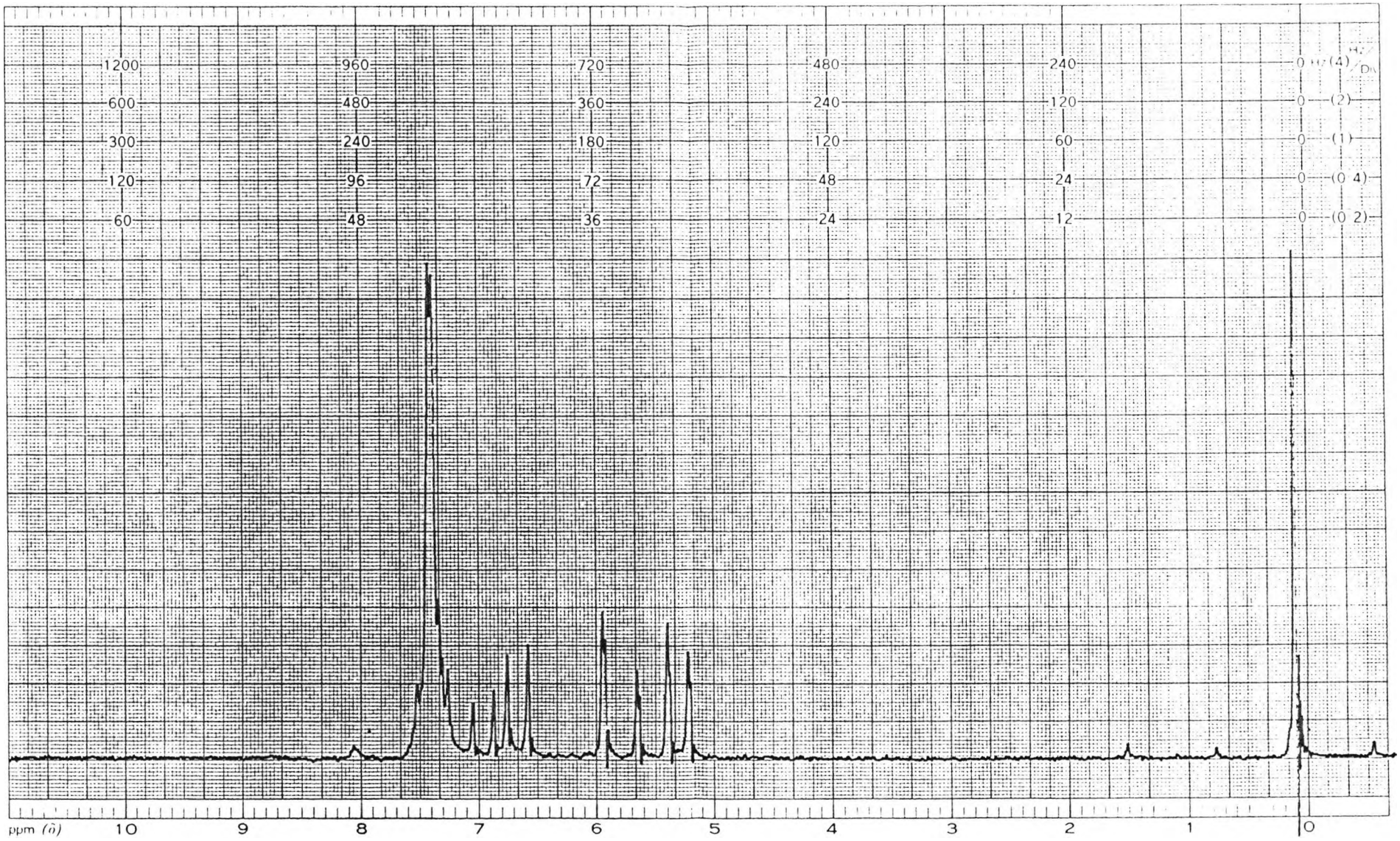

Fig. 3.22: ^{1}H n.m.r. ($CDCl_3$) spectrum of crude product mixture from the reaction of styrene (0.01 mol dm^{-3}) with nitrogen dioxide (0.1 mol dm^{-3}) in cyclohexane at 30°C for 1 h



Fig. 3.23: ^{1}H n.m.r. ($CDCl_3$) spectrum of 4-phenylbut-1-ene

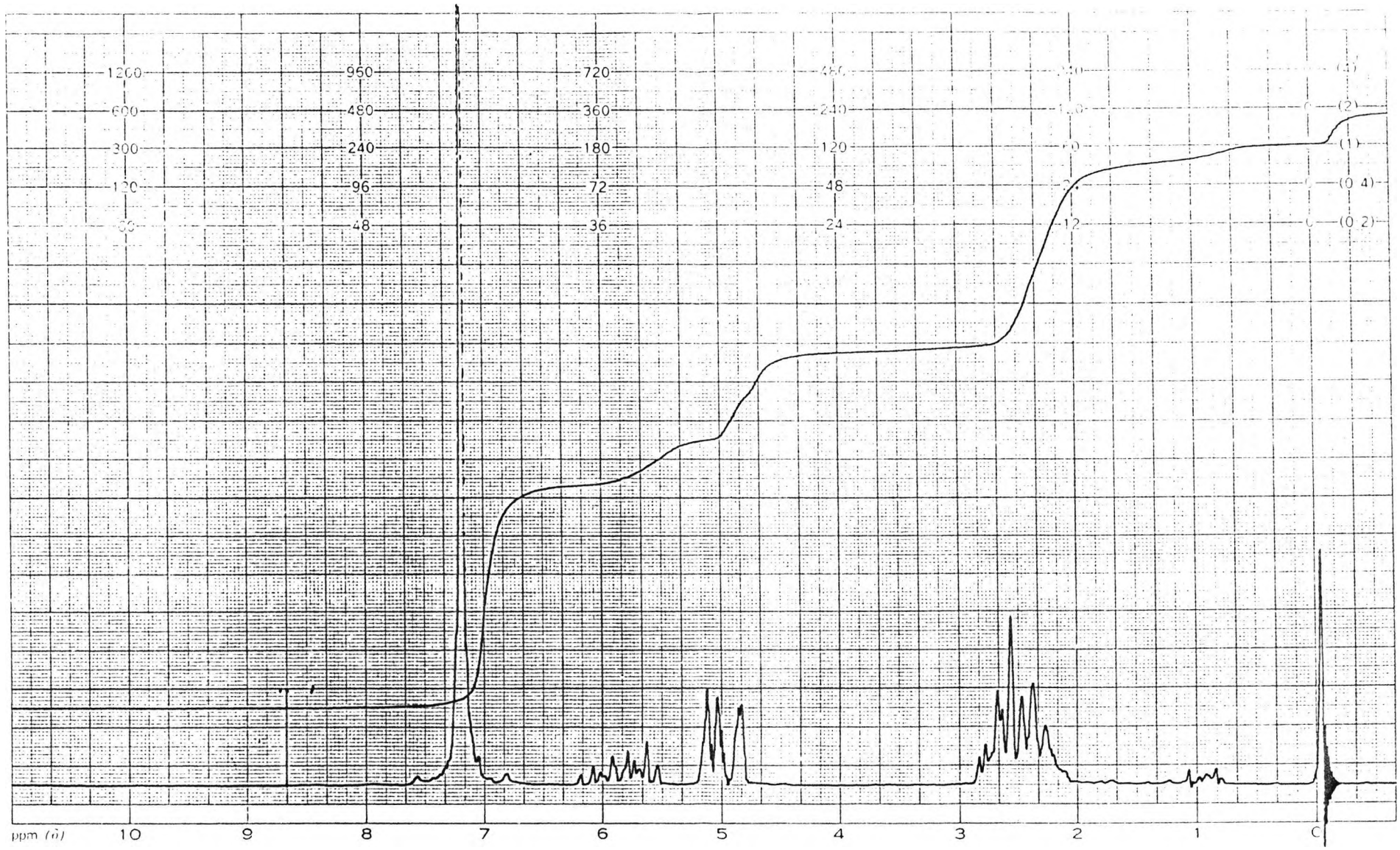

Fig. 3.24: ^{1}H n.m.r. ($CDCl_3$) spectrum of crude product mixture from the reaction of 4-phenylbut-1-ene (0.01 mol dm^{-3}) with nitrogen dioxide (0.1 mol dm^{-3}) in cyclohexane at 30°C for 1 h

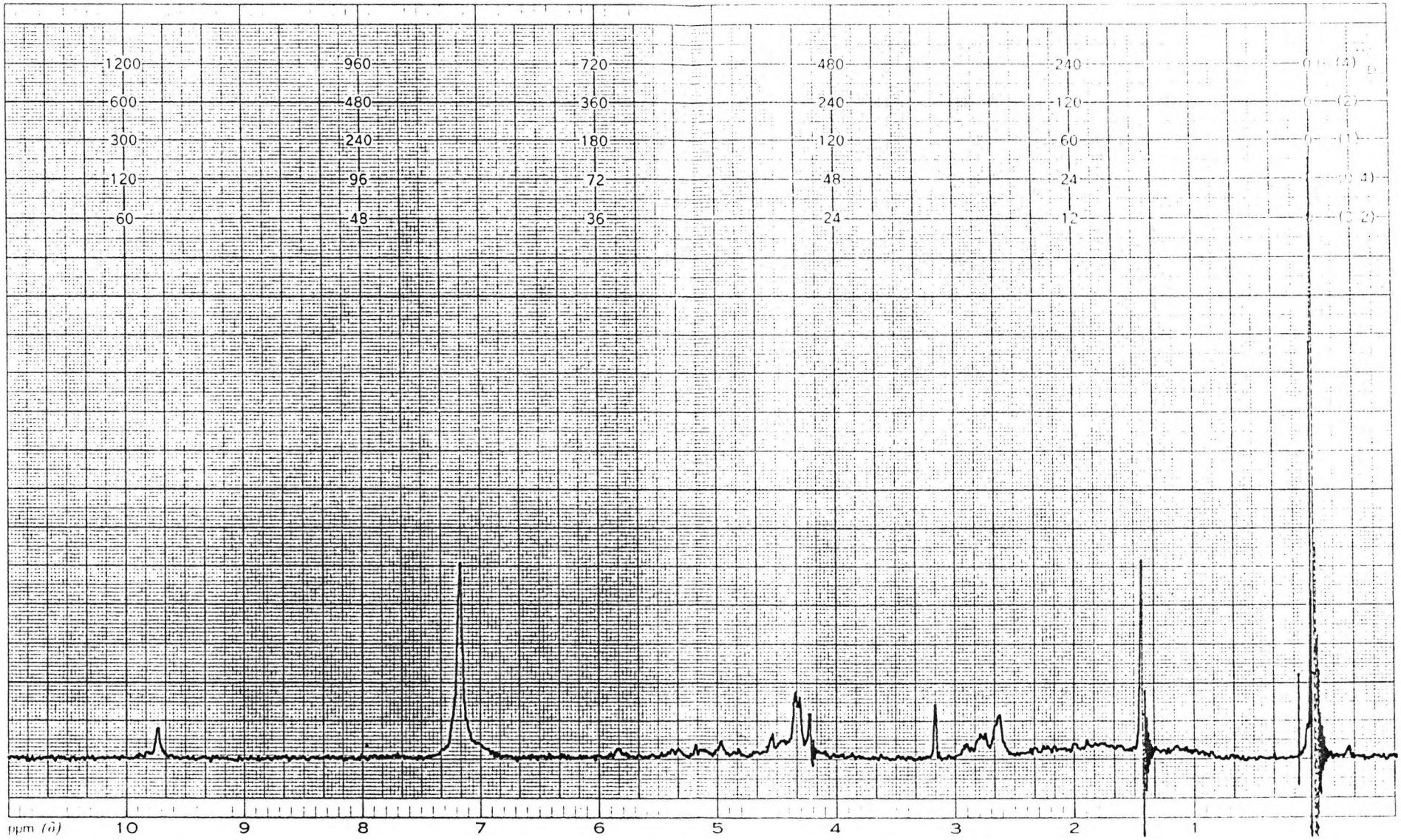

Fig. 3.25: ^{1}H n.m.r. ($CDCl_3$) spectrum of 1-dodecene

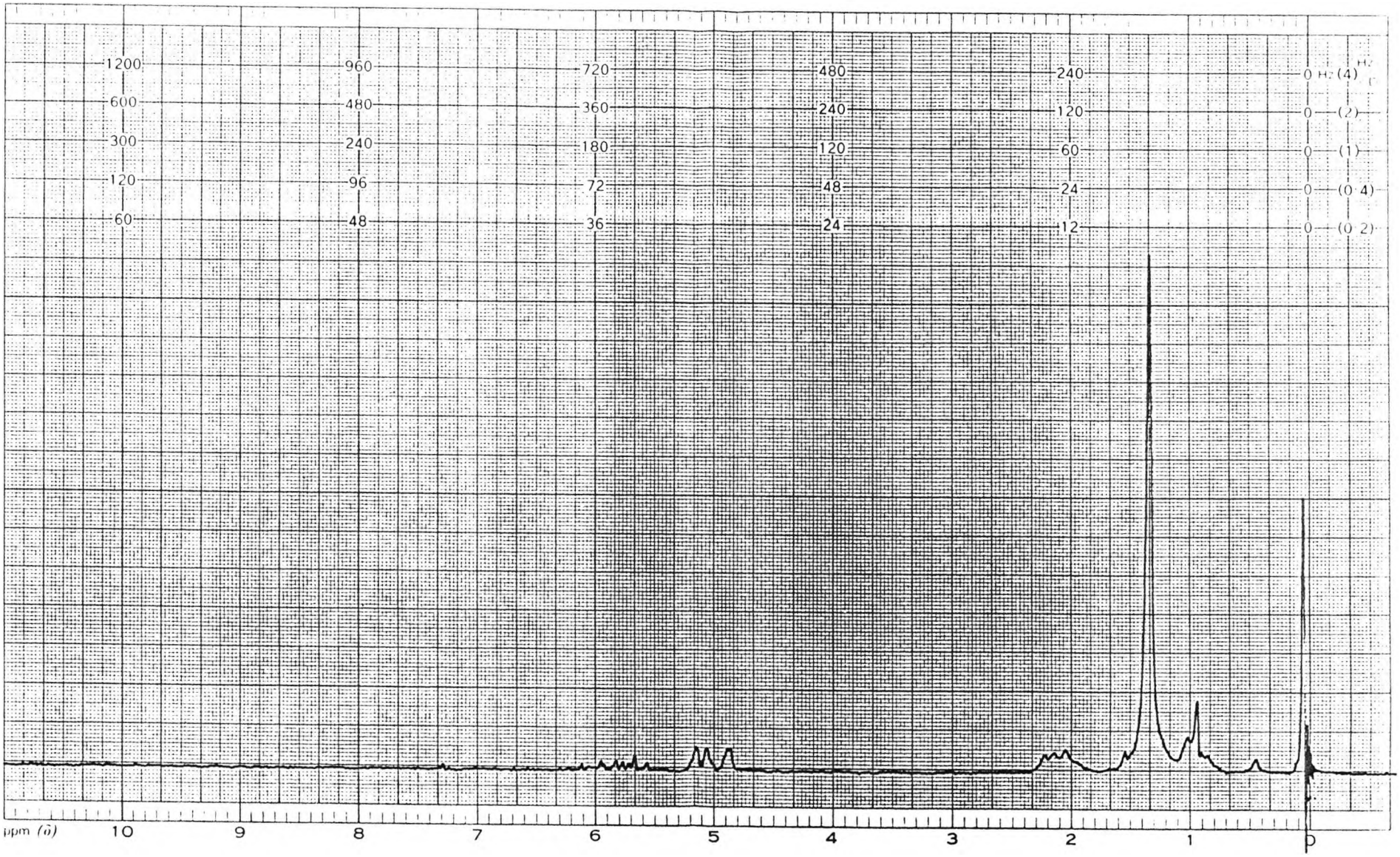

Fig.3.26: ^{1}H n.m.r. ($CDCl_3$) spectrum of crude product mixture from the reaction of 1-dodecene (5×10^{-3} mol dm^{-3}) with nitrogen dioxide (0.05 mol dm^{-3}) in cyclohexane at 30°C for 1 h

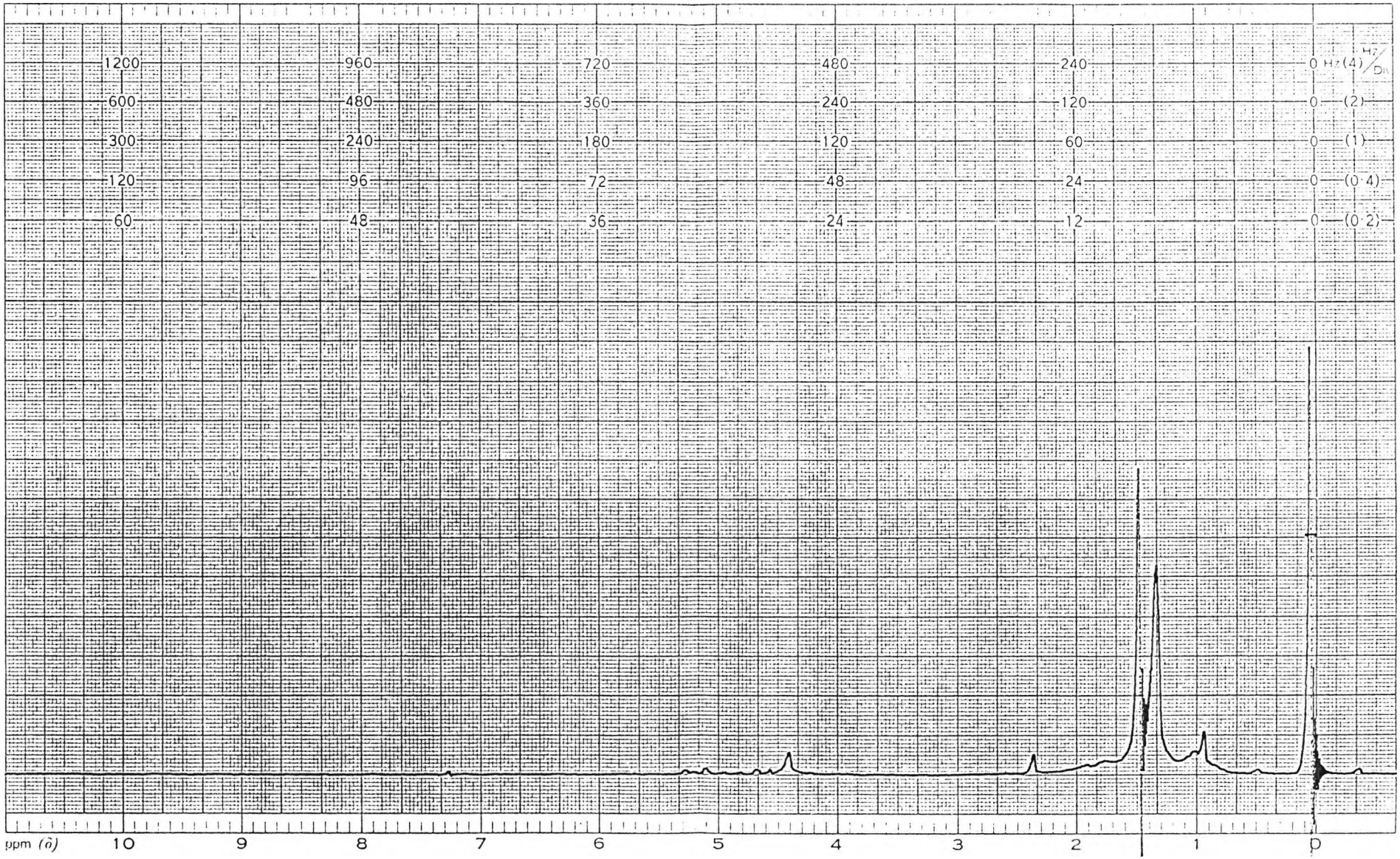

Table 3.10: I.R. spectrum of crude product mixture from the reaction of styrene (0.01 mol dm^{-3}) with nitrogen dioxide (0.1 mol dm^{-3}) in cyclohexane at 30°C for 1 h (thin film)

Peak, cm^{-1}	Assignment
3558 (m)	free and hydrogen bonded O-H
3065 (w)	aromatic = C-H stretch
3031 (m)	
2927 (m)	aliphatic C-H stretch
COMBINATION AND OVERTONE BANDS (w) 2000 - 1700 cm^{-1} 4 peaks (monosubstitution - typically 4 peaks in the range 2000 - 1650 cm^{-1})	
1642 (m)	asymmetric -O-NO_2 stretch
1619 (m)	aromatic C=C stretch
1495 (m)	
1553 (s)	asymmetric N=O stretch -NO_2
1380 (s)	symmetric N=O stretch
1278 (m → s)	symmetric -O-NO_2 stretch

Table 3.11: I.R. spectrum of crude product mixture from the reaction of 4-phenylbut-1-ene (0.01 mol dm^{-3}) with nitrogen dioxide (0.1 mol dm^{-3}) in cyclohexane at 30°C for 1 h (thin film)

Peak, cm^{-1}	Assignment
3558 (m)	free and hydrogen bonded O-H
3064 (w) 3028 (m)	aromatic = C-H stretch
2927 (m → s)	aliphatic C-H stretch
COMBINATION AND OVERTONE BANDS (w) 2000 - 1700 cm^{-1} 4 peaks (monosubstitution - typically 4 peaks in the range 2000 - 1650 cm^{-1})	
1642 (m)	asymmetric -O-NO_2 stretch
1603 (m) 1495 (m)	aromatic C=C stretch
1554 (s)	asymmetric N=O stretch -NO_2
1382 (s)	symmetric N=O stretch
1277 (m → s)	symmetric -O-NO_2 stretch

Table 3.12: I.R. spectrum of crude product mixture from the reaction of 1-dodecene (5×10^{-3} mol dm^{-3}) with nitrogen dioxide (0.05 mol dm^{-3}) in cyclohexane at 30°C for 1 h (thin film)

Peak, cm^{-1}	Assignment
3558 (m)	free and hydrogen bonded O-H
2925 (s)	aliphatic C-H stretch
1642 (m)	asymmetric O-NO_2 stretch
1554 (s)	asymmetric N=O stretch -NO_2
1378 (m)	symmetric N=O stretch
1467 (m)	CH_2 group
1276 (m)	symmetric -O-NO_2 stretch

Table 3.13: GC/CIMS(NH_3) chromatogram of crude product mixture from the reaction of styrene (0.01 mol dm^{-3}) with nitrogen dioxide (0.1 mol dm^{-3}) in cyclohexane at 30°C for 1 h (see Section 10·3·2)

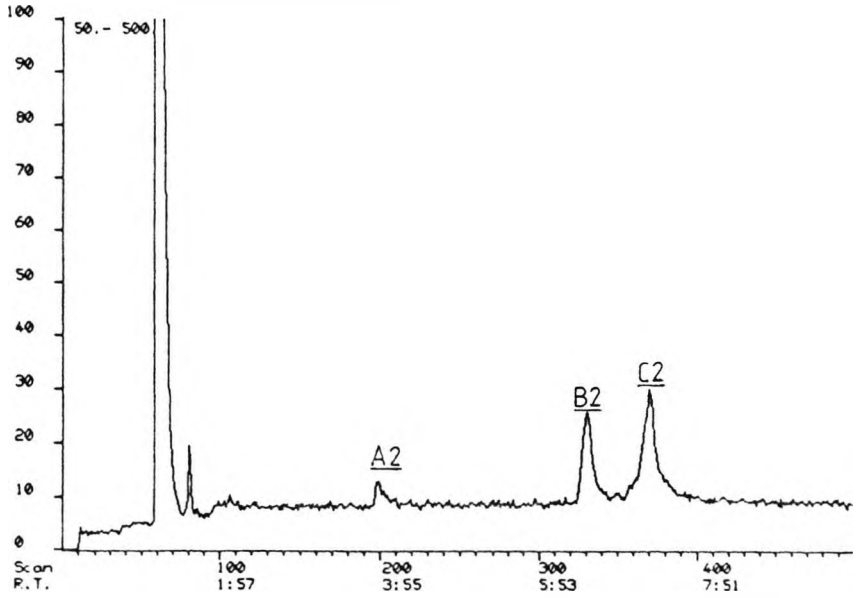

Peak		m/z
A2	$PhCH{=}CHNO_2$	149(5.3%;M^+),105(100%) 77(68%),51(25%)
B2	$PhCH{=}CHNO_2$	105(7%),81(15%) 55(100%)
C2	$PhCH(OH)\text{-}CH_2NO_2$	147(1.1%),105(6%), 83(100%),55(57%)

3.4 Discussion

Product analysis indicates that styrene, allylbenzene, 4-phenylbut-1-ene and 1-dodecene react with nitrogen dioxide in cyclohexane at 30°C to give the corresponding nitro-nitrite, dinitro and nitro-nitrate as the major products of reaction. I.R. studies of the reaction of allylbenzene with nitrogen dioxide suggest that 1-nitro-3-phenyl-2-propylnitrite is hydrolysed to 1-nitro-3-phenylpropan-2-ol as the reaction proceeds. The source of water for this reaction is assumed to be fortuitous water vapour since both the solvent and nitrogen dioxide were rigorously dried before use.

There is no significant change in products or proportions over the nitrogen dioxide concentrations used in the kinetic studies (see Table 3.13 and Chapter 5).

Peak C in the g.l.c. chromatogram of the product mixture from the reaction of allylbenzene (0.01 mol dm^{-3}) with nitrogen dioxide (0.1 mol dm^{-3}) - Fig. 3.5 - has been identified as 1-nitro-3-phenylpropan-2-ol. 1,2-dinitro-3-phenylpropane and 1-nitro-3-phenyl-2-propylnitrate both decompose in the GC/EIMS and GC/CIMS to give 1-nitro-3-phenylpropene. The peaks in the g.l.c. due to these compounds were tentatively assigned on the basis of the results obtained from the sparging experiments. In the g.l.c. chromatogram of the products from the reaction of allylbenzene with 50 ppm nitrogen dioxide, a peak at 6 min is seen, but no peak due to 1-nitro-3-phenylpropan-2-ol is detected. This reaction is expected to lead predominantly to formation of dinitro compound, with little nitro-nitrate being formed because of the low concentrations of nitrogen dioxide used. Thus, the peak at 6 min is likely to be due to 1,2-dinitro-3-phenylpropane. Comparison of the chromatogram from this experiment with that from above suggests that Peak A in Fig. 3.5 (retention time = 6.9 min) is 1,2-dinitro-3-phenylpropane. By a process of elimination Peak B is therefore 1-nitro-3-phenyl-2-propylnitrate.

The reason for the absence of the 1-nitro-3-

phenylpropan-2-ol peak in the chromatogram of the products from the reaction of allylbenzene with 50 ppm nitrogen dioxide is not clear. Reactions at low concentrations of nitrogen dioxide must involve a reaction between allylbenzene and nitrogen dioxide which favours the dinitro product.

These results are in good agreement with similar work carried out on the reaction of substituted alkenes with nitrogen dioxide.[44] The formation of 1,2-dinitro-2-phenylethane was not reported, however, in a recent study of the reaction of styrene with nitrogen dioxide.[44]

CHAPTER 4

C.I.D.N.P. STUDIES OF THE REACTIONS OF STYRENE, ALLYLBENZENE, 4-PHENYLBUT-1-ENE AND 1-DODECENE WITH NITROGEN DIOXIDE

4. C.I.D.N.P. studies of the reactions of styrene, allylbenzene, 4-phenylbut-1-ene and 1-dodecene with nitrogen dioxide

4.1 Introduction

If n.m.r. spectra are obtained of a solution in which a radical reaction is taking place, then the n.m.r. signals due to the starting materials and the products may show anomalous intensities (either enhanced absorption or emission). These anomalies arise from the phenomenon of chemically induced dynamic nuclear polarisation or C.I.D.N.P.

The phenomenon of C.I.D.N.P. was first observed independently by Bargon, Fischer and Johnsen,[101] and Ward and Lawler.[102] Initial attempts to explain the phenomenon in terms of the Overhauser effect or dynamic nuclear polarisation led to it being called C.I.D.N.P., but did not explain all of the experimental results.

Closs,[103] and Kaptein and Oosterhoff[104] independently proposed the radical pair or C.K.O. theory,which explained all the experimental results, and all discussion of C.I.D.N.P. is now made in terms of this theory. Both experimental and theoretical aspects of C.I.D.N.P. have been extensively reviewed.[105]

4.2 C.K.O. Theory

Consider two radicals R$^{\bullet}$ and S$^{\bullet}$ in a solvent caged radical pair. The radical pair could be formed by diffusion together of the radicals (an F precursor), by homolysis of an R-S bond (an S precursor), or by electron transfer between R^+ and S^- (an F precursor) to give either a singlet or triplet radical pair as shown below (Scheme 4.1):

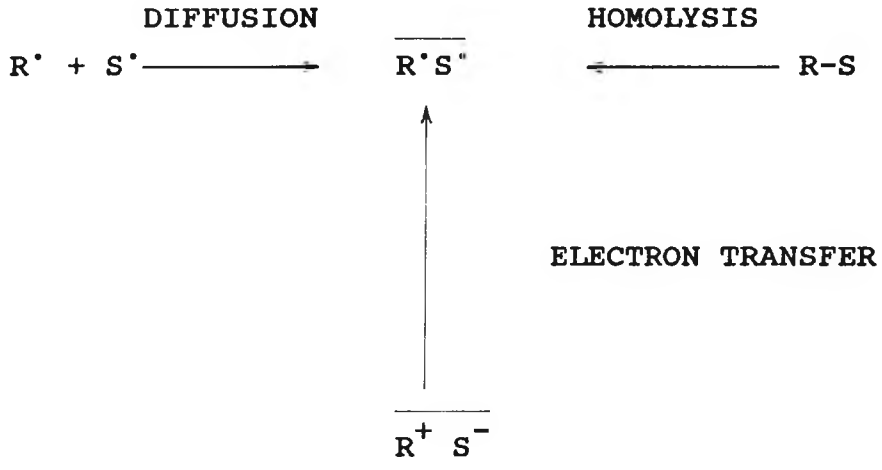

Scheme 4.1

Competition between reaction (to give cage products) and diffusion apart (to give escape products) results in anomalous nuclear spin state distributions, and hence n.m.r. signal intensities, in the products and, potentially, the starting materials. The phase of the net polarisation, Γ, can be predicted from Kaptein's rule.[106] For use with ^{15}N n.m.r. spectroscopy, Kaptein's rule has to be modified[107] to allow for the negative gyromagnetic ratio of the ^{15}N nucleus (equation 4.1).

Kaptein's rule:

$$\Gamma = - \mu\epsilon a_N(g_{R\cdot} - g_{S\cdot}) \qquad (4.1)$$

Sign of Γ is POSITIVE FOR ABSORPTION

NEGATIVE FOR EMISSION

where μ = + when the radical pair is formed from a triplet precursor or by diffusion together of free radicals

\- when the radical pair is formed from a singlet precursor

ϵ = + for recombination products

\- for products of radicals that have escaped from the cage

a_N = sign of the hyperfine coupling constant for the nucleus under consideration

$(g_{R\cdot} - g_{S\cdot})$= sign of the difference of g values of the two radicals, where $R^{\cdot}$ is the radical containing the nucleus under consideration

The emission and absorption signals can also be rationalised in the following, somewhat simplified, way. For a system of two coupled electrons, (the situation in a radical pair), the total spin quantum number, S, equals 0 or 1. If S equals 0 then the system is in a singlet state; if S equals 1 then the system is in a triplet state. In the singlet state the spins are opposed, in the triplet state they can have three relative configurations or sub-states (Fig. 4.1):

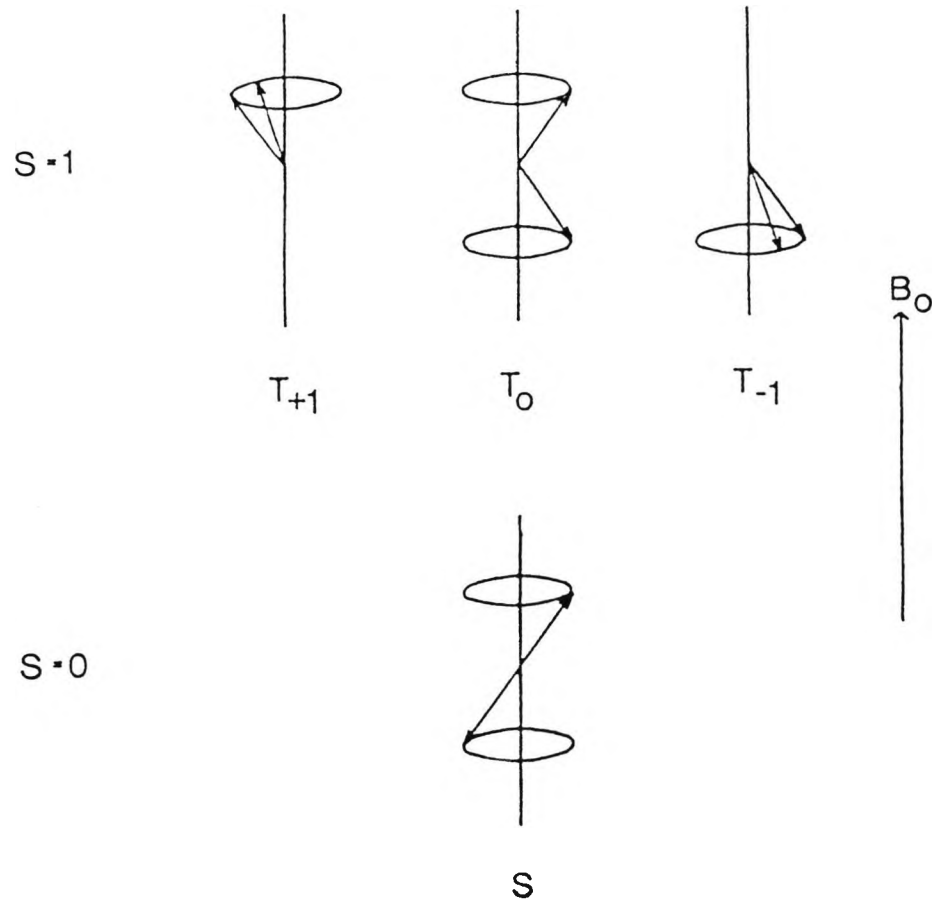

Fig. 4.1

If the spins are opposed as the two radicals interact (singlet state) they can combine to form a product. The triplet state, however, can only form products if it is converted to the singlet state before the radicals fully separate. If the two electrons in the T_0 state are not precessing at the same frequency then the S and T_0 states can interconvert. Since the electron and spin states are coupled, the interconversion between singlet and triplet states is affected by the interaction of nuclear and electron spin states. In the absence of nuclear coupling, the rate of this interconversion, or intersystem crossing, is equal to the difference in the rates of precession of the two electrons (see Appendix):

$$(w_{R\cdot} - w_{S\cdot}) = \frac{2\pi\beta}{h}(g_{R\cdot} - g_{S\cdot}) \qquad (4.2)$$

If the unpaired electron in radical $R^{\cdot}$ is coupled to a nucleus with spin, the expression becomes

$$(w_{R\cdot} - w_{S\cdot}) = \frac{2\pi\beta}{h}[(g_{R\cdot} - g_{S\cdot})B + am_I] \qquad (4.3)$$

The product will then have preferentially the nuclear spin states that favour the necessary spin inversion to singlet pairing. The result is that radical pairs that have their nuclei and electrons in certain spin states are more likely to yield products, whereas radical pairs in other spin states are more likely to escape. The product therefore has abnormal populations of some nuclear spin states giving abnormal relative line intensities in the n.m.r. spectrum.

A similar reasoning applies to a pair formed initially in the singlet state. In this case, however, product formation will occur in those radical pairs which have nuclear spin states which least favour the singlet - triplet interconversion, as the latter will lead to preferential escape from the cage.

4.3 Experimental

The nitrations of styrene, allylbenzene, 4-phenylbut-1-ene and 1-dodecene by ^{15}N-labelled nitrogen dioxide in cyclohexane were studied by ^{15}N n.m.r. spectroscopy, to detect the presence or absence of a ^{15}N C.I.D.N.P. effect in the nitration products. The reactions were carried out at room temperature (r.t.) using a Bruker-300 Fourier transform spectrometer. The n.m.r. machine was stable during these experiments and therefore was not locked on deuterium. Nitrobenzene labelled with ^{15}N was used as an internal standard for intensity measurements and chemical shifts.

The ^{15}N n.m.r. spectra taken during reaction had 8 pulses with a delay time of 15s and a pulse angle of 25°. 500 pulses were used in recording the spectra of reaction products.

In all the studies, the time ascribed to each spectrum, with the exception of the infinity spectrum, was the mid-point of the accumulation.

4.4 Results

4.4.1 The reaction of styrene with ^{15}N-labelled nitrogen dioxide

The rate of reaction of styrene (0.26 mol dm^{-3}) with ^{15}N-labelled nitrogen dioxide (0.25 mol dm^{-3}) was too fast to be monitored by ^{15}N n.m.r. Hence, very little product information could be obtained during the early stages of reaction, and a C.I.D.N.P. effect was not observed. The spectrum taken at the end of the reaction, however, shows four nitro signals and one nitrite signal to low field of the standard, ^{15}N-labelled nitrobenzene (set at 0 p.p.m.), with chemical shifts 4.69, 6.90, 11.90, 12.87 and 193.82 p.p.m. respectively, indicating the formation of 1,2-dinitro-2-phenylethane, 2-nitro-1-phenylethylnitrite and 2-nitro-1-phenylethanol (Fig. 4.2), by analogy with the results from allylbenzene.

4.4.2 The reaction of allylbenzene with ^{15}N-labelled nitrogen dioxide

The ^{15}N n.m.r. spectra taken during the nitration of allylbenzene (0.23 mol dm^{-3}) by ^{15}N-labelled nitrogen dioxide (0.22 mol dm^{-3}) are shown in Fig. 4.3. In the initial spectrum (1 min), two absorption signals appear at 4.94 p.p.m. and 7.75 p.p.m. corresponding to the 1-nitro groups of 1,2-dinitro-3-phenylpropane and 1-nitro-3-phenyl-2-propylnitrite respectively. Both are strongly enhanced, the intensities of the two peaks being greater than their final values by a factor of 14. A third nitro group appears as a strong emission signal at 13.14 p.p.m. corresponding to the 2-nitro group of 1,2-dinitro-3-phenylpropane. The intensity of this signal is increased by a factor of 288. All three peaks are to low field of the standard, ^{15}N-labelled nitrobenzene, 0 p.p.m. Subsequent spectra in Fig. 4.3 show the stages when the absorption and emission signals become progressively weaker and comparable in intensity with the standard as the reaction proceeds.

The T_{∞} spectrum shows the four nitro absorption signals and one nitrite signal obtained at the end of the reaction, corresponding to the formation of 1,2-dinitro-3-phenylpropane, 1-nitro-3-phenyl-2-propylnitrite and 1-nitro-3-phenylpropan-2-ol. The above signals were assigned according to the region in which they lie in the spectrum and by comparison with the ^{15}N proton coupled n.m.r. spectral studies in Chapter 3 (Section 4.5).

4.4.3 The reaction of 4-phenylbut-1-ene with ^{15}N-labelled nitrogen dioxide

The ^{15}N n.m.r. spectra taken during the nitration of 4-phenylbut-1-ene (0.25 mol dm^{-3}) by ^{15}N-labelled nitrogen dioxide (0.22 mol dm^{-3}) are shown in Fig. 4.4. In the initial spectrum (1 min), two absorption signals appear at 5.18 p.p.m. and 7.86 p.p.m. corresponding to the 1-nitro groups of 1,2-dinitro-4-phenylbutane and 1-nitro-4-phenyl-

2-butylnitrite. Both are strongly enhanced, the intensities of the two peaks being greater than their final values by a factor of 6 and 12 respectively. A third nitro group appears as a strong emission signal at 14.56 p.p.m. corresponding to the 2-nitro group of 1,2-dinitro-4-phenylbutane. The intensity of this signal is increased by a factor of 141. All three peaks are to low field of the standard, ^{15}N-labelled nitrobenzene, 0 p.p.m. Subsequent spectra in Fig. 4.4 shows the stages when the absorption and emission signals become progressively weaker and comparable in intensity with the standard as the reaction proceeds.

The T_{∞} spectrum shows the four nitro absorption signals and one nitrite signal obtained at the end of the reaction, corresponding to the formation of 1,2-dinitro-4-phenylbutane, 1-nitro-4-phenyl-2-butylnitrite and 1-nitro-4-phenylbutan-2-ol. The above assignments were made by comparison with the results from the reaction of allylbenzene with ^{15}N-labelled nitrogen dioxide.

4.4.4 The reaction of 1-dodecene with ^{15}N-labelled nitrogen dioxide

The ^{15}N n.m.r. spectra taken during the nitration of 1-dodecene (0.23 mol dm^{-3}) by ^{15}N-labelled nitrogen dioxide (0.23 mol dm^{-3}) are shown in Fig. 4.5. In the initial spectrum (1 min) two absorption signals appear at 5.39 p.p.m. and 8.10 p.p.m. corresponding to the 1-nitro groups of 1,2-dinitrododecane and 1-nitro-2-dodecylnitrite. Both are strongly enhanced, the intensities of the two peaks being greater than their final values by a factor of 6 and 13 respectively. A third nitro group appears as a strong emission signal at 15.70 p.p.m. corresponding to the 2-nitro group of 1,2-dinitrododecane. The intensity of this signal is increased by a factor of 134. All three peaks are to low field of the standard, ^{15}N-labelled nitrobenzene, 0 p.p.m. Subsequent spectra in Fig. 4.5 show the stages when the absorption and emission signals become progressively weaker and comparable in intensity with the standard as the reaction

proceeds.

The T_{∞} spectrum shows the four nitro absorption signals and one nitrite signal obtained at the end of the reaction, corresponding to the formation of 1,2-dinitrododecane, 1-nitro-2-dodecylnitrite and 1-nitrododecan-2-ol. The above assignments were made by comparison with the results from the reaction of allylbenzene with ^{15}N-labelled nitrogen dioxide.

Fig. 4.2: T_∞ spectrum (45 min, 500 pulses) obtained at the end of reaction of styrene (0.26 mol dm^{-3}) with ^{15}N-labelled nitrogen dioxide (0.25 mol dm^{-3}) in cyclohexane at r.t.

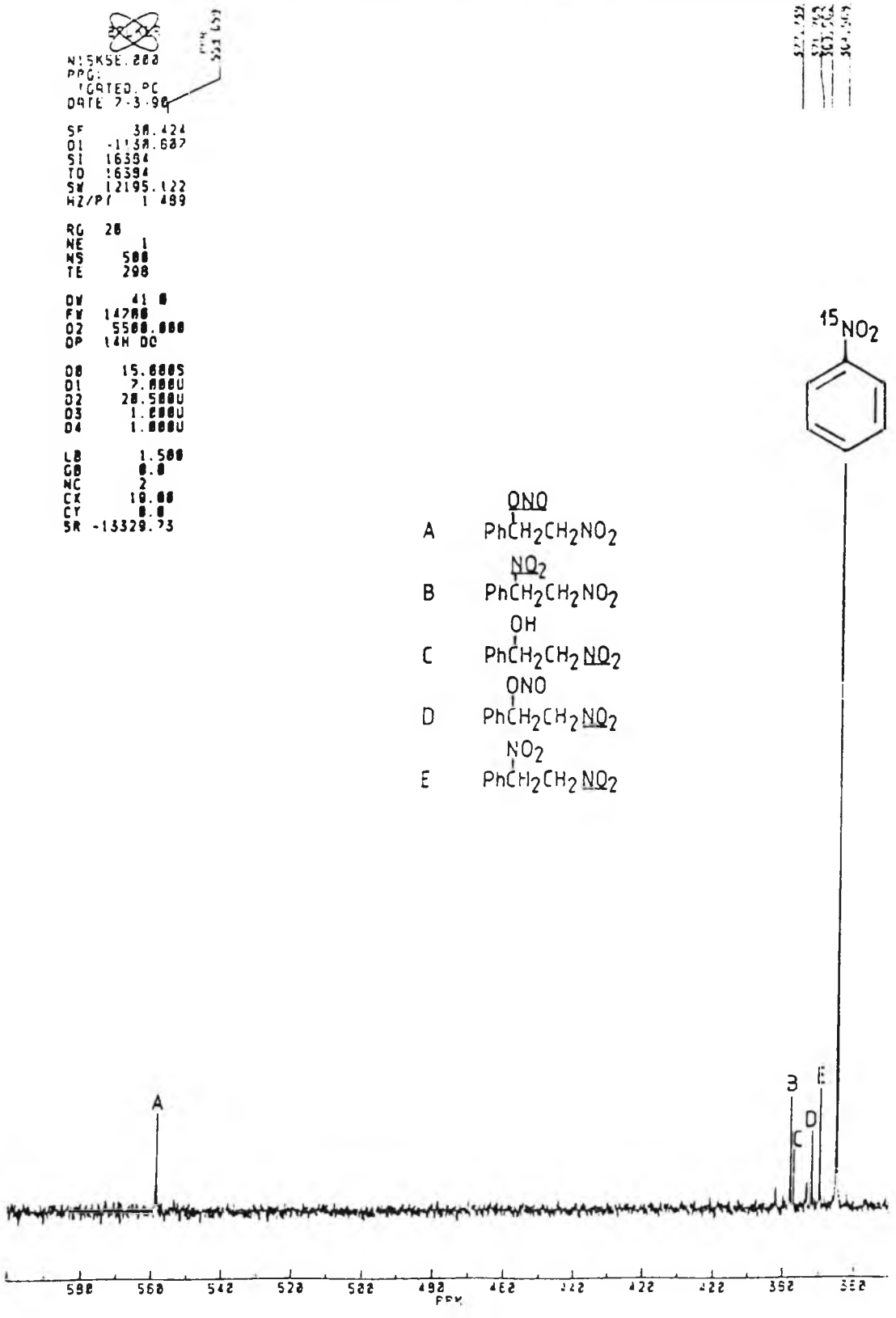

A $PhCH(ONO)CH_2NO_2$

B $PhCH(NO_2)CH_2NO_2$

C $PhCH(OH)CH_2NO_2$

D $PhCH(ONO)CH_2NO_2$

E $PhCH(NO_2)CH_2NO_2$

Fig. 4.3: ^{15}N n.m.r. spectra during the reaction of allylbenzene (0.23 mol dm^{-3}) with ^{15}N-labelled nitrogen dioxide (0.22 mol dm^{-3}) in cyclohexane at r.t.

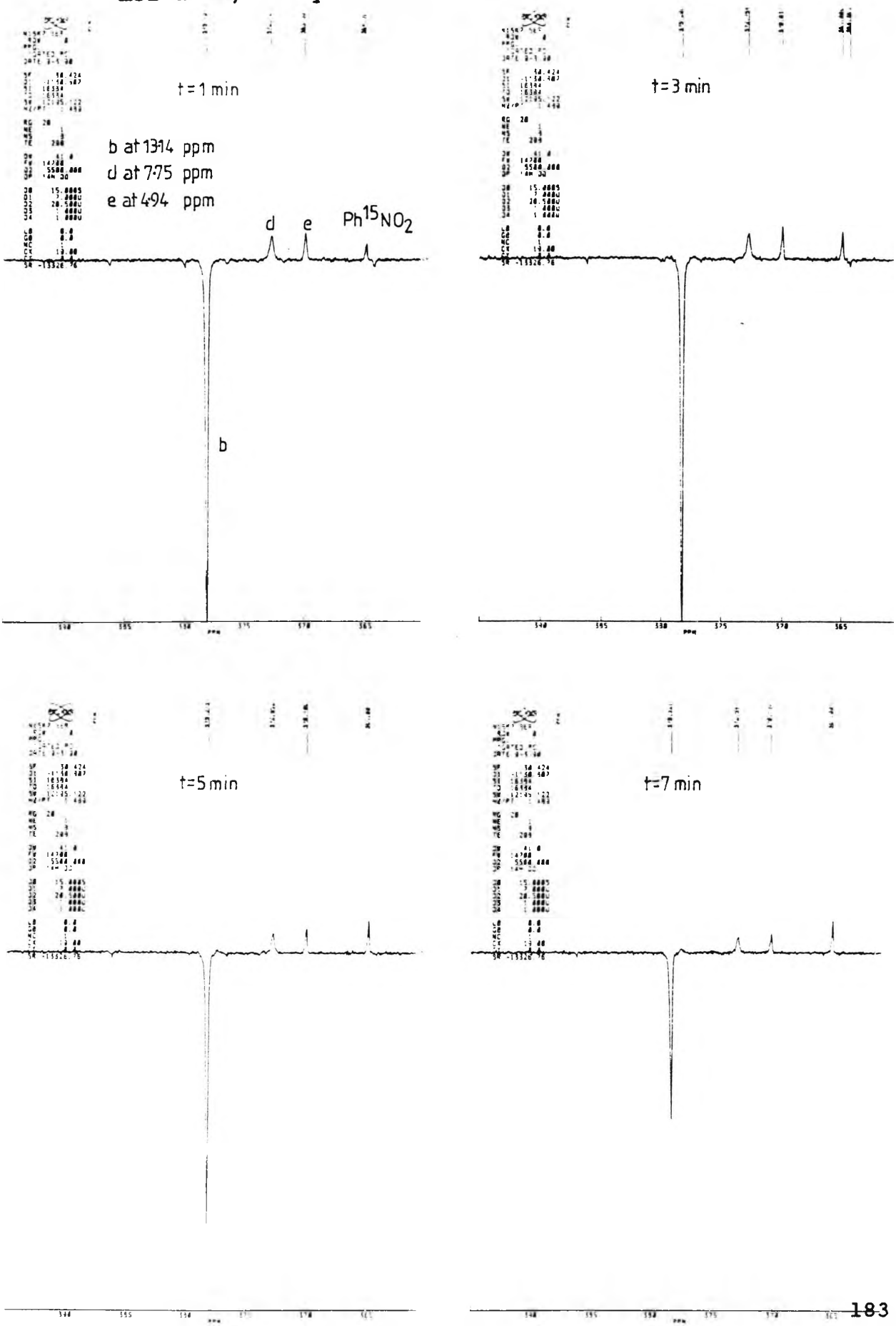

Fig. 4.3: .....cont'd

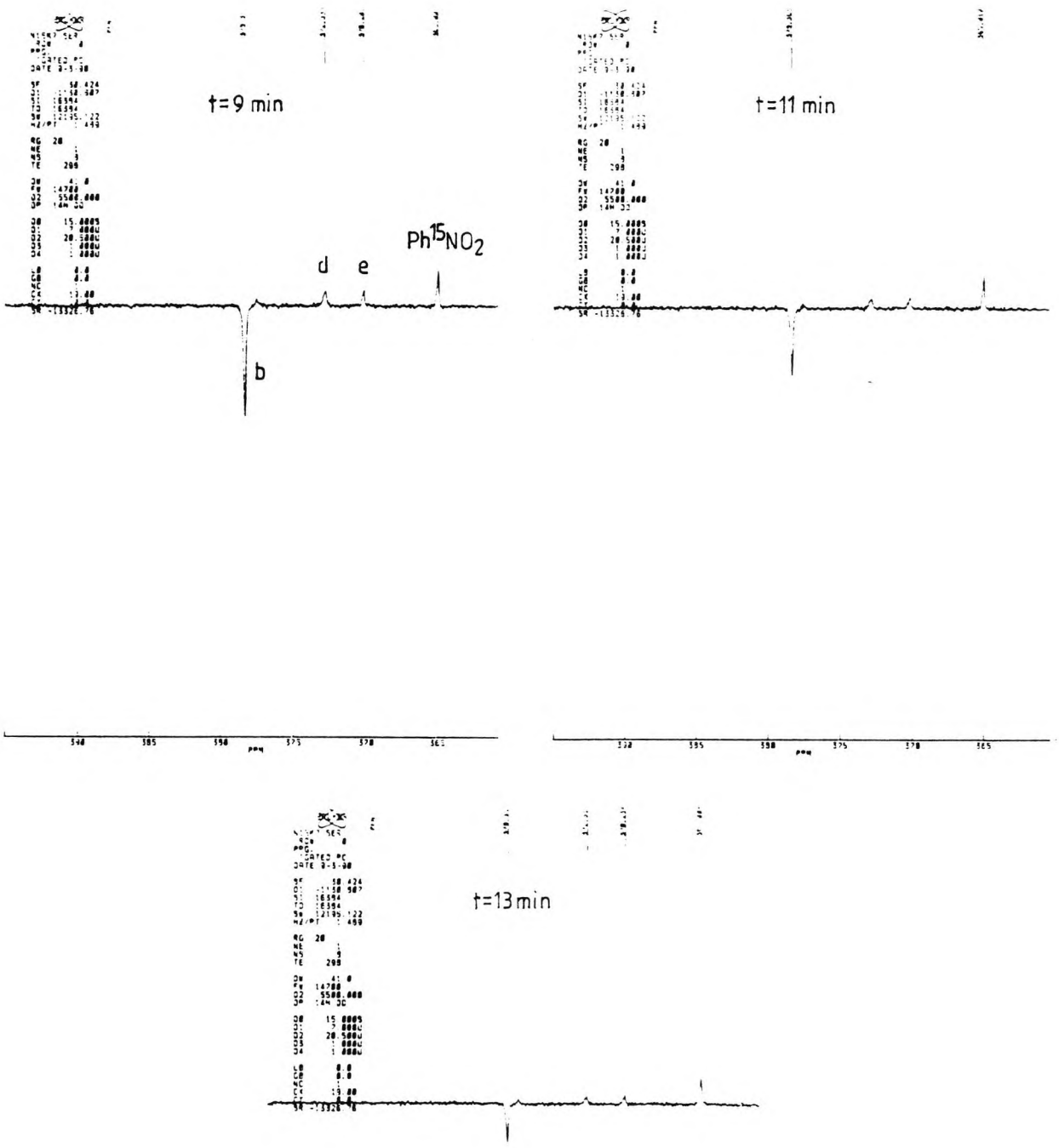

Fig. 4.3: .....cont'd

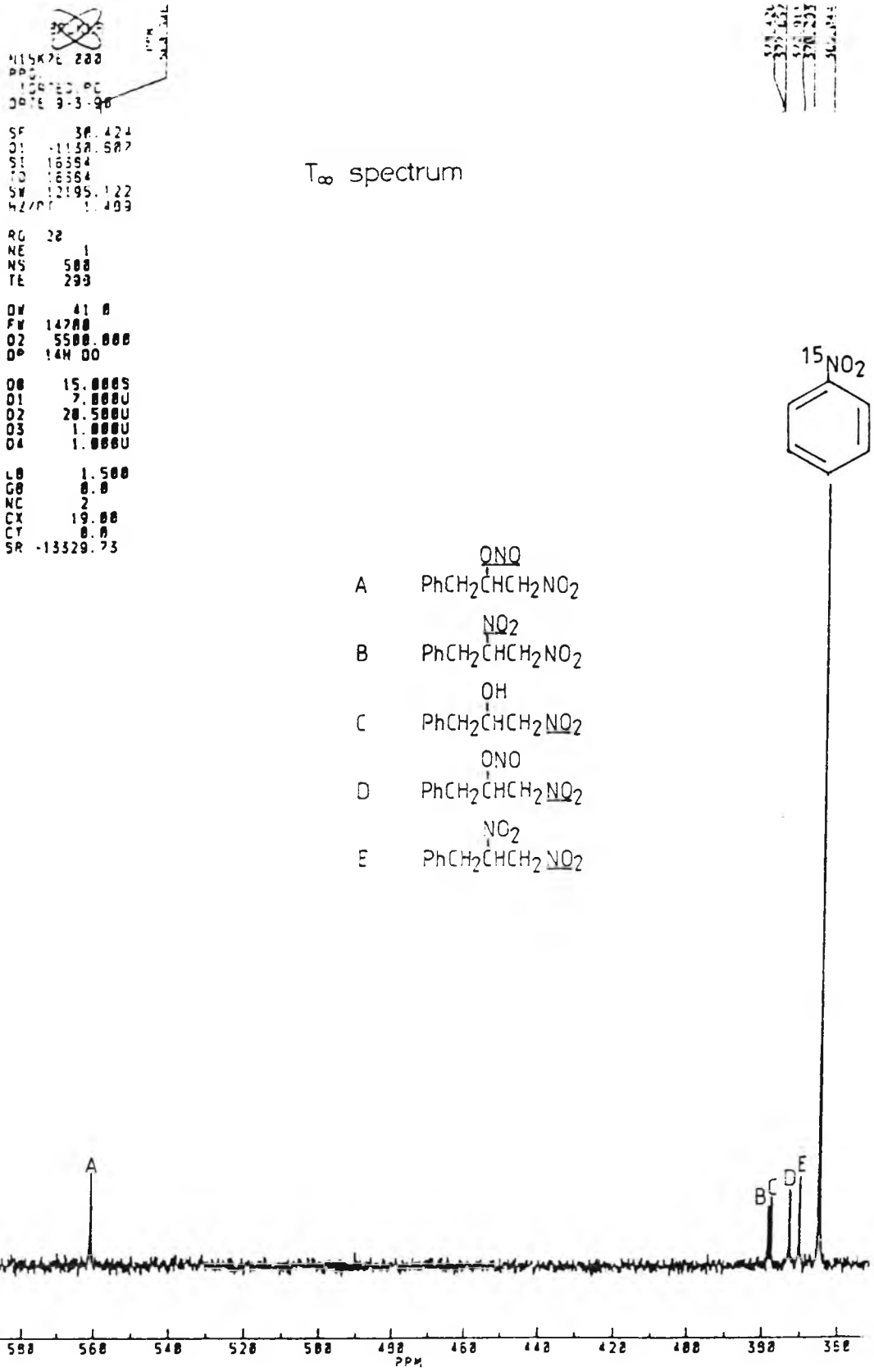

T∞ spectrum
15NO2
A PhCH2CHCH2NO2 (ONO)
B PhCH2CHCH2NO2 (NO2)
C PhCH2CHCH2NO2 (OH)
D PhCH2CHCH2NO2 (ONO)
E PhCH2CHCH2NO2 (NO2)
A
B C D E
PPM

Fig. 4.4: ^{15}N n.m.r. spectra during the reaction of 4-phenylbut-1-ene (0.25 mol dm^{-3}) with ^{15}N-labelled nitrogen dioxide (0.22 mol dm^{-3}) in cyclohexane at r.t.

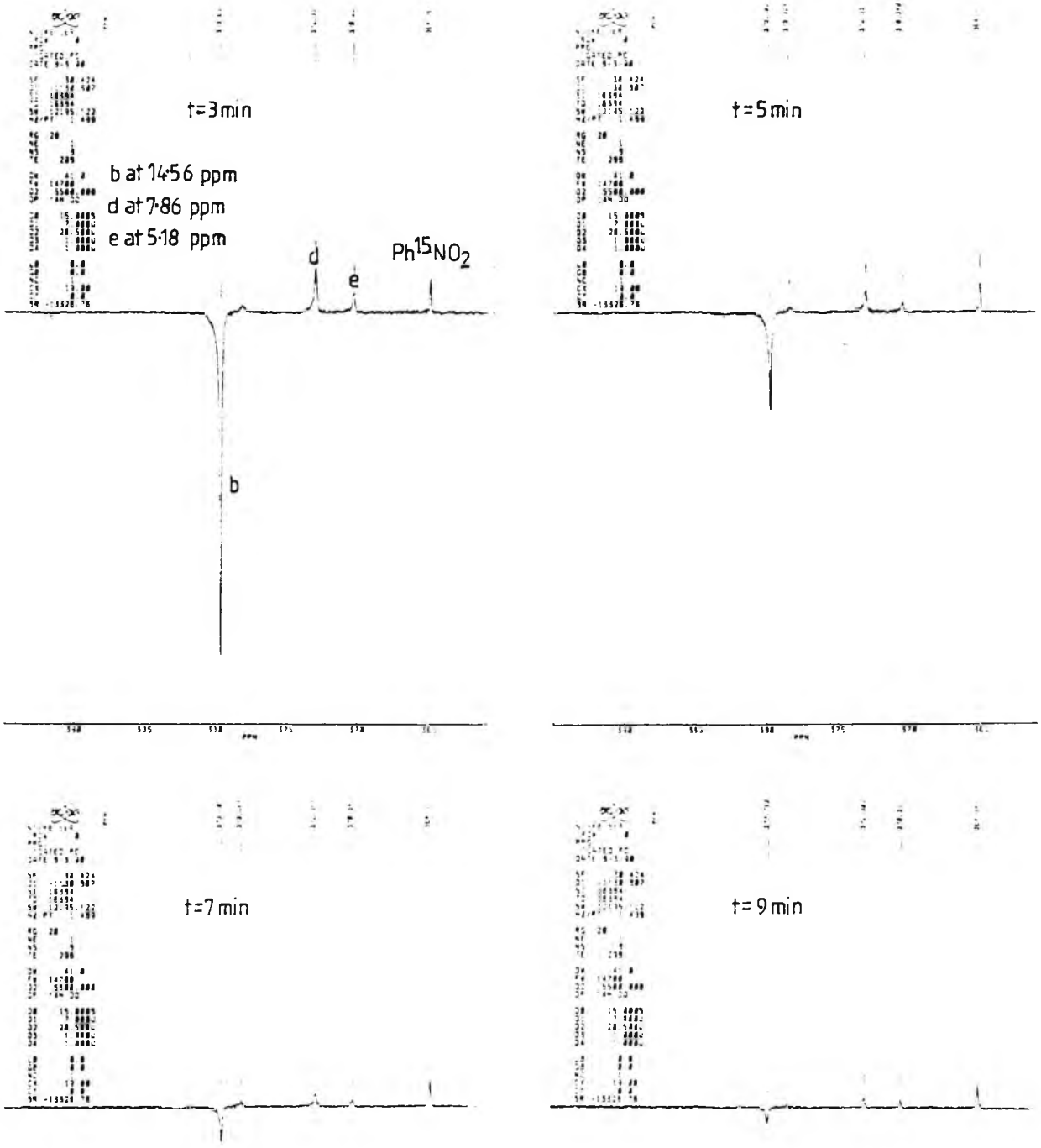

Fig. 4.4: .....cont'd

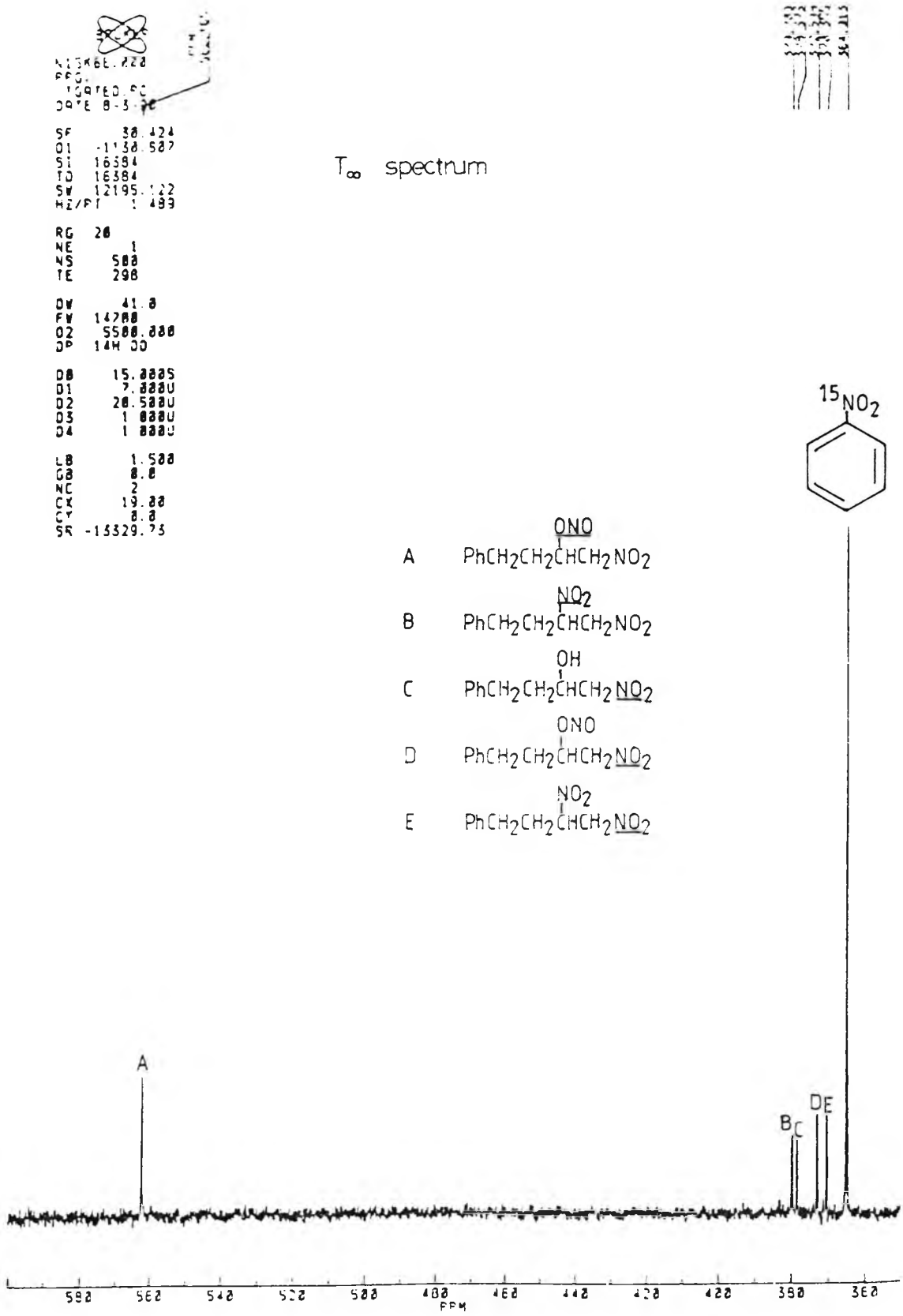

SF 30.424
O1 -1130.507
SI 16384
TD 16384
SW 12195.122
HZ/PT 1.489
RG 20
NE 1
NS 500
TE 298
DW 41.0
FW 14700
O2 5500.000
DP 14H DD
D0 15.000S
D1 7.000U
D2 20.500U
D3 1.000U
D4 1.000U
LB 1.500
GB 0.0
NC 2
CX 19.00
CY 0.0
SR -13329.73
T∞ spectrum
15NO2
A PhCH2CH2CHCH2NO2 (ONO)
B PhCH2CH2CHCH2NO2 (NO2)
C PhCH2CH2CHCH2NO2 (OH)
D PhCH2CH2CHCH2NO2 (ONO)
E PhCH2CH2CHCH2NO2 (NO2)
A
B C
D E
580 560 540 520 500 480 460 440 420 400 380 360
PPM

Fig. 4.5: ^{15}N n.m.r. spectra during the reaction of 1-dodecene (0.23 mol dm^{-3}) with ^{15}N-labelled nitrogen dioxide (0.23 mol dm^{-3}) in cyclohexane at r.t.

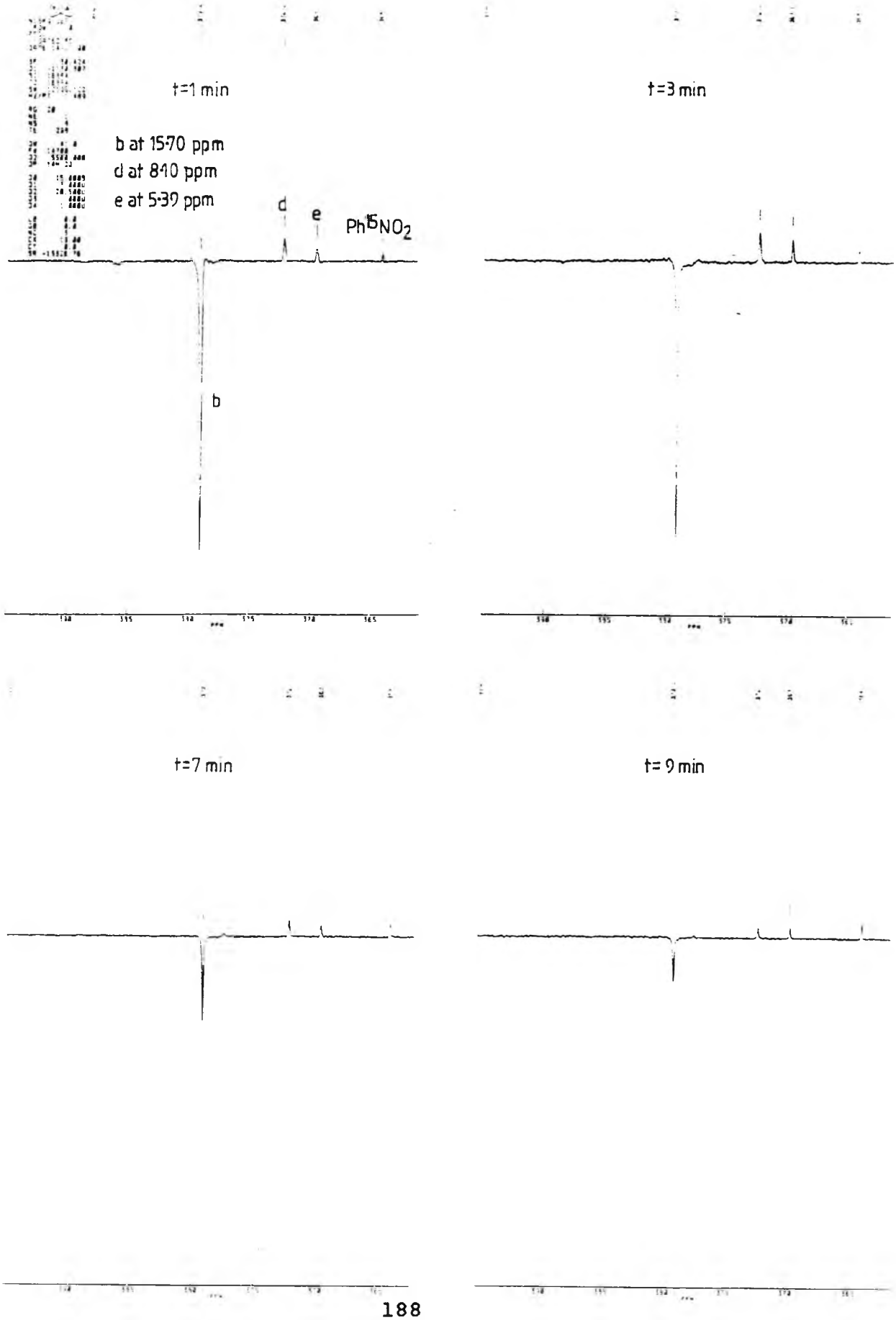

Fig. 4.5: .....cont'd

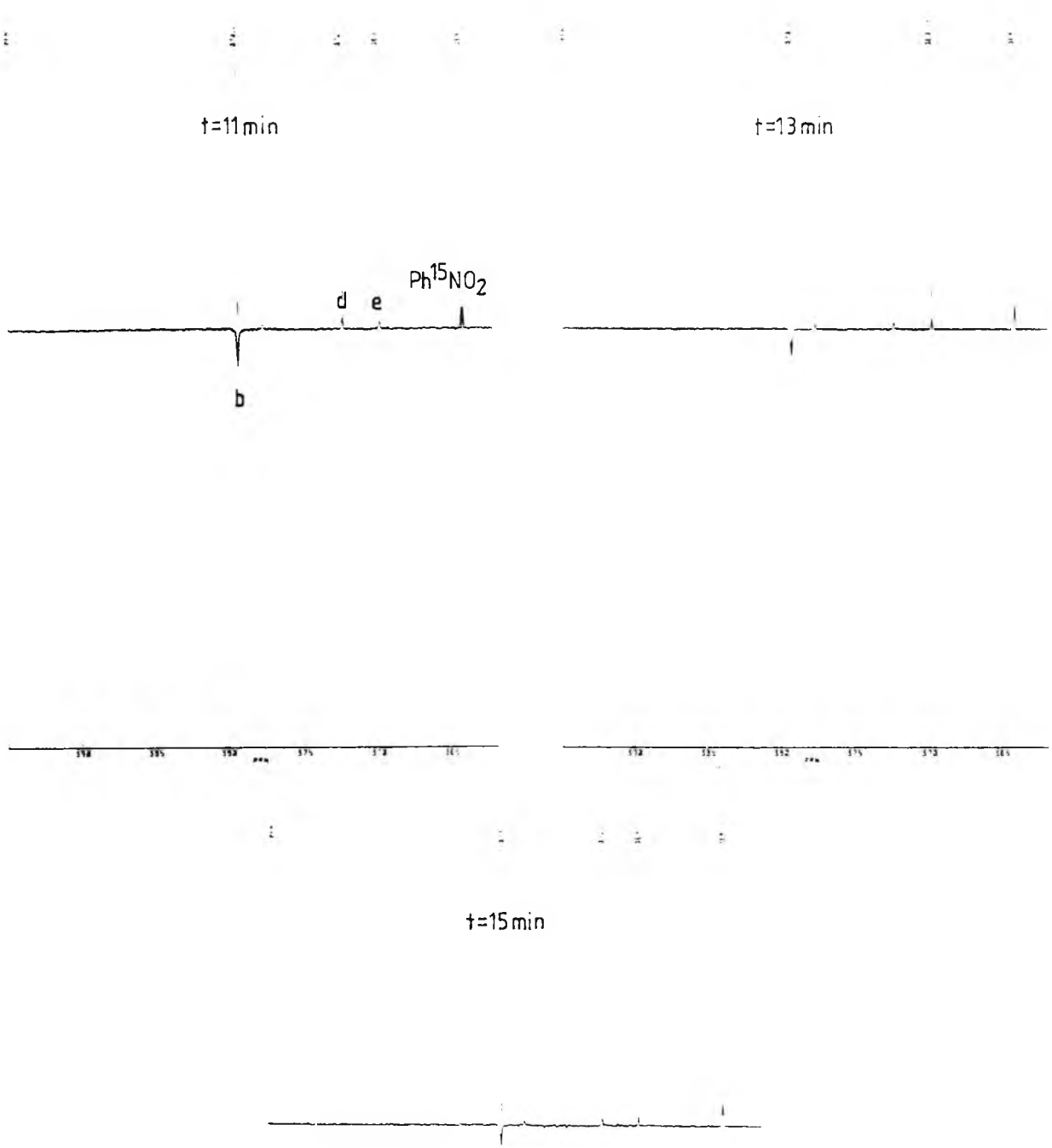

Fig. 4.5: .....cont'd

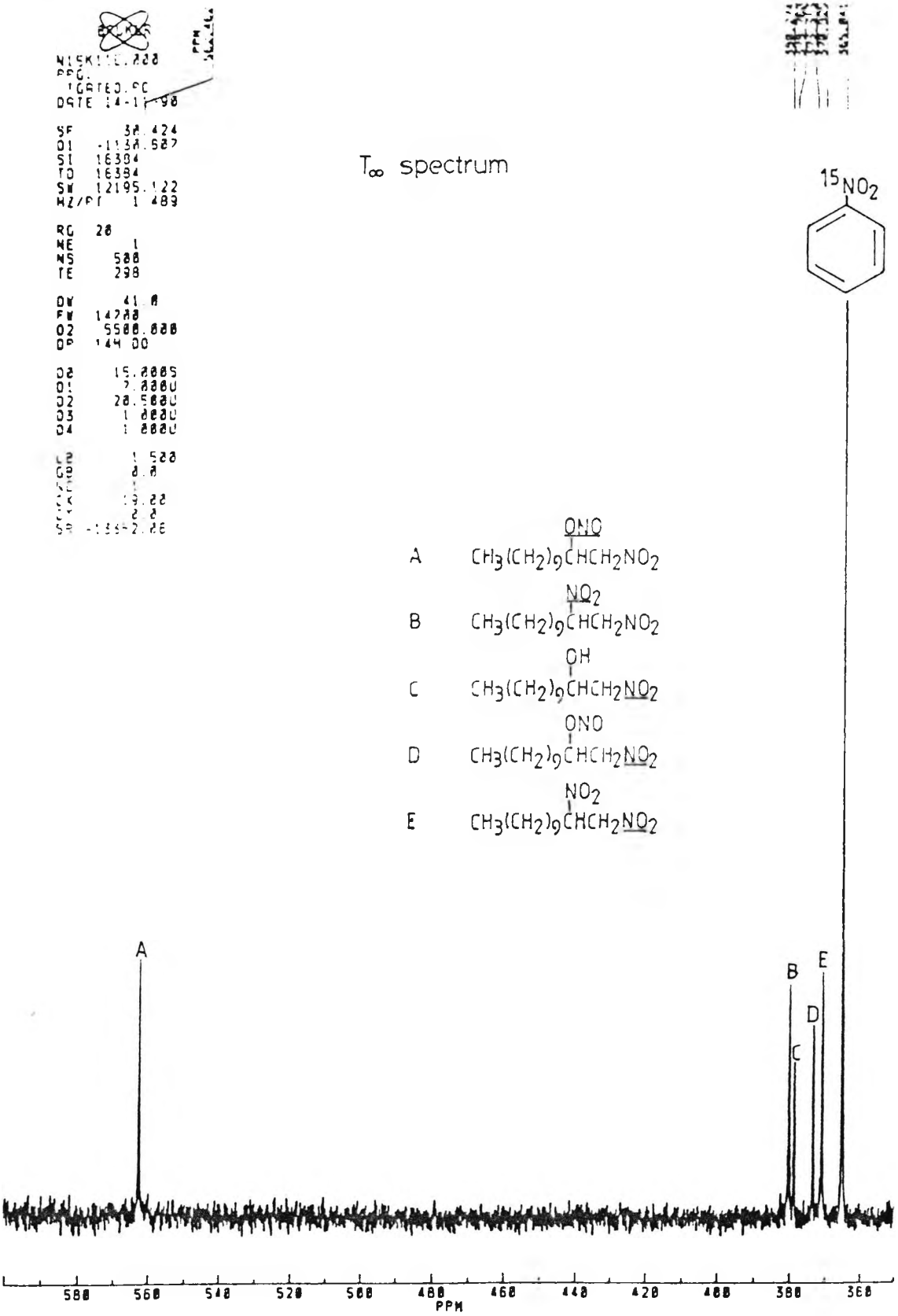

T∞ spectrum
15NO2
A CH3(CH2)9CHCH2NO2 (ONO)
B CH3(CH2)9CHCH2NO2 (NO2)
C CH3(CH2)9CHCH2NO2 (OH)
D CH3(CH2)9CHCH2NO2 (ONO)
E CH3(CH2)9CHCH2NO2 (NO2)
A
B
C
D
E
580 560 540 520 500 480 460 440 420 400 380 360
PPM

4.5 Discussion

The formation of nitro compounds by the addition of nitrogen dioxide to alkenes can be considered to occur via two mechanisms, as previously discussed in Chapter 2. The first mechanism proposed involves the reversible addition of $NO_2^{\bullet}$ to the alkene to give the more stable of the two possible radicals, followed by the addition of a second $NO_2^{\bullet}$ to this radical. The kinetics of the reaction in solution also suggest that part of the initial reaction of the alkene is with N_2O_4 to form the same radical pair. These reaction paths are shown in Scheme 4.2 for the reaction of allylbenzene with ^{15}N-labelled nitrogen dioxide.

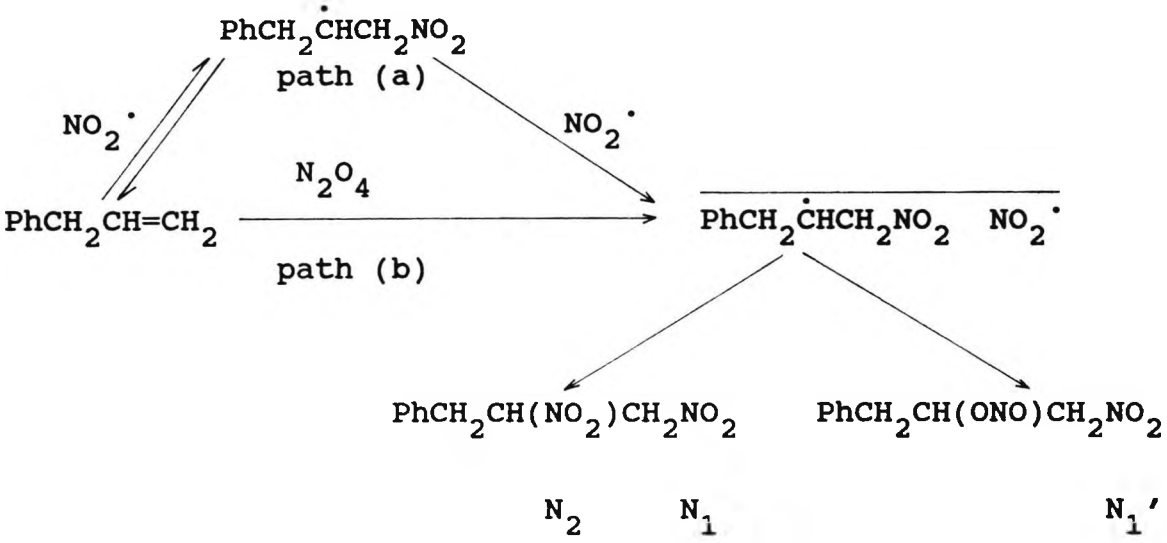

Scheme 4.2

Although the same radical pair is involved in the two reaction paths, the implications of these paths for any possible ^{15}N nuclear polarisation in the products are very different. This arises because the radical pair from path (a) is formed by diffusion and hence the radicals have uncorrelated

spins (an F precursor), whilst that from path (b) must be initially in a singlet state (an S precursor). The application of Kaptein's rules leads to the predicted phases of ^{15}N polarisation in the products shown in Table 4.1.

Table 4.1: Predicted phases of ^{15}N nuclear polarisation in the dinitro and nitro-nitrito products. The subscripts indicate the carbon atom to which the nitrogen atom is bonded (Scheme 4.2).

	N_1	N_2	N_1'
F Precursor	Enhanced Absorption	Emission	Enhanced Absorption
S Precursor	Emission	Enhanced Absorption	Emission

In the C.I.D.N.P. spectra of the reaction of allylbenzene with ^{15}N-labelled nitrogen dioxide, the signals due to the dinitro compound were assigned by comparison with previous spectra of crude product solutions (Section 3.3). The final T_∞ spectrum contained a further nitro peak (at 372.91 p.p.m.) assigned to the nitro-nitrite compound, which was absent from previous product spectra, and which also gave a peak at 560.85 p.p.m. in the region expected for a nitrite group. Also, in the T_∞ spectrum a further nitro group appears which was assigned to the nitro-hydroxy compound.

The ^{15}N n.m.r. spectra of the product mixture from the reaction of allylbenzene with nitrogen dioxide from the C.I.D.N.P. experiment (T_∞ run) and from a product studies experiment using C_6H_{12}/C_6D_{12} as the solvent (Fig. 3.12) are shown in Fig. 4.6. On comparison, it can be seen that although the difference in chemical shifts between the nitro

Fig. 4.6: ^{15}N n.m.r. spectra of the product mixture from the reaction of allylbenzene with nitrogen dioxide from the C.I.D.N.P. experiment and from a product studies experiment

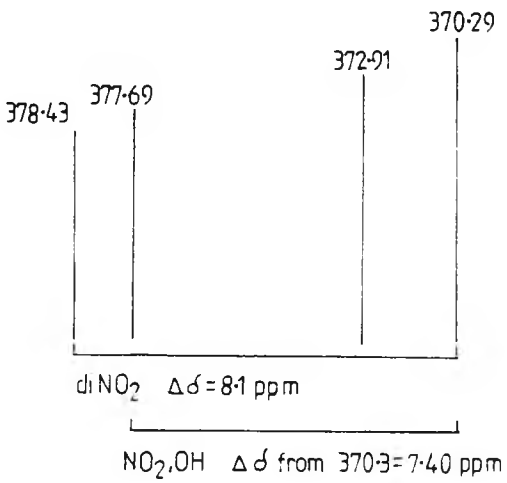

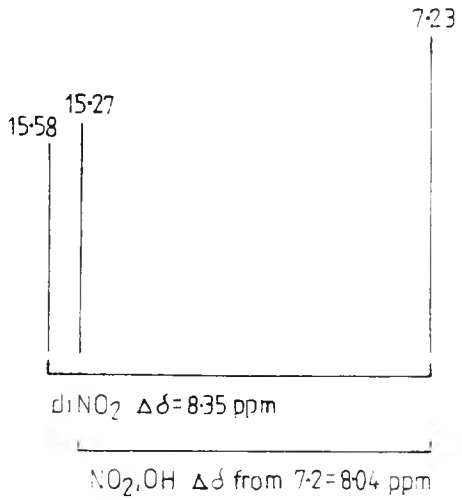

groups of the dinitro compound is similar in the two spectra (8.1 cf. 8.4), the $\Delta\delta$ value (from the 1-nitro group of the dinitro compound) of the NO_2 group of $PhCH_2CH(OH)CH_2NO_2$ is less in the C.I.D.N.P. spectrum (7.4 cf. 8.0). The chemical shift value of the NO_2 group of the nitro-hydroxy compound may be susceptible to the wetness of the solvent and to the nature of the other solutes present. In the sample used in the product experiment, a nitro-nitrate compound was present, which was only slightly soluble in C_6H_{12}/C_6D_{12}, along with dinitro and nitro-hydroxy compounds. The sample examined in the C.I.D.N.P. experiment contained dinitro, nitro-nitrite and nitro-hydroxy compounds, and no nitro-nitrate since equimolar proportions of allylbenzene and nitrogen dioxide were used. The concentrations of reactants used in the C.I.D.N.P. experiment were higher than those used in the product experiment, and this may also contribute to the difference in $\Delta\delta$ values mentioned above.

The predictions of Table 4.1 were based on the following deductions. With reference to equation 4.1

Kaptein's rule:

$$\Gamma = -\mu\epsilon a_N (g_R. - g_S.) \qquad (4.1)$$

The value of the hyperfine coupling constant (a_N) for the nitrogen atom in nitrogen dioxide should be negative because of the negative gyromagnetic ratio for the ^{15}N nucleus and the results of MNDO calcuations.[108]

For the reaction of allylbenzene with ^{15}N-labelled nitrogen dioxide the radical pair consists of $[PhCH_2\dot{C}HCH_2\ ^{15}NO_2\quad ^{15}NO_2\cdot]$. The g values for a number of aromatic radicals with alkyl side chains lie in the range 2.0026 - 2.00264.[109] For $^{15}NO_2\cdot$ the g value is equal to 2.0000.[110] The sign of the term ($g_R. - g_S.$) will therefore be positive for the 1-nitro group in both 1,2-dinitro-3-phenylpropane (DNPP) and

1-nitro-3-phenyl-2-propylnitrite (NPPN) and negative for the 2-nitro group in 1,2-dinitro-3-phenylpropane.

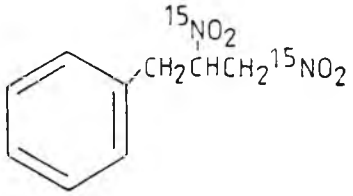

DNPP

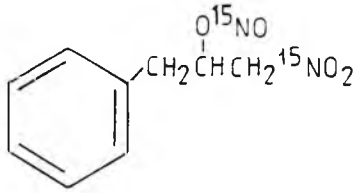

NPPN

Considering firstly reaction <u>via</u> path (a), the nitration of allylbenzene occurs by the diffusion together and essentially complete combination of the radicals, $PhCH_2\dot{C}HCH_2{}^{15}NO_2$ and $^{15}NO_2^{\cdot}$ (i.e. μ= +ve, ϵ= +ve). The ^{15}N spectrum of the product mixture should therefore show two enhanced absorption signals for the addition of the 1-nitro groups in DNPP and NPPN, and one emission signal for the addition of the 2-nitro group in NPPN.

From Kaptein's rule:

FOR THE ADDITION OF THE 1-NITRO GROUPS:

Γ = - + + - + = + ENHANCED ABSORPTION

FOR THE ADDITION OF THE 2-NITRO GROUP:

Γ = - + + - - = - EMISSION

Also, the emission peak should be much more enhanced than the absorption peaks because the ^{15}N hyperfine coupling constant of the $PhCH_2\dot{C}HCH_2{}^{15}NO_2$ radical at the 2-position is much less than that in nitrogen dioxide (a_N 50G), because the ^{15}N nucleus in $PhCH_2\dot{C}HCH_2{}^{15}NO_2$ is 2 bonds away from the radical centre.

These emission and absorption signals can also be rationalised in the following qualitative way. When the radicals $PhCH_2\dot{C}HCH_2{}^{15}NO_2$ and ${}^{15}NO_2{}^{\cdot}$ diffuse together, the resulting radical pair can be in either a singlet or triplet state. If the radical pair is in a singlet state, there need be no barrier to combination. If the radical pair is in a triplet state, combination cannot occur unless a triplet-singlet conversion occurs before the radicals finally separate.

Considering the 2-nitro group in DNPP, it has been shown above that the radical pair is formed mainly in the triplet state and the electron of ${}^{15}NO_2{}^{\cdot}$ precesses more slowly in the external field (B) than does that of radical $PhCH_2\dot{C}HCH_2{}^{15}NO_2$ (i.e. $g_{{}^{15}NO_2} < g_{PhCH_2\dot{C}HCH_2{}^{15}NO_2}$). If ${}^{15}NO_2{}^{\cdot}$ contains an electron coupled to a ${}^{15}N$ nucleus of $m_I = +\frac{1}{2}$ with a negative hyperfine coupling constant, the opposition of hyperfine and external fields will lead to a relatively lower pressional frequency for ${}^{15}NO_2{}^{\cdot}$, and a more rapid intersystem crossing. The product will therefore have an overpopulation of the $+\frac{1}{2}$ nuclear state and will show net n.m.r. emission.

Considering the 1-nitro groups in DNPP and NPPN, since $(g_{R\cdot} - g_{S\cdot})$ is positive, the triplet-singlet interconversion is faster when the ${}^{15}N$ nucleus is in the lower of the two permitted states ($m_I = -\frac{1}{2}$). The products will therefore contain initially an excess of nuclei in this state and hence give rise to enhanced absorption signals.

If, however, the radicals are formed initially in the singlet state, i.e. reaction via path (b), and then combine to form products, the polarisation will be precisely opposite to that resulting from spin selection in the T. pair. The ${}^{15}N$ spectrum of the product mixture should therefore show two emission signals for the addition of the 1-nitro groups in DNPP and NPPN, and one enhanced absorption signal for the addition of the 2-nitro group in NPPN. Also in view of the expected relative hyperfine coupling constants the absorption

peak should be much more enhanced than the emission peaks.

From Kaptein's rule

FOR THE ADDITION OF THE 1-NITRO GROUPS:

Γ = - - + - + = - EMISSION

FOR THE ADDITION OF THE 2-NITRO GROUP

Γ = - - + - - = + ENHANCED ABSORPTION

The emission and absorption signals for this second mechanism can also be rationalised qualitatively. For the 2-nitro group in DNPP, the radical pair is formed mainly in the singlet state and the electron of $^{15}NO_2^{\cdot}$ precesses more slowly in the external field than does that of radical $PhCH_2\dot{C}HCH_2{}^{15}NO_2$. After some time, the more rapid precession of the electron of $PhCH_2\dot{C}HCH_2{}^{15}NO_2$ will lead to the T_o state. If, however, $^{15}NO_2^{\cdot}$ contains a ^{15}N nucleus of $m_I = -\frac{1}{2}$, coupled to the unpaired electron with a negative hyperfine coupling constant, the hyperfine field will supplement the external field and will lead to a relatively higher precessional frequency for the electron in $^{15}NO_2^{\cdot}$, and consequently a longer time required to reach the triplet state. If $m_I = +\frac{1}{2}$, the opposition of hyperfine and external fields leads to a lower precessional frequency for $^{15}NO_2^{\cdot}$ and a more rapid intersystem crossing. Clearly, in the case of $m_I = -\frac{1}{2}$, the radical pair with higher singlet character will have a greater opportunity to lead to product. This product will have an overpopulation of the $-\frac{1}{2}$ nuclear state and will show net n.m.r. absorption. The T_o pairs, enriched in the $+\frac{1}{2}$ state, will have a longer life and a higher probability of dissociation or escape.

For the 1-nitro groups in DNPP and NPPN, since $(g_{R.} - g_{S.})$ is positive, the triplet-singlet interconversion is

least favoured when the ^{15}N nucleus is in the upper of the two permitted states ($m_I = +\frac{1}{2}$). The products will therefore contain initially an excess of nuclei in this state and hence give rise to emission signals.

The C.I.D.N.P. spectra from the reactions of 4-phenylbut-1-ene and 1-dodecene with ^{15}N-labelled nitrogen dioxide can be explained similarly.

The comparison of the intensities of the resulting signals of the product mixtures with the standard shows clearly that the early signals are strongly polarised with the phases and relative magnitudes expected from an F precursor and hence from reaction by path (a) (Table 4.2).

Table 4.2 Predicted and observed phases of ^{15}N nuclear polarisation in the dinitro and nitro-nitrito products from the reactions of allylbenzene, 4-phenylbut-1-ene and 1-dodecene with ^{15}N-labelled nitrogen dioxide. The subscripts indicate the carbon atom to which the nitrogen atom is bonded (Scheme 4.2)

	N_1	N_2	N_1'	relative signal magnitude
		PREDICTED		
F precursor	Enhanced Absorption	Emission	Enhanced Absorption	E > A
S precursor	Emission	Enhanced Absorption	Emission	A > E
		OBSERVED		
Allylbenzene	Enhanced Absorption (14)*	Emission (288)	Enhanced Absorption (14)	E > A
4-Phenylbut-1-ene	Enhanced Absorption (6)	Emission (141)	Enhanced Absorption (12)	E > A
1-Dodecene	Enhanced Absorption (6)	Emission (134)	Enhanced Absorption (13)	E > A

*The numbers in brackets refer to the approximate degree of enhancement

The fact that the signals for N_1 and N_2 are of opposite phase shows that the polarisation cannot arise in some other process and be carried over into the dinitro product. The enhanced absorption signal (N_1') seen for the nitro group in the nitro-nitrite ($PhCH_2CH(ONO)CH_2NO_2$) indicates that this compound, which is formed concurrently with the dinitro product, is also derived from a radical pathway. The observed phases of ^{15}N nuclear polarisation also suggests that path (b) is swamped by path (a) as far as C.I.D.N.P. is concerned (Chapter 5).

The fall-off in the intensity of the emission signal with time has been used to calculate the T_1 relaxation time for the 2-^{15}N nucleus in 1,2-dinitro-3-phenylpropane; the variation in the intensity (I) of this signal during the nitration of allylbenzene is shown in Table 4.3. A plot of $\log_{10}(I-I_\infty)$ against time[111] gives T_1 for the 2-^{15}N nucleus as 254s (Fig. 4.7). The relaxation time of this nucleus can also be determined conventionally by the fast inversion recovery method but this experiment was not carried out. $^{15}NO_2$ groups usually have relaxation times of ca. 180s: T_1 for the $^{15}NO_2$ group in nitrobenzene is 170s.

Table 4.3: The intensities of the emission signal in the ^{15}N n.m.r. spectrum of the reaction mixture during the nitration of allylbenzene

$PhCH_2CH(NO_2)CH_2NO_2$

t/min	2-$^{15}NO_2$(I)	[^{15}N]-Nitrobenzene	$\log_{10}(I-I_\infty)$
0-2	-3599.01	7.20	3.55
2-4	-2036.59	12.70	3.31
4-6	-1354.26	14.60	3.13
6-8	-827.03	14.50	2.91
8-10	-492.97	13.50	2.68
10-12	-337.71	11.90	2.51
12-14	-233.09	10.00	2.34
14-16	-132.38	8.50	2.08
45	12.5	160.75	

$I_\infty = 18.6$

Fig. 4.7: Plot of $\log_{10}(I-I_\infty)$ against time for the 2-^{15}N nucleus in 1,2-dinitro-3-phenylpropane during the nitration of allylbenzene

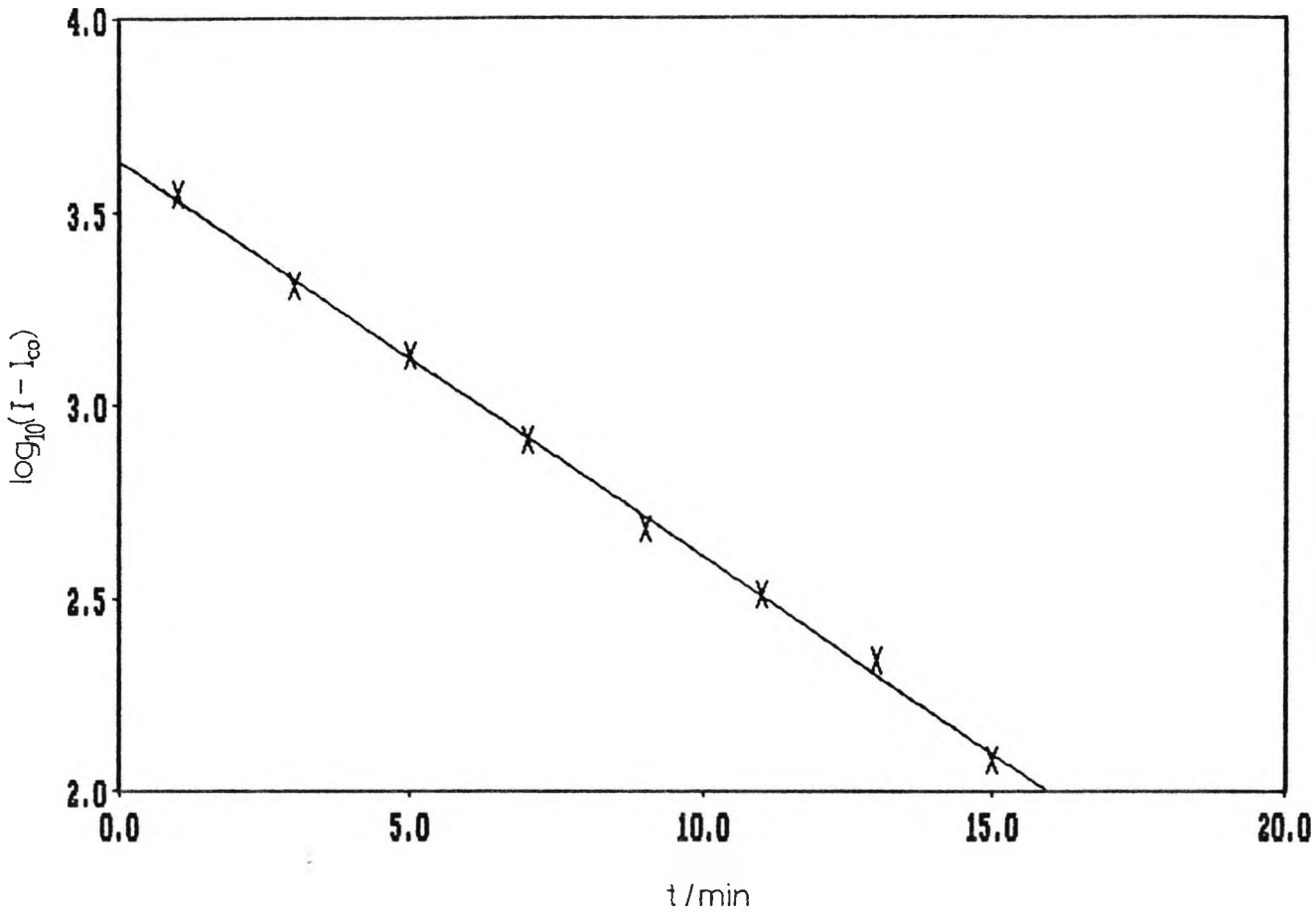

CHAPTER 5

CONCLUDING DISCUSSION FOR THE REACTIONS OF STYRENE, ALLYLBENZENE, 4-PHENYLBUT-1-ENE AND 1-DODECENE WITH NITROGEN DIOXIDE

5. Concluding discussion for the reactions of styrene, allylbenzene, 4-phenylbut-1-ene and 1-dodecene with nitrogen dioxide

5.1 Mechanistic implications

Kinetic, product and C.I.D.N.P. observations for the reactions of the title alkenes with nitrogen dioxide can be explained by the mechanism shown in Scheme 5.1.

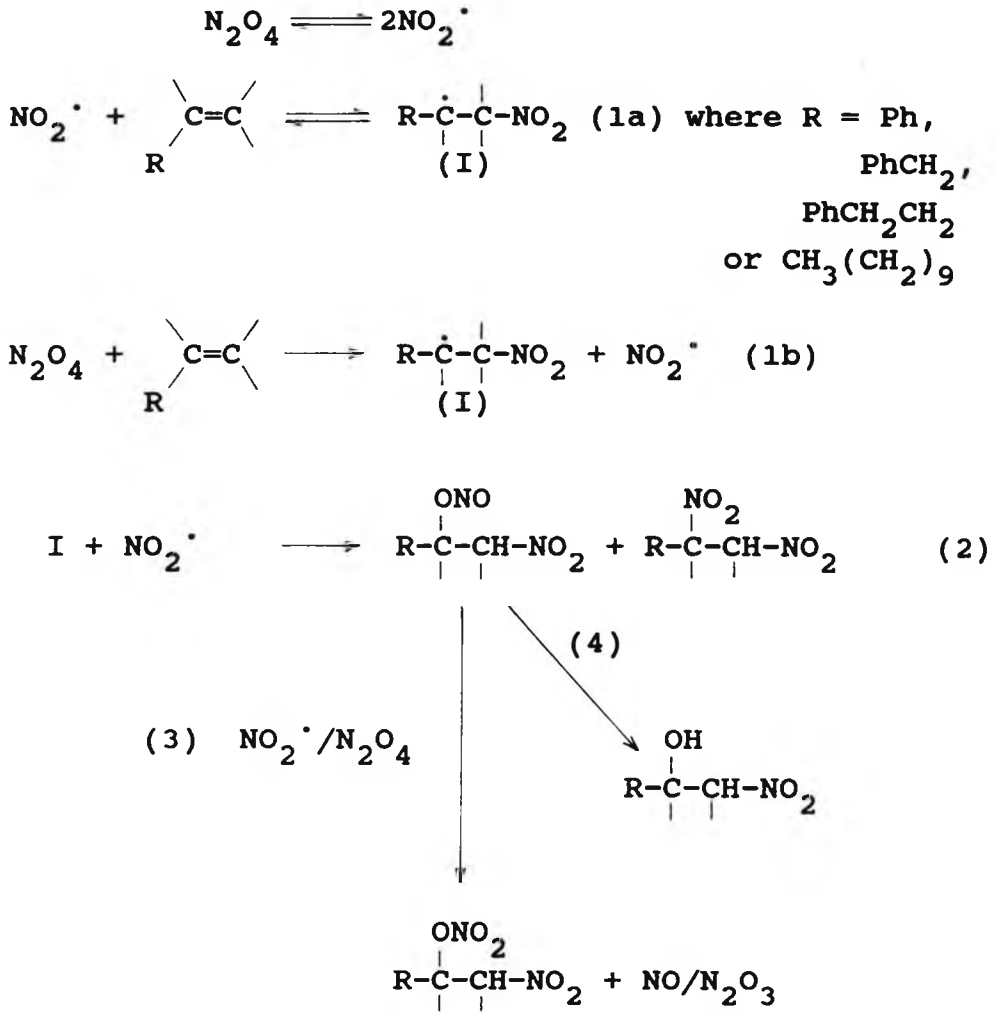

Scheme 5.1

The initial step involves addition of $NO_2^{\cdot}$ and N_2O_4 to the double bond in concurrent reactions to form the carbon-centred radical I. Radical I then reacts with more $NO_2^{\cdot}$ to give a

dinitro compound and a nitro-nitrite, which can in turn react further with nitrogen dioxide to form a nitro-nitrate compound. There is no significant change in products or proportions over the range of nitrogen dioxide concentrations used in the kinetic studies, and so reaction of radical I with N_2O_4 is unlikely. The nitrite ester is converted to the nitro-alcohol as the reaction proceeds.

The formation of a nitro-nitrate compound *via* direct oxidation of a nitro nitrite compound has been proposed earlier.[44] Further evidence for this pathway (Step 3) has been found in the present study. In the C.I.D.N.P. experiments, where equimolar amounts of alkene and nitrogen dioxide were used, ^{15}N n.m.r. signals assignable to 4 NO_2 groups and 1 -ONO group were seen, and no $-ONO_2$ groups were detected (Section 4.4). The ^{15}N n.m.r. spectrum of the product mixture from the reaction of allylbenzene with excess ^{15}N-labelled nitrogen dioxide, however, shows 2 peaks due to a NO_2 group and a $-ONO_2$ group in addition to those due to 1,2-dinitro-3-phenylpropane and 1-nitro-3-phenylpropan-2-ol, thus indicating that 1-nitro-3-phenyl-2-propylnitrite can react further with nitrogen dioxide to form 1-nitro-3-phenyl-2-propylnitrate (Section 3.3.1).

Evidence for step (4) was obtained by following the reaction of allylbenzene with nitrogen dioxide by I.R. spectroscopy (Section 3.3.1). This was supported by ^{15}N n.m.r. spectra obtained at the end of the C.I.D.N.P. experiments (Section 4.4), where a NO_2 group corresponding to a nitro-hydroxy compound was detected alongside the NO_2 groups of $R\text{-}CH(NO_2)CH_2NO_2$ and $R\text{-}CH(ONO)CH_2NO_2$.

An anomaly arises when the C.I.D.N.P. results are examined from a kinetic point of view. The rate data and relative values of $NO_2^{\bullet}$ and N_2O_4 concentrations present in solution indicate that reaction *via* path (1b) should be of equal significance to reaction *via* path (1a). Representative values are shown below for the reaction of allylbenzene with ^{15}N-labelled nitrogen dioxide.

$$\frac{-d[\text{Alkene}]}{dt} = k_2[\text{Alkene}][NO_2^{\cdot}] + k_2'[\text{Alkene}][N_2O_4]$$

At 30°C $k_2 = 0.26\ mol^{-1}dm^3s^{-1}$ $k_2' = 9.20 \times 10^{-3} mol^{-1}dm^3s^{-1}$

At 25.4°C $[NO_2^{\cdot}] = 6.3 \times 10^{-3} mol\ dm^{-3}$ $[N_2O_4] = 0.22\ mol\ dm^{-3}$

$k_2[NO_2^{\cdot}] \approx 1.67 \times 10^{-3} s^{-1}$ $k_2[N_2O_4] \approx 2.02 \times 10^{-3} s^{-1}$

In the C.I.D.N.P. spectra, however, only reaction *via* path (1a) is observed. This may be accounted for by the following. When the two radicals $R\text{-}CH_2\dot{C}HCH_2{}^{15}NO_2$ and $^{15}NO_2^{\cdot}$ come together in the singlet state (path 1b), reaction occurs rapidly and faster than the rate of interconversion of singlet and triplet states, and so any C.I.D.N.P. effect is smaller than that from an F precursor. In the case of path (1a), the radical pair is formed by diffusion, and therefore must undergo a triplet-singlet interconversion before product formation can take place. This may allow time for more radicals to escape from the cage allowing a more significant C.I.D.N.P. effect to arise. Path (1a) then dominates the results. The above findings are consistent with recent C.I.D.N.P. work on the addition of nitrogen dioxide to 2-ethylbut-1-ene,[43] which concluded that reaction occurred *via* path (1a).

Nitrogen dioxide has been reported to react with phenylethenes to yield several products[44] (e.g. for styrene : PhCHO, PhCOCN, $PhCO_2H$, $PhCH{=}CHNO_2$, $PhCOCH_2NO_2$, $PhCH(OH)CH_2NO_2$) that were also explained by radical addition of two $NO_2^{\cdot}$ molecules These were identified by GC/MS using injector temperatures of 200°C, which would lead to thermal degradation of any dinitro compounds formed to nitroalkene compounds, and would explain why dinitro compounds were not detected. Pryor and his co-workers[39] have shown in earlier work that the mechanism of nitrogen dioxide-alkene reactions changes from predominantly addition to predominantly hydrogen abstraction as the nitrogen dioxide concentration (in a carrier gas) decreases from high percent (50%) to below 10000 ppm (1%) levels. Whilst our product studies agree with those carried out with cyclohexene at high concentrations of nitrogen dioxide, an allylic-H abstraction pathway is not found with our alkenes at low [nitrogen dioxide] i.e. 50 p.p.m., even with allylbenzene when it would be favoured structurally. The

kinetic studies have already been discussed in some depth (Chapter 2). C.I.D.N.P. results have now provided conclusive evidence for an initial addition reaction of $NO_2^{\cdot}$ at high nitrogen dioxide concentrations.

CHAPTER 6

THE REACTIONS OF NAPHTHALENE AND 2-METHYLNAPHTHALENE WITH NITROGEN DIOXIDE

6. The reactions of naphthalene and 2-methylnaphthalene with nitrogen dioxide

6.1 Introduction

In recent years the reaction between dinitrogen tetraoxide or its monomer, nitrogen dioxide, with polycyclic aromatic hydrocarbons (PAHs) has received considerable interest as a possible route to the formation of, in many cases mutagenic, nitro derivatives of PAHs in airborne matter and exhausts from combustion engines.

Naphthalene and 2-methylnaphthalene were selected as model compounds for the present study because they are known to be the major diaromatics in the mineral oil of a lubricant. One of the main objectives of this study was to compare the reactivities of these compounds with those of the aromatic/alkene substrates. Kinetics of the reactions were performed in carbon tetrachloride at 25°C and 50°C and were followed by ^{1}H n.m.r. G.L.C. and ^{13}C n.m.r. techniques were used to determine the main products of reaction. The reactivities of naphthalene and 2-methylnaphthalene relative to benzene were also measured by competition experiments.

6.2 Experimental

6.2.1 Kinetic measurements

A stock solution of nitrogen dioxide was made up in carbon tetrachloride and was thermostatted at the temperature of the experiment for 15 min. 1 cm^3 of this solution was diluted in a 1 cm quartz cell and the nitrogen dioxide concentration was measured. A small quantity of the original nitrogen dioxide stock solution was then transferred to a n.m.r. tube fitted with a suba seal. The nitrogen dioxide solution was thermostatted in a waterbath for 15 min before addition of the aromatic compound. The reaction was followed by ^1H n.m.r. by removing the n.m.r. tube from the waterbath at periodic intervals and recording the n.m.r. spectrum of the reaction products (the n.m.r. spectrometer was not thermostatted at the temperature of the experiment).

6.2.2 Product measurements

At the end of each kinetic run, the reaction solution was poured into a 10 ml round-bottomed flask. The solvent was removed on a rotary evaporator and a small amount of the product mixture was transferred to a 10 ml volumetric flask. A known amount of internal standard (1-ethylnaphthalene) was added, and the resulting mixture was made up to the mark with methanol. Small volumes of the solutions (typically 1μl) were then injected into the gas chromatograph for analysis. For the naphthalene product mixtures a 2 metre x 31.75 mm silicone 5% SE30 column at 125°C and a nitrogen flow rate of 25 ml min^{-1} were used; for the 2-methylnaphthalene product mixtures the temperature of the column was increased to 150°C.

The yields of products were determined by a method based on relative response factors (Section 10.2). Standard solutions containing authentic samples of the products together with an internal standard (1-ethylnaphthalene) in known amounts were separated by g.l.c. and the peak areas measured. Values of f_x and f_s were determined, and by applying equation 6.1

$$c_x = c_s \frac{f_s}{f_x} \frac{A_x}{A_s} \qquad (6.1)$$

to the peak areas of the reaction mixture chromatograms, the amounts of products, c_x were determined, and hence the % yields.

Reaction mixtures from the kinetic runs were also analysed by ^{13}C n.m.r.

6.2.3 Measurement of reactivities by the competition technique

A solution of aromatic compound and benzene was made up in cyclohexane. 20 ml of this solution was transferred to a round-bottomed flask and was thermostatted in a waterbath at 25°C for 15 min. A stock solution of nitrogen dioxide was made up in the same solvent and was also thermostatted at 25°C. A small quantity of the nitrating solution was then added to the aromatic solution, the aromatics being maintained in a large excess, and the reaction mixture was left for 164 h. Small samples (0.5ml) were removed and treated with water to prevent further reaction, and the organic layer was analysed quantitatively by g.l.c. Analysis was possible with a 2 metre x 31.75 mm column of silicone 5% SE30 at 130°C and a nitrogen flow rate of 25 ml min^{-1}.

The yields of nitro products were determined by a method based on relative response factors, and hence the reactivities of naphthalene and 2-methylnaphthalene relative to benzene were determined.

6.3 Results

6.3.1 The reaction of naphthalene with nitrogen dioxide

6.3.1.1 Kinetic and product measurements

The reaction of naphthalene (0.35 mol dm^{-3}) with nitrogen dioxide (0.80 mol dm^{-3}) in carbon tetrachloride at 25°C was followed by ^{1}H n.m.r. and spectra were recorded at the following times:

spectrum	t/min
1	20.5
2	33.8
3	121.4
4	232.3
5	276.9

A change in the aromatic region of the spectrum (8.2δ - 9δ) was not observed over the course of the reaction, indicating that nitro products were not formed under the above conditions, (Fig. 6.1), cf. 1-nitronaphthalene in $CDCl_3$: δ, ppm. 8.5 (d).

The reaction of naphthalene (0.52 mol dm^{-3}) with nitrogen dioxide (0.64 mol dm^{-3}) in carbon tetrachloride at 50°C was followed by ^{1}H n.m.r. and spectra were recorded at the following times:

spectrum	t/min
1	15.6
2	175.4
3	240.6

Again, no change in the aromatic region of the spectrum (8δ - 9δ) was observed over a period of 4 h (Fig. 6.2).

The products from the above two kinetic runs were analysed quantitatively by g.l.c. Peaks due to the formation of 1-nitronaphthalene (retention time = 24 min) or 2-nitronaphthalene (retention time = 28.9 min) were not detected in the chromatograms (compare Fig. 6.3 with Figs. 6.4 and 6.5). The ^{13}C n.m.r. spectra of the products from the reaction carried out at 25°C (Fig. 6.6) and 50°C (Fig. 6.7) also indicate the absence of 1-nitronaphthalene (δ, ppm. for $C-NO_2$ is 146.6) and 2-nitronaphthalene (δ, ppm. for $C-NO_2$ is 145.6).

6.3.2 The reaction of 2-methylnaphthalene with nitrogen dioxide

6.3.2.1 Kinetic measurements

The reaction of 2-methylnaphthalene (0.69 mol dm^{-3}) with nitrogen dioxide (0.69 mol dm^{-3}) in carbon tetrachloride at 25°C was followed by ^{1}H n.m.r. and spectra were recorded at the following times

spectrum	t/min
1	40.8
2	135.4
3	288.7

The reaction of 2-methylnaphthalene (0.63 mol dm^{-3}) with nitrogen dioxide (0.65 mol dm^{-3}) in carbon tetrachloride at 50°C was followed by ^{1}H n.m.r. and spectra were recorded at the following times:

spectrum	t/min
1	15.8
2	21.7
3	26.1
4	77.5
5	127.4
6	193.3
7	241.5
8	270.4

In both the above kinetic runs (Figs. 6.8 and 6.9), a peak appears to high field of the $-CH_3$ signal of 2-methylnaphthalene (peak at 2.39δ in Fig. 6.8; no reference standard was used in the reaction carried out at 50°C so it is not possible to quote the δ value of the nitro compound in this experiment) and corresponds to the formation of 2-methyl-1-nitronaphthalene, c.f. 2-methyl-1-nitronaphthalene in $CDCl_3$: δ, ppm. 2.38 (s, Me).

6.3.2.2 **Product Measurements**

The product from the kinetic run carried out at 25°C and that from the reaction of 2-methylnaphthalene (0.69 mol dm^{-3}) with nitrogen dioxide (0.65 mol dm^{-3}) at 50°C were analysed quantitatively by g.l.c. Comparison of the chromatograms (peak at 9.2 min in Fig. 6.11 and peak at 9.2 min in Fig. 6.12) with that obtained using a standard solution (peak at 10.0 min in Fig. 6.10) indicated a yield of 11.4% and 11.7% of 2-methyl-1-nitronaphthalene at 25°C and 50°C respectively. The formation of this compound was confirmed by ^{13}C n.m.r. The spectra of the products from the reaction carried out at 25°C (Fig. 6.13) and 50°C (Fig. 6.14) contain a signal at 17.78 δ, c.f. 2-methyl-1-nitronaphthalene in $CDCl_3$: δ, ppm. 17.93 (s, 2-Me).

Fig. 6.1: ^{1}H N.M.R. spectra recorded during the reaction of naphthalene (0.35 mol dm^{-3}) with nitrogen dioxide (0.80 mol dm^{-3}) in carbon tetrachloride at 25°C

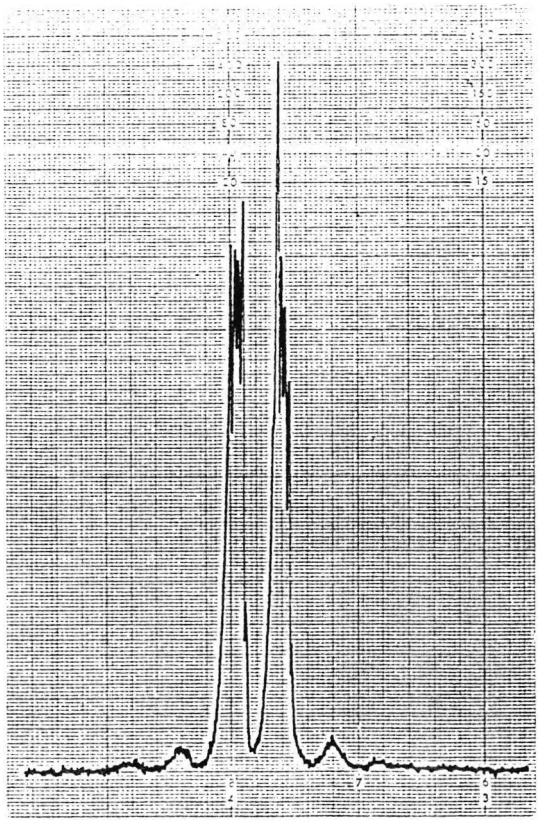

t=20·5 min

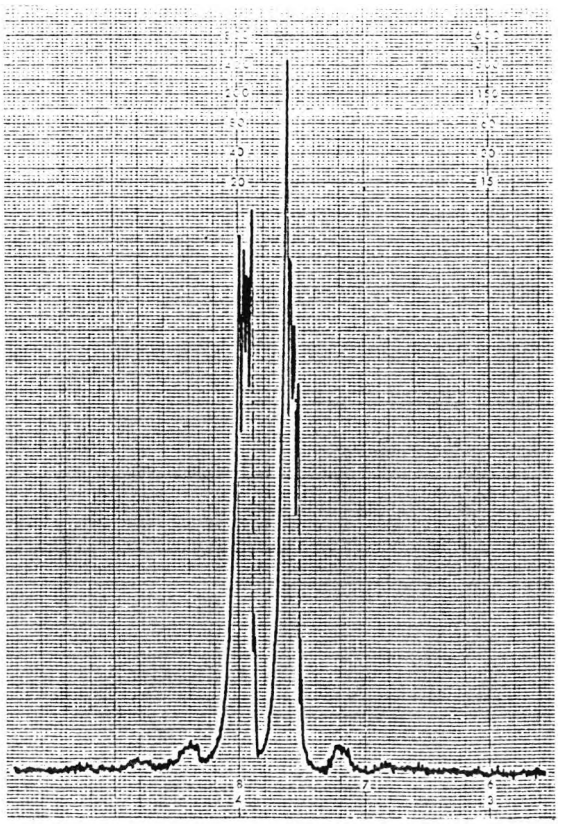

t=33·8 min

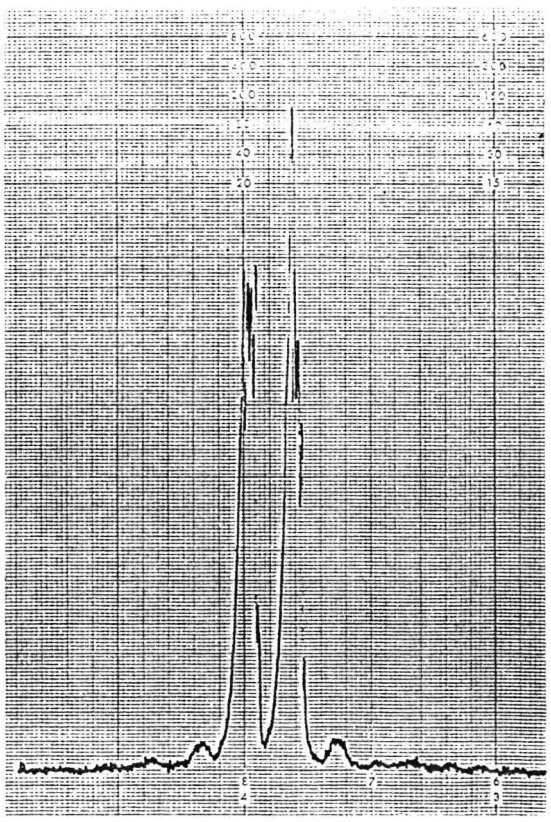

t=121·4 min

Fig. 6.1: .....cont'd

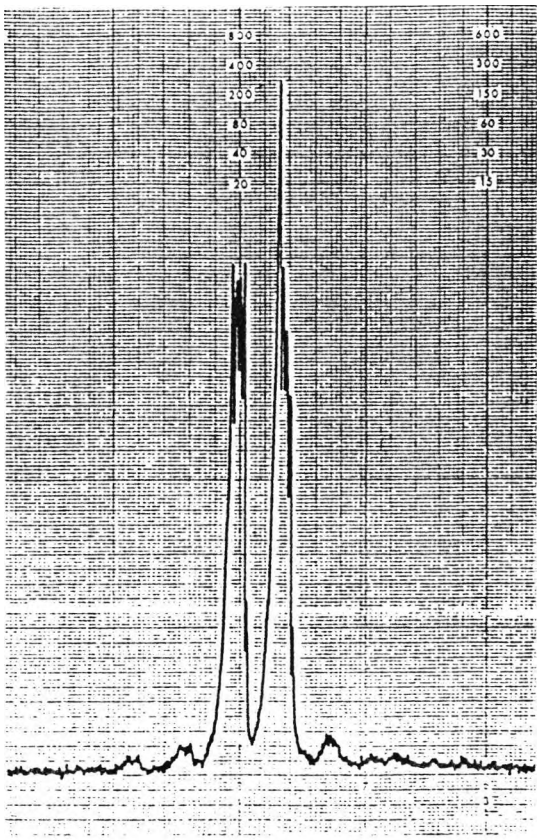

t=232·3 min

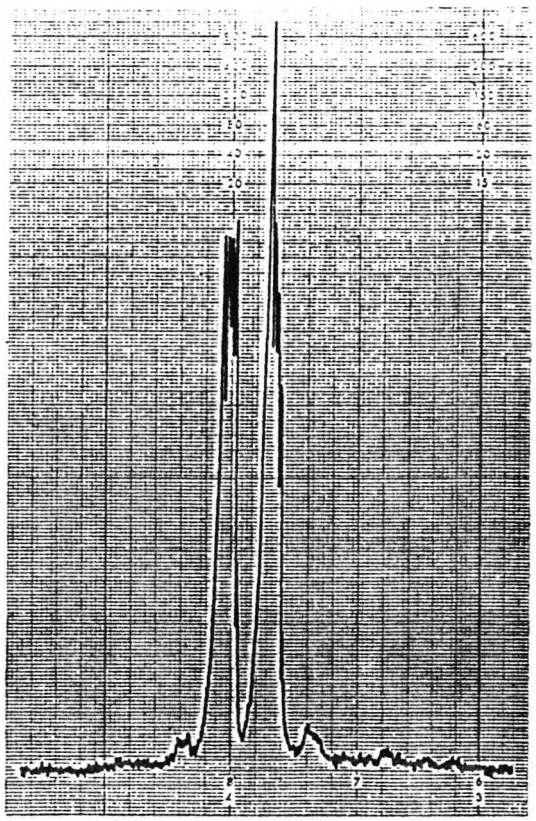

t=276·9 min

Fig.6.2: ^{1}H N.M.R. spectra recorded during the reaction of naphthalene (0.52 mol dm^{-3}) with nitrogen dioxide (0.64 mol dm^{-3}) in carbon tetrachloride at 50°C

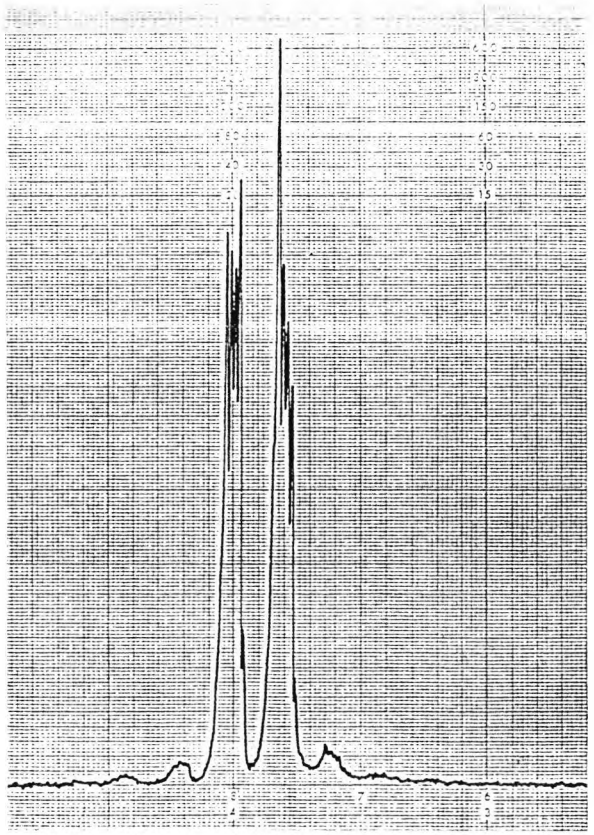

t = 15·6 min

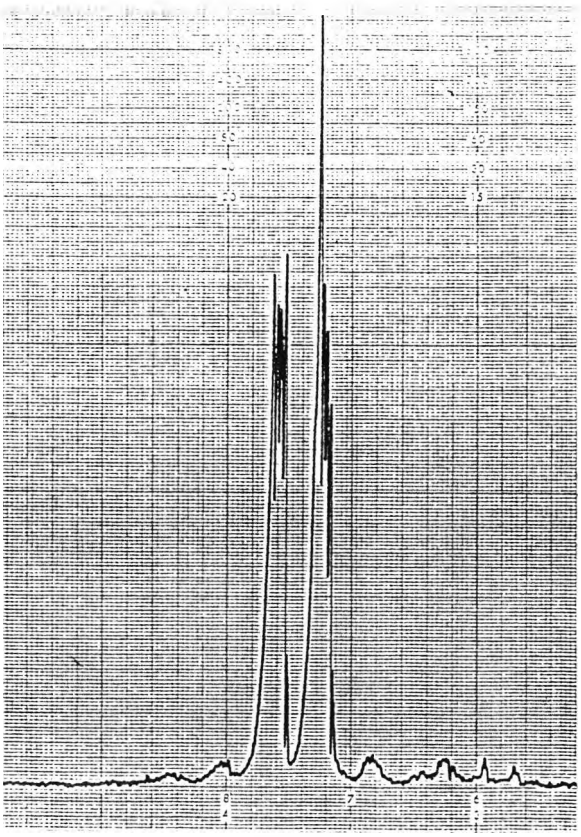

t=175·4 min

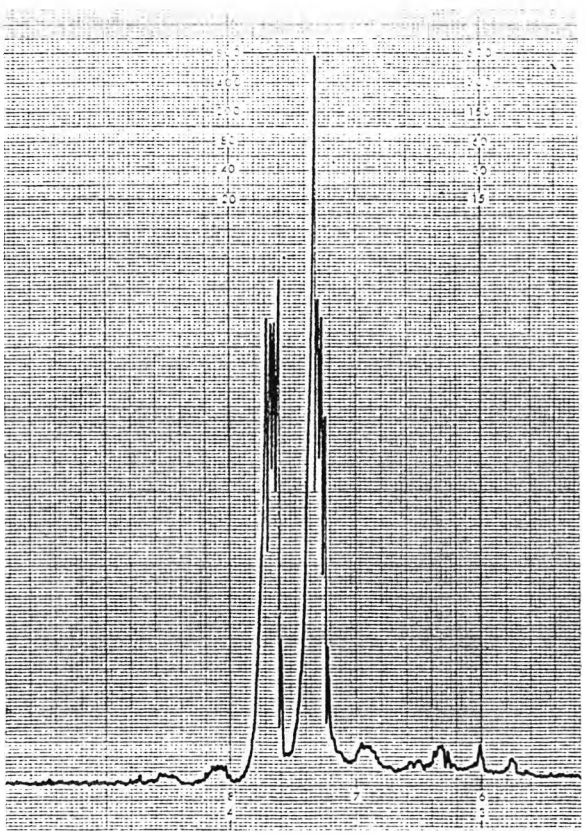

t=240·6 min

Fig.6.3: G.L.C. chromatogram of a standard solution of naphthalene, 1-nitronaphthalene, 2-nitronaphthalene and 1-ethylnaphthalene

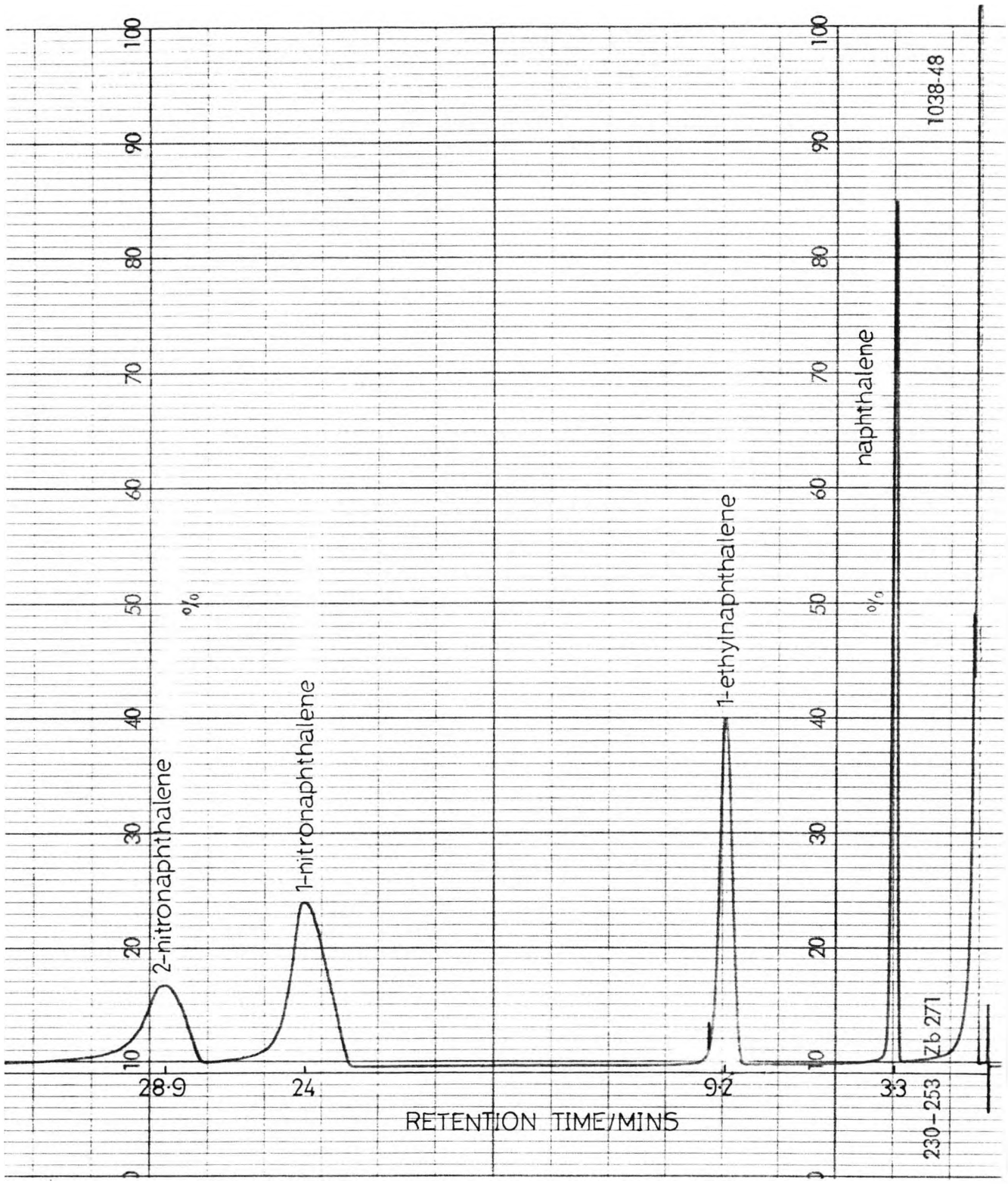

Fig.6.4: G.L.C. chromatogram of the products from the reaction of naphthalene (0.35 mol dm^{-3}) with nitrogen dioxide (0.80 mol dm^{-3}) in carbon tetrachloride at 25°C



Fig. 6.5: G.L.C. chromatogram of the products from reaction of naphthalene (0.52 mol dm^{-3}) with nitrogen dioxide (0.64 mol dm^{-3}) in carbon tetrachloride at 50°C

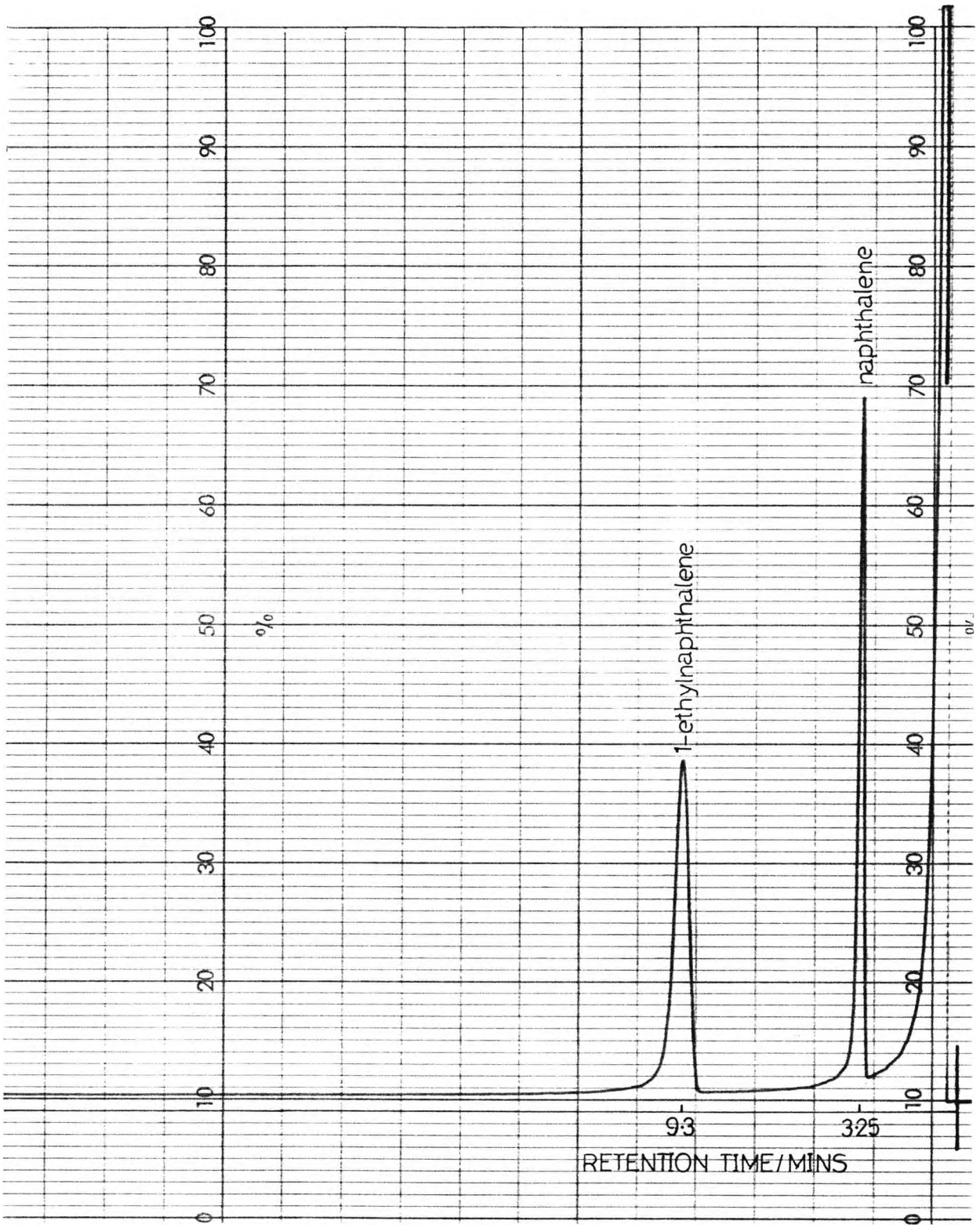

Fig. 6.6: ^{13}C N.M.R. spectrum of the products from the reaction of napthhthalene (0.35 mol dm^{-3}) with nitrogen dioxide (0.80 mol dm^{-3}) in carbon tetrachloride at 25°C

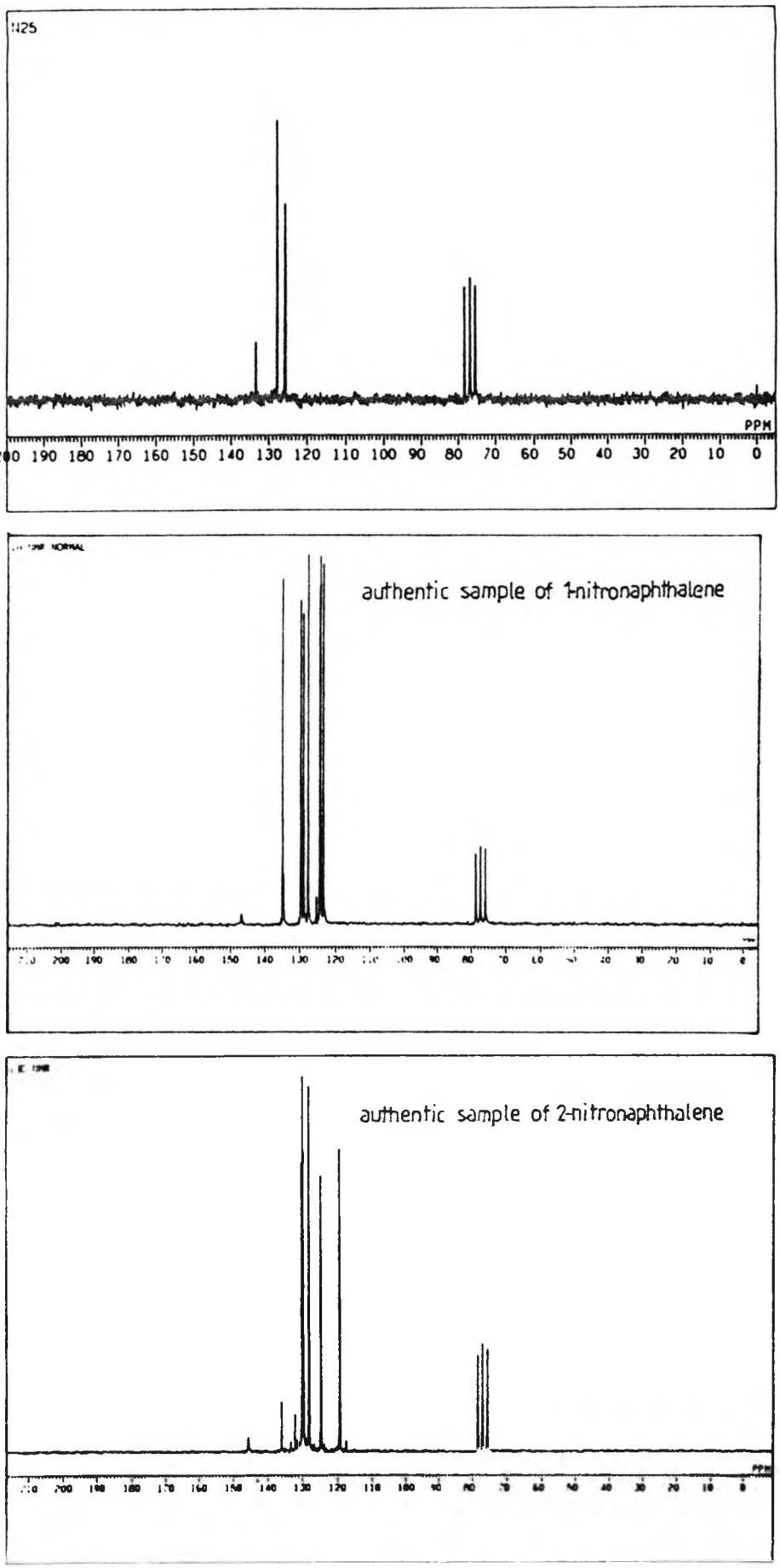

Fig.6.7: ^{13}C N.M.R. spectrum of the products from the reaction of naphthalene (0.52 mol dm^{-3}) with nitrogen dioxide (0.64 mol dm^{-3}) in carbon tetrachloride at 50°C

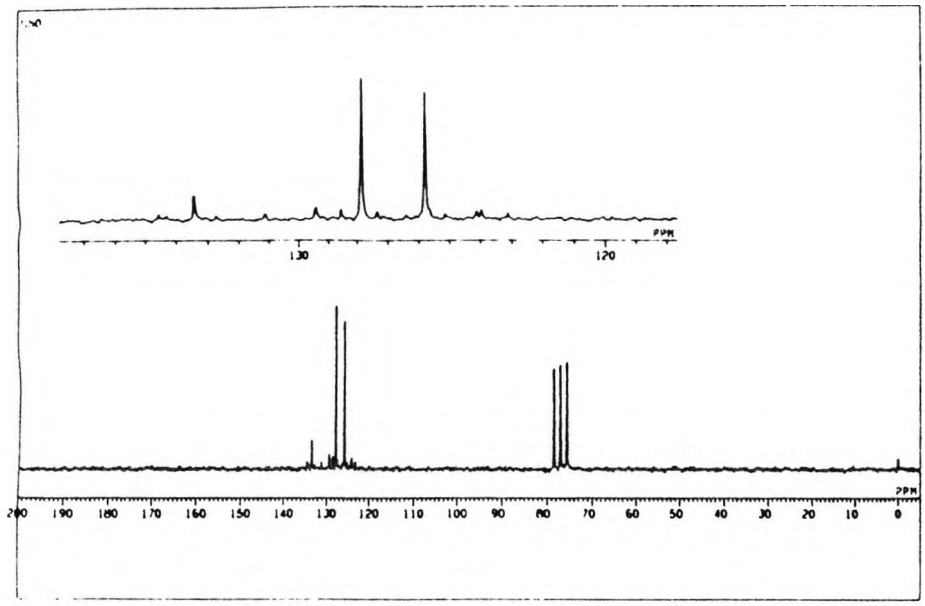

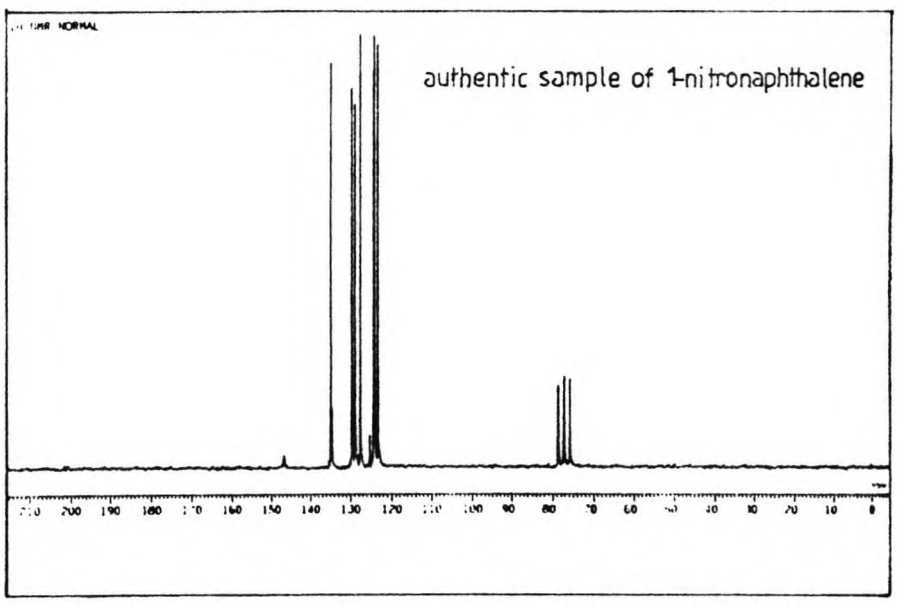

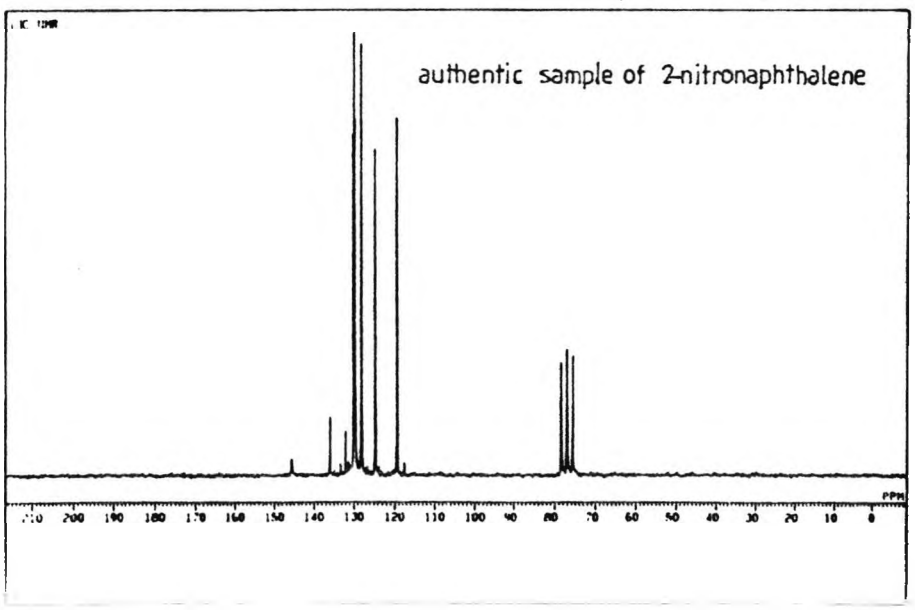

Fig. 6.8: ^{1}H N.M.R. spectra recorded during the reaction of 2-methylnaphthalene (0.69 mol dm^{-3}) with nitrogen dioxide (0.69 mol dm^{-3}) in carbon tetrachloride at 25°C

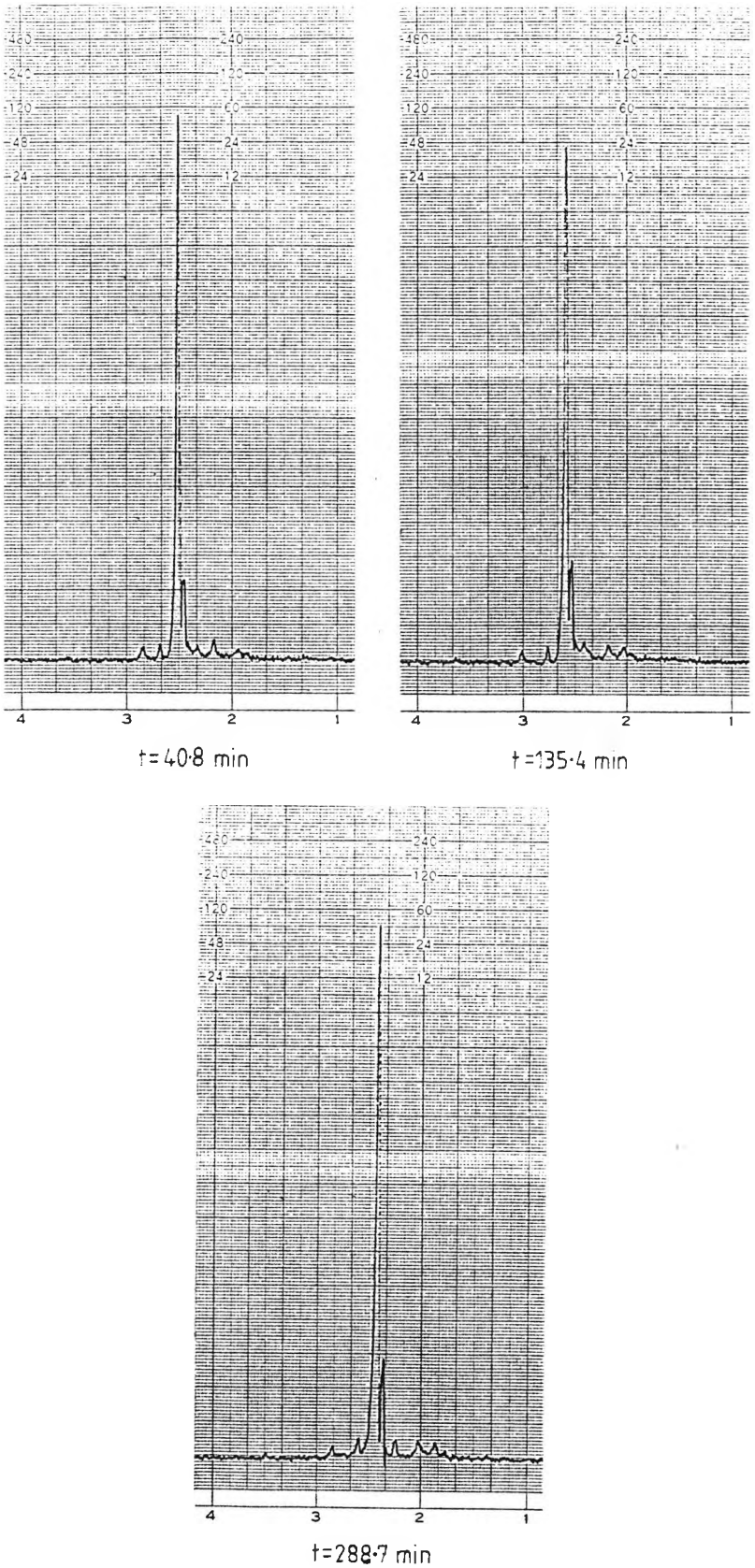

Fig. 6.9: ^{1}H N.M.R. spectra recorded during the reaction of 2-methylnaphthalene (0.63 mol dm^{-3}) with nitrogen dioxide (0.65 mol dm^{-3}) in carbon tetrachloride at 50°C

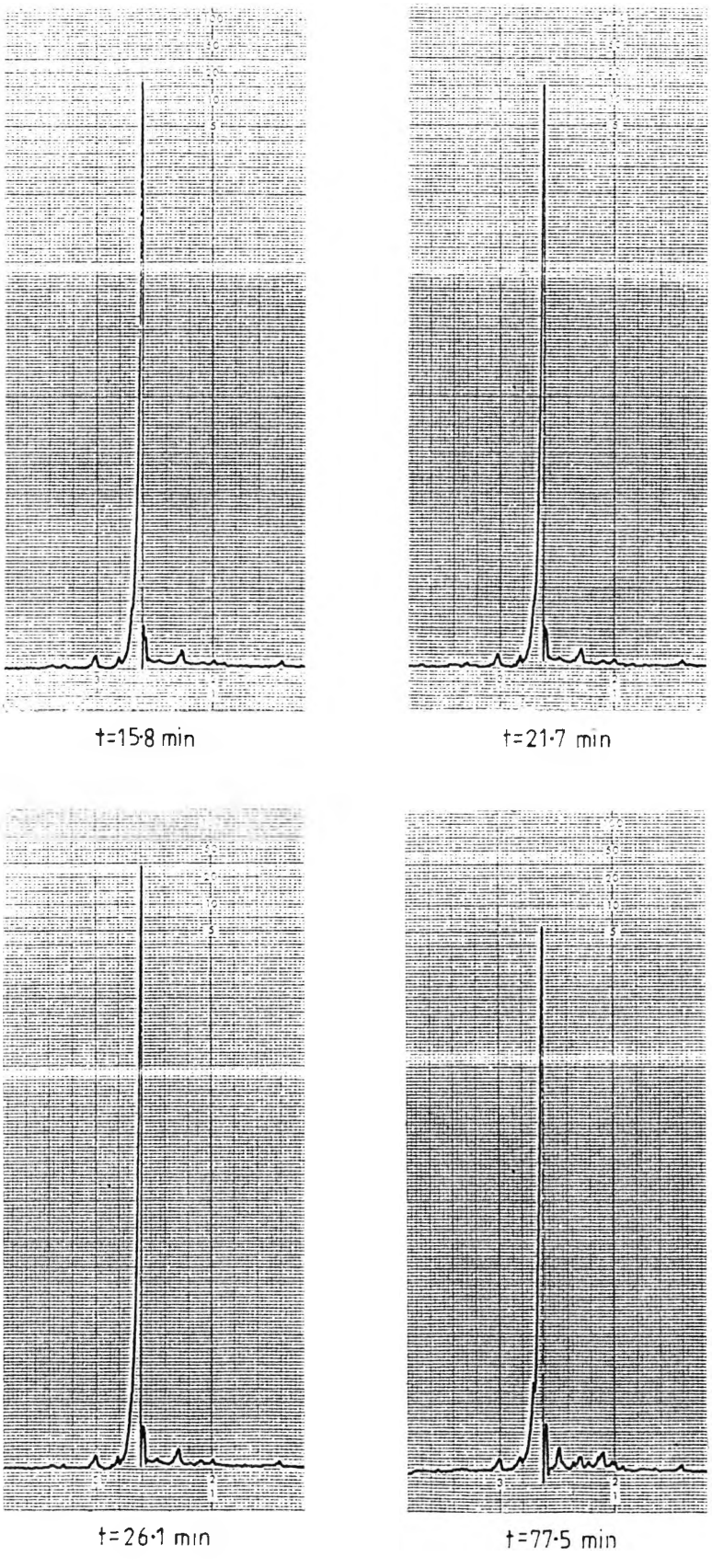

Fig. 6.9: ..... cont'd

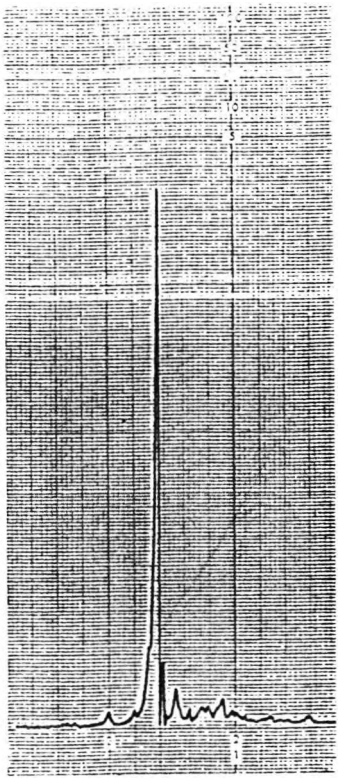

t=127·4 min

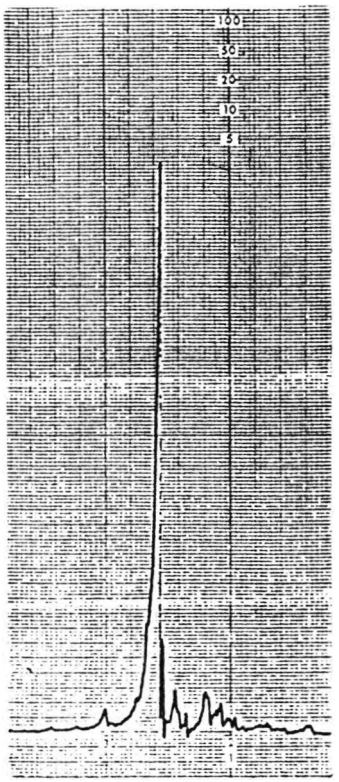

t=193·3 min

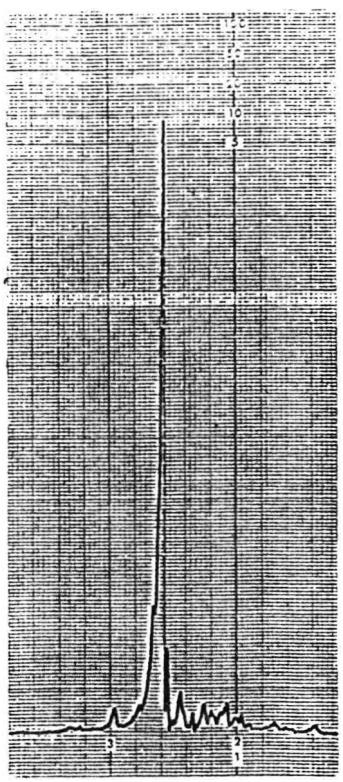

t=241·5 min

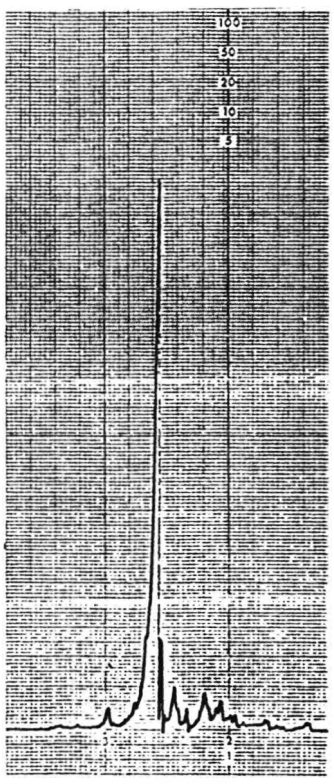

t=270·4 min

Fig. 6.10: G.L.C. chromatogram of a standard solution of 2-methylnaphthalene, 2-methyl-1-nitronaphthalene and 1-ethylnaphthalene

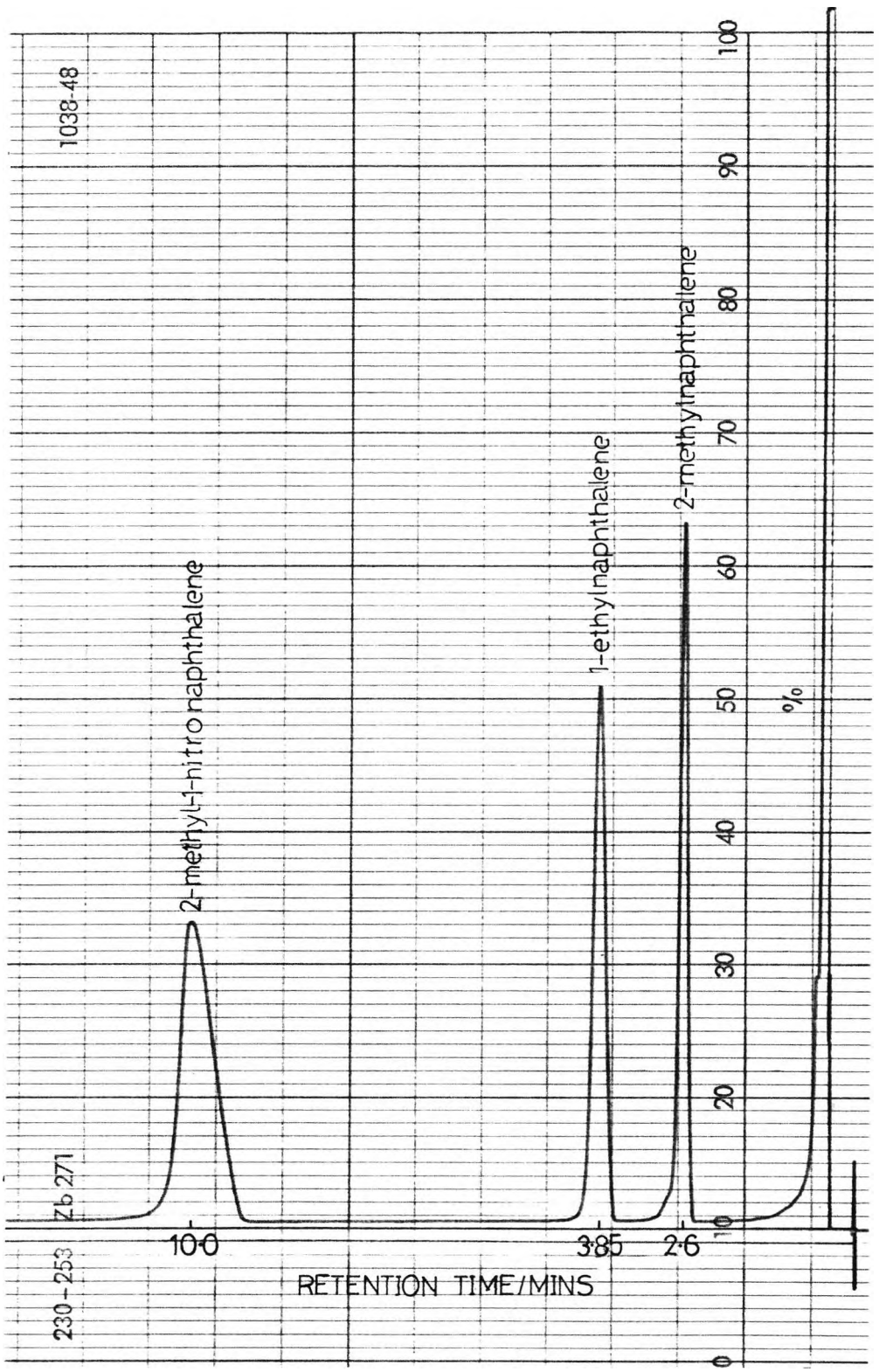

Fig. 6.11: G.L.C. chromatogram of the products from the reaction of 2-methylnaphthalene (0.69 mol dm^{-3}) with nitrogen dioxide (0.69 mol dm^{-3}) in carbon tetrachloride at 25°C

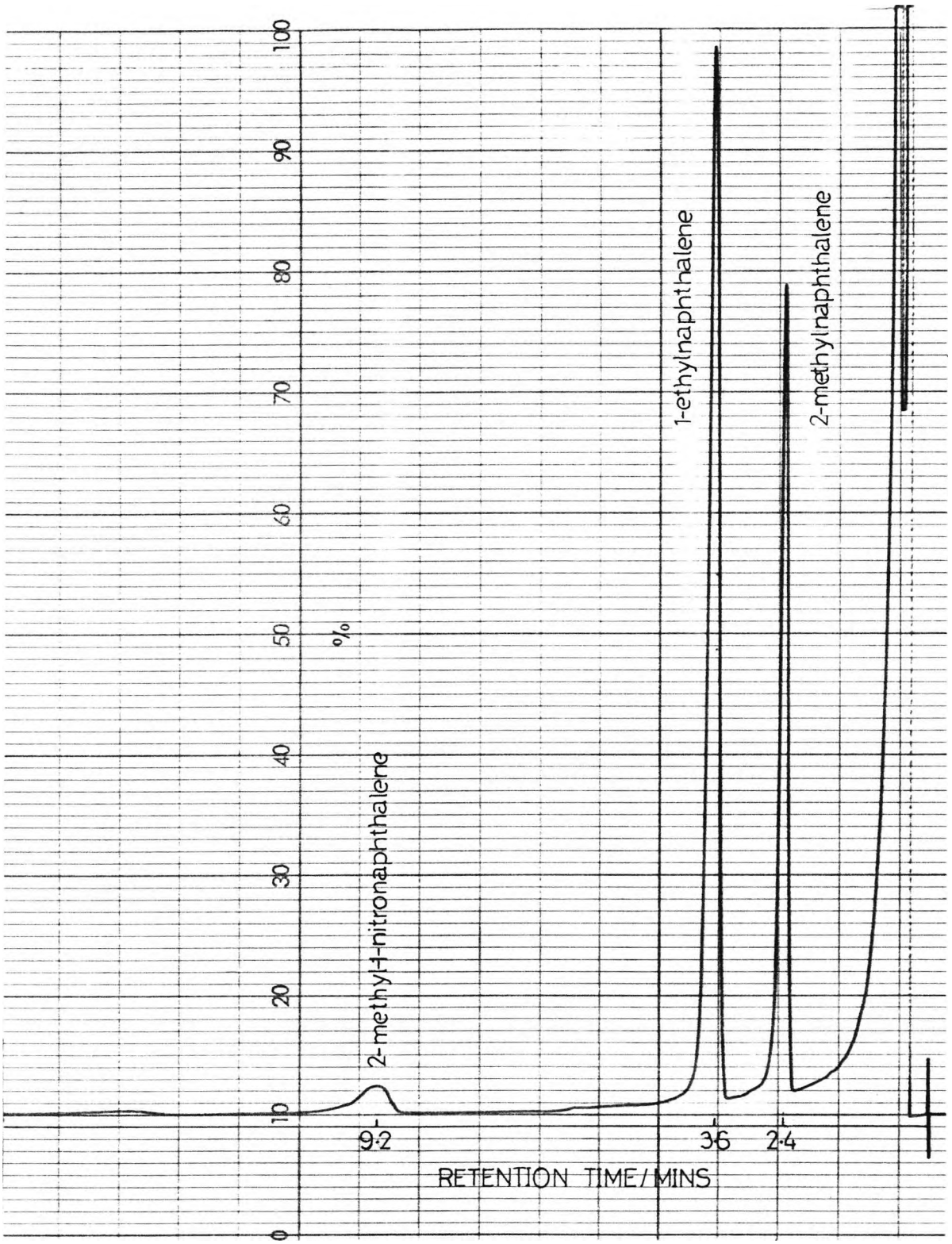

Fig. 6.12: G.L.C. chromatogram of the products from the reaction of 2-methylnaphthalene (0.69 mol dm^{-3}) with nitrogen dioxide (0.65 mol dm^{-3}) in carbon tetrachloride at 50°C

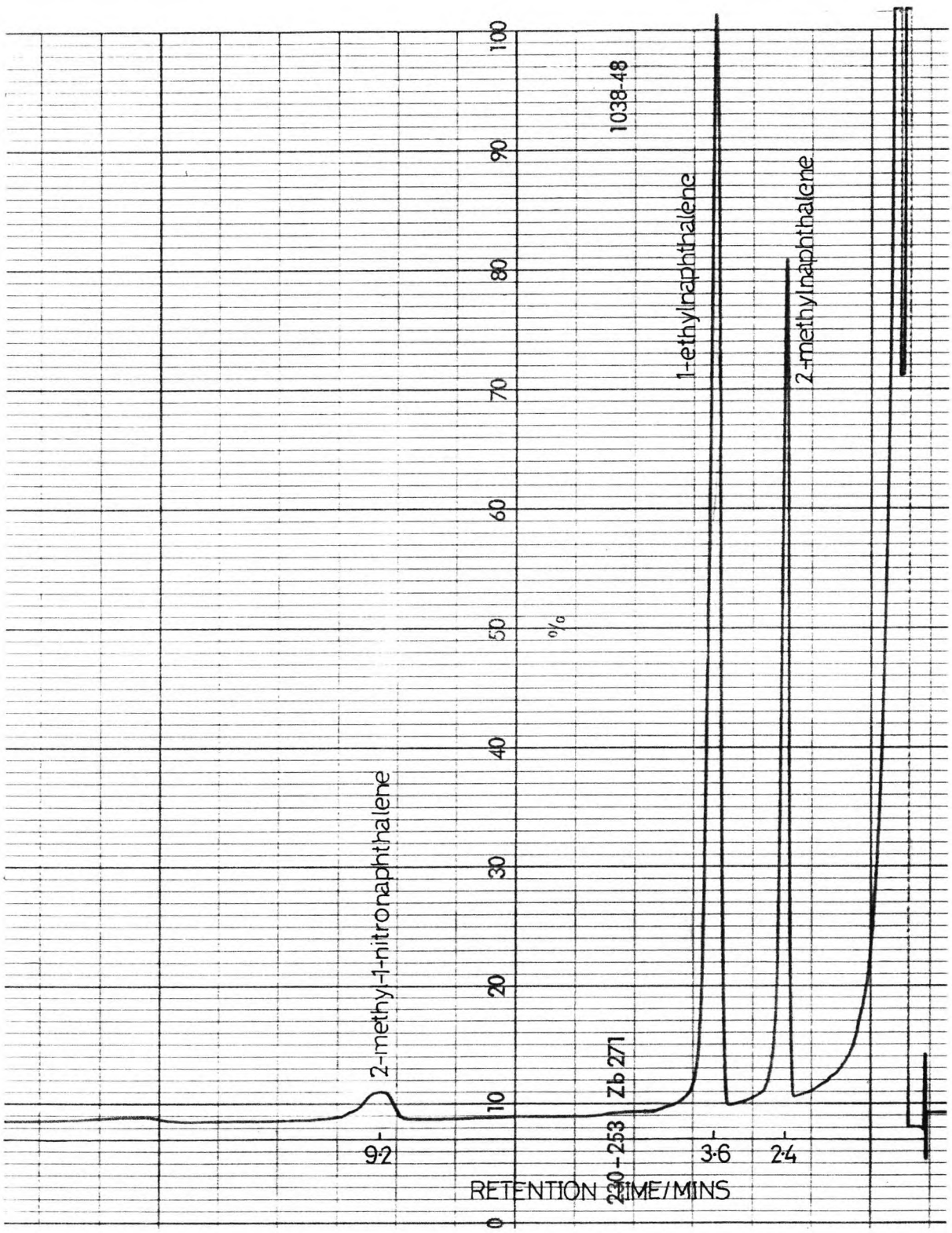

Fig. 6.13: ^{13}C N.M.R. of the products from the reaction of 2-methylnaphthalene (0.69 mol dm^{-3}) with nitrogen dioxide (0.69 mol dm^{-3}) in carbon tetrachloride at 25°C

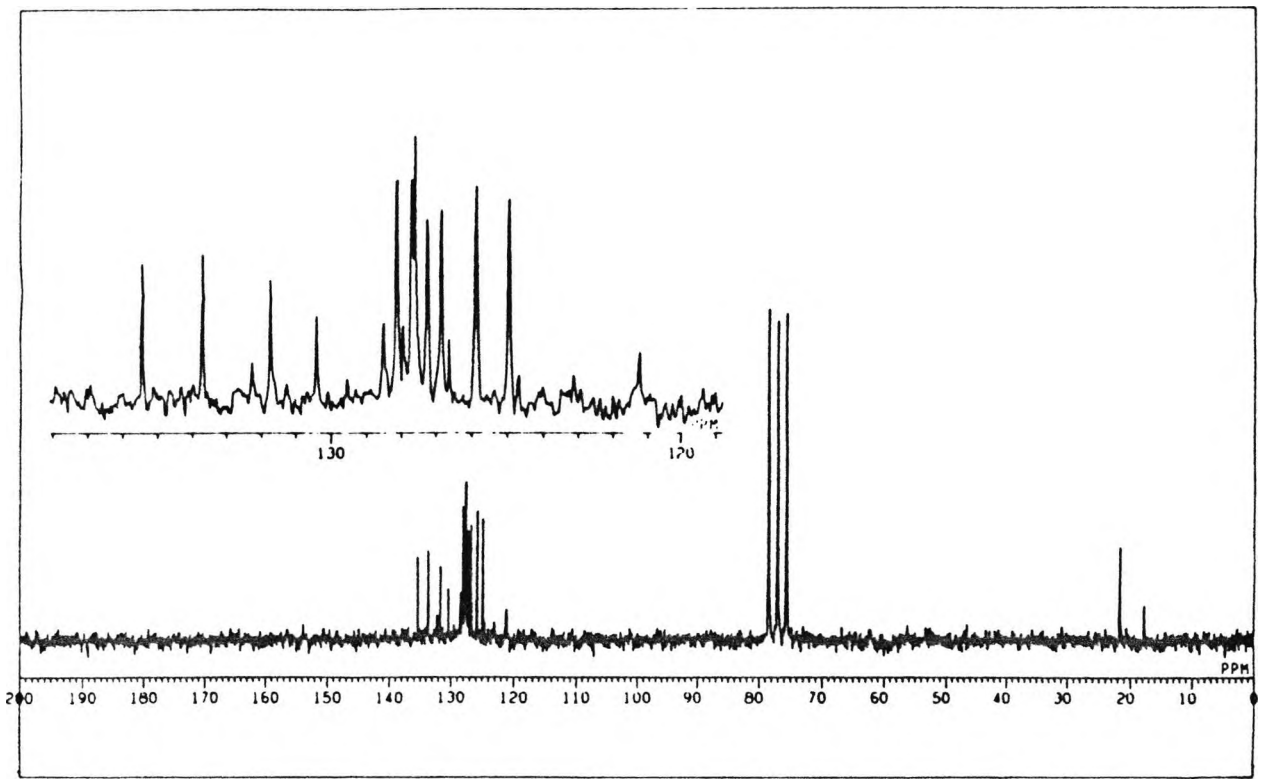

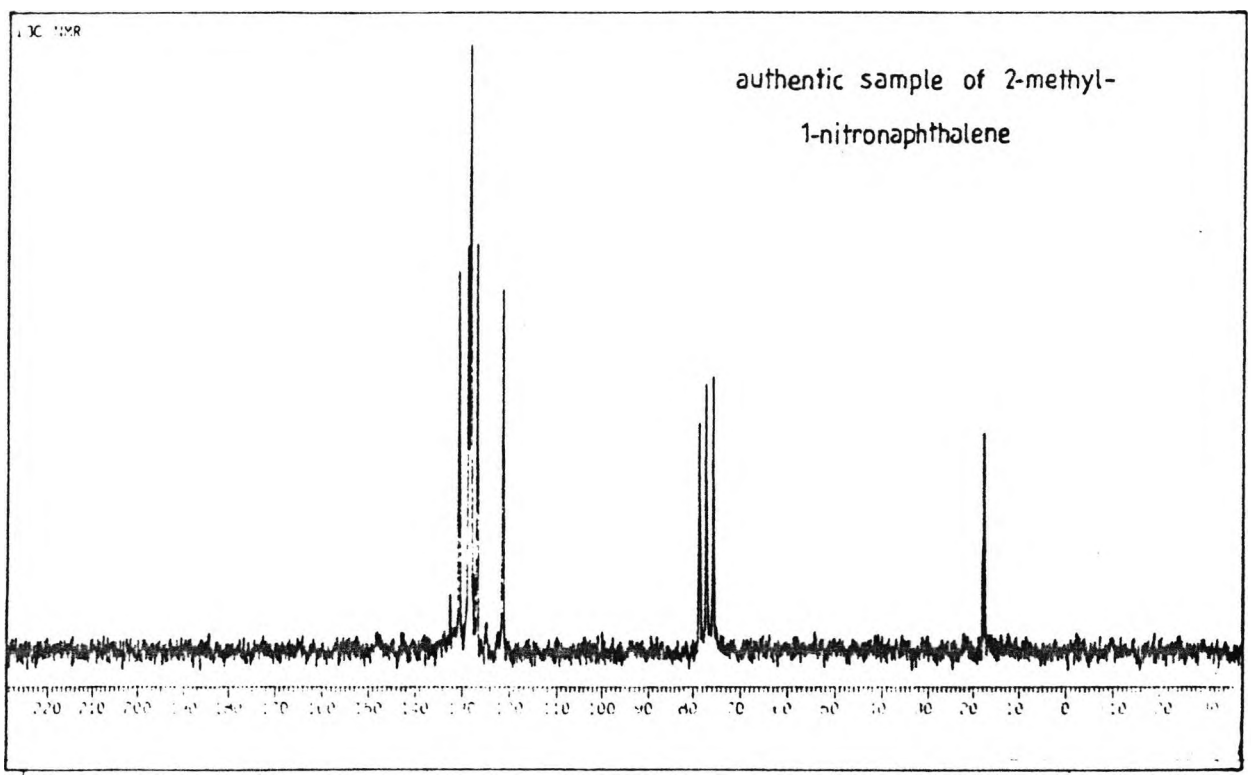

Fig. 6.14: ^{13}C N.M.R. of the products from the reaction of 2-methylnaphthalene (0.69 mol dm^{-3}) with nitrogen dioxide (0.65 mol dm^{-3}) in carbon tetrachloride at 50°C

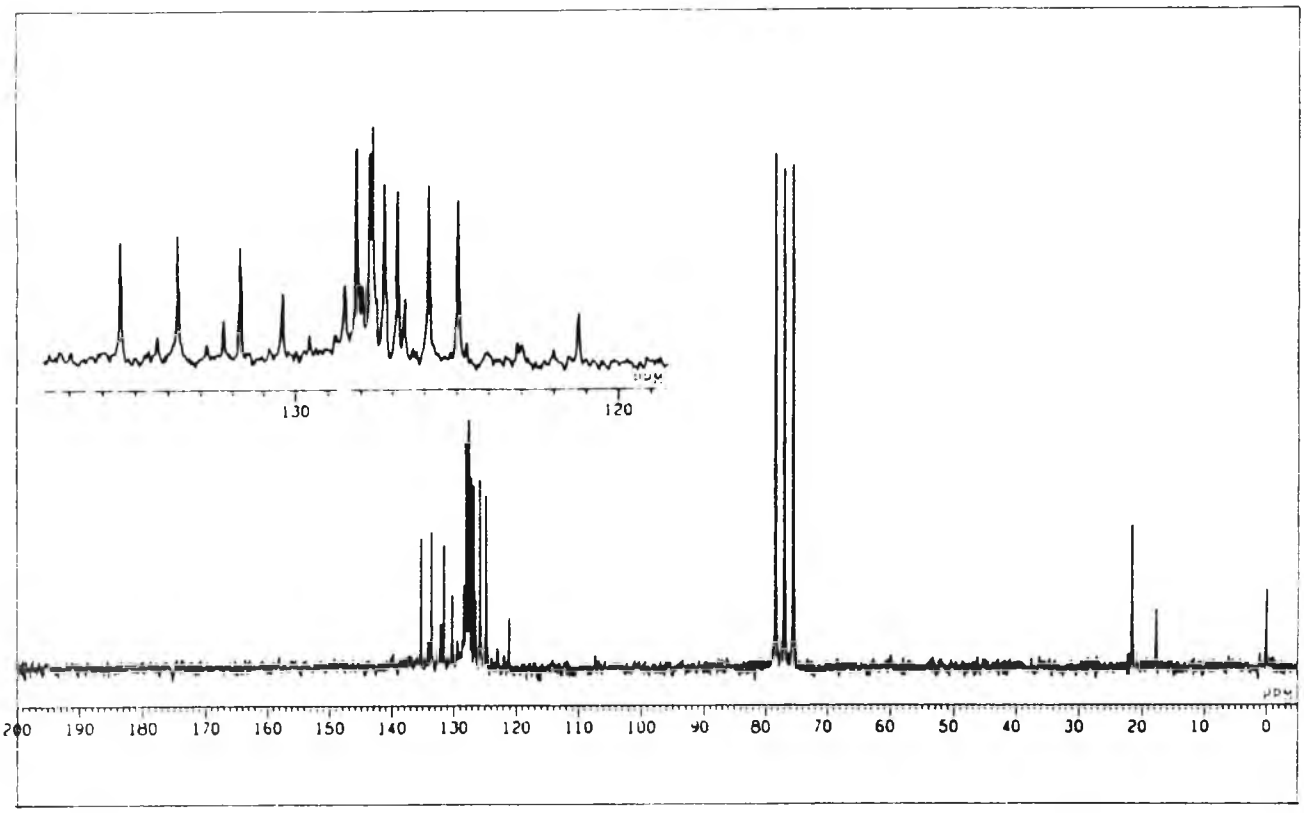

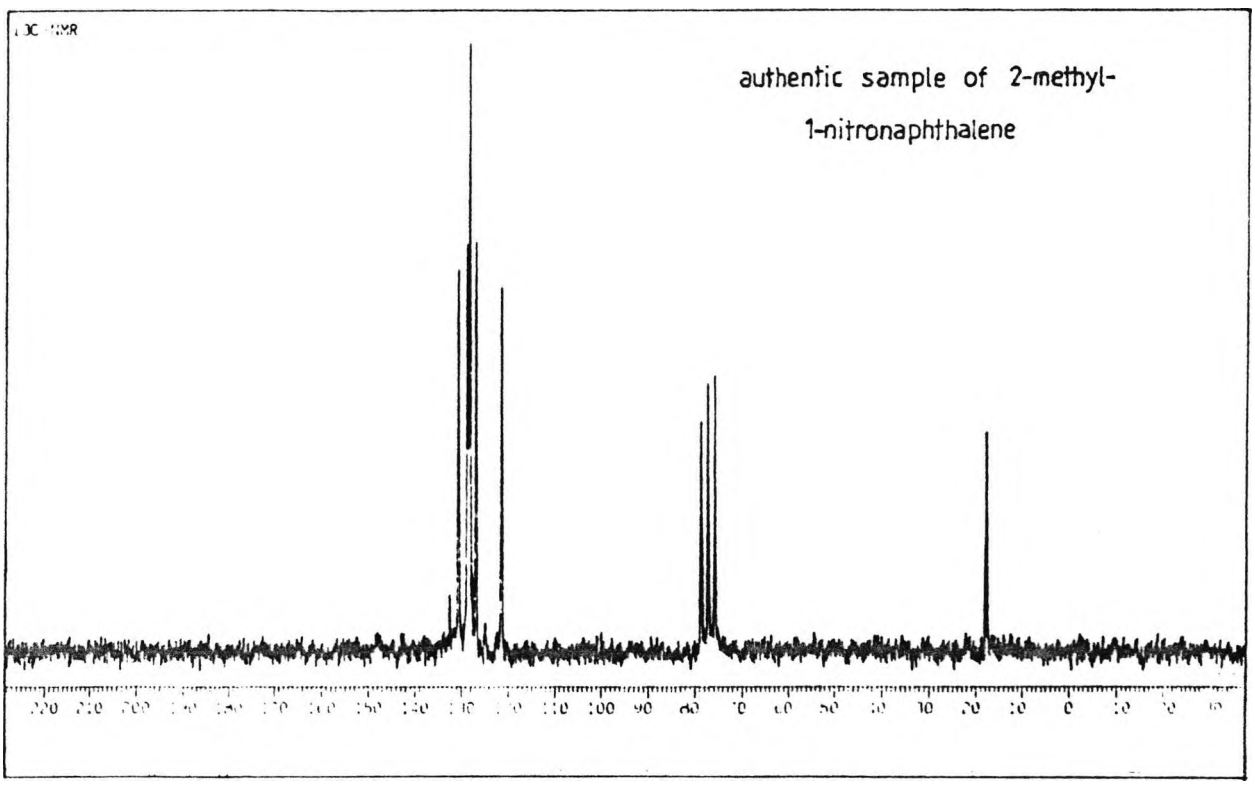

6.3.3 Relative reactivities

6.3.3.1 Naphthalene

The results (Table 6.1) and subsequent calculation required for a typical determination of relative rate for the nitration of naphthalene are given below:

Table 6.1: Relative reactivity of naphthalene to nitrogen dioxide in carbon tetrachloride by competition

	Experiment	Reaction period	Rate relative to benzene
RUN 1	[Naphthalene]=1.1M [Benzene]=0.95M $[N_2O_4]_t$ = 0.08M	164 h	21
RUN 2	[Naphthalene]=1.1M [Benzene]=0.95M $[N_2O_4]_t$ = 0.09M	164 h	20

$$\frac{k_{NAPH}}{k_{BENZENE}} = \frac{[1\text{-nitronaphthalene}]/4}{[\text{nitrobenzene}]/6} \Big/ \frac{[\text{naphthalene}]_o}{[\text{benzene}]_o} \qquad (6.2)$$

From equation 6.1

$$[1\text{-nitronaphthalene}]=C_{NN} = C_s \times \frac{A_x}{A_s} \times \frac{f_s}{f_x} \qquad (6.3)$$

$$[\text{nitrobenzene}]=C_{NB} = C_s \times \frac{A_x'}{A_s} \times \frac{f_s}{f_x'} \qquad (6.4)$$

$$\frac{[1\text{-nitronaphthalene}]}{[\text{nitrobenzene}]} = \frac{A_x}{A_x'} \times \frac{f_x'}{f_x} \qquad (6.5)$$

The g.l.c. chromatogram of a standard solution of 1-nitronaphthalene (1.15×10^{-2} mol dm^{-3}) and nitrobenzene (1.75×10^{-2} mol dm^{-3}) is shown in Fig. 6.15.

$$A_x = 86.01 \text{ mm}^2$$
$$A_x' = 182.14 \text{ mm}^2$$

where A_x = area of 1-nitronaphthalene peak
A_x' = area of nitrobenzene peak

From equation 6.1

$$\frac{f_x'}{f_x} = \frac{C_x}{C_s} \times \frac{A_x'}{A_x}$$

$$= \frac{0.0115}{0.0175} \times \frac{182.14}{86.01}$$
$$= 1.3916$$

The g.l.c. chromatogram of the products from the reaction of naphthalene (1.1 mol dm^{-3}) and benzene (0.95 mol dm^{-3}) with nitrogen dioxide (0.08 mol dm^{-3}) - RUN 1 (table 6.1) is shown in Fig. 6.16.

$$A_x = 347.15 \text{ mm}^2$$
$$A_x' = 30 \text{ mm}^2$$

Substituting these values into equation 6.5 gives

$$\frac{[\text{1-nitronaphthalene}]}{[\text{nitrobenzene}]} = \frac{347.15}{30} \times 1.3916$$

$$\frac{k_{NAPH}}{k_{BENZENE}} = \frac{6 \times 347.15 \times 1.3916}{4 \times 30} \Big/ 1.1/0.95$$

$$= 21$$

In the competition experiments, naphthalene was nitrated predominantly at C(1). The g.l.c. chromatogram

of the products from RUN 2 was recorded at high sensitivity and from the areas of the product peaks the 1NNAP/2NNAP was found to be 250 (Fig. 6.17).

Fig. 6.15: G.L.C. chromatogram of a standard solution of nitrobenzene and 1-nitronaphthalene

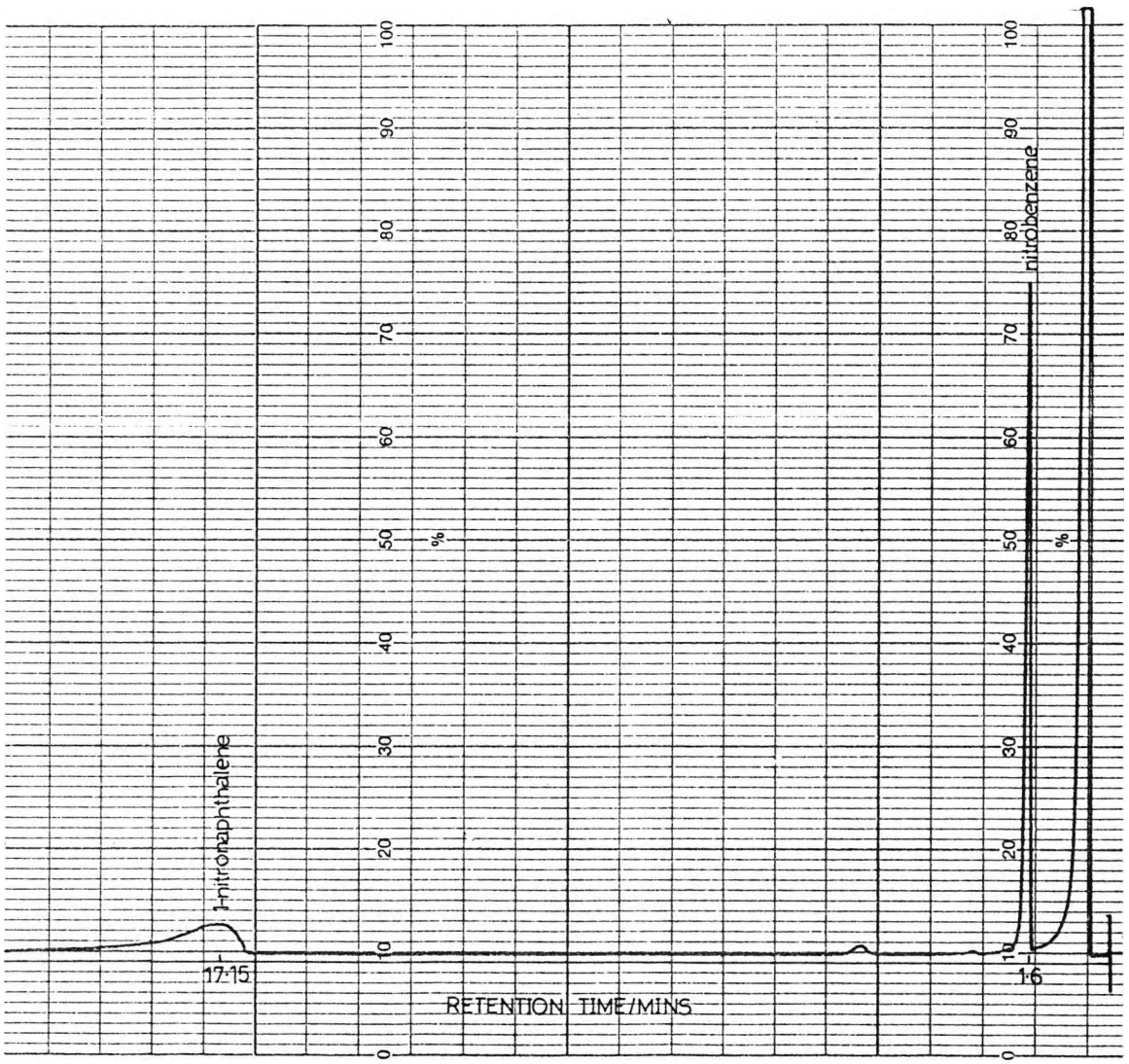

Fig. 6.16: G.L.C. chromatogram of the products from the reaction of naphthalene (1.1 mol dm^{-3}) and benzene (0.95 mol dm^{-3}) with nitrogen dioxide (0.08 mol dm^{-3})

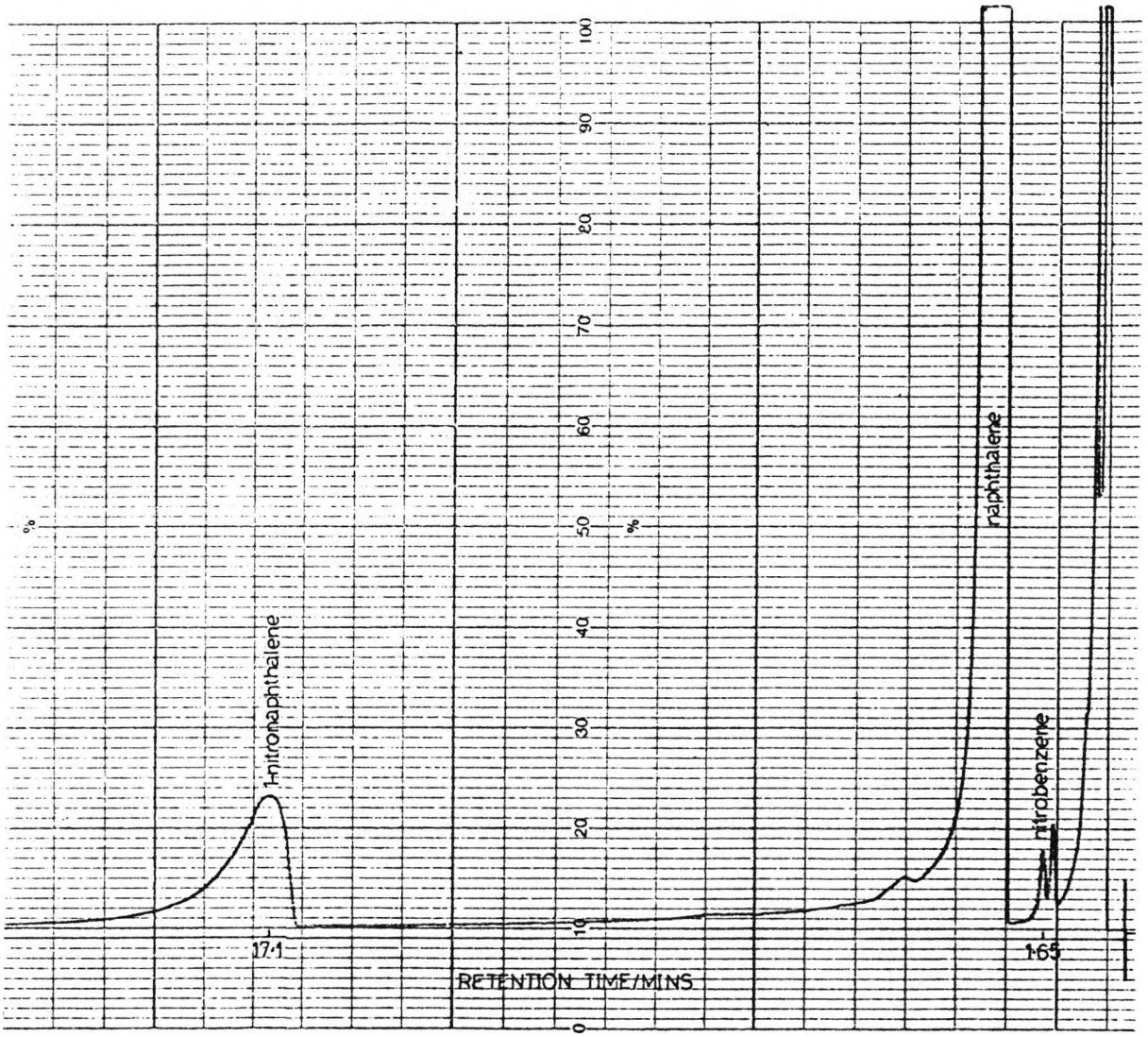

Fig. 6.17: G.L.C. chromatogram of the products from the reaction of naphthalene (1.1 mol dm^{-3}) and benzene (0.95 mol dm^{-3}) with nitrogen dioxide (0.09 mol dm^{-3}) recorded at high sensitivity

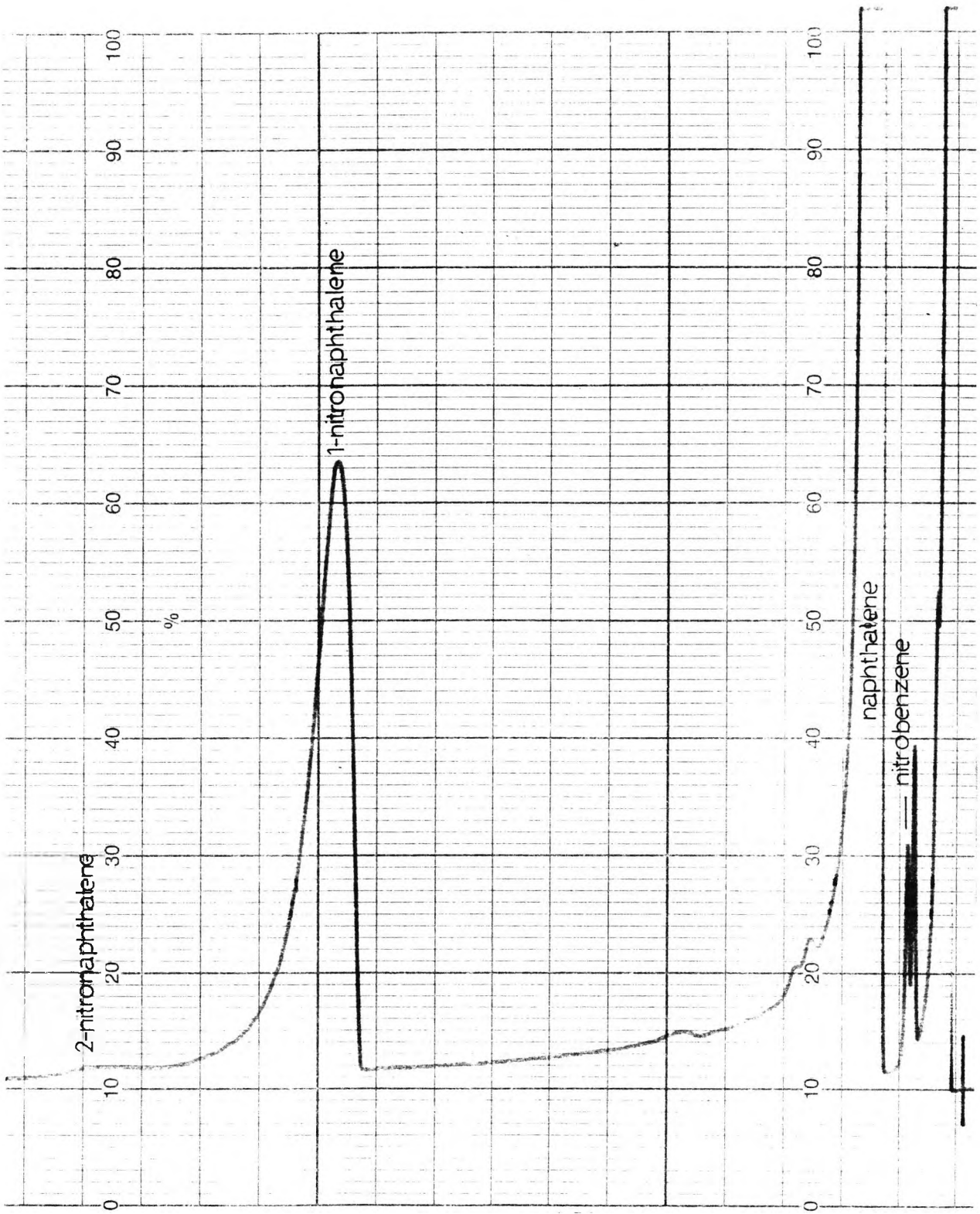

6.3.3.2 2-Methylnaphthalene

The results (Table 6.2) and subsequent calculation required for a typical determination of relative rate for the nitration of 2-methyl-1-nitronaphthalene are given below:

Table 6.2: Relative reactivity of 2-methylnaphthalene to nitrogen dioxide in carbon tetrachloride by competition

	Experiment	Reaction period	Rate relative to benzene
RUN 1	[2-Methylnaphthalene]=2.8M [Benzene]=2.6M $[N_2O_4]_t$ = 0.22M	164 h	409
RUN 2	[2-Methylnaphthalene]=2.9M [Benzene]=2.6M $[N_2O_4]_t$ = 0.22M	164 h	514

$$\frac{k_{2\text{-MeN}}}{k_{BENZENE}} = \frac{[\text{2-methyl-1-nitronaphthalene}]}{\text{nitrobenzene}/6} \Big/ \frac{[\text{2-methylnaphthalene}]_o}{[\text{benzene}]_o} \quad (6.6)$$

From equation 6.1

$$[\text{2-methyl-1-nitronaphthalene}]=c_{MN} = C_s \times \frac{A_x''}{A_s} \times \frac{f_s}{f_x''} \quad (6.7)$$

$$[\text{nitrobenzene}] = C_{NB} = C_s \times \frac{A_x'}{A_s} \times \frac{f_s}{f_x'} \quad (6.8)$$

$$\frac{[\text{2-methyl-1-nitronaphthalene}]}{[\text{nitrobenzene}]} = \frac{A_x''}{A_x} \times \frac{f_x'}{f_x''} \quad (6.9)$$

The g.l.c. chromatogram of a standard solution of 2-methyl-1-nitronaphthalene (9.83×10^{-2} mol dm^{-3}) and nitrobenzene (1.51×10^{-2} mol dm^{-3}) is shown in Fig. 6.18.

$$A_x'' = 102.25 \text{ mm}^2$$
$$A_x' = 162.68 \text{ mm}^2$$

where A_x'' = area of 2-methyl-1-nitronaphthalene peak
A_x' = area of nitrobenzene peak

from equation 6.1

$$\frac{f_x'}{f_x''} = \frac{C_{MN}}{C_{NB}} \times \frac{A_x'}{A_x''}$$

$$= \frac{9.83 \times 10^{-3}}{1.51 \times 10^{-2}} \times \frac{162.68}{102.25}$$

$$= 1.0357$$

The g.l.c. chromatogram of the products from the reaction of 2-methylnaphthalene (2.8 mol dm^{-3}) and benzene (2.6 mol dm^{-3}) with nitrogen dioxide (0.22 mol dm^{-3}) - RUN 1 (Table 6.2) - is shown in Fig. 6.19.

$$A_x'' = 1551.24 \text{ mm}^2$$
$$A_x' = 21.87 \text{ mm}^2$$

Substituting these values into equation 6.9 gives

$$\frac{[\text{2-methyl-1-nitronaphthalene}]}{[\text{nitrobenzene}]} = \frac{1551.24}{21.87} \times 1.0357$$

$$\frac{k_{2\text{-MeN}}}{k_{\text{BENZENE}}} = \frac{6 \times 1551.24 \times 1.0357}{21.87} \Big/ 2.8/2.6$$

$$= 409$$

Fig. 6.18: G.L.C. chromatogram of a standard solution of nitrobenzene and 2-methyl-1-nitronaphthalene

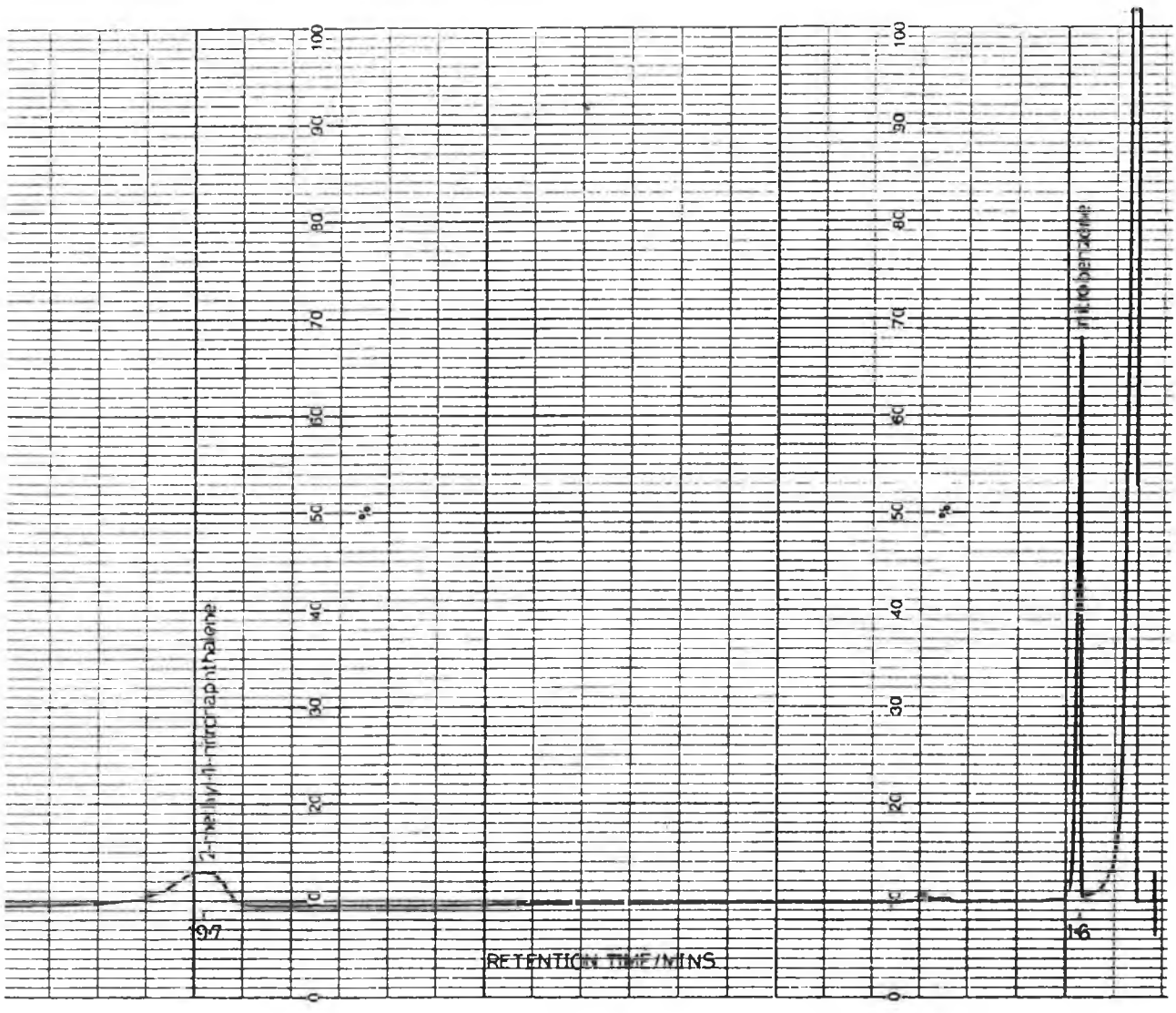

Fig. 6.19: G.L.C. chromatogram of the products from the reaction of 2-methylnaphthalene (2.8 mol dm^{-3}) and benzene (2.6 mol dm^{-3}) with nitrogen dioxide (0.22 mol dm^{-3})

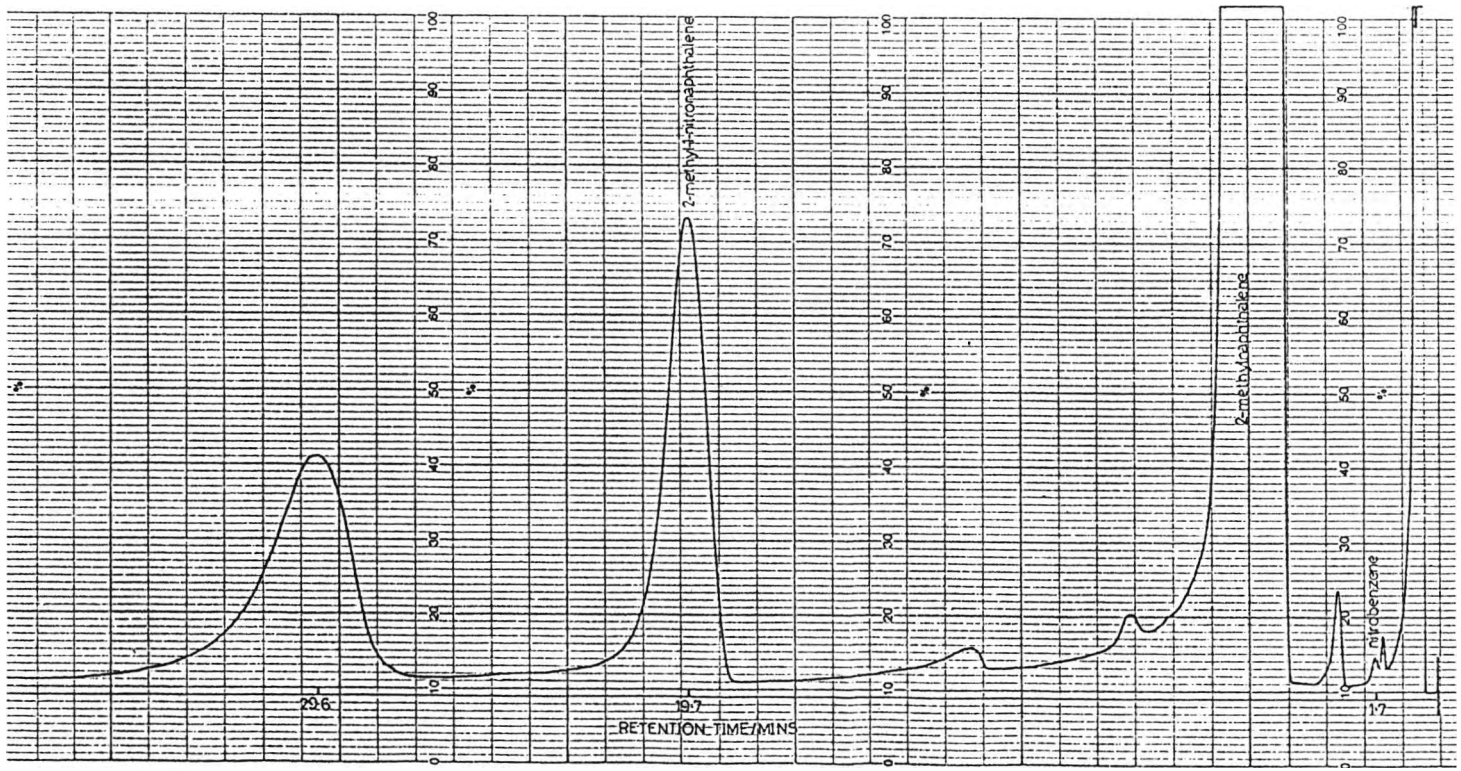

6.4 Discussion

The nitration of naphthalene (NAP) has been the subject of several studies and the 1-nitronaphthalene/2-nitronaphthalene (1NNAP/2NNAP) ratios obtained vary under the conditions used (Table 6.3). The reaction of NAP with liquid dinitrogen tetraoxide at 18 - 20°C has been reported to yield 1NNAP exclusively.[59] The nitration of NAP with nitrogen dioxide in CCl_4 occurs by a free radical mechanism and gives a 1NNAP/2NNAP ratio of 10,[66] similar to that obtained in nitrations by the nitronium ion[112] (or a strongly solvated modification thereof). It also affords a 1NNAP/2NNAP ratio markedly lower than that obtained with nitrogen dioxide in more polar solvents like sulpholane or acetonitrile (about 20). In the case of the nitration of naphthalene by dinitrogen tetraoxide in dichloromethane at room temperature, the yield was reported as 59% after a 48 h reaction period with a 1-nitro:2-nitro ratio of 24.[62] However, when 2,6-di-t-butylpyridine (DTBP) was used as a scavenger of acids in CH_2Cl_2,[66] a lower 1NNAP/2NNAP ratio (about 4) was obtained, and the reaction rate was also slower, comparable to that obtained in CCl_4 (DTBP did not significantly change the products when the nitration was carried out in CCl_4). Thus, nitric and/or nitrous acid are efficient catalysts of an ionic nitration pathway in solvents more polar than CCl_4. The 1NNAP/2NNAP ratios obtained from electrophilic, presumably nitronium ion, nitration are still the subject of some controversy - values of 7-13 have recently been reported.[115]

The most striking feature of the nitration of NAP with nitrogen dioxide in CCl_4 detailed in Pryor's study[66] (Scheme 1.16) is the formation of the unexpected dinitronaphthalene isomers, 1,3-dinitronaphthalene (1,3-diNNAP) and 2,3-dinitronaphthalene (2,3-diNNAP) even at low conversions. The reaction of naphthalene (2M;1.5 ml) with nitrogen dioxide (2M;2.4 ml) for 24 h in CCl_4, for example, led to a 12% conversion with a 1-nitro:2-nitro ratio of 9.7 at 25°C, and a 19% and a 16% yield of 1,3-diNNAP and 2,3-diNNAP, respectively. The production of these diNNAPS was believed to

occur too early in the nitration of NAP for their formation to arise from futher free radical nitration of either 1NNAP or 2NNAP, and so the involvement of a postulated tetranitrotetrahydronaphthalene intermediate was suggested. The formation of 1,3-dinitro compounds has also been observed in the nitration of benzene in liquid dinitrogen tetraoxide when nitric oxide and oxygen are simultaneously bubbled through the solution.[48] Dinitrobenzenes were formed though nitrobenzene was not nitrated under similar conditions. In this case, however, a radical mechanism involving $NO_3^{\cdot}$ as a one-electron oxidant was proposed.

In the present study the rate of nitration of naphthalene and 2-methylnaphthalene with nitrogen dioxide in carbon tetrachloride was found to be extremely low. Nitro products were not detected from the reaction of naphthalene with nitrogen dioxide and 11.4% and 11.7% yields of 2-methyl-1-nitronaphthalene were obtained from the nitration of 2-methylnaphthalene at 25°C and 50°C, respectively (Table 6.4).

A free radical pathway is obviously not prevalent here since there is no evidence of the low 1NNAP/2NNAP ratios or dinitro products observed in Pryor's naphthalene work.[66] The operation of an electron transfer mechanism[60] or a mechanism involving initial attack of $N_2O_4NO^+$,[63] proposed in two independent studies of the reactions of PAHs with nitrogen dioxide in CH_2Cl_2, can also be eliminated since these would lead to low (11.6) and higher (24) 1NNAP/2NNAP ratios respectively.

In the competition experiments carried out in cyclohexane, naphthalene was nitrated predominantly at C(1) with a 1NNAP/2NNAP ratio of 250. 2-Methylnaphthalene was also nitrated mainly at C(1), but an additional peak (at 29.6 min in Fig. 6.19) due to an unidentified isomer was also detected in the g.l.c. chromatograms. The value of the relative reactivity obtained for naphthalene and benzene is that expected for an electrophile less selective than the nitronium ion (149±15),[116] although the species selects quite well between

naphthalene and 2-methylnaphthalene. No further conclusions can be reached as to the nature of this nitrating species except to say that the reaction appears to be analogous to that carried out in the absence of solvent.[59]

Table 6.3: Nitration of naphthalene under different conditions

reagent	solvent	temp/°C	1NN/2NN	ref
NO_2BF_4	sulpholane	25	10	113
NO_2BF_4	nitromethane	25	12	113
$C(NO_2)_4$	gas phase	300	1	113
NO_2	acetonitrile	25	24	113
NO_2	sulpholane	25	19	114
NO_2	CH_2Cl_2	r.t.	24	62
NO_2	CH_2Cl_2	25	11.6	60
NO_2	CH_2Cl_2[a]	25	4	66
NO_2	CCl_4	25	10	66
NO_2	CCl_4[a]	25	8	66
NO_2	CCl_4	50	4.5	66
NO_2	no solvent	18-20	1NNAP only	59
HNO_3/H_2SO_4	CH_3CN	25	10.9	112

a 2,6-di-t-butylpyridine was added to scavenge nitric and nitrous acids

Table 6.4: Kinetic and product studies of the reactions of naphthalene and 2-methylnaphthalene with nitrogen dioxide in carbon tetrachloride

Experiment	Temp	Reaction period	% yield of nitro products
[Naphthalene]=0.35M	25°C	4.75 h	-
$[N_2O_4]_t$ = 0.80M			
[Naphthalene]=0.52M	50°C	4.25 h	-
$[N_2O_4]_t$ = 0.64M			
[2-Methylnaphthalene]=0.69M	25°C	5.25 h	11.4
$[N_2O_4]_t$ = 0.69M			
[2-Methylnaphthalene]=0.69M	50°C	6.00 h	11.7
$[N_2O_4]_t$ = 0.65M			

C H A P T E R 7

THE REACTION OF 1-METHYLBUTYLBENZENE WITH NITROGEN DIOXIDE

7 The reaction of 1-methylbutylbenzene with nitrogen dioxide

7.1 Introduction

The reactivity of 1-methylbutylbenzene with gaseous nitrogen dioxide has been investigated over the temperature range 25°C - 150°C, in order to compare the rate of H abstraction with substitution of the ring.

7.2 Experimental

7.2.1 The reaction of 1-methylbutylbenzene with gaseous nitrogen dioxide

A dilute solution of 1-methylbutylbenzene in cyclohexane was placed in a two-necked flask fitted with a condenser, purged with nitrogen at 55 ml min^{-1} for 15 min, exposed to 10000 ppm gaseous nitrogen dioxide/N_2 at 55 ml min^{-1} for 2 h at 25°C and purged again with N_2 at 55 ml min^{-1} for 15 min, to remove any unreacted nitrogen dioxide.

Similar experiments were carried out with dilute and concentrated solutions of 1-methylbutylbenzene in hexadecane at 150°C, and with hexadecane alone at 150°C. In the latter two cases, a nitrogen dioxide/N_2 flow rate of 31 ml min^{-1} was used.

Reaction solutions were analysed directly by g.l.c. (2 metre x 31.75 mm silicone 5% SE30 column using a temperature program : 120°C for 6 min, 10°C min^{-1}, 200°C for 5 min and a nitrogen flow rate of 25 ml min^{-1}) after addition of a known amount of 1-ethylnaphthalene as a standard.

7.2.2 Measurement of the reactivity of 1-methylbutylbenzene by the competition technique

A solution of 1-methylbutylbenzene and benzene was made up in cyclohexane. 20 ml of this solution was transferred to a

round-bottomed flask and was thermostatted in a waterbath at 25°C for 15 min. A stock solution of nitrogen dioxide was made up in the same solvent and was also thermostatted at 25°C. A small quantity of the nitrating solution was then added to the aromatic solution, the aromatics being in a large excess to maintain the proportions of the two substrates, and the reaction mixture was left for 164 h. A small sample (0.5 ml) was removed and treated with water to prevent further reaction, and the organic layer was analysed quantitatively by g.l.c. Analysis was possible with a 2 metre x 31.75 mm silicone 5% SE30 column at 130°C using a nitrogen flow rate of 25 ml min^{-1}.

7.3 Results

7.3.1 The reaction of 1-methylbutylbenzene with gaseous nitrogen dioxide

The extent of reaction in each experiment was measured in terms of the disappearance of 1-methylbutylbenzene and is shown in Table 7.1. The concentration of 1-methylbutylbenzene in the product solutions was determined by a method based on relative response factors (Section 10.2 and Table 7.2).

Products resulting from the nitration of 1-methylbutylbenzene *via* either H abstraction or ring substitution were not detected by g.l.c. The unidentified peak that was observed in the chromatogram of the 1-methylbutylbenzene/nitrogen dioxide reaction solution at low concentration at 150°C (peak at 17.4 min. in Fig. 7.3) was also seen in the chromatogram of the products from the reaction of hexadecane alone with nitrogen dioxide (Fig. 7.1). The peaks at 11.1 min. in Figs. 7.2, 7.3, 7.4 and 14.7 min in Fig. 7.3 are due to impurities in the solvent, hexadecane.

Table 7.1: Nitration of 1-methylbutylbenzene with gaseous nitrogen dioxide

	Experiment	Temp.	% Reaction
Fig. 7.1	Reaction of hexadecane with 1% nitrogen dioxide/N_2 for 2 h	150°C ± 4°C	-
Fig. 7.2	Reaction of 1-methylbutylbenzene (0.01 mol dm^{-3}) with 1% nitrogen dioxide/N_2 for 2 h	25°C	12%
Fig. 7.3	Reaction of 1-methylbutylbenzene (0.01 mol dm^{-3}) with 1% nitrogen dioxide/N_2 for 2 h	150°C ± 2°C	28%
Fig. 7.4	Reaction of 1-methylbutylbenzene (0.23 mol dm^{-3}) with 1% nitrogen dioxide/N_2 for 2 h	150°C ± 4°C	10%

Table 7.2: Calculation of the constant f_s/f_x

amount of internal standard, 1-ethylnaphthalene = 8.99×10^{-3} mol dm^{-3}

amount of 1-methylbutylbenzene = 1.15×10^{-2} mol dm^{-3}

c_x/mol dm^{-3}	c_s/mol dm^{-3}	A_x/mm^2	A_s/mm^2	$f = f_s/f_x$
1.15×10^{-2}	8.99×10^{-3}	128.92	103.25	1.0291
		123.60	99.36	1.0330
		119.10	97.60	1.0530

Average value of f = 1.0384

Fig. 7.1: GLC chromatogram of the products from the reaction of hexadecane with 10000 ppm gaseous nitrogen dioxide at 150°C for 2 h

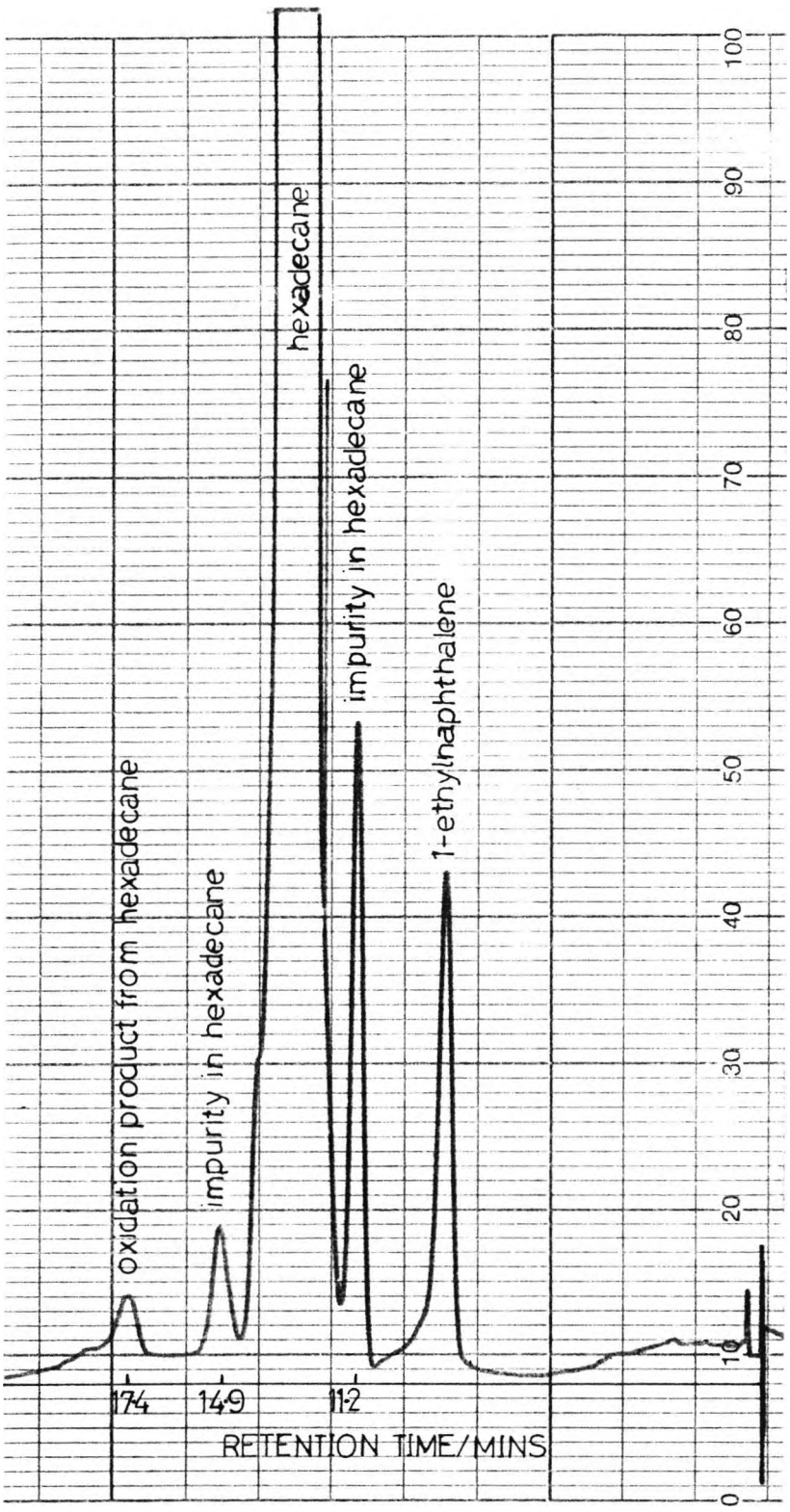

Fig. 7.2: GLC chromatogram of the products from the reaction of 1-methylbutylbenzene (0.01 mol dm^{-3}) with 10000 ppm gaseous nitrogen dioxide in hexadecane at 25°C for 2 h

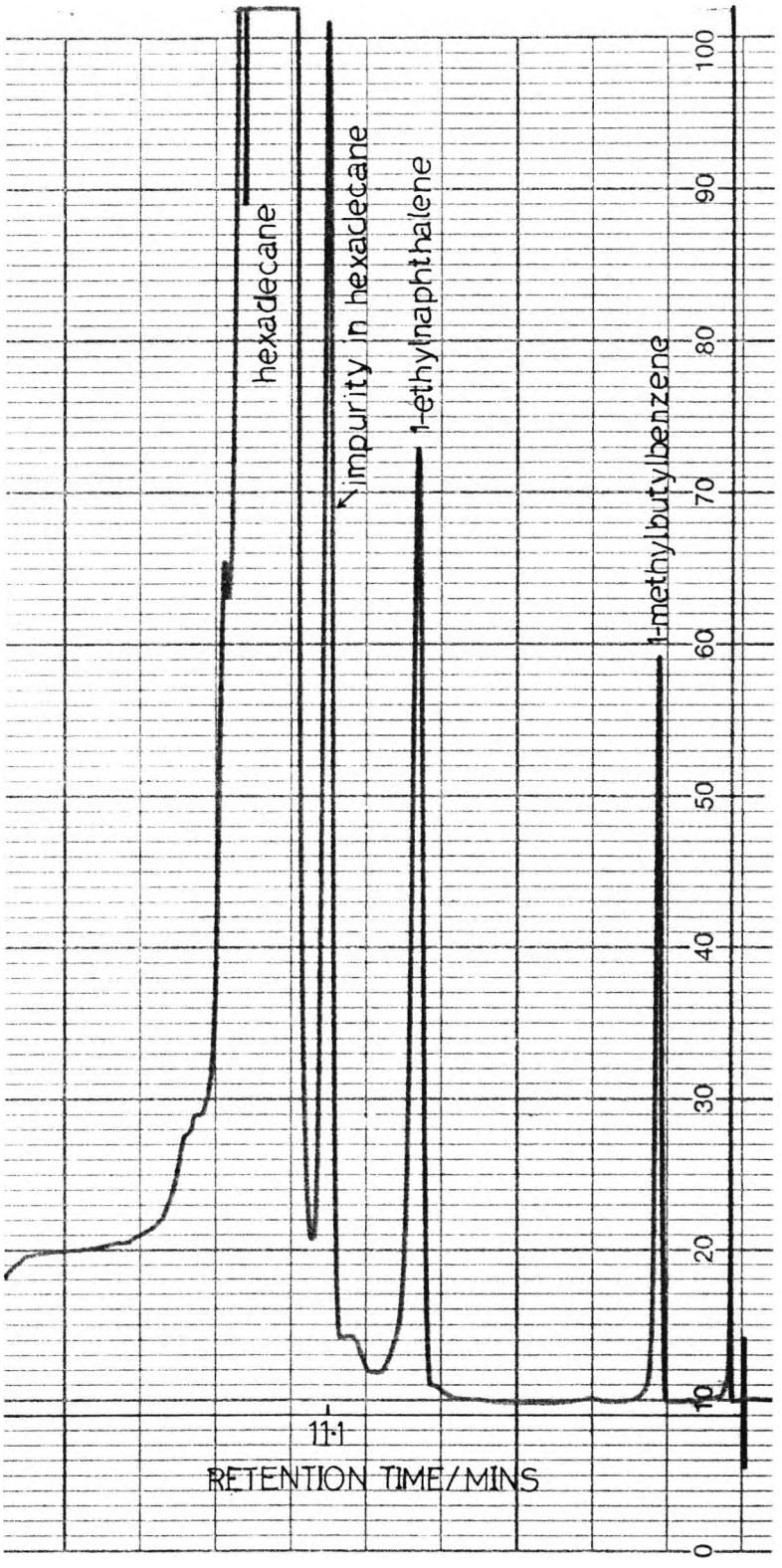

Fig. 7.3: GLC chromatogram of the products from the reaction of 1-methylbutylbenzene (0.01 mol dm^{-3}) with 10000 ppm gaseous nitrogen dioxide in hexadecane at 150°C for 2 h

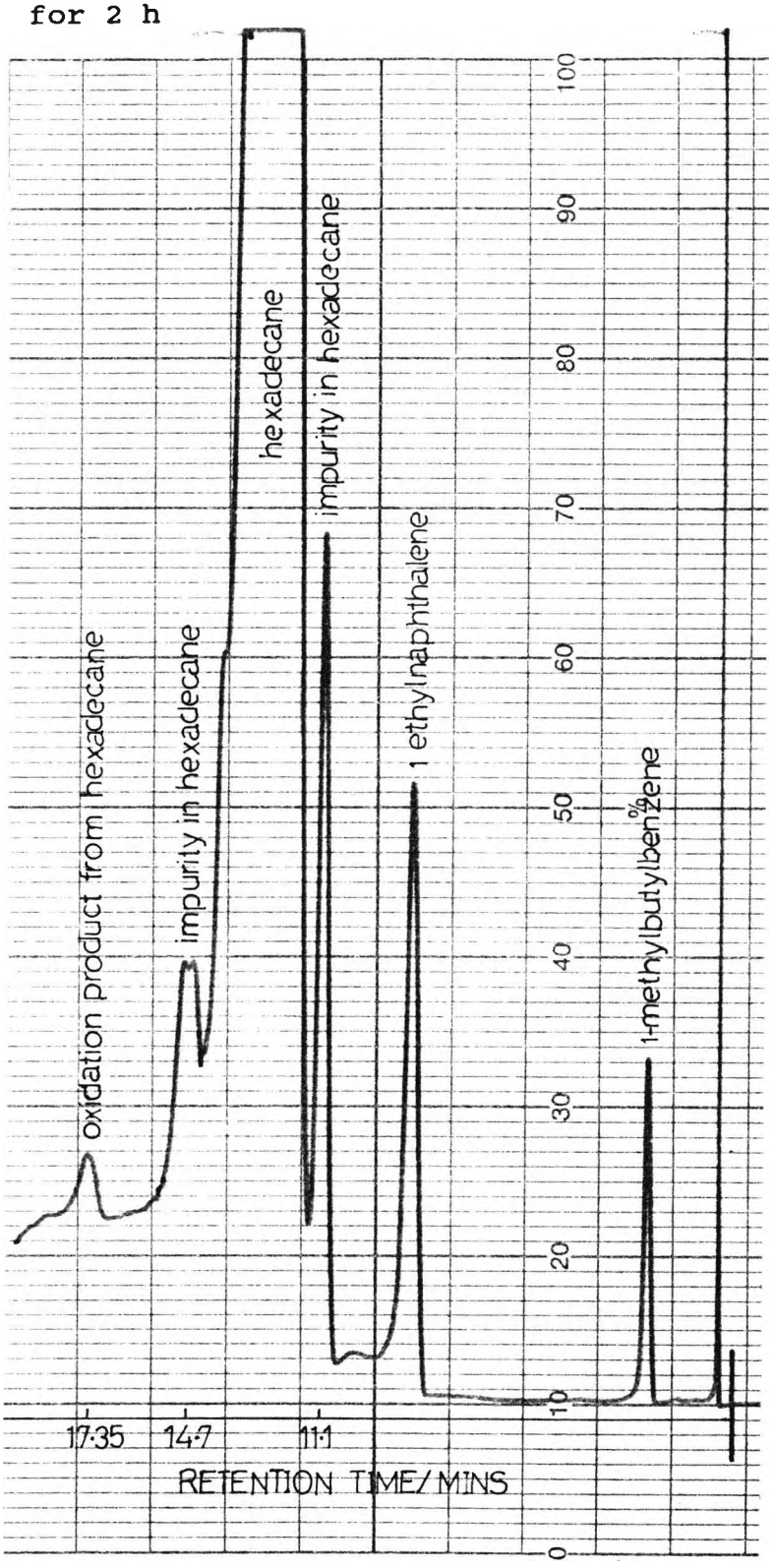

Fig. 7.4:GLC chromatogram of the products from the reaction of 1-methylbutylbenzene (0.23 mol dm^{-3}) with 10000 ppm gaseous nitrogen dioxide in hexadecane at 150°C for 2 h

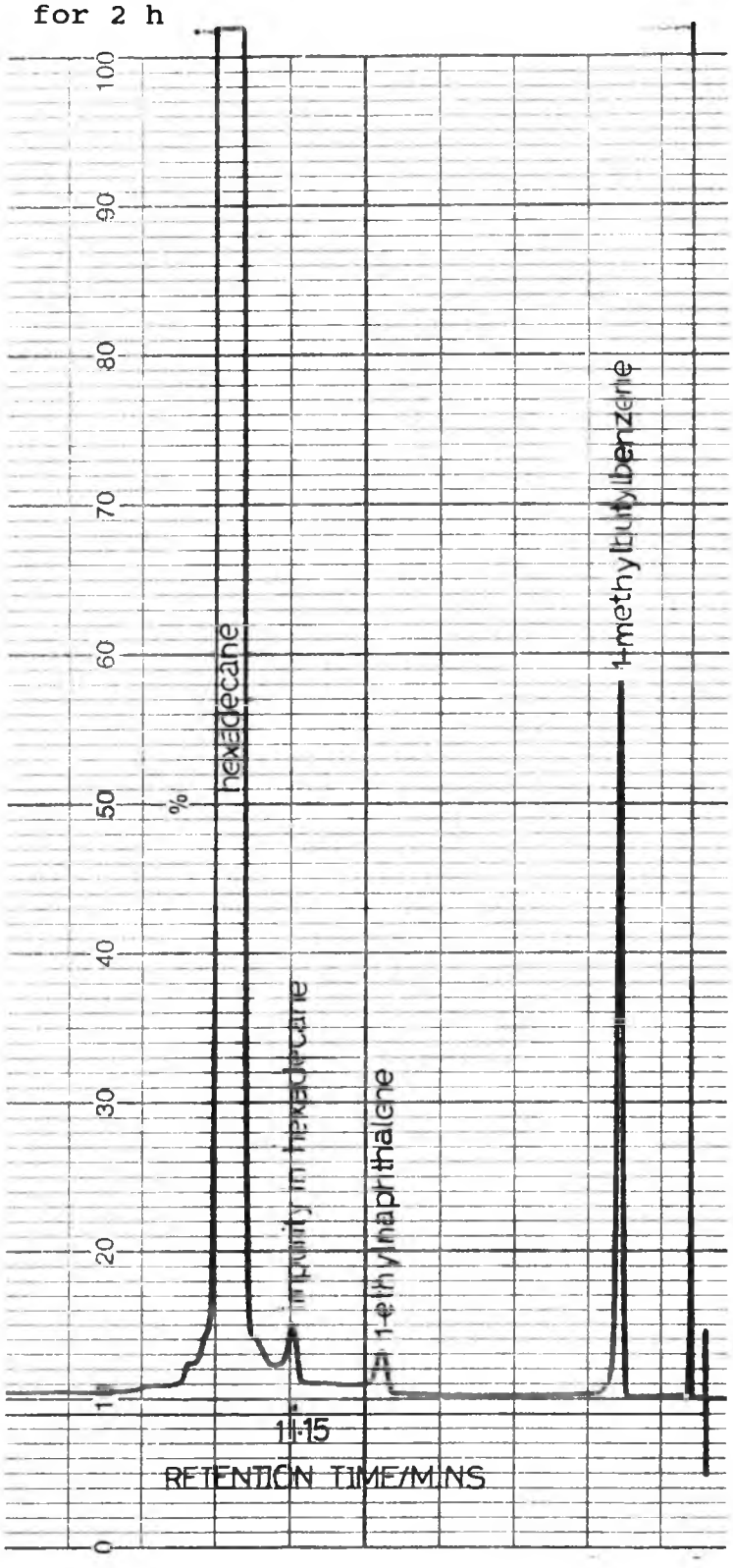

7.3.2 Measurement of the reactivity of 1-methylbutylbenzene by the competition technique

Attempts were made to determine the reactivity of 1-methylbutylbenzene relative to benzene by the competition technique. However, since no nitration products were detected from the reaction of 1-methylbutylbenzene (1.3 mol dm^{-3}) with nitrogen dioxide (0.16 mol dm^{-3}), it was not possible to estimate the relative reactivity of this compound (compare Fig. 7.5 and Fig. 7.6). Also, the amount of nitrobenzene formed could not be determined since this peak was masked by the 1-methylbutylbenzene peak in the g.l.c. chromatogram. Similarly, it was not possible to measure the relative heights of the 1-methylbutylbenzene and benzene signals since the benzene peak was masked by the cyclohexane peak. The peaks that were observed in the g.l.c. chromatogram (peaks at 6.05 min and 4.6 min in Fig. 7.5) were those due to the impurities present in the 1-methylbutylbenzene (Fig. 7.6).

Fig. 7.5: GLC chromatogram of 1-methylbutylbenzene (1.3 mol dm^{-3})/benzene (0.9 mol dm^{-3}) solution used in competition experiment

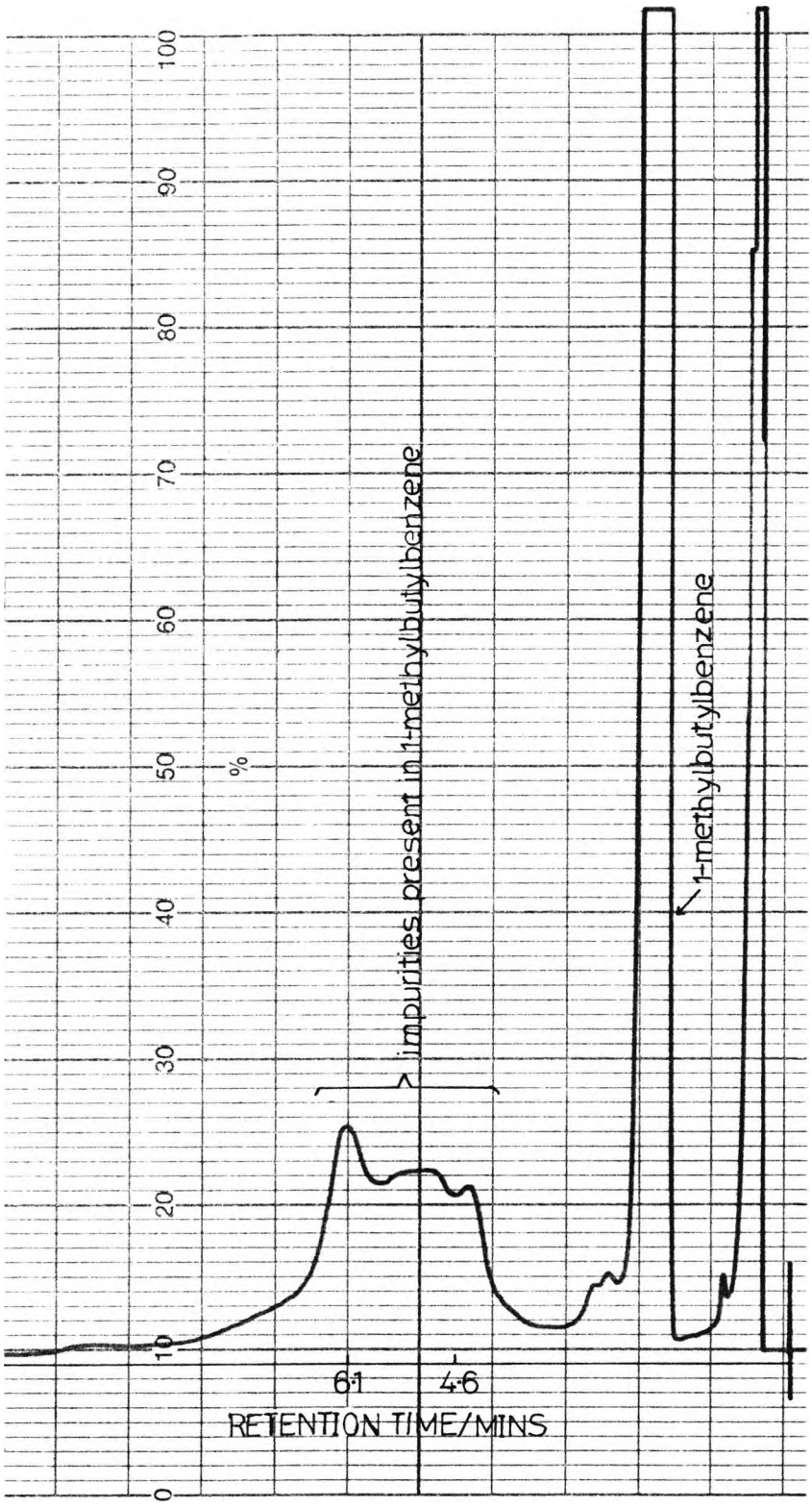

Fig. 7.6: GLC chromatogram of the products from the reaction of 1-methylbutylbenzene (1.3 mol dm^{-3}) and benzene (0.9 mol dm^{-3}) with nitrogen dioxide (0.16 mol dm^{-3}) in cyclohexane at 25°C for 164 h

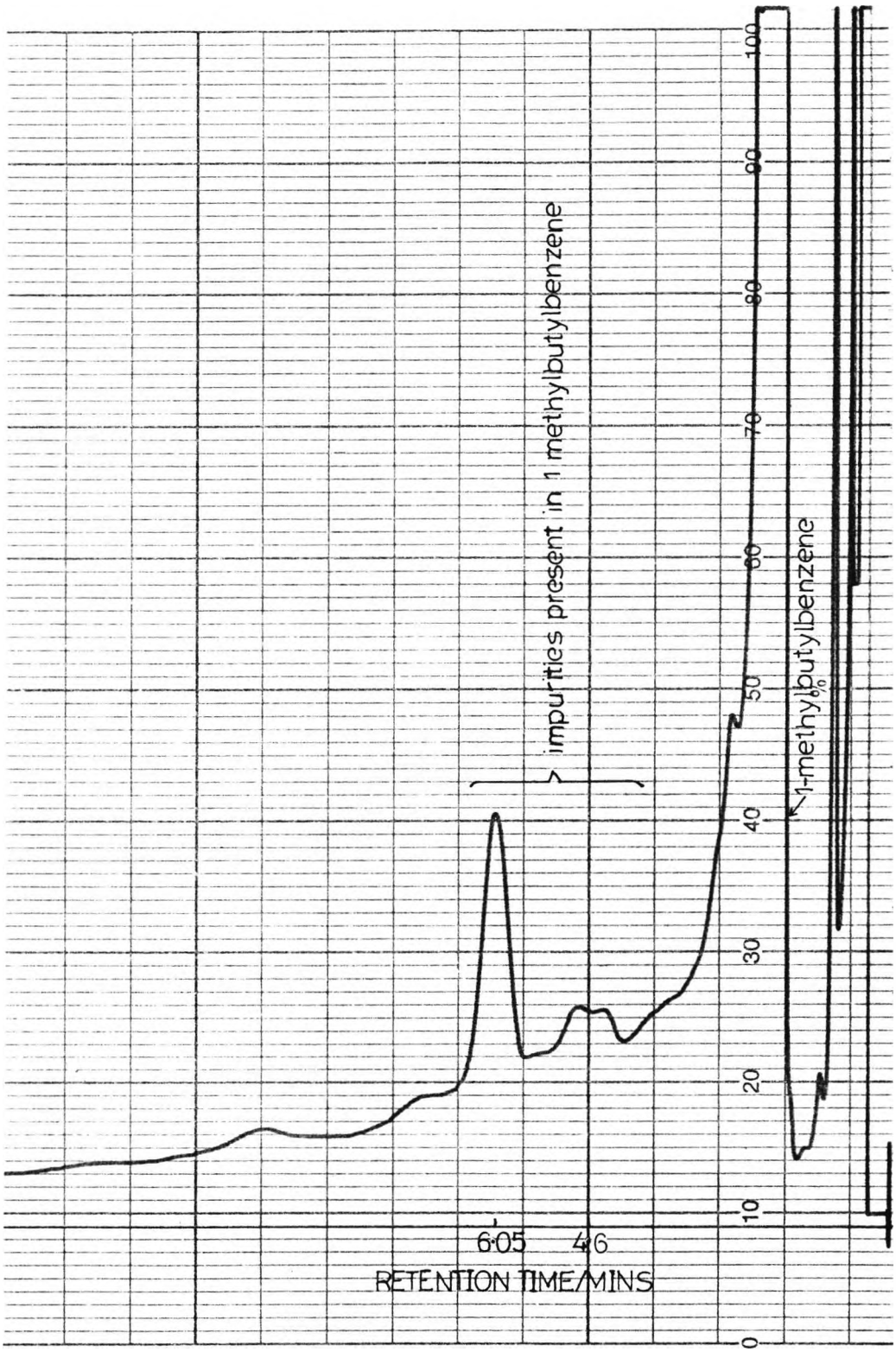

7.4 Discussion

The maximum extent of reaction of 1-methylbutylbenzene with nitrogen dioxide over a 2 h period was 12% at 25°C and this apparently increased to 28% at 150°C. Since no products were detected by g.l.c. the disappearance of 1-methylbutylbenzene could be accounted for by loss through evaporation as the nitrogen dioxide/N_2 gas mixture was bubbled through the substrate solution. Also, if the 12% reaction at 25°C is considered 'real', then we would expect a considerable increase in the rate of reaction at 150°C. Since no reaction envisaged is likely to have such a low activation energy as that implied then the loss, at least at 25°C, is likely to be due to evaporation.

It is possible that nitration products were formed in the reaction of 1-methylbutylbenzene with nitrogen dioxide at 150°C, but were either retained on the column or were masked in the g.l.c. chromatogram by the solvent peak, the impurities in the solvent (peaks at 11.1 min in Figs. 7.2, 7.3 and 7.4 and the peak at 14.7 min in Fig. 7.3) or the products from the reaction of the solvent with nitrogen dioxide (peak at 17.4 min in Fig. 7.3). It is unlikely that unstable nitration products were formed since no decomposition products were detected by g.l.c.

C H A P T E R 8

THE REACTIONS OF POLYSUBSTITUTED BISPHENOLS WITH NITROGEN DIOXIDE

8 The reactions of polysubstituted bisphenols with nitrogen dioxide

8.1 Introduction

The major reaction products are reported for bis(4-hydroxy-3,5-di-t-butylphenyl)methane (AN2) and 2,2-bis(4-hydroxy-3,5-di-t-butylphenyl)propane (IONOX 400). Kinetics of the initial reactions were found to be first-order in the aromatic when the nitrogen dioxide was in a large excess.

The sterically hindered phenols are important both in the lubricant and food industries (e.g. 2,4,6-tri-t-butyl- and 2,6-di-t-butyl-4-methylphenol and bis(4-hydroxy-3,5-di-t-butylphenyl)methane). The phenoxyl radicals are relatively stable and tend to inhibit autoxidation of hydrocarbons (Scheme 8.1) where ArOH is the phenol.

$$R^{\bullet} + O_2 \longrightarrow ROO^{\bullet}$$

$$ROO^{\bullet} + RH \longrightarrow ROOH + R^{\bullet}$$

$$2ROO^{\bullet} \longrightarrow \text{molecular products}$$

$$ROO^{\bullet} + ArOH \rightleftharpoons ROOH + ArO^{\bullet}$$

$$\left.\begin{matrix} ArO^{\bullet} + ROO^{\bullet} \\ 2ArO^{\bullet} \end{matrix}\right\} \longrightarrow \text{molecular products}$$

Scheme 8.1

Compounds with two rings have not previously been studied and provide a useful comparison with single ring substrates. The rates of reaction have been interpreted in terms of established mechanisms of reaction of phenol compounds with nitrogen dioxide.

8.2 Experimental

8.2.1 Kinetic Measurements

Kinetic studies were performed in cyclohexane at 25.4±0.1°C under conditions of a large excess of nitrogen dioxide using UV spectrophotometry. The reactions were carried out in 1 cm quartz cells fitted with silicone rubber septa, held in place with Quickfit screw-caps. Stock solutions of nitrogen dioxide and aromatic compound were prepared in cyclohexane and stored in 5 cm^3 volumetric flasks fitted with the same air-tight seals as the cells. Small quantities of stock solutions were transferred to the cells using a 0.5-, 1- or 10-μl syringe.

Samples of the solvent were thermostatted in the spectrophotometer for 15 min before nitrogen dioxide was added. The concentration of $NO_2^{\bullet}$ was measured using the gas-phase extinction coefficient of 150 $dm^3mol^{-1}cm^{-1}$ at 430 nm. The concentration of N_2O_4 was calculated using the equilibrium constant at the temperature of the experiment. The wavelength was then moved to a value suitable for the observation of the reaction and the aromatic compound was added to the solution. The cell was shaken and returned to the thermostatted cell compartment as quickly as possible for observation of the reaction.

8.2.2 Product Measurements

Product studies of the reactions of AN2 and IONOX 400 with nitrogen dioxide at high concentrations were carried out in order to identify the products formed in the kinetic experiments.

8.3 Results

8.3.1 The reaction of bis(4-hydroxy-3,5-di-t-butylphenyl) methane (AN2) with nitrogen dioxide

8.3.1.1 Product Measurements

Bis(4-hydroxy-3,5-di-t-butylphenyl)methane (0.1 mol dm^{-3}) in carbon tetrachloride (20 cm^3) was cooled to 0°C ⟶ -10°C in an ice/salt bath. A stock solution of nitrogen dioxide was made up in the same solvent and was thermostatted at 0°C ⟶ -10°C for 15 min. 1 cm^3 of this solution was diluted in a 1 cm quartz cell and the $NO_2^{\bullet}$ concentration was measured. A 1 cm^3 portion of the original stock solution (0.1 mol dm^{-3}) was then added to the AN2 solution and the reaction was left for 2 h at 0°C ⟶ -10°C. The excess nitrogen dioxide was then removed in a stream of nitrogen, and the solvent removed under high vacuum at room temperature to give a light yellow/green solid, identified as

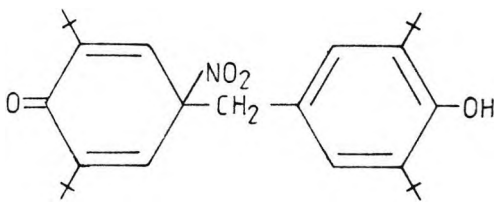

(I)

This was the only product formed in the reaction.

I.R.(KBr disc) : ν , cm^{-1}, 1365, 1550, 1664, 3620.
^1H NMR ($CDCl_3$) : δ, ppm : 1.23 (s, ^{t}Bu-dienone ring); 1.41 (s, ^{t}Bu-phenol ring); 3.31 (s, 2H, CH_2); 5.08 (s, 1H, OH); 6.77 (s, 4H, H-3,5).

The ^1H n.m.r. of the above dienone was studied at low temperatures in an attempt to resolve the aromatic signals of the dienone and phenol rings. AN2 (0.1 mol dm^{-3}) and nitrogen dioxide (0.12 mol dm^{-3}) were mixed in carbon tetrachloride at -5 ⟶ -8°C, a sample was removed after 45 min and the ^1H n.m.r. spectrum was recorded at -10°C. The spectrum showed

the presence of two aromatic signals, δ, ppm. : 1.24(s, ^{t}Bu); 1.42 (s, ^{t}Bu); 3.31 (s, 2H, CH_2); 5.18 (s, 1H, OH); 6.80(s, 2H, H-3,5); 6.82(s, 2H, H-3,5).

A solution of the dienone I (6.4×10^{-5} mol dm^{-3}) was made up in a 1 cm quartz cell and the UV spectrum recorded for comparison with the spectra obtained during the kinetic experiments.

8.3.1.2 **Kinetic Measurements**

AN2 reacts rapidly with nitrogen dioxide in cyclohexane at 25.4°C giving mainly the corresponding dienone(I):

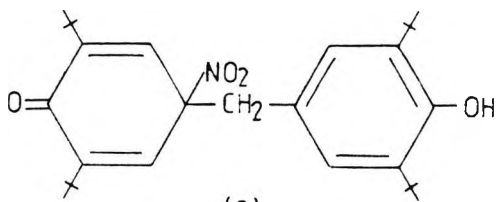

(I)

Kinetic studies were performed in cyclohexane under conditions of a large excess of nitrogen dioxide. The concentration of AN2 was 3.2×10^{-6} mol dm^{-3} and $[N_2O_4]_t$ was varied over the range 4.22×10^{-5} - 1.05×10^{-4} mol dm^{-3}. Under these conditions, the reaction was demonstrated to be first-order in AN2. The reaction was monitored at 260 nm. The results from a typical run are shown in Table 8.1 and Fig. 8.1. The change in absorbance during the kinetic runs and the change in the UV spectrum of the phenol on mixing with nitrogen dioxide are consistent with the formation of the dienone (I) as the major product (compare Figs. 8.2 and 8.3).

Table 8.2 shows the variation of the first-order rate coefficient with nitrogen dioxide concentration. It is apparent from these data (see Figs. 8.4 and 8.5) that the reaction rate obeys equation 8.1, which is kinetically equivalent to equation 8.2

$$\frac{-d[ArOH]}{dt} = k_2[N_2O_4]\ [ArOH] \qquad (8.1)$$

$$\frac{-d[ArOH]}{dt} = k_3[NO_2^{\cdot}]^2[ArOH] \qquad (8.2)$$

Table 8.1: Change in absorbance with time for a typical reaction of AN2 with nitrogen dioxide in cyclohexane at 25.4°C

t/s	$A_\infty - A_t$	$-\log_{10}(A_\infty - A_t)$
30	0.008	2.09
60	0.006	2.22
90	0.006	2.22
120	0.005	2.30
150	0.004	2.40
180	0.003	2.52
210	0.003	2.52
240	0.002	2.70
270	0.002	2.70
300	0.002	2.70
330	0.002	2.70
360	0.001	3.00

[ArOH] = 3.2×10^{-6} mol dm^{-3}; $[N_2O_4]_t = 5.76 \times 10^{-5}$ mol dm^{-3}

$k_{obs} = 5.53 \times 10^{-2} s^{-1}$

reaction monitored at 260 nm

Fig. 8.1: Typical first-order plot of $\log_{10}(A_\infty - A_t)$ against time for the reaction of AN2 with nitrogen dioxide in cyclohexane at 25.4°C

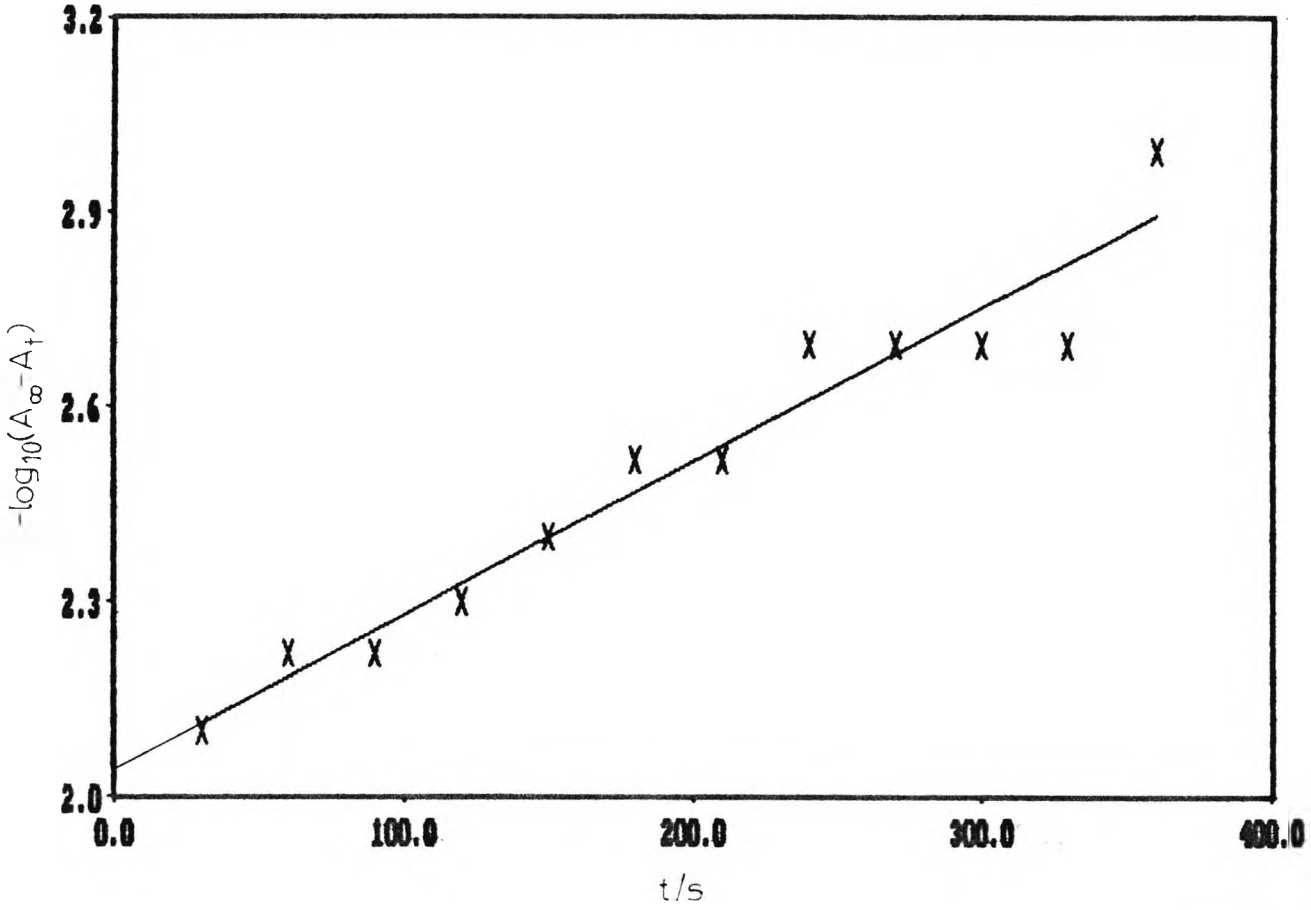

Fig. 8.2: Change in the UV spectrum of AN2 (—; 6.4 x 10^{-5} mol dm^{-3}) on mixing with nitrogen dioxide (1.51 x 10^{-4} mol dm^{-3}) in cyclohexane at 25.4°C. The spectra were recorded at 45 s intervals.

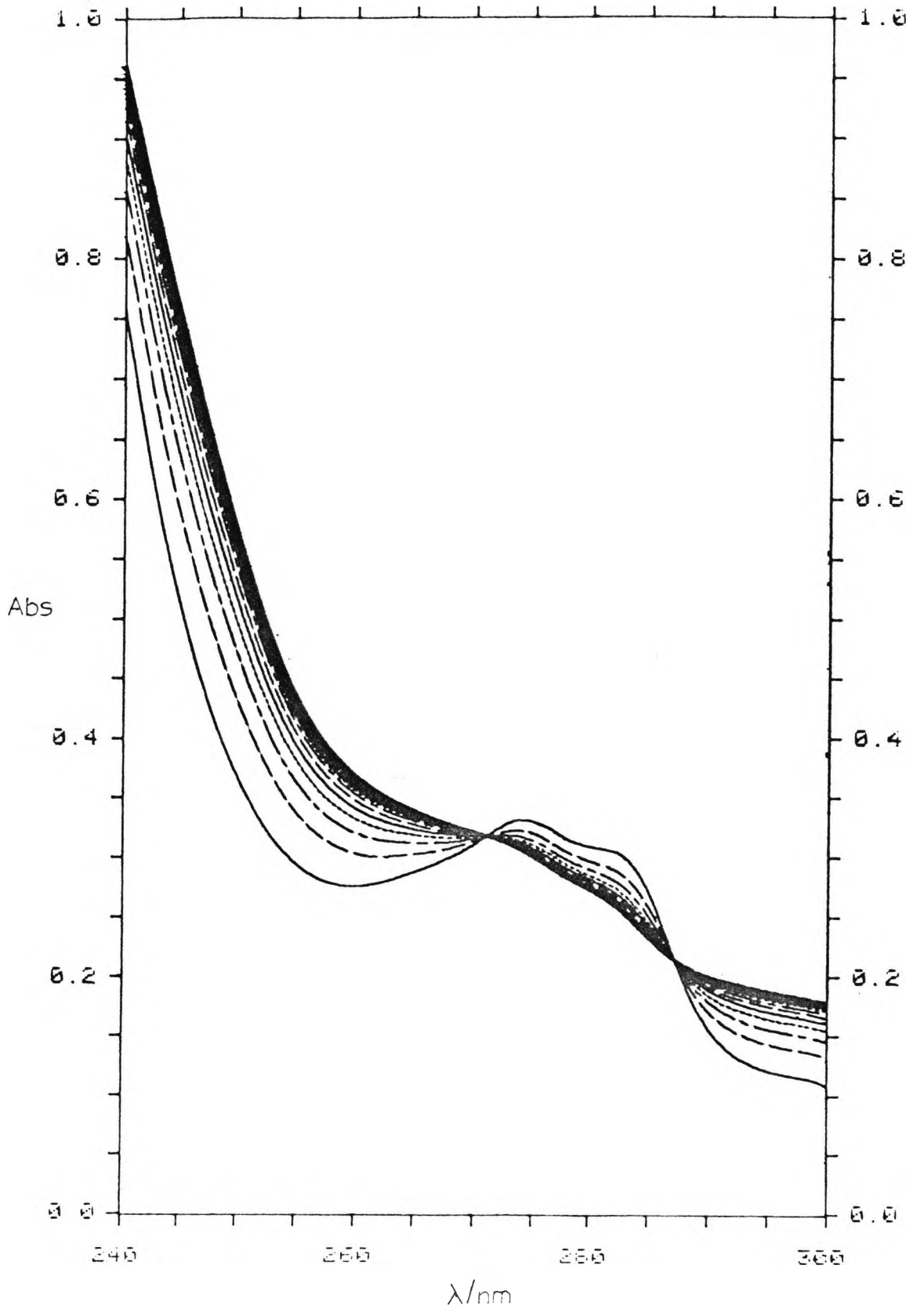

Fig. 8.3: UV spectra of AN2 (- - -; 6.4 x 10^{-5} mol dm^{-3}) and the dienone (6.4 x 10^{-5} mol dm^{-3}) in cyclohexane

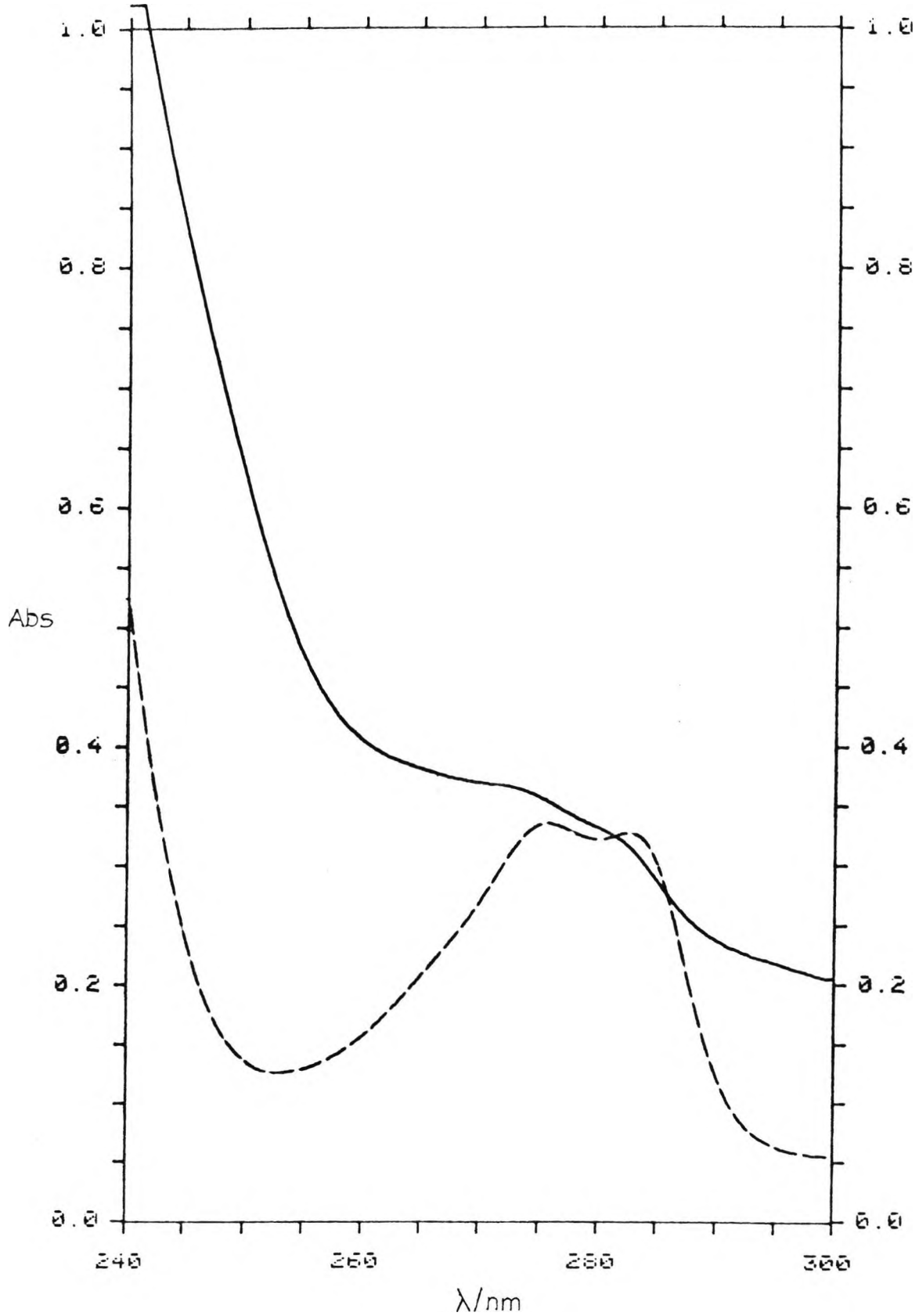

Table 8.2: Variation of k_{obs} with $[N_2O_4]_t$ for the reaction of AN2 with nitrogen dioxide in cyclohexane at 25.4°C

$10^2 k_{obs}/s^{-1}$	$10^4[N_2O_4]_t$/mol dm^{-3}	$10^4[N_2O_4]$/mol dm^{-3}	$10^4[NO_2^{\cdot}]$/mol dm^{-3}
0.274	0.422	0.155	0.533
0.500	0.497	0.197	0.600
0.553	0.576	0.243	0.667
0.873	0.661	0.294	0.733
1.000	0.750	0.350	0.800
1.138	0.943	0.476	0.933
1.184	1.050	0.546	1.000

Fig. 8.4: Plot of k_{obs} against $[N_2O_4]$ for the reaction of AN2 with nitrogen dioxide in cyclohexane at 25.4°C

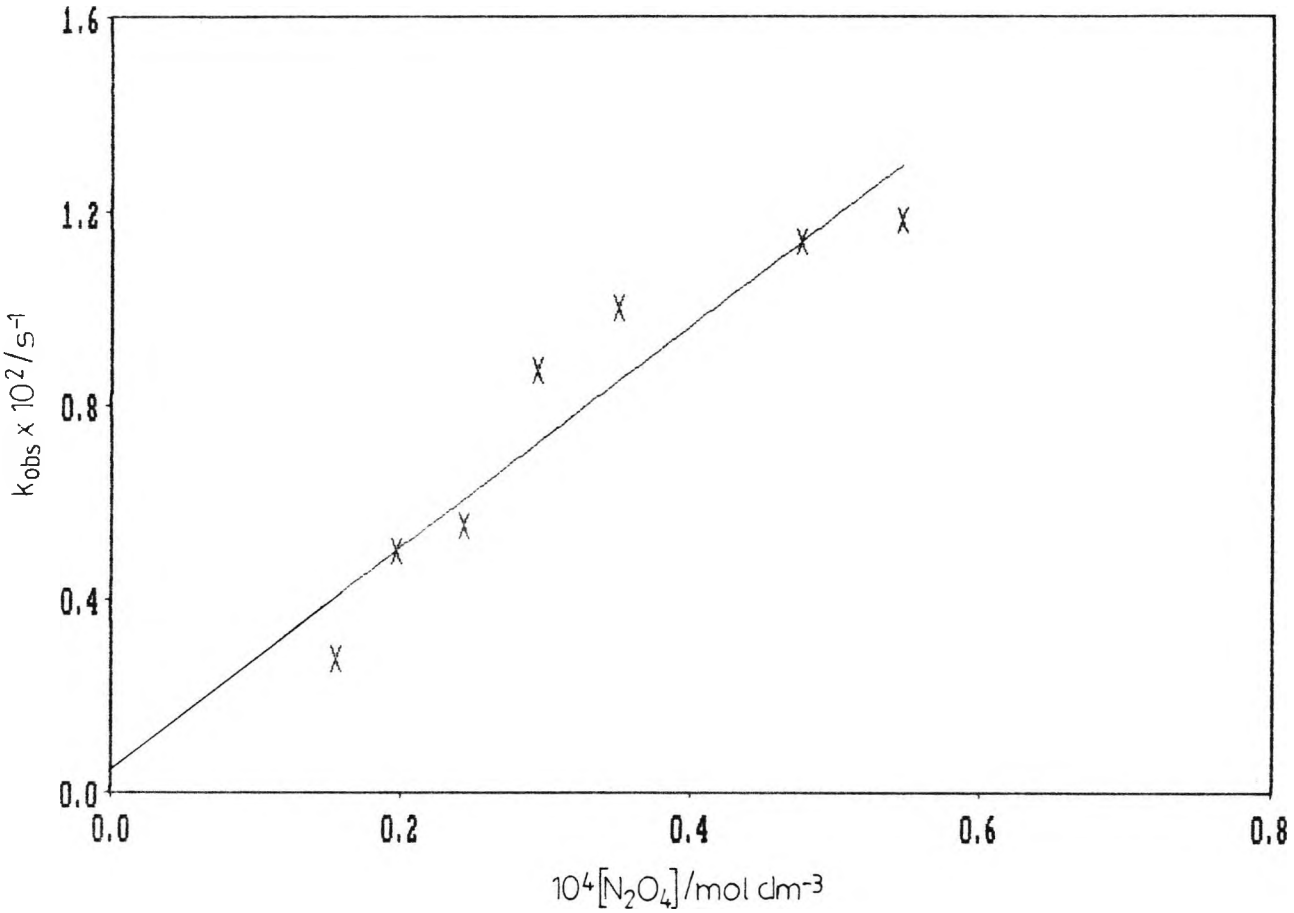

Fig. 8.5: Plot of k_{obs} against $[NO_2^{\bullet}]$ for the reaction of AN2 with nitrogen dioxide in cyclohexane at 25.4°C

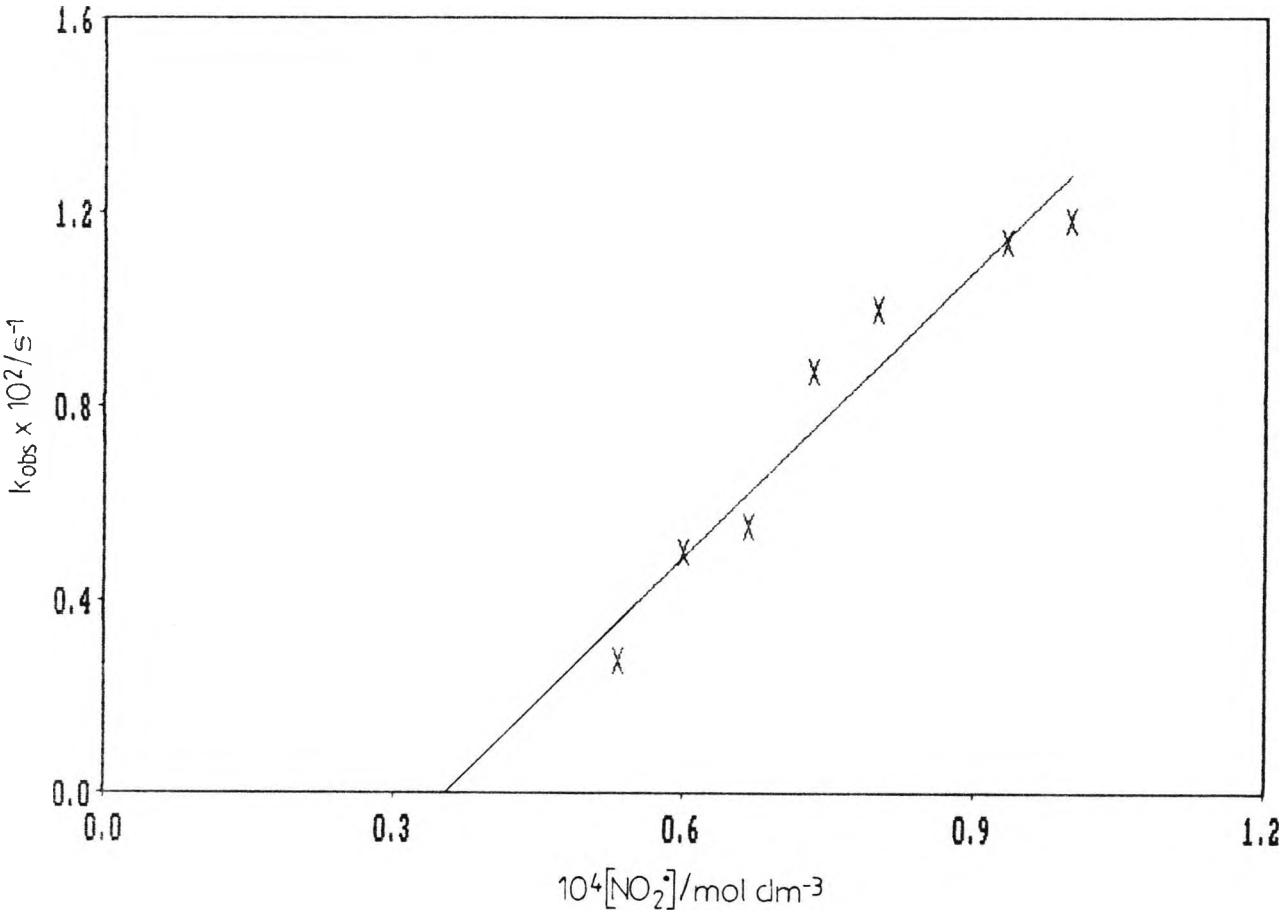

8.3.2 **The reaction of 2,2-bis(4-hydroxy-3,5-di-t-butylphenyl)propane (IONOX 400) with nitrogen dioxide**

8.3.2.1 **Product Measurements**

2,2-Bis(4-hydroxy-3,5-di-t-butylphenyl)propane (0.1 mol dm^{-3}) in carbon tetrachloride (20 cm^3) was cooled to 0°C ⟶ -10°C in an ice/salt bath. A stock solution of nitrogen dioxide was made up in the same solvent and was thermostatted at 0°C ⟶ -10°C for 15 min. 1 cm^3 of this solution was diluted in a 1 cm quartz cell and the NO_2 concentration was measured. A 1.4 cm^3 portion of the original stock solution (0.1 mol dm^{-3}) was then added to the IONOX 400 solution and the reaction was left for 2 h at 0°C ⟶ -10°C. The excess nitrogen dioxide was then removed in a stream of nitrogen, and the solvent removed under high vacuum at room temperature to give a yellow solid, identified as a mixture of

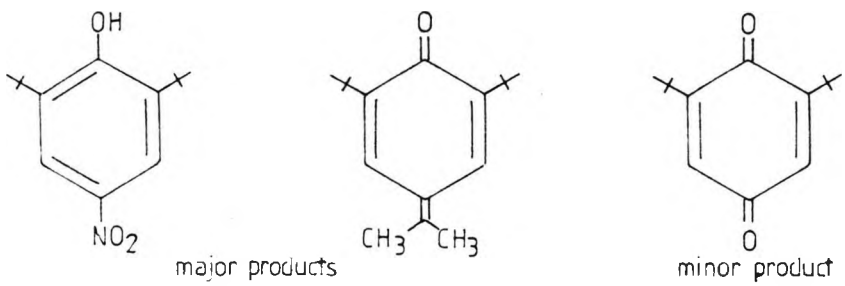

I.R.(KBr disc): ν, cm^{-1}, 1339, 1522, 1787, 3623.

^1H NMR(CCl_4) : δ, ppm:

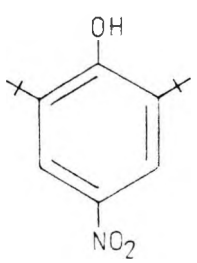

1.49 δ (s, ^tBu); 5.85 δ (s, 1H, OH); 8.03 δ (s, 2H, H-3,5)

This was assigned by comparison with an authentic sample.

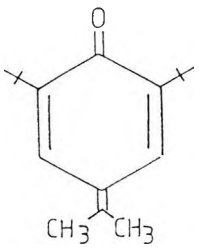

1.28 δ (s, ^{t}Bu); 2.19 δ (s, 6H, 1 x 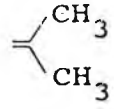

7.23 (s, 2H, H-3,5)

This is a tentative assignment.

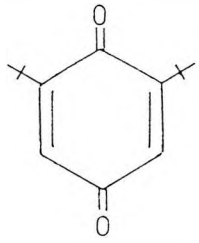

1.44 δ (s, ^{t}Bu); 7.15 δ (s, H-3,5)

This was assigned by comparison with an authentic sample of 2,6-dimethylbenzoquinone.

A solution of 2,6-di-t-butyl-4-nitrophenol (1 x 10^{-5} mol dm^{-3}) was made up in a 1 cm quartz cell and the UV spectrum recorded for comparison with the spectra obtained during the kinetic experiments.

8.3.2.2 **Kinetic Measurements**

IONOX 400 reacts rapidly with nitrogen dioxide in cyclohexane at 25.4°C giving mainly 2,6-di-t-butyl-4-nitrophenol.

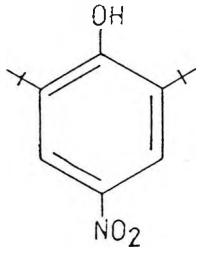

Kinetic studies were performed in cyclohexane under conditions of a large excess of nitrogen dioxide. The concentration of IONOX 400 was 1 x 10^{-5} mol dm^{-3} and $[N_2O_4]_t$ was varied over the range 7.50 x 10^{-5} - 2.84 x 10^{-4} mol dm^{-3}. The reaction was monitored at 270 nm. The results from a typical run are shown below:

[IONOX 400] = 1 x 10^{-5} mol dm^{-3}

$[N_2O_4]_{t,o}$ = 8.44 x 10^{-4} mol dm^{-3}

The change in concentration of IONOX 400 was monitored over eight half-lives (Table 8.3). The rate of nitration was shown to be first order in IONOX 400 by a linear plot of $\log_{10}$[IONOX 400] against time (Fig. 8.6). From the slope of this graph, the observed first-order rate coefficient, k_{obs} = $1.6 \times 10^{-3} s^{-1}$.

The change in absorbance during the kinetic runs and the change in the UV spectrum of the phenol on mixing with nitrogen dioxide are consistent with the formation of two equivalent amounts of 2,6-di-t-butyl-4-nitrophenol as the major product (compare Figs. 8.7 and 8.8).

Table 8.4 shows the variation of the first-order rate coefficient with nitrogen dioxide concentration. It is apparent from these data (see Figs. 8.9 and 8.10) that the reaction obeys equation 8.3.

$$\frac{-d[ArOH]}{dt} = k_1[NO_2^{\cdot}][ArOH] \qquad (8.3)$$

Table 8.3: Change in absorbance with time for a typical reaction of IONOX 400 with nitrogen dioxide in cyclohexane at 25.4°C

t/s	$A_\infty - A_t$	$-\log_{10}(A_\infty - A_t)$
60	0.032	1.49
90	0.029	1.54
120	0.026	1.59
150	0.024	1.62
180	0.022	1.66
210	0.020	1.70
240	0.019	1.72
270	0.018	1.74
300	0.017	1.77
330	0.016	1.80
360	0.015	1.82
390	0.014	1.85
450	0.013	1.89
510	0.012	1.92
540	0.011	1.96
720	0.009	2.05
780	0.008	2.10
840	0.008	2.10
900	0.007	2.15
1080	0.005	2.30
1320	0.004	2.40
1440	0.003	2.52
2100	0.001	3.00

$[ArOH] = 1 \times 10^{-5}$ mol dm^{-3}, $[N_2O_4]_t = 8.44 \times 10^{-5}$ mol dm^{-3}

$k_{obs} = 1.60 \times 10^{-3}\ s^{-1}$

reaction monitored at 270 nm

Fig. 8.6: Typical first-order plot of $\log_{10}(A_\infty - A_t)$ against time for the reaction of IONOX 400 with nitrogen dioxide in cyclohexane at 25.4°C

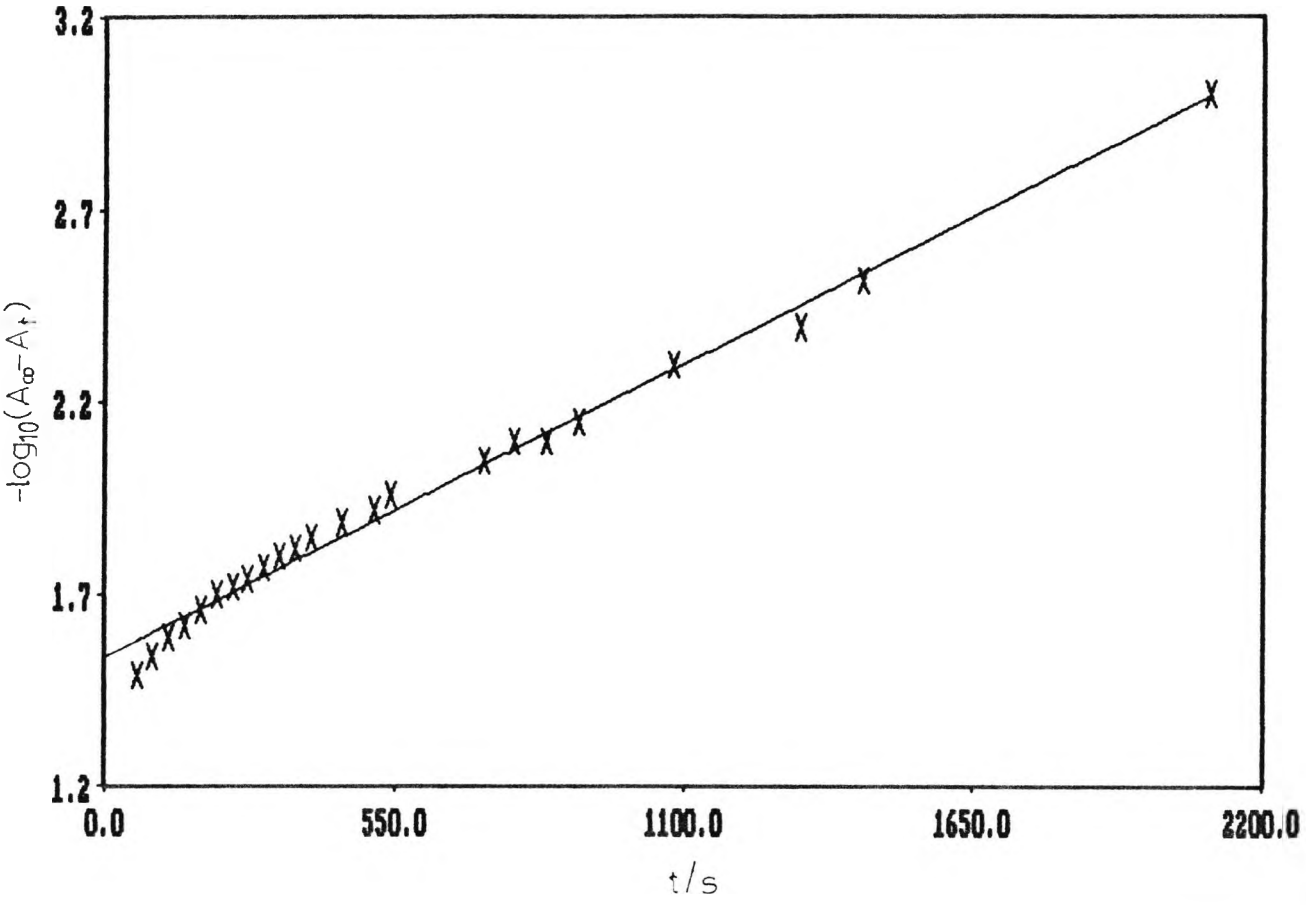

Fig. 8.7: Change in the UV spectrum of IONOX 400 (——— ; 1 x 10^{-5} mol dm^{-3}) on mixing with nitrogen dioxide 5.76 x 10^{-5} mol dm^{-3}) in cyclohexane at 25.4°C. The spectra were recorded at 1 min intervals.

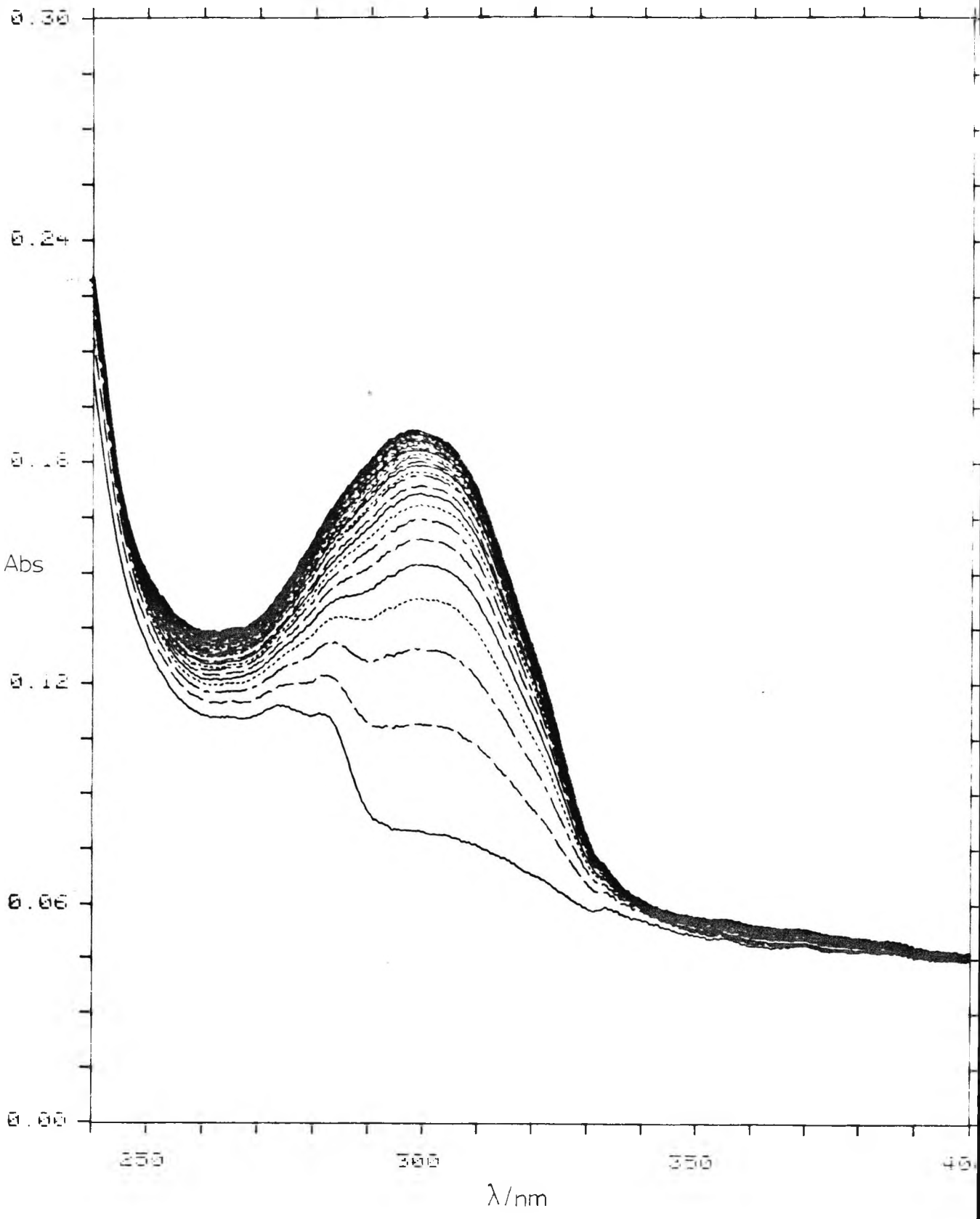

Fig. 8.8: UV spectrum of 2,6-di-t-butyl-4-nitrophenol (1 x 10^{-5} mol dm^{-3}) in cyclohexane

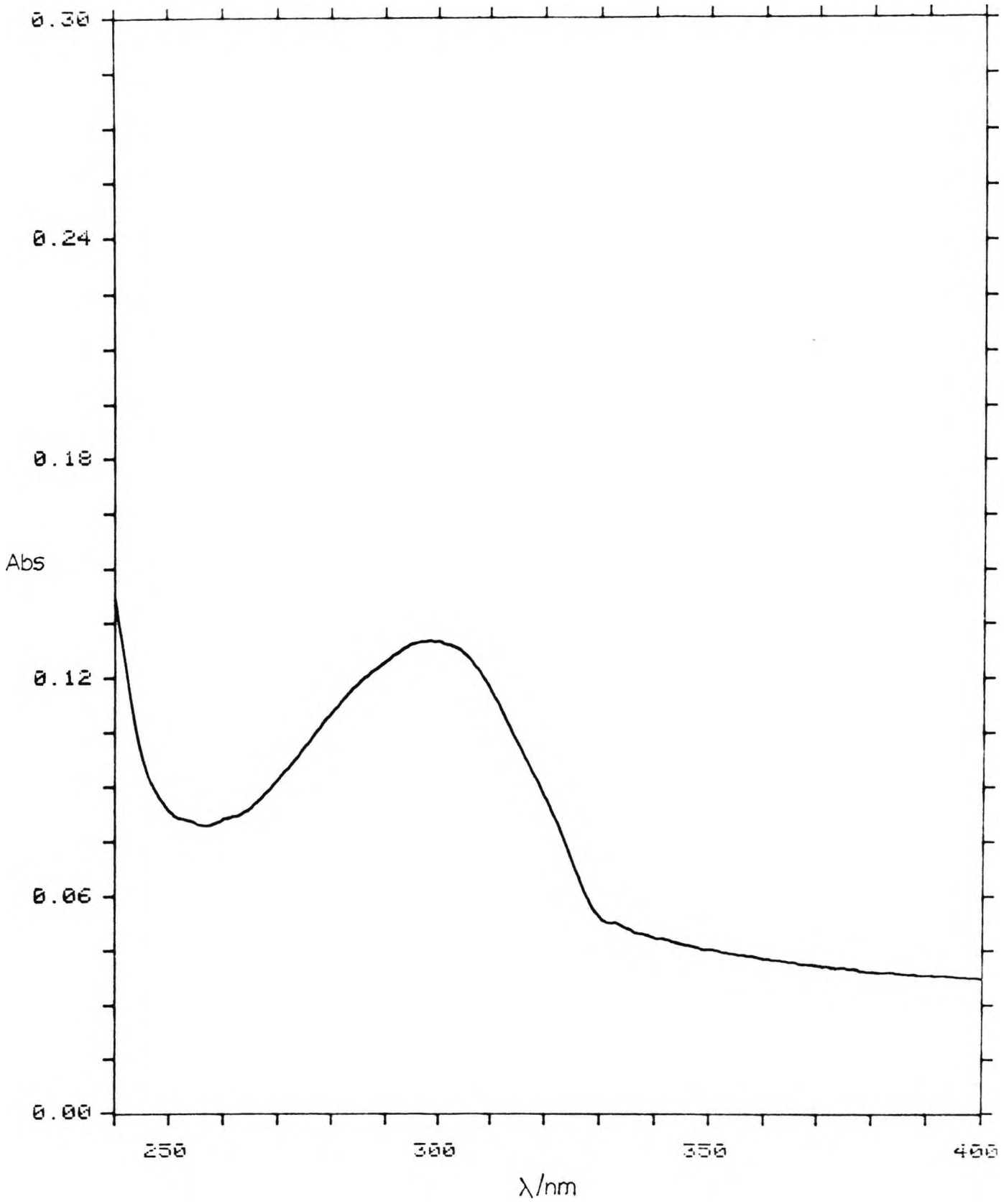

Table 8.4: Variation of k_{obs} with $[N_2O_4]_t$ for the reaction of IONOX 400 with nitrogen dioxide in cyclohexane at 25.4°C

$10^3 k_{obs}/s^{-1}$	$10^4[N_2O_4]_t$/mol dm^{-3}	$10^4[N_2O_4]$/mol dm^{-3}	$10^4[NO_2^{\cdot}]$/mol dm^{-3}
1.69	0.750	0.350	0.800
1.60	0.844	0.410	0.867
2.34	0.943	0.476	0.933
1.90	1.100	0.583	1.030
2.14	1.210	0.661	1.100
2.53	1.510	0.877	1.270
2.50	1.770	1.070	1.400
3.04	2.200	1.400	1.600
3.96	2.350	1.520	1.670
3.92	2.840	1.900	1.870

Fig. 8.9: Plot of k_{obs} against $[NO_2^{\bullet}]$ for the reaction of IONOX 400 with nitrogen dioxide in cyclohexane at 25.4°C

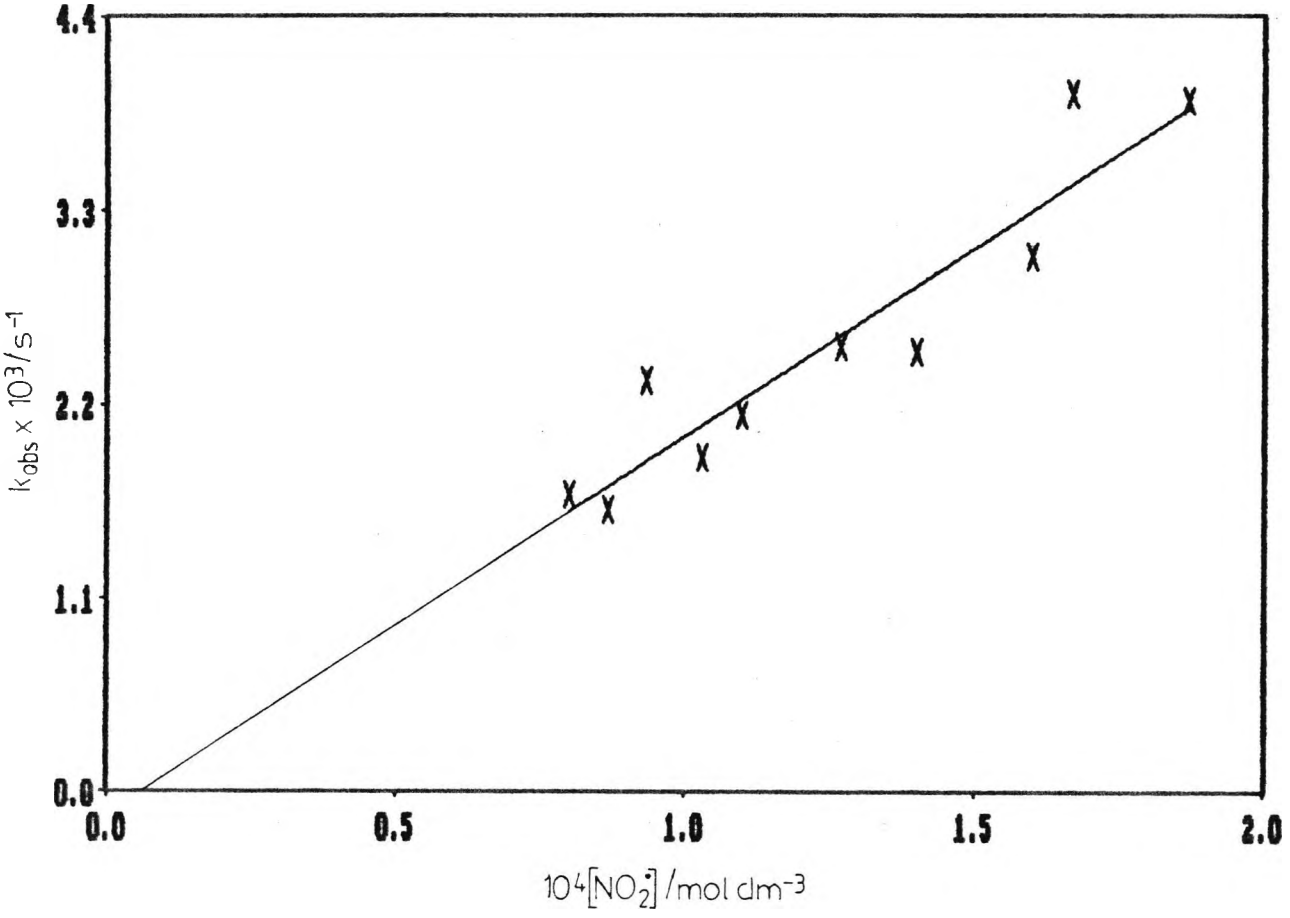

Fig. 8.10: Plot of k_{obs} against $[N_2O_4]$ for the reaction of IONOX 400 with nitrogen dioxide in cyclohexane at 25.4°C

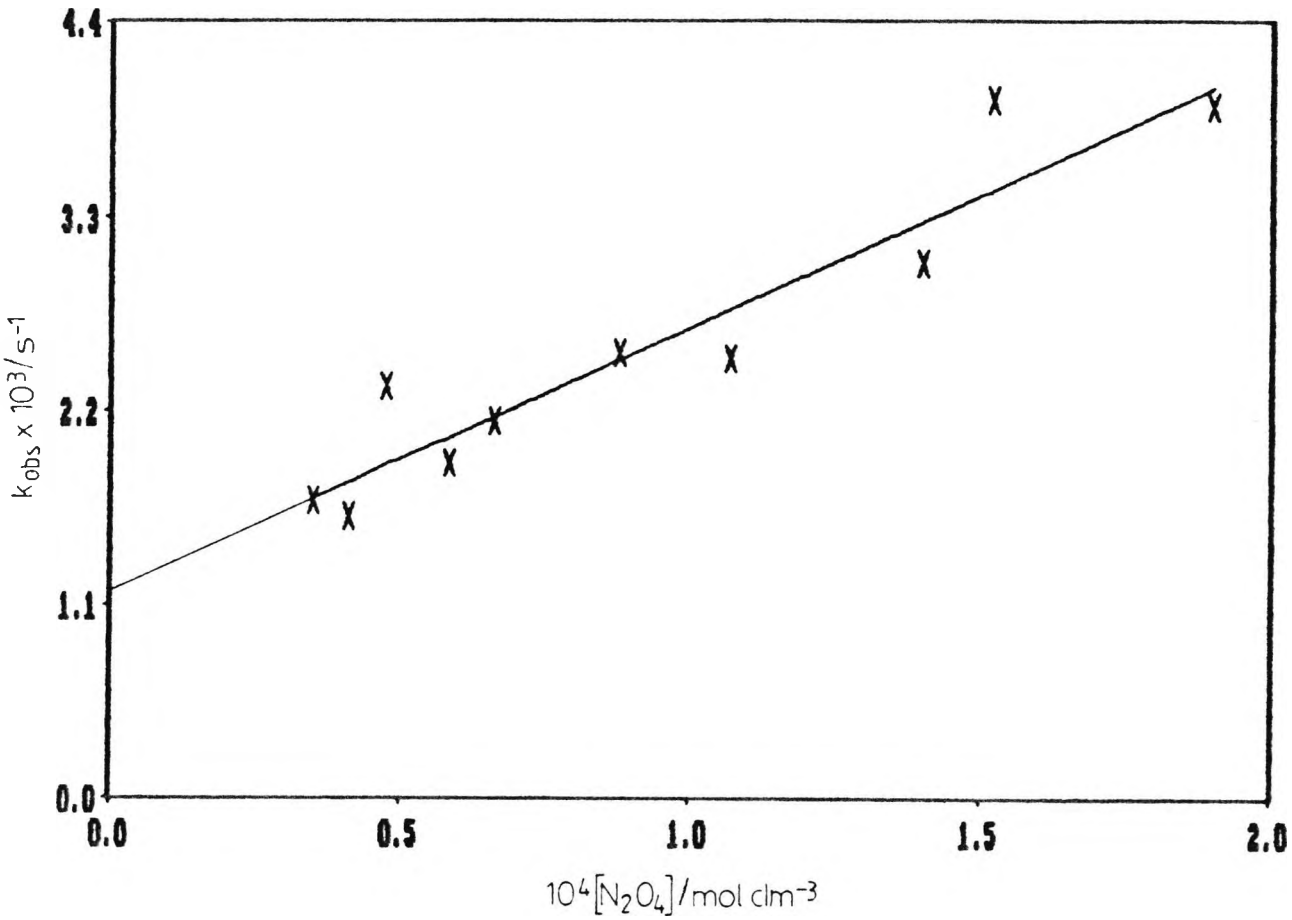

8.4 Discussion

The reactions of 2,4,6-trialkylphenols with nitrogen dioxide have been studied previously in great detail.[69] The reactions of 2,6-di-t-butyl-4-methylphenol and 2,4,6-tri-t-butylphenol,[69] in particular, with nitrogen dioxide serve as useful models for the present study.

2,6-di-t-butyl-4-methylphenol reacts rapidly with nitrogen dioxide in carbon tetrachloride at 25°C to give the dienone (II) as the major product.[69]

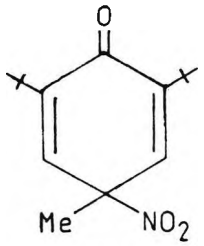

(II)

The dienone is relatively stable at room temperature but decomposes on warming in carbon tetrachloride (2h at 60°C), giving predominantly the starting phenol and some adduct (III). The adduct (III) is also formed along with (IV) when the dienone is reacted further with nitrogen dioxide in carbon tetrachloride at 25°C.

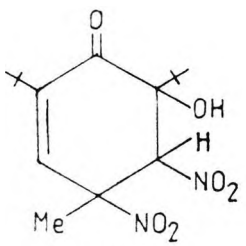

(III)

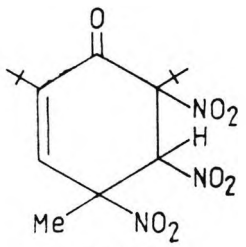

(IV)

The kinetics of the initial reaction giving rise to the dienone were studied in cyclohexane over the temperature range 20.5 - 63°C. The data obtained indicated that the reaction rate obeyed equation 8.1 which is kinetically equivalent to 8.2.

$$\frac{-d[ArOH]}{dt} = k_3[NO_2^{\cdot}]^2[ArOH] \qquad (8.1)$$

$$\frac{-d[ArOH]}{dt} = k_2[N_2O_4][ArOH] \qquad (8.2)$$

The two interpretations of the kinetic results gave rise to two sets of Arrhenius parameters, and the interpretation shown in equation 8.1 gave rise to a negative activation energy (-34 kJ mol^{-1}). The observed order of the reaction in $NO_2^{\cdot}$ was explained by the mechanism in Scheme 8.2, provided that $[HNO_2]$ remained constant.

$$ArOH + NO_2^{\cdot} \underset{k_{-a}}{\overset{k_a}{\rightleftharpoons}} ArO^{\cdot} + HNO_2$$

$$ArO^{\cdot} + NO_2^{\cdot} \underset{k_{-i}}{\overset{k_i}{\rightleftharpoons}} I$$

$$I \xrightarrow{k_r} \text{products}$$

Scheme 8.2

The alternative mechanism for the reaction involved attack of N_2O_4 on the phenol. This route did not explain, however, how the reaction with phenol became first-order in $NO_2^{\cdot}$ at high concentrations of nitrogen dioxide where there was proportionally less $NO_2^{\cdot}$ present. So for the mechanism to be consistent with the results obtained during the study of other phenols, reaction with $NO_2^{\cdot}$ as the reactive species was considered more likely.

Studies of 2,4,6-trimethylphenol and p-methoxyphenol led to the identification of I as the corresponding 6-nitrocyclohexa-2,4-dienone, e.g.

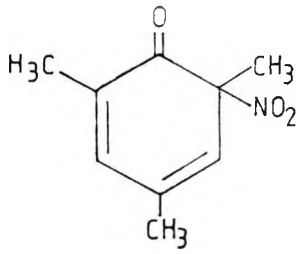

The reaction scheme is more complicated than that shown in Scheme 8.2 as some 2,5-dienone is always formed directly from ArO$^{\bullet}$.

2,4,6-tri-t-butylphenol also reacts rapidly with nitrogen dioxide in carbon tetrachloride at 25°C giving a good yield of the corresponding dienone (V).[69]

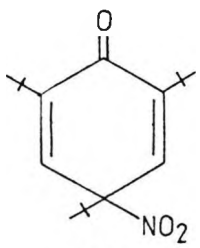

(V)

The dienone is unstable and decomposes in carbon tetrachloride to give a mixture of products, (VI) and (VII).

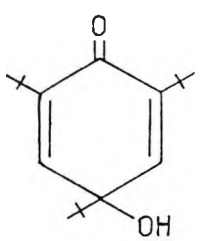

(VI)

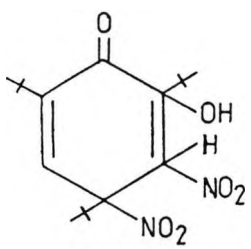

(VII)

The adduct (VII) is also formed when the dienone is reacted further with nitrogen dioxide.

The order in $NO_2^{\bullet}$ of the reaction was again accommodated in terms of Scheme 8.2. At low concentrations of nitrogen dioxide, both the pre-equilibria lay to the left-hand

side and below 6 x 10^{-4}mol dm^{-3} N_2O_4, the third step was rate-limiting, the reaction being second-order in $NO_2^{\bullet}$. Above 2.2 x 10^{-3} mol dm^{-3}, the equilibria lay to the right-hand side. The intermediate I was then formed rapidly in bulk and the rate of reaction was governed by the rate of rearrangement of I, the reaction becoming zeroth-order under these conditions.

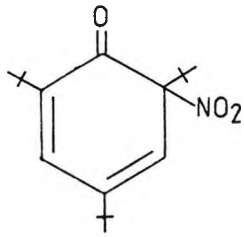

intermediate I

The zeroth-order reaction rate here was identical to that of reaction of the tri-t-butylphenoxy radical with $NO_2^{\bullet}$ over a much wider range of nitrogen dioxide concentrations.

The reaction of AN2 with nitrogen dioxide appears to be analogous with the reaction of 2,6-di-t-butyl-4-methylphenol with nitrogen dioxide. The formation of the dienone as the major product and the second-order dependence of rate in $[NO_2^{\bullet}]$ can be explained in terms of Scheme 8.3 and are consistent with the mechanism shown in Scheme 8.2

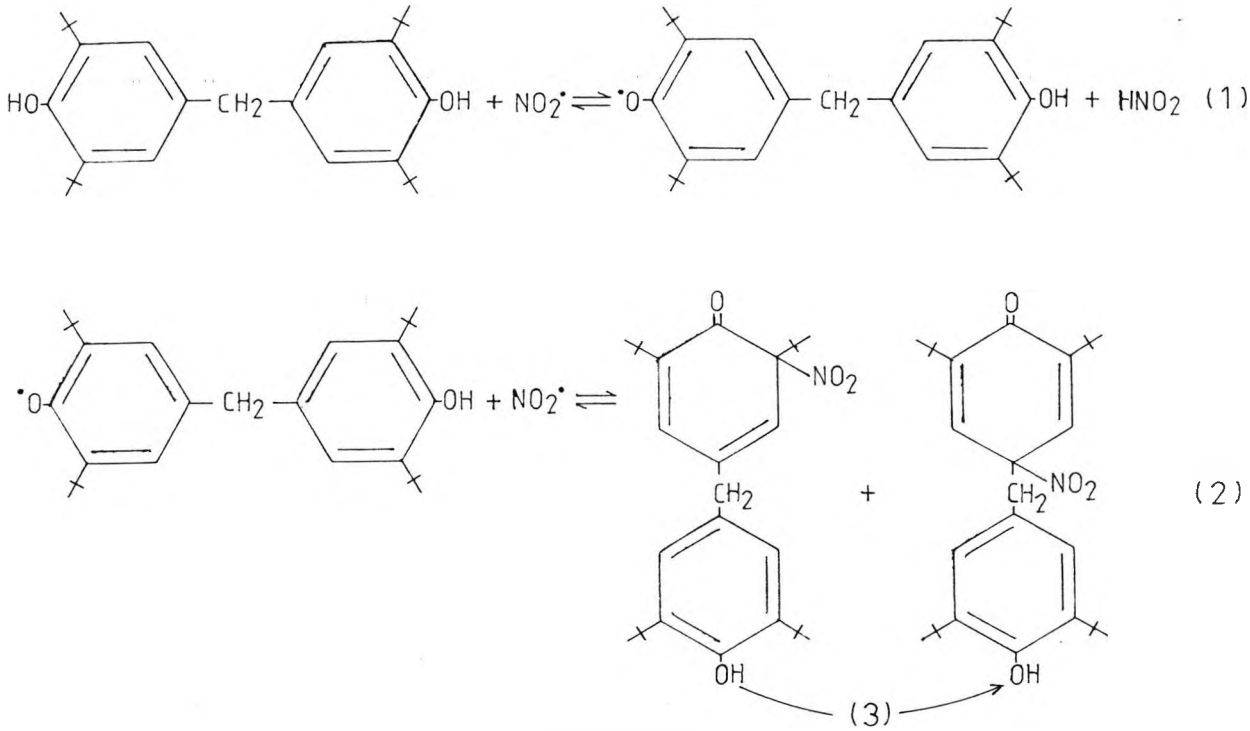

Scheme 8.3

On this interpretation, over the nitrogen dioxide concentration range studied, a step subsequent to step (1) is rate-limiting and this leads to a kinetic dependence that is second-order in $NO_2^{\bullet}$. The kinetic and spectral data reported in this thesis, however, do not rule out stage 2 being rate-limiting in this case. The fact that the reaction stops after mono-nitration is very likely to be due to the orientation of the cyclohexadiene rings of the dienone, which sterically hinders attack of $NO_2^{\bullet}$ at the p-position of the second ring. This is supported by models of the mono- and di-nitro products.

The reaction of IONOX 400 with nitrogen dioxide is first-order in $NO_2^{\bullet}$. This can be explained by step 1 in Scheme 8.2 becoming rate-limiting or to a separate bimolecular reaction between this substrate and $NO_2^{\bullet}$.

If step 1 of Scheme 8.2 becomes rate-limiting then $k_i[NO_2^{\bullet}]$ has become > $k_{-a}[HNO_2]$ or a new reaction between ArO$^{\bullet}$ and $NO_2^{\bullet}$ or N_2O_4 is occurring. It is not immediately apparent why the substitution of the two methyl groups on the central methylene which is the difference between AN2 and IONOX 400

should have this effect.

It is however perhaps possible that the increased stability of the tertiary radical (X) over (Y) is involved.



(X) (Y)

This could perhaps lead to a direct synchronous homolytic displacement of (X) by $NO_2^{\bullet}$ in IONOX 400

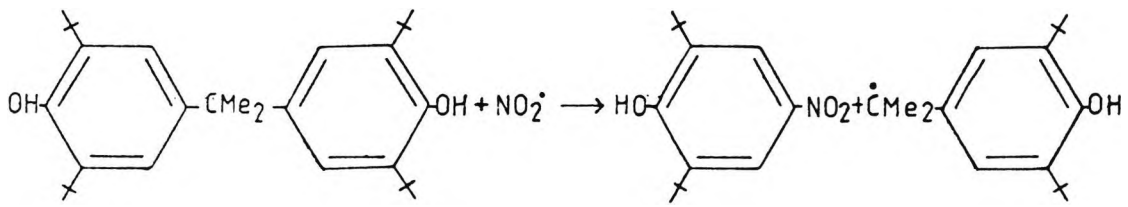

Scheme 8.4

or a rapid synchronous displacement of (X) by $NO_2^{\bullet}$ in the second stage of reaction.

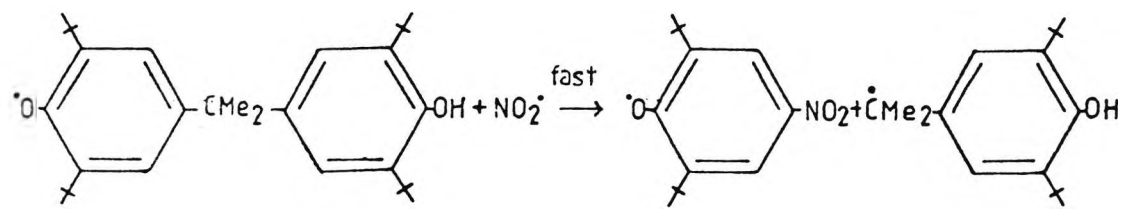

Scheme 8.5

The change in the UV spectrum (Fig. 8.7), where the concentration of 2,6-di-t-butyl-4-nitrophenol (1.7×10^{-5} mol dm^{-3}) is almost twice that of the starting material IONOX 400 (1×10^{-5} mol dm^{-3}), suggests formation of the nitro product from both rings and hence that (X) is also converted into the nitro product. A possible Scheme is

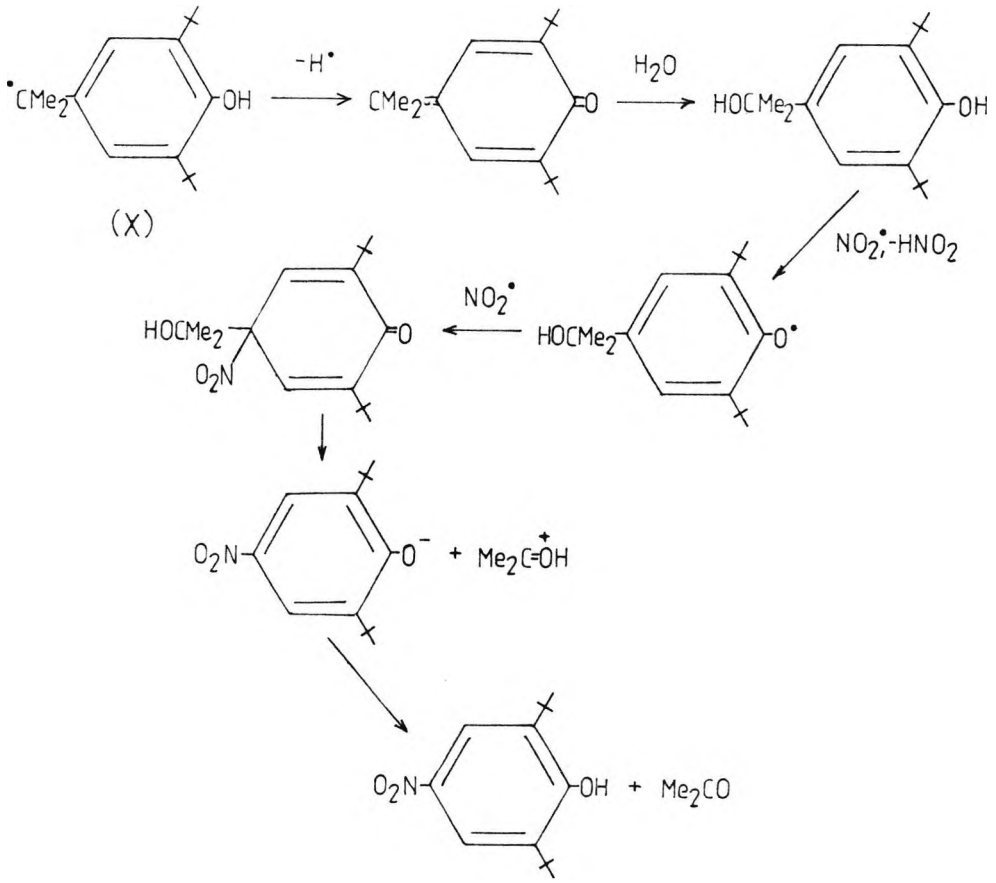

Scheme 8.6

Such a Scheme is consistent with the minor products detected in the product experiments at high concentrations.

CHAPTER 9

CONCLUDING DISCUSSION

9. Concluding Discussion

The reactions of styrene, allylbenzene, 4-phenylbut-1-ene and 1-dodecene with nitrogen dioxide were found to show excellent first-order behaviour in alkene over three half-lives. Kinetic, product and C.I.D.N.P. observations can be explained by the mechanism shown in Scheme 9.1 (see Chapter 5).

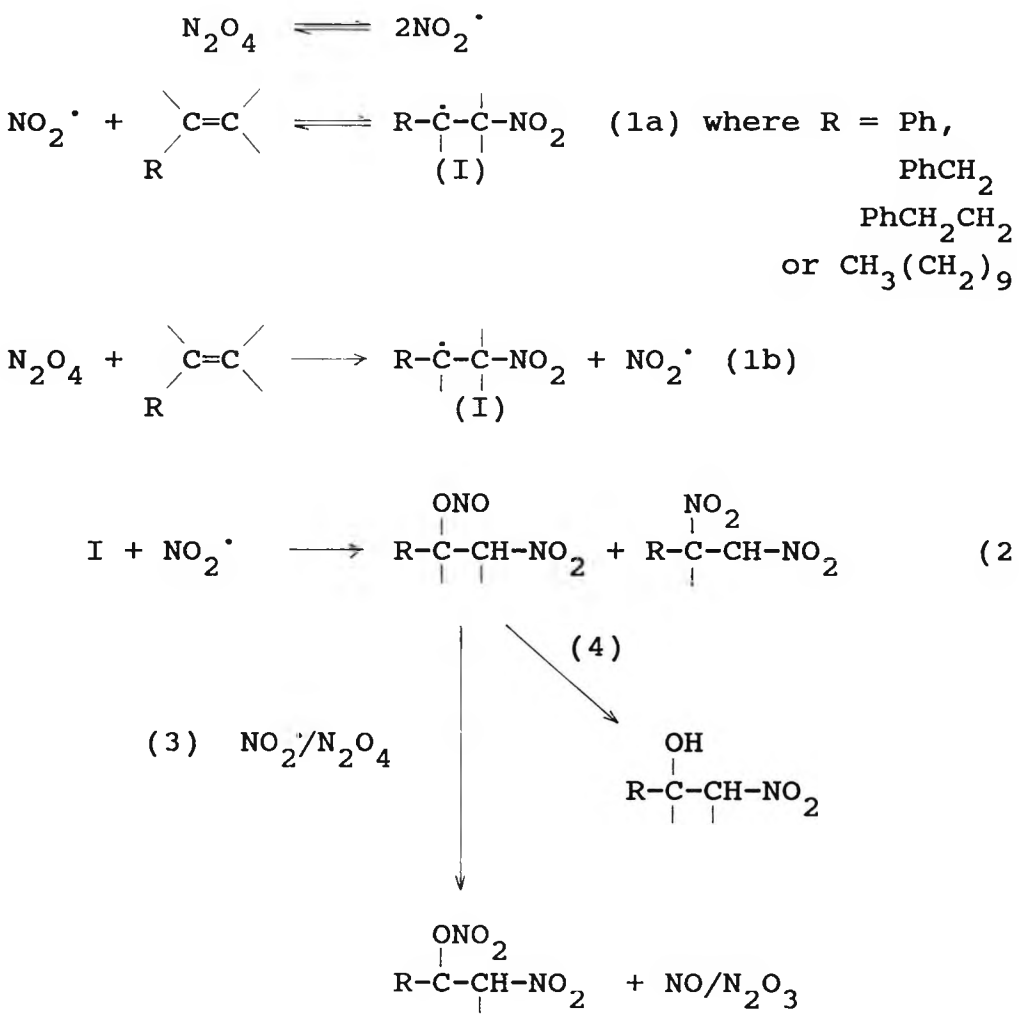

Scheme 9.1

Kinetic results provide conclusive evidence for the initial step of the reaction, which involves addition of $NO_2^{\cdot}$ and N_2O_4 to the double bond in concurrent reactions to form the carbon-centred radical I. C.I.D.N.P. results confirm steps

(1a) and (2). Radical I then reacts with more $NO_2^{\cdot}$ to give a dinitro compound and a nitro-nitrite, which can in turn react further with $NO_2^{\cdot}$ to form a nitro-nitrate compound. The nitrite ester is converted to the nitro-alcohol as the reaction proceeds. There is no change in products or proportions over the range of nitrogen dioxide concentrations used in the kinetic runs, indicating that the mechanism of reaction does not change as the proportion of N_2O_4 in the nitrating solution increases.

There is little reactivity of 1-methylbutylbenzene with nitrogen dioxide under the conditions studied. The maximum extent of reaction over a 2 h period is 12% at 25°C and this apparently increases to 28% at 150°C. Since no products were detected by g.l.c., the disappearance of 1-methylbutylbenzene is believed to be due to loss through evaporation as the nitrogen dioxide/N_2 gas mixture was bubbled through the substrate solution. Attempts were made to determine the reactivity of 1-methylbutylbenzene relative to benzene by the competition technique. However, since no nitration products were detected from the reaction of 1-methylbutylbenzene with nitrogen dioxide, it was not possible to estimate the relative reactivity of this substrate.

The rates of nitration of naphthalene and 2-methylnaphthalene with nitrogen dioxide were also found to be extremely low under the conditions used. Nitro products were not detected from the reaction of naphthalene with nitrogen dioxide and 11.4% and 11.7% yields of 2-methyl-1-nitronaphthalene were obtained from the nitration of 2-methylnaphthalene at 25°C and 50°C, respectively. The values of relative reactivity obtained for naphthalene and benzene are those expected for a species less selective than the nitronium ion. No further conclusion could be reached as to the nature of the reacting species or the mechanism of reaction.

In contrast, the rates of nitration of the bisphenol compounds studied is extremely high. The reactions were found to show excellent first-order behaviour in bisphenol over three

half-lives. The observed orders of the reactions in $NO_2^{\bullet}$ can be explained by the mechanism shown in Scheme 9.2.

$$ArOH + NO_2^{\bullet} \rightleftharpoons ArO^{\bullet} + HNO_2 \qquad (1)$$

$$ArO^{\bullet} + NO_2^{\bullet} \longrightarrow \longrightarrow \longrightarrow \text{products} \qquad (2)$$

Scheme 9.2

For the reaction of AN2 with nitrogen dioxide where the dienone is formed, a step subsequent to step (1) is rate-limiting and this leads to a kinetic dependence that is second-order in $NO_2^{\bullet}$. The kinetic and spectral data do not rule out the second stage being rate-limiting. The reaction stops after mono-nitration because of the orientation of the cyclohexadiene rings, which sterically hinders attack of $NO_2^{\bullet}$ at the p-position of the second ring.

The reaction of IONOX 400 with nitrogen dioxide is first-order in $NO_2^{\bullet}$. This can be explained by step (1) in Scheme 9.2 becoming rate-limiting or to a separate bimolecular reaction between this substrate and $NO_2^{\bullet}$. The increased stability of the tertiary radical (X) over (Y) may be involved.

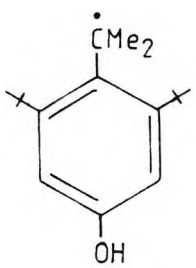

(X)

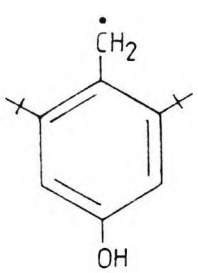

(Y)

The product, 2,6-di-t-butyl-4-nitrophenol, is formed from both rings.

The importance of the above reactions with respect to deposit formation in the crankcase of an internal combustion

engine is summarised in Table 9.1. The reactions have different orders in nitrogen dioxide and rate coefficient and half-life values have been calculated accordingly. The data are based on a concentration of 150 ppm $NO_2^{\bullet}$ in the lubricant and a temperature of ~25°C. Phenol, AN2, IONOL and IONOX 400 react at the fastest rates, with half-life values of 9×10^{-3}s, 5×10^{-2} s, 11×10^{-2}s and 10s respectively, followed by 1-dodecene, 4-phenylbut-1-ene and allylbenzene. Although there are no kinetic data for the last 4 compounds in the table, it is clear that $NO_2^{\bullet}$ reacts with naphthalenes in preference to benzenoid aromatics other than phenols. It should be noted that the above reactions will be considerably faster at crankcase/rocker cover temperatures, i.e. ambient to 150°C, and piston temperatures, i.e. 250°C - 300°C, leading to a higher rate of deposit formation.

In summary, the reactions of nitrogen dioxide with the aromatic/alkene, aromatic and diaromatic components of the fuel/lubricant are very much slower than those with the commercial antioxidant additives and the salicylates; the crankcase oil will be degraded by loss of the latter before the reactions of the former can become important contributors to sludge/lacquer formation.

Table 9.1: Absolute rates of reaction of organic substrates present in fuel/lubricant towards NO_2* at ~25°C

substrate	k/s^{-1}	$t_{½}/s$
Phenol[1]	80	9×10^{-3}
AN2[2]	14	5×10^{-2}
IONOL[1]	6	11×10^{-2}
IONOX 400[2]	7×10^{-2}	10
salicylates/methyl salicylate[1]	1.5×10^{-2}	5×10^{-4}
Styrene[2]	-	-
1-Dodecene[2]	1.8×10^{-3}	6 min
4-Phenylbut-1-ene[2]	1.7×10^{-3}	7 min
Allylbenzene[2]	1.2×10^{-3}	9½min
2-Methylnaphthalene[2]	↓	DECREASING RATE OF REACTIVITY TOWARDS NO_2
Naphthalene[2]		
1-Methylbutylbenzene[2]		
Benzene	V. SLOW	

*$[NO_2]$ = 150 ppm

1. A Diggle, PhD Thesis, The City University, 1987
2. J. Chatterjee, PhD Thesis, The City University, 1993

CHAPTER 10

EXPERIMENTAL

10. Experimental

10.1 Materials

10.1.1 Nitrogen dioxide and solvents

Nitrogen dioxide was obtained from Fisons (99.5%) and was normally used without further purification. The rate of reaction of nitrogen dioxide with cyclohexane is considerably lower than that of nitrogen dioxide with the aromatic substrates in this study, and kinetic studies showed that this result did not change with the rigorous drying of the nitrogen dioxide (codistillation from P_2O_5 under a stream of dry nitrogen) or the cyclohexane solvent. Cyclohexane (BDH spectrosol) and carbon tetrachloride (BDH spectrosol) were dried over type 4A molecular sieves before use. Hexadecane was obtained from BDH (99%) and was used without further purification. $CDCl_3$, CD_3COCD_3 and C_6D_{12} were used for ^1H n.m.r. and ^{15}N n.m.r. work. These were obtained from Aldrich and were used without further purification.

The 50 ppm and 10000 ppm nitrogen dioxide/N_2 gas mixtures were obtained from Electrochem.

10.1.2 Aromatic Compounds

All samples of aromatic compounds were used without further purification. Allylbenzene, benzene, 1-ethylnaphthalene, naphthalene, nitrobenzene, 1-nitronaphthalene, 2-nitronaphthalene, 2-methylnaphthalene, 4-nitroveratrole and styrene were obtained from Aldrich. 1-methylbutylbenzene and 4-phenylbut-1-ene were Aldrich Rare chemicals. 1-Dodecene was obtained from BDH and 1-nitro-2-methylnaphthalene from Koch Light. AN2 and IONOX 400 were obtained from Shell International Chemical Company Ltd.

10.2 Gas-liquid chromatography

Reactant concentrations and yields of products were determined by a method based on relative response factors. The relative response factors of the reactants or products were measured with respect to a reference standard which was added to the sample prior to analysis. The area, A_p of a given peak is proportional to the amount of the respective solute, c_p

$$A_p = f_p c_p \qquad (10.1)$$

where f_p is a constant depending on the properties of the component, p. Using this relationship, it is possible to obtain expressions for two peaks, of components x and s where s is a standard and x is to be determined.

$$A_s = f_s c_s \qquad (10.2)$$
$$A_x = f_x c_x \qquad (10.3)$$

Dividing equation 10.3 by 10.2 gives

$$\frac{c_x}{c_s} = \frac{A_x f_s}{A_s f_x} \qquad (10.4)$$

The constant $f_s/f_x = f$ can be readily obtained from a standard mixture of reference standard and unknown, and hence

$$c_x = c_s \, f \, \frac{A_x}{A_s} \qquad (10.5)$$

10.2.1 GLC conditions for allylbenzene/nitrogen dioxide product mixtures

All allylbenzene/nitrogen dioxide product mixtures were analysed on a 2 metre x 31.75 mm silicone 5% SE30 column at 125°C and a nitrogen flow rate of 25 ml min^{-1}.

10.3 GLC/MS Analysis

10.3.1 GC/EIMS

GC/EIMS analysis was performed by first separating the sample mixture on a fused silica column (2 metre x 31.75 mm silicone 5% SE30 on WHP support). The following temperature profile was used : heating at 100°C for 5 min, 100°C - 125°C at 5°C min^{-1} then heating at 125°C. 1 μl of a dilute solution of the reaction products was introduced via the injector port (175°C) and helium was used as the carrier gas (25 ml min^{-1}). The separated components passed via the transfer line (150°C - 200°C) into the ion source of an AEI MS30 double beam high resolution mass spectrometer where ionisation was performed by electron impact (EI).

10.3.2 GC/CIMS

GC/CIMS analysis was carried out by the mass spectrometry service at King's College London. The allylbenzene/nitrogen dioxide reaction mixture was analysed on a BP1 25 metre capillary column (0.22 mm i.d.), using a split injection (injector temperature 175°C). The oven temperature employed was 140°C. For the styrene, 4-phenylbut-1-ene, 1-dodecene reaction mixtures the oven and injector temperatures were altered to 100°C and 130°C respectively. Injection volumes were 2 μl and ammonia was used to produce the reagent ions; helium was used as eluent. Scans were taken every 1s and a scanning range up to m/z 500 was possible.

10.4 Instrumentation

Ultraviolet-visible spectra were measured on a Perkin-Elmer Lambda-5 spectrophotometer, and all spectra are of the solution in the cell versus air. Gas liquid chromatography was performed on a Perkin Elmer Sigma 3 gas chromatograph fitted with a flame ionisation detector. ^{1}H nuclear magnetic resonance spectra were measured using Jeol FX 60 and FX 100 spectrometers and ^{13}C n.m.r. spectra on a Jeol FX 90 instrument. Infrared

spectra were recorded using a Perkin Elmer 983G infrared spectrophotometer.

10.5 Temperature Measurements

All thermometers were compared with a standard thermometer of the British Standard Institution Testing and Approvals Centre at the end of all experimental work.

APPENDIX

The abbreviations used in the text refer to the following:

PAH(s) polyaromatic hydrocarbon(s)
TLC/t.l.c. thin layer chromatography
GLC gas liquid chromatography
GLC/MS combined gas liquid chromatography/mass spectrometry
GC/EIMS combined gas liquid chormatography/mass spectrometry
GC/CIMS combined gas liquid chromatography/mass spectrometry
I.R. infrared spectroscopy
$^{1}H/^{13}C/^{15}N$ n.m.r. $^{1}H/^{13}C/^{15}N$ nuclear magnetic resonance spectroscopy
UV ultraviolet spectroscopy
r.t. room temperature

Definition of terms:

β Bohr magneton

h Plank's constant

a Hyperfine coupling constant

m_I Spin quantum number of nucleus

B Applied/external magnetic field

REFERENCES

1. G.G. Havens, Phys. Rev., 1932, 41, 337.

2. J.H. van Vleck, "The Theory of Electric and Magnetic Susceptibility", OUP, London, 1932, p.275.

3. R.J. Kandel, J. Chem. Phys., 1955, 23, 84.

4. H.O. Pritchard, Chem. Revs., 1953, 52, 555.

5. M. Brown and M.K. Wilson, J. Chem. Phys., 1954, 22, 955.

6. G.E. Moore, J. Opt. Soc. Amer., 1953, 43, 1045.

7. R.G. Snyder and I.C. Hisatsune, J. Mol. Spectrosc., 1957, 1, 139.

8. G.M. Begun and W.H. Fletcher, J. Mol. Spectrosc., 1960, 4, 388.

9. J. Laane and J.R. Ohlsen, Prog. Inorg. Chem., 1980, 27, 465.

10. R.F. Holland and W.B. Maier. J. Chem. Phys., 1983, 78, 2928.

11. D.W. Smith and K. Hedberg, J. Chem. Phys., 1956, 25, 1282.

12. J.S. Broadley and J.M. Robertson, Nature, 1949, 164, 914.

13. J.W. Mellor, "A Comprehensive Treatise on Inorganic and Theoretical Chemistry", Vol. VIII, Longmans, Green and Company, London, 1928, pp. 529 - 48.

14. T. Carrington and N. Davidson, J. Phys. Chem., 1953, 57, 418.

15. I.C. Hisatsune, J. Phys. Chem., 1961, 65, 2249.

16. T.F. Redmond and B.B. Wayland, J. Phys. Chem., 1968, 72, 1626.

17. T.C. Hall and F.E. Blacet, J. Phys. Chem., 1952, 20, 1745.

18. H. Wieland, Liebig's Ann., 1903, 328, 154; 1903, 329, 225; 1905, 340, 63; 1908, 360, 299; 1921, 424 71.

19. H. Wieland and H. Stenzel, Chem. Ber., 1907, 40, 4825.

20. J.H. Ridd and R.P. Claridge, unpublished results.

21a. A. Michael and G.H. Carlson, J. Org. Chem., 1940, 5 14 - 23.

b. A. Michael and G.H. Carlson, J. Org. Chem., 1940, 5, 1 - 13.

22. N.Y. Demianov and K.V. Sidorenko, Zh. russk. khim. obshch., 1909, 41, 832.

23. N.Y. Demianov, Zh. russk. khim. obshch., 1904, 36, 15; Anilo-krasoch. prom., 1934, 4, 132.

24. J. Schmidt, Chem. Ber., 1903, 36, 1775.

25. A. Michael and G.H. Carlson, J. Amer. Chem. Soc., 1937, 59, 843.

26. A.Smith, Amer. Pat. 2384087; Chem. Abstr., 1946, 40, 347.

27. H. Baldock and A. Smith, Ind. Eng. Chem., 1952, 44, 2041.

28a. N. Levy and C.W. Scaife, J. Chem. Soc., 1946, 1093; N. Levy, C.W. Scaife and A.E. Wilder-Smith, J. Chem. Soc., 1946, 1096.

b. N. Levy and C.W. Scaife, J. Chem. Soc., 1946, 1100.

29. N. Levy, C.W. Scaife and A.E. Wilder-Smith, J. Chem. Soc., 1948, 52.

30. H. Baldock, N. Levy and C.W. Scaife, J. Chem. Soc., 1949, 2627.

31. C.K. Ingold, "Structure and Mechanism in Organic Chemistry", Cornell Univ. Press, New York, 1953, p. 670.

32. K.N. Campbell, J. Shavel and B.K. Campbell, J. Amer. Chem Soc., 1953, 75, 2400.

33. J.P. Freeman and W.D. Emmons, J. Amer. Chem. Soc., 1957, 79, 1712.

34. H. Schechter and F. Conrad, J. Amer. Chem. Soc., 1953, 75, 5610.

35. A.I. Titov, Tetrahedron, 1963, 19, 557-580.

36. J.C.D. Brand and I.D.R. Stevens, J. Chem. Soc., 1958, 629.

37. H.S. Schechter, J.J. Gardikes, T.S. Cantrell and G.V.D. Tiers, J. Amer. Chem. Soc., 1967, 89, 3005.

38. W.K. Siefert, J. Org. Chem., 1963, 28, 125.

39. W.A. Pryor, J.W. Lightsey and D.F. Church, J. Amer. Chem. Soc., 1982, 104, 6685.

40. W.A. Pryor, M. Tamura and D.F. Church, J. Amer. Chem. Soc., 1984, 106, 5073.

41. A. Rockenbauer, M. Gyor and F. Tudos, Tetrahedron Lett., 1986, 27, 3425.

42. D.H. Giamalva, G.B. Kenion, D.F. Church and W.A. Pryor, J. Amer. Chem. Soc., 1987, 109, 7059.

43. J.L. Powell, J.H. Ridd and J.P.B. Sandall, J. Chem. Soc., Chem. Commun., 1990, 402.

44. D.K. Bryant, B.C. Challis and J. Iley, J. Chem. Soc., Chem. Commun., 1989, 1027.

45. H. Wieland, Chem. Ber., 1921, 54, 1776.

46. L.H. Friedburg, J. Amer. Chem. Soc., 1882, 4, 252.

47. L.W. Bass and T.B. Johnson, J. Amer. Chem. Soc., 1924, 46, 456.

48. D.S. Ross and W.G. Blücher, Report 1980, ARO-13831.3.CX, Avail. NTIS.

49. A. Schaarschmidt and F. Smolla, Chem. Ber., 1921, 57, 32; P.P. Shorygin and A. Topchiev, Chem. Ber., 1934, 67 1362.

50. M.I. Bogdanov, Anilinokrasochnaya prom., 1933, 3, 133; A. Schaarschmidt, Z. angew. Chem., 1924, 37, 933.

51. A.I. Titov, J. Gen. Chem. USSR (Engl. Transl.), 1937, 7, 591.

52. G.R. Underwood, R.S. Silverman and A. Vanderwalde, J. Chem. Soc., Perkin II, 1973, 1177.

53. L.W. Russell, Ph.D. Thesis, The City University, 1974.

54. V. Gold, Ph.D. Thesis, University of London, 1945; G.H. Williams, Ph.D. Thesis, University of London, 1950; V. Gold, E.D. Hughes, C.K. Ingold and G.H. Williams, J. Chem. Soc., 1950, 2452.

55. K.E. Spratley, Ph.D. Thesis, The City University, 1982.

56. T.G. Bonner, R.A. Hancock, G. Yousif and F.R. Rolle, J. Chem. Soc. (B), 1969, 1237.

57. P.P. Shorygin, A.V. Topchiev and V.A. Anal'ina, J. Gen. Chem. USSR (Engl. Transl.), 1938, 8, 981.

58. M.A. Ilynskii, Zh. obshch. khim. (USSR), 1928, 5, 469.

59. A.V. Topchiev, "Nitration of Hydrocarbons and other Organic Compounds", Pergamon Press, London, 1959, p.239.

60. W.A. Pryor, G.J. Gleicher, J.P. Cosgrove and D.F. Church, J. Org. Chem., 1984, 49, 5189.

61. H. Tokiwa, R. Nakagawa, K. Morita and U. Ohnishi, Mutat. Res., 1981, 85, 195.

62. F. Radner, Acta Chem. Scand. (B), 1983, 37, 65.

63. L. Eberson and F. Radner, Acta Chem. Scand. (B), 1985, 39, 343.

64. R.J. Schmitt, S.E. Buttrill, Jr. and D.S. Ross, J. Amer. Chem. Soc., 1984, 106, 926.

65. L. Eberson and F. Radner, Acta Chem. Scand. (B), 1986, 40, 71 - 78.

66. G.L. Squadrito, F.R. Fronczek, D.F. Church and W.A. Pryor, J. Org. Chem., 1989, 54, 548.

67. P.F. Frankland and R.C. Farmer, J. Chem. Soc., 1901, 79, 1356.

68. A. Purgotti, Ann. ist. super. agrar. Portici [3], 1929, 3, 41.

69. A.W. Diggle, Ph.D. Thesis, The City University, 1987.

70. R.S. Spindt, C.L. Wolfe and D.R. Stevens, "Nitrogen Oxides, Combustion, and Engine Deposits", SAE Trans., 1956, 64, 797.

71. E. Dimitroff and R.D. Quillian, Jr., "Low Temperature Engine Sludge - What? - Where? - How?", SAE Technical Paper 650255, 1965.

72. E. Dimitroff, J.V. Moffitt and R.D. Quillian Jr., "Why, What, How:Engine Varnish", Transactions of the ASME, 1969, 91, 406.

73. D.J. Smolenski and S.P. Bergin, "Development of the ASTM Sequence IIIE Engine Oil Oxidation and Wear Test", SAE Technical Paper, 881576, 1988.

74. S. Korcek and M.D. Johnson, "Effects of NO_x on Liquid Phase Oxidation and Inhibition at Elevated Temperatures", Ford Motor Company, Dearborn, USA.

75. C.E. Welling, G.C. Hall and J.S. Stepanski, SAE Transactions, 1961, 69, 448.

76. W.E. Morris and K.T. Dishart, ASTM Meeting, Toronto, 1970.

77. H.H.Oelert, W. Mayer-Gurr and J. Zajontz, Erdol and Kohle, Erdgas, Petrochemie vereinigt mit Brennstoff-Chemie, 1974, 27, No. 3, 146.

78. J.B. Edwards and D.M. Teague, "Unravelling the Chemical Phenomena Occurring in Spark Ignition Engines", SAE Paper 700489.

79. W.A. Waters, "Mechanisms of Oxidation of Organic Compounds", Methuen and Company Ltd., John Wiley and Sons, New York, 1964.

80. N.M. Emanuel, "The Oxidation of Hydrocarbons in the Liquid Phase", The Macmillan Company, New York, 1965.

81. A.P. Altschulter and I. Cohen, Int. J. Air and Water Pollution, 1961, 4, 55.

82. J.F. Brown, JR., J. Amer. Chem. Soc., 1957, 79, 2480.

83. B.D. Vineyard and A.Y. Coran, "Gasoline Engine Deposition: I Blowby Collection and the Identification of Deposit Precursors", Preprints, Div. Petrol, Chem., ACS, 1969, 14(4), A25 - A32.

84. I.J. Spilners, J.F. Hedenburg and C.R. Spohn, Preprints, Div. Petrol. Chem., ACS, March 29 - April 3 1981, Atlanta.

85. W.H. Crouse and D.L. Anglin, "Automotive Fuel, Lubricating and Cooling Systems", McGraw-Hill Book Company, 1976.

86. J.L. Sprung, H. Akimoto and J.N. Pitts, Jr., J. Amer. Chem. Soc., 1974, 96, 6549.

87. R. Atkinson, S.M. Aschmann, A.M. Winer and J.N. Pitts, Jr., Int. J. Chem. Kinet., 1984, 16, 697.

88. S. Jaffe, "Chemical Reactions in Urban Atmospheres"; C.S. Tuesday, Ed., Elsevier, New York, 1971.

89. T. Ohta, H. Nagura and S. Suzuki, Int. J. Chem. Kinet., 1986, 18, 1.

90. H. Niki, P.D. Maker, C.M. Savage, L.P. Breitenbach, M.D. Hurley, Int. J. Chem. Kinet., 1986 18, 1235.

91. G.B. Kenion, J.P. Cosgrove, D.H. Giamalva, D.F. Church and W.A. Pryor, unpublished results.

92. H. Schechter, Rec. Chem. Prog., 1964, 25, 55.

93. T.L. Cottrell and T.E. Graham, J. Chem. Soc., 1953, 556.

94. T.L. Cottrell and T.E. Graham, J. Chem. Soc., 1954, 3644.

95. P.A. Bristow and R.G. Coombes, Chem. Ind. (London), 1969, 135.

96. J.W. Roddy and C.F. Coleman, Talanta, 1968, 15(II), 1281.

97. B.D. Pearson and J.E. Ollerenshaw, Chem. Ind. (London), 1966, 370; R.C. Meeker, F. Critchfield and E.T. Bishop, Analyt. Chem., 1962, 52, 3568.

98. W.A. Pryor, L. Castle and D.F. Church, J. Amer. Chem. Soc., 1985, 107, 211.

99. P. Sykes, "A Guidebook to Mechanism in Organic Chemistry", 2 ed., 1965 Longman, London.

100. G.C. Levy and R.B. Lichter, "^{15}N Nuclear Magnetic Resonance Spectroscopy", John Wiley & Sons, New York, 1979.

101. J. Bargon, H. Fischer and U. Johnsen, Z. Naturforsch, 1967, 22a, 1551.

102. H.R. Ward, J. Amer. Chem. Soc., 1967, 89, 5517; H.R. Ward and R.G. Lawler, J. Amer. Chem. Soc., 1967, 89, 5518.

103. G.L. Closs, J. Amer. Chem. Soc., 1969, 91, 4552; G.L. Closs and A.P. Trifunac, J. Amer. Chem. Soc., 1970, 92, 2183.

104. R. Kaptein and L.J. Oosterhoff, Chem. Phys. Lett., 1969, 4, 195; R. Kaptein and L.J. Oosterhoff, Chem. Phys. Lett., 1969 4, 214.

105a. D. Bethell and M.D. Brinkman, Adv. Phys. Org. Chem., 1973, 10, 53.

b. R.G. Lawler and H.R. Ward, Det. Org. Struc. Phys. Meth., 1973, 5, 99.

c. G.L. Closs, Adv. Mag. Res., 1974, 7, 157.

d. H.Fischer, Top. Curr. Chem., 1971, 24, 1.

e. R. Kaptein, Adv. Free Rad. Chem., 1975, 5, 319.

f. H.R. Ward, "Free Radicals" (J.K. Kochi Ed.), John Wiley & Sons 1973, Volume 1, p. 239.

g. H.R. Ward, Acc. Chem. Res., 1972, 5, 18.

h. R.G. Lawler, Acc. Chem. Res., 1972, 5, 25.

i. C. Richard and P. Granger, "Chemically Induced Dynamic Nuclear and Electron Polarisations - C.I.D.N.P. and C.I.D.E.P. (N.M.R. - Basic Principles and Progress Series Editors P. Diehl, E. Fluck and R. Kosfeld Volume 8)", Springer Verlag, Berlin, 1974.

j. A.L. Buchachenko and F.M.Zhidornirov, Usp. khim., 1971, 40, 801.

k. R.G. Lawler, Prog. N.M.R. Spec., 1973, 9, 149.

l. S.H. Pine, J. Chem. Ed., 1972, 49, 664.

m. A.R. Lepley and G.L. Closs (Eds.), "Chemically Induced Magnetic Polarisation", John Wiley & Sons, New York, 1973.

n. K.M. Salikhov, Yu. N. Molin, R.Z. Sagdeev and A.L. Buchachenko," Spin Polarisation and Magnetic Effects in Radical Reactions" (Yu. N. Holin Ed.) (Studies in Physical and Theoretical Chemistry Volume 22)", Elsevier, 1984.

106. R. Kaptein, J. Chem. Soc., Chem. Comm., 1971, 732.

107. W.A. Porter, G.R. Dubay and J.G. Green, J. Amer. Chem. Soc., 1978, 100, 920.

108. J.F. Johnston, University of London, Ph.D. Thesis, 1990.

109. M.S. Blois, H.W. Brown and J.E. Maling, Neuvième Colloque Ampère, Geneva:Librarie Payot, 1960, 243.

110. J.R. Morton, K.F. Preston and S.J. Strach, J. Phys. Chem., 1979, 83, 553.

111. See Ref. 105 m, Ch. 8.

112. C.L. Perrin, J. Amer. Chem. Soc., 1977, 99, 5516.

113. G.A. Olah, S.C. Narang and J.A. Olah, Proc. Natl. Acad. Sci. USA., 1981, 78 3298.

114. A. Boughriet, A. Bremard and M.J. Wartel, New J. Chem., 1987, 11, 245.

115a. E.K. khim, T.M. Bockman and J.K. Kochi, J.Chem. Soc., Perkin Trans.2, 1992, 1879.

b. S. Sankararaman and J.K. Kochi, J.Chem. Soc., Perkin Trans.2, 1991, 1.

116. D.J. Clark and D.J. Fairweather, Tetrahedron, 1969, 5525.